

**UCLA**

**UCLA Electronic Theses and Dissertations**

**Title**

Geographic Information Systems (GIS) for Misaligned Variables: Advances in Small-Area Analyses for Environmental Health Sciences

**Permalink**

<https://escholarship.org/uc/item/0xd470vq>

**Author**

Lipsitt, Jonah Michael

**Publication Date**

2022

Peer reviewed|Thesis/dissertation

UNIVERSITY OF CALIFORNIA

Los Angeles

Geographic Information Systems (GIS) for Misaligned Variables:  
Advances in Small-Area Analyses for Environmental Health Sciences

A dissertation submitted in partial satisfaction of the  
requirements for the degree Doctor of Philosophy  
in Environmental Health Sciences

by

Jonah Michael Lipsitt

2022

© Copyright by  
Jonah Michael Lipsitt  
2022

## ABSTRACT OF THE DISSERTATION

Geographic Information Systems (GIS) for Misaligned Variables:  
Advances in Small-Area Analyses for Environmental Health Sciences

by

Jonah Michael Lipsitt

Doctor of Philosophy in Environmental Health Sciences

University of California, Los Angeles, 2022

Professor Michael Leo B. Jerrett, Chair

Geospatial methods are increasingly used to evaluate environmental exposures in epidemiologic studies. Geospatial data are often acquired from different sources and time periods and at different spatial resolutions. This dissertation presents methods for combining datasets that do not overlap in space and, or time and are essential for the accurate quantification of metrics used in Environmental Health Sciences. In three chapters, we demonstrated and compared advances in small-area geospatial methods used to reduce misalignment and misclassification of key variables (e.g., exposure).

First, we showed how small-area analyses of COVID-19 can benefit from spatial aggregation to account for areal misalignment. In an analysis of the association between air pollution levels and COVID-19 incidence and mortality, we used residential building footprints to combine misaligned COVID-19 outcomes recorded at the neighborhood level, population

demographics recorded at the census-tract level, and NO<sub>2</sub> interpolated surfaces recorded at 30-meter grids. We found NO<sub>2</sub> to be positively associated with COVID-19 incidence and mortality for neighborhoods in Los Angeles.

Second, we used data acquired through the PASTA-LA study to attribute daily green space exposure for physically-active spaces (PASs) where activity, location, and green space data were misaligned. We used tracking data from accelerometers and smartphones to attribute green-space exposure using 21 geospatial methods. We found that exposures attributed to home-address buffers, a commonly used method, can result in exposure misclassification. We also found a large range in correlation depending on tracking device used and the way physical activity was categorized across the 21 methods, suggesting that the method selected is key to the findings.

Finally, third, also using PASTA-LA data, we studied the association between heat exposure and physical activity in which temperature, green space, and participant-level covariates were misaligned. We showed that heat exposure was associated with increased physical activity and that exposure to green space modified this association in only some models. In this chapter, and in all chapters of this dissertation, we demonstrated how choice in geospatial approach to spatiotemporal misalignment can yield different study results.

The dissertation of Jonah Michael Lipsitt is approved.

Sudipto Banerjee

Brian L. Cole

Yifang Zhu

Michael Leo B. Jerrett, Committee Chair

University of California, Los Angeles

2022

## **DEDICATION**

Dedicated to my family, friends, and colleagues who have helped me personally and professionally throughout my life and academic career.

## TABLE OF CONTENTS

<b>ABSTRACT OF THE DISSERTATION</b> .....	<b>II</b>
<b>DEDICATION</b> .....	<b>V</b>
<b>TABLE OF CONTENTS</b> .....	<b>VI</b>
<b>LIST OF FIGURES</b> .....	<b>X</b>
<b>LIST OF TABLES</b> .....	<b>XI</b>
<b>GLOSSARY</b> .....	<b>XII</b>
<b>ACKNOWLEDGEMENTS</b> .....	<b>XIV</b>
<b>VITA</b> .....	<b>XVII</b>
<b>CHAPTER 1 : INTRODUCTION AND OVERVIEW OF THE ORGANIZATION OF THE DISSERTATION</b> .....	<b>1</b>
1.1 OVERVIEW .....	1
1.2 SUMMARY OF AIMS.....	2
1.3 RESEARCH SETTING .....	3
1.4 AREAL MISALIGNMENT IN AN INVESTIGATION OF COVID-19 AND TRAFFIC- RELATED AIR POLLUTION.....	4
1.5 SPATIOTEMPORALLY MISALIGNED DATA IN A COMPARISON OF PHYSICAL ACTIVITY SPACE METHODS FOR GREEN SPACE EXPOSURE ATTRIBUTION .....	6
1.6 SPATIOTEMPORALLY MISALIGNED DATA METHODS IN THE ASSESSMENT OF PHYSICAL ACTIVITY, HEAT, AND GREEN SPACE .....	8
1.7 REFERENCES FOR CHAPTER 1 .....	11
<b>CHAPTER 2 : SPATIAL ANALYSIS OF COVID-19 AND TRAFFIC-RELATED AIR POLLUTION IN LOS ANGELES</b> .....	<b>18</b>
2.1 INTRODUCTION .....	18
2.2 MATERIAL AND METHODS.....	21
2.2.1 Setting.....	21
2.2.2 Data sources.....	21
2.2.3 Quantification of variables .....	23
2.2.4 Statistical Modeling .....	24
2.3 RESULTS .....	25

2.4	DISCUSSION AND CONCLUSION .....	27
2.5	Appendix A. Adjusted association of NO <sub>2</sub> and COVID-19 from three models for the period between March 16 <sup>th</sup> and September 8 <sup>th</sup> , 2020 .....	36
2.6	Appendix B. Adjusted association of NO <sub>2</sub> and COVID-19 from three models for the period between March 16 <sup>th</sup> and September 8 <sup>th</sup> , 2020 – sensitivity analyses including hypertension and diabetes covariates.....	37
2.7	Appendix C. Adjusted association of NO <sub>2</sub> and COVID-19 from three models for the period between September 8 <sup>th</sup> , 2020 and February 23 <sup>rd</sup> , 2021 .....	38
2.8	REFERENCES FOR CHAPTER 2 .....	39

### **CHAPTER 3 : PHYSICAL ACTIVITY SPACE METHODS FOR GREEN SPACE EXPOSURE**

	<b>ATTRIBUTION: A MULTI-METHOD COMPARISON STUDY .....</b>	<b>64</b>
3.1	INTRODUCTION .....	64
3.2	METHODS.....	70
3.2.1	Participants .....	70
3.2.2	PASTA-LA data collection .....	71
3.2.3	Inclusion criteria and data cleaning .....	73
3.2.4	Moderate-to-vigorous physical activity.....	74
3.2.5	Physical activity spaces .....	75
3.2.6	Green space exposure attribution .....	78
3.2.7	Comparison and evaluation.....	79
3.2.8	Software.....	79
3.3	RESULTS .....	80
3.3.1	Summary of 21 PAS methods .....	80
3.3.2	Quantification of green space for 21 PAS methods .....	82
3.4	DISCUSSION .....	84
3.5	CONCLUSION.....	88
3.6	REFERENCES FOR CHAPTER 3 .....	107

### **CHAPTER 4 : HEAT, GREEN SPACE, AND PHYSICAL ACTIVITY IN LOS ANGELES: AN ACTIVITY SPACES APPROACH .....**

	<b>ACTIVITY SPACES APPROACH .....</b>	<b>132</b>
4.1	INTRODUCTION .....	132
4.2	METHODS.....	134
4.2.1	Participants .....	134

4.2.2	Participant data collection .....	135
4.2.3	Inclusion criteria and data cleaning .....	137
4.2.4	Moderate-to-vigorous physical activity.....	137
4.2.5	Physical activity space .....	138
4.2.6	Temperature attribution.....	138
4.2.7	Green space attribution.....	139
4.2.8	Statistical modeling .....	140
4.3	RESULTS .....	142
4.4	DISCUSSION .....	145
4.5	CONCLUSION.....	148
4.6	APPENDIX A. Supplemental Table 1: Description of sample from four exposure methods .....	156
4.7	APPENDIX B. Supplemental Table 2: Adjusted models of association for temperature and MVPA – for four exposure methods.....	157
4.8	APPENDIX C. Supplemental Table 1: Adjusted models of association for temperature and MVPA, including interaction between temperature <sup>2</sup> and NDVI – for four exposure methods .....	158
4.9	APPENDIX D. Supplemental Table 4: Adjusted models of association for temperature and MVPA – for four exposure methods using overlapping samples by PAS type.....	159
4.10	APPENDIX E. Supplemental Table 5: Adjusted models of association for temperature and MVPA, including interaction between temperature <sup>2</sup> and NDVI – for four exposure methods using overlapping samples by PAS type.....	160
4.11	APPENDIX F. Supplemental Table 6: Adjusted models of association for temperature and MVPA—for four exposure methods using overlapping samples by MVPA conversion equation .....	161
4.12	APPENDIX G. Supplemental Table 7: Adjusted models of association for temperature and MVPA, including interaction between temperature <sup>2</sup> and NDVI – for four exposure methods using overlapping samples by MVPA conversion equation.....	162
4.13	APPENDIX H. Supplemental Figure 1: Predicted MVPA associated with daily maximum temperature for minimum convex polygon PASs created from <i>Freedson 1998</i> MVPA .....	163
4.14	APPENDIX I. Supplemental Figure 2: Predicted MVPA associated with daily maximum temperature, stratified by median NDVI, for minimum convex polygon PASs created from <i>Freedson 1998</i> MVPA.....	164

4.15 REFERENCES FOR CHAPTER 4 ..... 165

**CHAPTER 5 : SUMMARY OF DISSERTATION FINDINGS AND FUTURE RESEARCH**

**RECOMMENDATIONS ..... 172**

5.1 INTRODUCTION ..... 172

5.2 COVID-19 AND TRAFFIC-RELATED AIR POLLUTION ..... 173

5.3 PHYSICAL ACTIVITY SPACE METHODS ..... 174

5.4 HEAT, GREEN SPACE, AND PHYSICAL ACTIVITY ..... 175

5.5 CONCLUDING REMARKS ON GIS METHODS FOR MISALIGNED VARIABLE  
QUANTIFICATION IN ENVIRONMENTAL HEALTH SCIENCES ..... 176

5.6 REFERENCES FOR CHAPTER 5 ..... 178

## LIST OF FIGURES

Figure 2.1. Maps of NO <sub>2</sub> and COVID-19 case, mortality, and case-fatality rates by neighborhood .....	34
Figure 3.1. Flow chart of participant sample utilized for analyses.....	96
Figure 3.2. Map of participant activity and location data from MOVES app .....	97
Figure 3.3. Map of participant activity and location data from Actigraph+GPS.....	98
Figure 3.4. Map example of 250-meter location buffer PAS with true-color satellite image and NDVI .....	99
Figure 3.5. Map examples of PAS polygons with NDVI .....	100
Figure 3.6. Overview of study procedures used to quantify green space exposure by PASs, including major software and software packages utilized .....	101
Figure 3.7. Flow chart of methods to extract green space (mean NDVI) from home location buffers while anonymizing data for cloud computing .....	102
Figure 3.8. Proportion of person-days of observation excluded for each of 21 methods.....	103
Figure 3.9. Comparison of 2018 versus 2016 extracted NDVI values for 7 PAS methods.....	104
Figure 3.10. Comparison of NDVI extracted using 7 PAS methods versus NDVI extracted using 250-meter home address buffers .....	105
Figure 3.11. Comparison of NDVI extracted from MOVES-based PASs versus NDVI extracted from Actigraph+GPS-based PASs for seven PAS methods utilizing MVPA categorized by step-rate (Abel et al., 2011).....	106
Figure 4.1: Predicted MVPA associated with daily maximum temperature .....	154
Figure 4.2: Predicted MVPA associated with daily maximum temperature, stratified by median NDVI .....	155

## LIST OF TABLES

Table 2.1. Data sources and spatiotemporal dimensions for model of association between NO <sub>2</sub> and COVID-19 case, mortality, and case-fatality rates in Los Angeles County .....	33
Table 2.2. Adjusted association of NO <sub>2</sub> and COVID-19 from three models.....	35
Table 3.1. Data sources utilized for the assessment of green-space exposure attribution by physical activity space (PAS) .....	89
Table 3.2. Participant demographics and tracking data sample size .....	89
Table 3.3. Description of sample, minutes of MVPA included, and size of PAS polygons from activity and location data, for 21 methods .....	90
Table 3.4: Green space (areal mean NDVI derived from NAIP imagery) values attributed to PASs for 21 methods .....	91
Table 3.5. Green space (areal mean NDVI derived from NAIP imagery) values attributed to home address buffers .....	92
Table 3.6. Comparison of 2018 versus 2016 extracted NDVI values for seven PAS methods...	93
Table 3.7: Comparison of NDVI extracted from 250-meter home address buffers versus NDVI extracted from seven PAS methods.....	94
Table 3.8: Comparison of NDVI extracted from MOVES versus Actigraph+GPS (using step-count MVPA conversion—Abel 2011) for seven PAS methods .....	95
Table 4.1: Data sources utilized for the assessment of exposure to heat on physical activity..	149
Table 4.2: Description of sample for main model.....	150
Table 4.3: Adjusted models of association for temperature and MVPA .....	151
Table 4.4: Adjusted models of association for temperature and MVPA, including interaction between temperature <sup>2</sup> and NDVI.....	152
Table 4.5: Comparison of model results for four methods .....	153

## GLOSSARY

<b>Abbreviation</b>	<b>Name</b>
°C	Temperature in degrees Celsius
ACS	U.S. Census Bureau's American Community Survey
API	Application programming interface
app	Smartphone application
BMI	Body mass index
CADPH	California Department of Public Health
CAR	Conditional auto-regressive model
CDC	U.S. Centers for Disease Control and Prevention
CI	95% confidence interval
CrI	Credible interval
CSA	Countywide statistical area
DBSCAN	Density-based spatial clustering applications
ESRI	Environmental Systems Research Institute
GIS	Geographic Information Systems
GPS	Global Positioning System
HDBSCAN	Hierarchical density-based spatial clustering applications
ICC	Intraclass correlation coefficient
ID	Participant identifying number
iOS	Apple's mobile-technology operating system
IQR	Interquartile range
IRB	Institutional Review Board
IRR	Incidence rate ratio
KDR	Kernel-density ranking
kg	Kilogram
LA	Los Angeles
LAC	Los Angeles County
LACDPH	Los Angeles County Department of Public Health
Log <sub>e</sub>	Natural logarithm (base e)
LUR	Land-use regression

M	Mean
m	Meter
MET	Metabolic equivalent of task ratio
mins	Minutes
MOVES	"MOVES" smartphone application
MVPA	Moderate-to-vigorous physical activity
NAIP	National Agriculture Imagery Program
NASA	National Aeronautics and Space Administration
NDVI	Normalized Difference Vegetation Index
OPTICS	Ordering points to identify clustering structure (process)
PAS	Physical activity space
PASTA	Physical Activity through Sustainable Transport Approaches (European) study
PASTA-LA	Physical Activity through Sustainable Transport Approaches in Los Angeles study
PM	Particulate matter
ppb	Parts per billion
R	'R' statistical programming language
r	Sample correlation coefficient
REML	Restricted maximum likelihood
s	Second
SARS	Severe Acute Respiratory Syndrome
SD	Standard deviation
TRAP	Traffic-related air pollution
U.K.	United Kingdom
U.S.	United States of America
UCLA	University of California, Los Angeles
USDA	U.S. Department of Agriculture
WIFI	Wireless technology used to connect devices

## ACKNOWLEDGEMENTS

Thank you to my PhD advisor and mentor, Michael Jerrett. For over ten years, he has guided me through a meandering career and has helped me embrace my multidisciplinary background. His deep understanding of geographic information systems (GIS) applied to the field of Environmental Health Sciences has provided me an immeasurable source of continued learning and inspiration. He has been a source of great support and care throughout my academic career—at both UC Berkeley and UCLA.

I would also like to thank my doctoral committee members: Yifang Zhu, Brian Cole and Sudipto Banerjee. Yifang has provided me great support in my writing and helped me navigate the student experience at UCLA. Brian has taught me the importance of assessing impact and been a great source of personal support throughout my doctoral degree. Sudipto has been an inspiring scientific mentor and has helped me collaborate better with other statistical professionals.

My research has involved many colleagues, and my doctoral studies have provided me many peers. Thank you to Owen Hall for helping me create data collection and analysis protocols for PASTA-LA. Thank you to Christina Batteate who managed PASTA-LA data collection. Thank you to Alec Chan-Golston for teaching me many of the statistical methods used in my research. Thank you to Marco Mingione and Pierfrancesco Alaimo Di Loro for helping me with cleaning, interpolating, and analyzing the PASTA-LA dataset. Thank you to Rachel Connolly for helping me access satellite data with limited internet resources due to COVID-19 lockdowns. I would also like to thank Jonathan Liu, Doug Morrison, and Ellen Do for their programming help and collaboration.

I would like to thank my friends and family for all of their support. My mother and father, who gave me my love of education and learning – thank you. Tiffany Dang, thank you for always

being there for me. I owe a special thanks to John Conroy, a friend and life coach who has guided me through doctoral work-life balance.

My graduate studies have been financially supported by several fellowships, awards, and grants, including:

- UCLA Department of Environmental Health Sciences, Departmental Fellowship;
- Southern California Education and Research Center, Student Pilot Project Award;
- National Institutes of Health, Research Project Grant Program (R01).

I have also received financial support for my research from the UCLA Sustainable LA Grand Challenge, the UCLA Department of Transportation, and the UCLA Healthy Campus Initiative.

Chapter 2 is a version of a published manuscript from *Environment International*. The original version published in March 2021 was updated slightly (in December 2021) to reflect changes to the literature on COVID-19. No analyses were altered—only descriptions of the literature and of COVID-19 case, mortality and case-fatality rate metrics. Figures and tables were altered slightly to fit within the formatting and labeling constraints of this dissertation. For this (chapter 2) manuscript, I conducted the data acquisition, data analysis, and writing; Alec Chan-Golston (co-author) advised on statistical methods; Jason Su (co-author) provided land-use regression products, from a previous paper, for NO<sub>2</sub> exposure attribution. Co-authors Yifang Zhu and Jonathan Liu provided expert advice throughout the project and assisted in editing the paper. Michael Jerrett (co-author) was principal investigator of the project and guided overall research.

Chapter 3 is a manuscript in preparation for submission in summer 2022. Data was collected from PASTA-LA participants with the help of Christina Batteate. Pierfrancesco Alaimo di Loro and Marco Mingione cleaned and interpolated the device data so that it could be used for subsequent analysis (Alaimo et al., 2021); Owen Hall assisted in coding analyses, specifically the

automation of analyses involving Google Earth Engine; Rachel Connolly advised on the creation of satellite-derived vegetation layer; Sudipto Banerjee and Alec Chan-Golston advised on statistical and modeling methods; Ellen Do helped clean device and questionnaire data; and Michael Jerrett aided in research design, management and manuscript editing.

Chapter 4 is also a manuscript in preparation for submission in summer 2022. This manuscript uses similar data and analyses compared to Chapter 3. The responsibilities of my collaborators were, therefore, the same.

## VITA

### EDUCATION

- 2014–2015 MSc, Public Health | London School of Hygiene and Tropical Medicine  
2011–2013 Post-baccalaureate, Pre-Health | New York University  
2005–2010 BA, Geography | University of California-Berkeley

### AWARDS & HONORS

- 2017 Student Pilot Project Award, National Institute of Occupational Safety & Health-Southern California Education & Research Center (NIOSH SC-ERC)  
2017 Voted “Favorite Environmental Health Teaching Assistant”

### ACADEMIC POSITIONS

- 2015–2021 Graduate Student Researcher | UCLA, Fielding School of Public Health  
2016–2019 Teaching Associate | UCLA  
2014 Spatial Data Analyst | NYC Department of Health and Mental Hygiene  
2012–2014 Geospatial Consultant/Research Assistant | Berkeley, CA and Limpopo, S. Africa  
Center for Environmental Research and Children's Health (CERCH)  
2007–2010 Research Assistant/Geospatial Analyst | Berkeley Lab, Berkeley, CA  
2011–2014 Research Consultant/Spatial Analyst | UC, Berkeley, Berkeley, CA  
2009–2011 Research Assistant/Geospatial Analyst | UC, Berkeley, Berkeley, CA

### PEER-REVIEWED PUBLICATIONS

- Oroumijeh, F., Jerrett, M., Del Rosario, I., **Lipsitt, J.**, Liu, J., Paulson, S. E., Ritz, B., Schauer, J. J., Shafer, M. M., & Shen, J. 2022. Elemental composition of fine and coarse particles across the greater Los Angeles area: Spatial variation and contributing sources. *Environmental Pollution*, 292, 118356.
- **Lipsitt, J.**, Chan-Golston, A. M., Liu, J., Su, J., Zhu, Y., & Jerrett, M. 2021. Spatial analysis of COVID-19 and traffic-related air pollution in Los Angeles. *Environment International*. Available online only.

- Di Loro, P. A., Mingione, M., **Lipsitt, J.**, Batteate, C. M., Jerrett, M., & Banerjee, S. 2021. Bayesian hierarchical modeling and analysis for physical activity trajectories using actigraph data. *ArXiv Preprint ArXiv:2101.01624*.
- Liu, J., **Lipsitt, J.**, Jerrett, M., & Zhu, Y. 2020. Decreases in Near-Road NO and NO<sub>2</sub> Concentrations during the COVID-19 Pandemic in California. *Environmental Science & Technology Letters*, 8(2), 161–167.
- Gaspar, F. W., Chevrier, J., Quirós-Alcalá, L., **Lipsitt, J. M.**, Barr, D. B., Holland, N., Bornman, R., & Eskenazi, B. 2017. Levels and determinants of DDT and DDE exposure in the VHEMBE cohort. *Environmental Health Perspectives*, 125(7), 077006.
- Su, J. G., Apte, J. S., **Lipsitt, J.**, Garcia-Gonzales, D. A., Beckerman, B. S., de Nazelle, A., Texcalac-Sangrador, J. L., & Jerrett, M. 2015. Populations potentially exposed to traffic-related air pollution in seven world cities. *Environment International*, 78, 82–89.
- Eskenazi, B., Quirós-Alcalá, L., **Lipsitt, J. M.**, Wu, L. D., Kruger, P., Ntimbane, T., Nawn, J. B., Bornman, M. R., & Seto, E. 2014. mSpray: A mobile phone technology to improve malaria control efforts and monitor human exposure to malaria control pesticides in Limpopo, South Africa. *Environment International*, 68, 219–226.
- Jarjour, S., Jerrett, M., Westerdahl, D., de Nazelle, A., Hanning, C., Daly, L., **Lipsitt, J.**, & Balmes, J. 2013. Cyclist route choice, traffic-related air pollution, and lung function: A scripted exposure study. *Environmental Health*, 12(1), 1–12.

## SELECTION OF PRESENTATIONS

- “Global Positioning System (GPS) Assessments of Green Space Exposure and Use” International Society of Exposure Science Conference, Online, Oral Presentation. Oakland, CA, September 2021.
- “Research Training Seminar: A Methodology for Selecting Air Monitoring Locations for Measuring Brake and Tire Wear Emissions” California Air Resources Board (CARB), Online, Oral Presentation. Sacramento, CA, June 2021
- “Traffic-Related Air Pollution Exposure and COVID-19 Case-Fatality in Los Angeles Neighborhoods: A Spatial Approach” University of California-Merced COVID-19 Seminar Series, Online, Oral Presentation. Merced, CA, October 2020.

# CHAPTER 1: INTRODUCTION AND OVERVIEW OF THE ORGANIZATION OF THE DISSERTATION

## 1.1 OVERVIEW

'Big data' is getting bigger, but it also provides many new opportunities for application in the field of Public Health. Not too long ago, utilizing datasets involving millions of observations required teams of analysts and thousands of dollars in computing hardware and software. Now datasets often include exponentially more observations and are significantly more complex. Many 'big data' datasets, however, can now be processed more quickly and for less cost. Cloud computing has allowed better access to previously cost-restrictive hardware.

According to a review of 'big data' in Public Health, investigators identified five measurement-type data utilized for research: (1) biological (e.g., genomics), (2) contextual (e.g., descriptors of spatial surroundings), (3) administratively-collected (e.g., census data), (4) rapidly-automated (e.g., GPS data), and (5) electronically-compiled data (e.g., data from social media) (Mooney and Pejaver, 2018). These data types can be even more useful in combination. For example, (2) contextual and (4) rapidly-automated information can be combined to describe momentary exposure.

Public Health data often come from multiple sources, in multiple formats, and are reported for regions or time periods that do not overlap, leading to challenges when combining these disparate and possibly non-interoperable datasets for research purposes. Aggregation is often used to combine the disparate data into one spatiotemporal scale for the purposes of subsequent statistical analyses. Spatial aggregation of misaligned areal datasets can, however, lead to areal unit problems, where individuals or values are assigned to more than one location. Furthermore, aggregation of misaligned exposure (gridded) datasets can lead to exposure misclassification.

This dissertation presents three case studies in which we demonstrate advancements in geospatial methods to account for spatiotemporal misalignment. We utilize contemporary geospatial methods for context or exposure quantification from spatiotemporally misaligned ‘big data’ datasets. In **Chapter 2**, COVID-19 was studied at a small-area population level, but the data utilized were from misaligned geographies—neighborhoods and census-tracts. The methods in this chapter demonstrate the use of residential building footprints to better aggregate these areal datasets. In **Chapter 3**, we were interested in evaluating methods used to quantify green-space exposure for individuals engaged in physical activity. We demonstrate multiple methods for using misaligned contextual (green space) data, rapidly-automated (GPS, accelerometer, and smartphone) data, and electronically compiled (online questionnaire) data for attributing green space exposure to study participants based on their location and activity level. In **Chapter 4**, we were interested in examining how choices in the geospatial methods used for exposure attribution (i.e., presented in Chapter 3) could impact the results from exposure assessment health studies. We investigated the association between heat exposure (another misaligned contextual measurement) and physical activity as modified by green space exposure, and demonstrated how these different methods choices impacted results.

## 1.2 SUMMARY OF AIMS

This dissertation aims to assess GIS methods for combining misaligned datasets for use in Environmental Health Sciences. This is achieved by demonstrating methods used in three case studies. In **Chapter 2**, we use spatial aggregation to account for data misalignment in our assessment of the association between air pollution and COVID-19. In **Chapter 3**, we compare multiple GIS methods for quantifying exposure within regions of physically active behavior by using activity and location data. And in **Chapter 4**, we demonstrate how these GIS exposure attribution methods are used in the study of the association of daily heat exposure and physical

activity. In these case studies (**Chapters 2-4**) the dissertation aims to demonstrate how GIS can be used to avoid variable and exposure misclassification. These methods build on previous methods by taking advantage of advancements in software, hardware and data availability. Specifically, we aim to add to previous investigation of activity spaces and aim to develop new methods for the assessment of exposure within *physical* activity spaces. The work presented may guide future health research efforts and offers discussion on how previous research may have been impacted by choices in GIS method.

### **1.3 RESEARCH SETTING**

All three research chapters (**Chapters 2-4**) involve research situated in Los Angeles (LA) County. The population size of LA County is 10.0 million, spread across 4,057 square miles or 10,508 square kilometers (US Census Bureau, 2020). LA County is racially, ethnically, and socioeconomically diverse (51% White, 48% Latino, 15% Asian, and 8.3% Black) with a median income of approximately \$64,000 dollars. LA County is comprised of 88 incorporated cities with separate city councils (Los Angeles County, 2018), each city council conducts its own land use and urban planning.

LA County has considerable urban development and sprawl, with 38% of land considered impervious surface (e.g., concrete). This includes 21,825 miles of roads comprising 514 miles of interstates and freeways, 4,819 miles of high-capacity arterial roads, and 16,489 miles of lower-capacity local roads (Caltrans, 2020). LA County has 10 of the top 25 most trafficked expressways in the US (by annual average daily traffic) (Federal Highway Administration, 2019). In 2018, the American Community Survey (US Census Bureau, 2018) showed that 78% of commuters in LA County used single-occupancy vehicles (drove alone), 10% used carpools, 6% used public transit, and less than 6% used forms of active transport (such as walking and biking) (Federico et al., 2017).

LA County, however, also has a growing patchwork of mobility infrastructure (e.g., bike lanes, pedestrian walkways, e-scooters rentals); and numerous green spaces (e.g., local and state parks, playgrounds, and beaches). The *County of Los Angeles: Bicycle Master Plan*, implemented in March 2012, included intentions to add over 800 miles of bicycle infrastructure by 2032 to the already existing 144 miles (Los Angeles County, 2012). The built and natural environments of LA are also designed for recreation, with 34% of the total land in LA County considered protected, including over 1,602 local parks such as Griffith Park—the largest urban park in the United States (Los Angeles County, 2018). In 2019, under the direction of Mayor Garcetti, the City of Los Angeles began to implement its “Green New Deal” sustainable city plan to improve its communities, targeting (to name a few) environmental justice, healthy buildings, active and public transit, air and water quality improvements, and quality green-space initiatives (Garcetti, 2019).

#### **1.4 AREAL MISALIGNMENT IN AN INVESTIGATION OF COVID-19 AND TRAFFIC-RELATED AIR POLLUTION**

As of May 21<sup>st</sup>, 2022, there have been 2.9 million confirmed cases of COVID-19 in LA County, the most of any county in California—with 29,000 cases confirmed per 100,000 people (Mayo Clinic, 2022). Although COVID-19 has been heavily researched, continued investigation is needed to determine how exposure risk factors may impact the disease. **Chapter 2** includes an investigation of the association between NO<sub>2</sub> exposure and COVID-19 incidence, mortality, and case-fatality rates.

NO<sub>2</sub> is a gaseous pollutant that serves as a marker for traffic-related air pollution (TRAP) and demonstrates considerable intra-urban variation, especially in LA County (Su et al., 2020, 2009; Zeldovich, 2015). Current literature suggests that exposure to TRAP is associated with respiratory morbidities and all-cause mortality (Bai et al., 2018; Dales et al., 2008; Franklin et al., 2015; Jerrett et al., 2008, 2005a; Sydbom et al., 2001). Emerging literature has reported an

association between NO<sub>2</sub> (Liang et al., 2020b; Xiao Wu et al., 2020a) and COVID-19 outcomes, but only a few studies, as of yet, have conducted small-area analyses. For the first period of COVID-19, area-based aggregate counts of COVID-19 outcomes were the best-available data for researchers (Liang et al., 2020b; Xiao Wu et al., 2020a). As COVID-19 outcome data has become more available, other studies have been able to use individual-level outcomes (Yu et al., 2022). These small-area studies are important because reductions in spatiotemporal misalignment may reduce possibility of misclassification when the exposure being measured has high spatial variability (i.e., traffic-related air pollution, green space) (Apte et al., 2017; Ma et al., 2020).

In **Chapter 2**, we used annual air pollution surfaces derived from land-use regression products (Su et al., 2020), which have a spatial resolution of 30 meters, COVID-19 cases and deaths reported at the neighborhood level, and demographic data reported by census tract. Neighborhoods and census tracts intersect, i.e., census tracts may overlap with multiple neighborhoods and neighborhoods may overlap with multiple tracts. The intention was to not count populations more than once, so population-level covariates from both tracts and neighborhoods were aggregated into one unified geography. In this Chapter, we used neighborhoods because they included the main outcome (COVID-19 case and death counts).

To account for misalignment among geographies, most studies have used areal densities to aggregate partial counts between partial geographies (Auchincloss et al., 2009; Gething et al., 2006). This aggregation technique can be problematic for geographies with substantial variability in population density (e.g., census tracts with both urban centers and rural suburbs). We demonstrate a method using residential building footprints (Holt et al., 2013) as an intermediate aggregation geography for dealing with the misalignment between where people live and the mapped area used to describe them.

In **Chapter 2**, we studied the relationship between TRAP exposure and COVID-19 outcomes and compared the results from three adjusted models: a zero-inflated Poisson model; a zero-inflated negative binomial model; and a conditional auto-regressive Poisson model (that accounts for spatial variability). Discussion of spatial methods utilized, including data aggregation and modeling methods, may inform similar research involving spatiotemporally misaligned data.

## **1.5 SPATIOTEMPORALLY MISALIGNED DATA IN A COMPARISON OF PHYSICAL ACTIVITY SPACE METHODS FOR GREEN SPACE EXPOSURE ATTRIBUTION**

The built and natural environments heavily impact an individual's environmental exposures and their level of physical activity; however, measuring or quantifying the spatial context of activity can be challenging (Bowler et al., 2010b; Smith et al., 2017; Twohig-Bennett and Jones, 2018). Spatial context is most accurately quantified using repeated measurements of location and activity due to the natural mobility of most individuals (Almanza et al., 2012). The study of physical activity has benefited greatly from advancements in location and activity tracking technologies—specifically geographic positioning system (GPS) and accelerometry-based sensor devices (Dons et al., 2015; Ku et al., 2018; Lee and Kwan, 2018; Trifan et al., 2019). Wearable devices, including smartphones, smartwatches, and research-grade devices, have made individual tracking easier and cheaper—allowing for more complete snap shots of location and activity. Over 85% of American adults now own smartphones (Perrin, 2021), which have gyroscopes, accelerometers, and GPS sensors—all used for measuring location and activity (Lane et al., 2010; Shoaib et al., 2014). Whereas previous exposure attribution methods may have used only the home location to describe context (Dadvand et al., 2015; Olsen et al., 2019), these wearable sensors allow for continuous tracking and exposure assessment. Although many studies have discussed incomplete exposure limitations when using home location to assign context or exposure for daily activity, few studies have investigated alternative assessment

methods and fewer have quantified differences in context or exposure assigned (Holliday et al., 2017).

In **Chapter 3**, we utilized tracking data from the Physical Activity through Sustainable Transport Approaches in Los Angeles (PASTA-LA) study. Participants were equipped with Actigraph accelerometers, GlobalSat GPSs, and the MOVES smartphone app to assess location and activity and infer context. Actigraph and GlobalSat are commonly used for research purposes (Dunton et al., 2014), while the MOVES app, which has been less-commonly utilized (Donaire-Gonzalez et al., 2013; Kooiman et al., 2015), was included to investigate the efficacy of using a cheaper, commercially available smartphone option. To compare these data, methods accounting for spatiotemporal misalignments were needed as Actigraph accelerometers measure momentary acceleration at an epoch of 10 seconds, GlobalSats measures location at an epoch of 15 seconds, and the MOVES app recorded data at a variable epoch (between 5 seconds and over 6 hours), depending on a proprietary battery-conserving feature. Interpolation methods, data cleaning, and spatial aggregation were used to create overlapping datasets in both time and space. When combined with data describing the natural or built environment, these wearable sensors can be used to describe the context for regions of activity. In this study, we were interested in regions of moderate-to-vigorous levels of physical activity (MVPA), defined using GPS and accelerometry outcomes. We constructed these physical activity spaces (PASs), using seven discrete polygon-drawing approaches, and used them to quantify environmental context for study participants.

Green space exposure was assigned to each PAS to demonstrate methods for environmental context or exposure quantification. Exposure to green space has been demonstrated to benefit human health (Almanza et al., 2012; Bowler et al., 2010a; Wolch et al., 2014a), but there is little scientific agreement on the best practices for attributing exposure to green space (McCrorie et al., 2014). **Chapter 3** presents a comprehensive assessments of

geospatial methods for green space exposure attribution—possibly the only assessment for green space exposure attribution for physically-active regions (PASs). This study demonstrates how the selection between multiple geospatial methods may influence numerical quantification of context (green space) due to differences in spatiotemporal misalignment and limitations of each method. We compared and contrast the various PAS methods used and compare them the commonly used standard for exposure attribution using home addresses. Home addresses with circular buffers are commonly used for exposure attribution (Amoly et al., 2015; Dadvand et al., 2015; van den Berg et al., 2010). Our results may impact future decisions that researchers make regarding geospatial method selection and may help minimize exposure misclassification by allowing researchers better comparisons of best practices.

## **1.6 SPATIOTEMPORALLY MISALIGNED DATA METHODS IN THE ASSESSMENT OF PHYSICAL ACTIVITY, HEAT, AND GREEN SPACE**

Studies of heat and green space exposure have been limited by the availability of activity- and location-tracking data and have often used home location to attribute daily exposure (Amoly et al., 2015; Dadvand et al., 2015, 2012b; Dzhambov et al., 2018; Fuertes et al., 2016; Klompaker et al., 2018; Laurent et al., 2013). For the average US adult, more than half of daily activity is spent outside the home (U.S. Department of Labor, 2021); therefore, when studying physical activity, repeated measures of activity and location allow for better assessment of daily exposure. Methods to account for spatiotemporal misalignment of the combined tracking and exposure datasets should be considered in order to not introduce exposure misclassification.

Due to climate change, daily temperatures in Los Angeles are likely to increase with the number of days exceeding 35°C (95° Fahrenheit) to increase from six, observed in 2015, to 54, projected for 2100 (Sun et al., 2015). Although increases in extreme heat are expected to reduce physical activity rates (Stamatakis et al., 2013) and increase excess mortality (Hayhoe et al., 2004), moderate increases in daily temperature are potentially associated with increased physical

activity (Obradovich and Fowler, 2017). Furthermore, these changes in active behavior due to heat exposure may be modified by access to green spaces (Chan et al., 2006; Ho et al., 2021).

In **Chapter 4**, we demonstrated how geospatial methods can be applied to activity and location tracking data to assess the relationship of heat exposure on physical activity and the effect modification by green space. We utilized the data produced and cleaned in **Chapter 3**, and in addition, implemented physical activity space (PAS) polygons to extract meteorological surfaces derived from satellite and ground-based sensor data. These extracted raster means were used to describe areal means of daily maximum temperature and green space (normalized difference vegetation index, NDVI). We used 1,000-meter daily temperature rasters from the Daymet, version 4 product, which was interpolated from ground sensors (Oak Ridge National Laboratory and NASA, 2022; Thornton et al., 2020); and 60-centimeter annual NDVI rasters, derived from the U.S. Department of Agriculture's National Agriculture Imagery Program (USDA NAIP) multispectral images (USDA NAIP GeoHub, 2022). Given the difference in spatial and temporal resolutions between the temperature data and the green space data, exposure misclassification was likely when extracting raster means by the same PASs; however, as is shown in **Chapter 3**, the potential for misclassification was substantially reduced by using PAS polygons to quantify exposure compared to using home location buffers. **Chapter 4** demonstrated how choices in methodology for attributing heat and green space exposure (as well as choices in method to quantify minutes of MVPA) can impact models of association when investigating the relationship between heat exposure and daily MVPA, as modified by exposure to green space.

**Chapters 3 and 4**, combined, offer a framework for selecting geospatial methods intended to assess these or similar environmental factors influencing momentary behavior. From data collection to modeling, with regards to geospatial methods, certain choices are more impactful on

results than others, so conclusions are meant to assist future researchers in prioritizing research protocols.

## 1.7 REFERENCES FOR CHAPTER 1

- Almanza, E., Jerrett, M., Dunton, G., Seto, E., Ann Pentz, M., 2012. A study of community design, greenness, and physical activity in children using satellite, GPS and accelerometer data. *Health Place* 18, 46–54. <https://doi.org/10.1016/j.healthplace.2011.09.003>
- Amoly, E., Dadvand, P., Fornas, J., López-Vicente, M., Basagaña, X., Julvez, J., Alvarez-Pedrerol, M., Nieuwenhuijsen, M.J., Sunyer, J., 2015. Green and blue spaces and behavioral development in barcelona schoolchildren: The BREATHE project. *Environ. Health Perspect.* 122. <https://doi.org/10.1289/ehp.1408215>
- Apte, J.S., Messier, K.P., Gani, S., Brauer, M., Kirchstetter, T.W., Lunden, M.M., Marshall, J.D., Portier, C.J., Vermeulen, R.C.H., Hamburg, S.P., 2017. High-Resolution Air Pollution Mapping with Google Street View Cars: Exploiting Big Data. *Environ. Sci. Technol.* 51. <https://doi.org/10.1021/acs.est.7b00891>
- Auchincloss, A.H., Diez Roux, A. V, Mujahid, M.S., Shen, M., Bertoni, A.G., Carnethon, M.R., 2009. Neighborhood resources for physical activity and healthy foods and incidence of type 2 diabetes mellitus: the Multi-Ethnic study of Atherosclerosis. *Arch. Intern. Med.* 169, 1698–1704. <https://doi.org/10.1001/archinternmed.2009.302>
- Bai, L., Chen, H., Hatzopoulou, M., Jerrett, M., Kwong, J.C., Burnett, R.T., Van Donkelaar, A., Copes, R., Martin, R. V., Van Ryswyk, K., Lu, H., Kopp, A., Weichenthal, S., 2018. Exposure to ambient ultrafine particles and nitrogen dioxide and incident hypertension and diabetes. *Epidemiology* 29. <https://doi.org/10.1097/EDE.0000000000000798>
- Bowler, D.E., Buyung-Ali, L., Knight, T.M., Pullin, A.S., 2010a. Urban greening to cool towns and cities: A systematic review of the empirical evidence. *Landsc. Urban Plan.* <https://doi.org/10.1016/j.landurbplan.2010.05.006>
- Bowler, D.E., Buyung-Ali, L.M., Knight, T.M., Pullin, A.S., 2010b. A systematic review of evidence for the added benefits to health of exposure to natural environments. *BMC Public Health* 10. <https://doi.org/10.1186/1471-2458-10-456>
- Caltrans, 2020. Highway Performance Monitoring System (HPMS) Data [WWW Document]. URL <https://dot.ca.gov/programs/research-innovation-system-information/highway-performance-monitoring-system> (accessed 5.2.22).
- Chan, C.B., Ryan, D.A.J., Tudor-Locke, C., 2006. Relationship between objective measures of physical activity and weather: A longitudinal study. *Int. J. Behav. Nutr. Phys. Act.* 3, 1–9. <https://doi.org/10.1186/1479-5868-3-21/FIGURES/2>
- Dadvand, P., de Nazelle, A., Triguero-Mas, M., Schembari, A., Cirach, M., Amoly, E., Figueras,

- F., Basagaña, X., Ostro, B., Nieuwenhuijsen, M., 2012. Surrounding greenness and exposure to air pollution during pregnancy: An analysis of personal monitoring data. *Environ. Health Perspect.* 120. <https://doi.org/10.1289/ehp.1104609>
- Dadvand, P., Villanueva, C.M., Font-Ribera, L., Martinez, D., Basagaña, X., Belmonte, J., Vrijheid, M., Gražulevičienė, R., Kogevinas, M., Nieuwenhuijsen, M.J., 2015. Risks and benefits of green spaces for children: A cross-sectional study of associations with sedentary behavior, obesity, asthma, and allergy. *Environ. Health Perspect.* 122. <https://doi.org/10.1289/ehp.1308038>
- Dales, R., Wheeler, A., Mahmud, M., Frescura, A.M., Smith-Doiron, M., Nethery, E., Liu, L., 2008. The Influence of Living Near Roadways on Spirometry and Exhaled Nitric Oxide in Elementary Schoolchildren. *Environ. Health Perspect.* 116, 1423–1427. <https://doi.org/10.1289/ehp.10943>
- Donaire-Gonzalez, D., de Nazelle, A., Seto, E., Mendez, M., Nieuwenhuijsen, M.J., Jerrett, M., 2013. Comparison of Physical Activity Measures Using Mobile Phone-Based CalFit and Actigraph. *J. Med. Internet Res.* 15, e111. <https://doi.org/10.2196/jmir.2470>
- Dons, E., Götschi, T., Nieuwenhuijsen, M., De Nazelle, A., Anaya, E., Avila-Palencia, I., Brand, C., Cole-Hunter, T., Gaupp-Berghausen, M., Kahlmeier, S., Laeremans, M., Mueller, N., Orjuela, J.P., Raser, E., Rojas-Rueda, D., Standaert, A., Stigell, E., Uhlmann, T., Gerike, R., Int Panis, L., 2015. Physical Activity through Sustainable Transport Approaches (PASTA): protocol for a multi-centre, longitudinal study Energy balance-related behaviours. *BMC Public Health* 15. <https://doi.org/10.1186/s12889-015-2453-3>
- Dunton, G.F., Almanza, E., Jerrett, M., Wolch, J., Pentz, M.A., 2014. Neighborhood park use by children: Use of accelerometry and global positioning systems. *Am. J. Prev. Med.* 46. <https://doi.org/10.1016/j.amepre.2013.10.009>
- Dzhambov, A., Hartig, T., Markevych, I., Tilov, B., Dimitrova, D., 2018. Urban residential greenspace and mental health in youth: Different approaches to testing multiple pathways yield different conclusions. *Environ. Res.* 160. <https://doi.org/10.1016/j.envres.2017.09.015>
- Federal Highway Administration, 2019. FHWA Office of Highway Policy Information Fact Sheet: The 25 Most Traveled Route Locations by Annual Daily Traffic (AADT) [WWW Document]. URL <https://www.fhwa.dot.gov/policyinformation/tables/02.cfm> (accessed 5.2.22).
- Federico, F., Rauser, C., Gold, M., 2017. 2017 Sustainable LA Grand Challenge Environmental Report Card for Los Angeles County Energy and Air Quality [WWW Document]. Univ. Calif. Escholarsh. URL <https://escholarship.org/uc/item/6xj45381> (accessed 5.2.22).
- Franklin, B.A., Brook, R., Arden Pope, C. 3rd, 2015. Air pollution and cardiovascular disease.

- Curr. Probl. Cardiol. 40, 207–238. <https://doi.org/10.1016/j.cpcardiol.2015.01.003>
- Fuertes, E., Markevych, I., Bowatte, G., Gruzieva, O., Gehring, U., Becker, A., Berdel, D., von Berg, A., Bergström, A., Brauer, M., Brunekreef, B., Brüske, I., Carlsten, C., Chan-Yeung, M., Dharmage, S.C., Hoffmann, B., Klümper, C., Koppelman, G.H., Kozyrskyj, A., Korek, M., Kull, I., Lodge, C., Lowe, A., MacIntyre, E., Pershagen, G., Standl, M., Sugiri, D., Wijga, A., Heinrich, J., 2016. Residential greenness is differentially associated with childhood allergic rhinitis and aeroallergen sensitization in seven birth cohorts. *Allergy Eur. J. Allergy Clin. Immunol.* 71. <https://doi.org/10.1111/all.12915>
- Garcetti, E., 2019. L.A.'s Green New Deal: Sustainable City Plan 2019. Los Angeles.
- Gething, P.W., Noor, A.M., Gikandi, P.W., Ogara, E.A.A., Hay, S.I., Nixon, M.S., Snow, R.W., Atkinson, P.M., 2006. Improving imperfect data from health management information systems in Africa using space-time geostatistics. *PLoS Med.* 3. <https://doi.org/10.1371/journal.pmed.0030271>
- Hayhoe, K., Cayan, D., Field, C.B., Frumhoff, P.C., Maurer, E.P., Miller, N.L., Moser, S.C., Schneider, S.H., Cahill, K.N., Cleland, E.E., Dale, L., Drapek, R., Hanemann, R.M., Kalkstein, L.S., Lenihan, J., Lunch, C.K., Neilson, R.P., Sheridan, S.C., Verville, J.H., 2004. Emissions pathways, climate change, and impacts on California. *Proc. Natl. Acad. Sci. U. S. A.* 101, 12422–12427. [https://doi.org/10.1073/PNAS.0404500101/SUPPL\\_FILE/04500FIG17.JPG](https://doi.org/10.1073/PNAS.0404500101/SUPPL_FILE/04500FIG17.JPG)
- Ho, J.Y., Zijlema, W.L., Triguero-Mas, M., Donaire-Gonzalez, D., Valentín, A., Ballester, J., Chan, E.Y.Y., Goggins, W.B., Mo, P.K.H., Kruize, H., van den Berg, M., Gražuleviciene, R., Gidlow, C.J., Jerrett, M., Seto, E.Y.W., Barrera-Gómez, J., Nieuwenhuijsen, M.J., 2021. Does surrounding greenness moderate the relationship between apparent temperature and physical activity? Findings from the PHENOTYPE project. *Environ. Res.* 197, 110992. <https://doi.org/10.1016/J.ENVRES.2021.110992>
- Holliday, K.M., Howard, A.G., Emch, M., Rodríguez, D.A., Evenson, K.R., 2017. Are buffers around home representative of physical activity spaces among adults? *Heal. Place* 45, 181–188. <https://doi.org/10.1016/j.healthplace.2017.03.013>
- Holt, J.B., Lo, C.P., Hodler, T.W., 2013. Dasymetric Estimation of Population Density and Areal Interpolation of Census Data. <http://dx.doi.org/10.1559/1523040041649407> 31, 103–121. <https://doi.org/10.1559/1523040041649407>
- Jerrett, M., Arain, A., Kanaroglou, P., Beckerman, B., Potoglou, D., Sahuvaroglu, T., Morrison, J., Giovis, C., 2005. A review and evaluation of intraurban air pollution exposure models. *J. Expo. Anal. Environ. Epidemiol.* <https://doi.org/10.1038/sj.jea.7500388>

- Jerrett, M., Shankardass, K., Berhane, K., Gauderman, W.J., Künzli, N., Avol, E., Gilliland, F., Lurmann, F., Molitor, J.N., Molitor, J.T., Thomas, D.C., Peters, J., McConnell, R., 2008. Traffic-related air pollution and asthma onset in children: A prospective cohort study with individual exposure measurement. *Environ. Health Perspect.* 116, 1433–1438. <https://doi.org/10.1289/ehp.10968>
- Klompaker, J.O., Hoek, G., Bloemsma, L.D., Gehring, U., Strak, M., Wijga, A.H., van den Brink, C., Brunekreef, B., Lebret, E., Janssen, N.A.H., 2018. Green space definition affects associations of green space with overweight and physical activity. *Environ. Res.* 160, 531–540. <https://doi.org/10.1016/J.ENVRES.2017.10.027>
- Koorman, T.J.M., Dontje, M.L., Sprenger, S.R., Krijnen, W.P., van der Schans, C.P., de Groot, M., 2015. Reliability and validity of ten consumer activity trackers. *BMC Sports Sci. Med. Rehabil.* 7, 24. <https://doi.org/10.1186/s13102-015-0018-5>
- Ku, P.W., Steptoe, A., Liao, Y., Sun, W.J., Chen, L.J., 2018. Prospective relationship between objectively measured light physical activity and depressive symptoms in later life. *Int. J. Geriatr. Psychiatry* 33. <https://doi.org/10.1002/gps.4672>
- Lane, N., Miluzzo, E., Lu, H., Peebles, D., Choudhury, T., Campbell, A., 2010. A survey of mobile phone sensing. *IEEE Commun. Mag.* 48, 140–150. <https://doi.org/10.1109/MCOM.2010.5560598>
- Laurent, O., Wu, J., Li, L., Milesi, C., 2013. Green spaces and pregnancy outcomes in Southern California. *Heal. Place* 24. <https://doi.org/10.1016/j.healthplace.2013.09.016>
- Lee, K., Kwan, M.P., 2018. Physical activity classification in free-living conditions using smartphone accelerometer data and exploration of predicted results. *Comput. Environ. Urban Syst.* 67. <https://doi.org/10.1016/j.compenvurbsys.2017.09.012>
- Liang, D., Shi, L., Zhao, J., Liu, P., Schwartz, J., Gao, S., Sarnat, J., Liu, Y., Ebel, S., Scovronick, N., Chang, H.H., 2020. Urban Air Pollution May Enhance COVID-19 Case-Fatality and Mortality Rates in the United States. *medRxiv Prepr. Serv. Heal. Sci.* <https://doi.org/10.1101/2020.05.04.20090746>
- Los Angeles County, 2018. LA County: Our County - Landscapes and Ecosystems [WWW Document]. Our Cty. Landscapes Ecosyst. Brief. URL [https://ourcountyla.lacounty.gov/wp-content/uploads/2018/10/Our-County-Landscapes-and-Ecosystems-Briefing\\_For-Web.pdf](https://ourcountyla.lacounty.gov/wp-content/uploads/2018/10/Our-County-Landscapes-and-Ecosystems-Briefing_For-Web.pdf) (accessed 5.2.22).
- Los Angeles County, 2012. County of Los Angeles: Bicycle Master Plan, Final Plan.
- Ma, X., Longley, I., Gao, J., Salmond, J., 2020. Assessing schoolchildren's exposure to air pollution during the daily commute - A systematic review. *Sci. Total Environ.* 737, 140389.

<https://doi.org/10.1016/J.SCITOTENV.2020.140389>

- Mayo Clinic, 2022. California COVID-19 Map: Tracking the Trends [WWW Document]. URL <https://www.mayoclinic.org/coronavirus-covid-19/map/california> (accessed 5.23.22).
- McCrorie, P.R., Fenton, C., Ellaway, A., 2014. Combining GPS, GIS, and accelerometry to explore the physical activity and environment relationship in children and young people - a review. *Int. J. Behav. Nutr. Phys. Act.* 11. <https://doi.org/10.1186/s12966-014-0093-0>
- Mooney, S.J., Pejaver, V., 2018. Big Data in Public Health: Terminology, Machine Learning, and Privacy. <https://doi.org/10.1146/annurev-publhealth-040617-014208> 39, 95–112. <https://doi.org/10.1146/ANNUREV-PUBLHEALTH-040617-014208>
- Oak Ridge National Laboratory, NASA, 2022. Daymet V4: Daily Surface Weather and Climatological Summaries [WWW Document]. URL <https://daymet.ornl.gov/> (accessed 5.15.22).
- Obradovich, N., Fowler, J.H., 2017. Climate change may alter human physical activity patterns. *Nat. Hum. Behav.* 2017 15 1, 1–7. <https://doi.org/10.1038/s41562-017-0097>
- Olsen, J.R., Mitchell, R., McCrorie, P., Ellaway, A., 2019. Children’s mobility and environmental exposures in urban landscapes: A cross-sectional study of 10–11 year old Scottish children. *Soc. Sci. Med.* 224, 11–22. <https://doi.org/10.1016/j.socscimed.2019.01.047>
- Perrin, A., 2021. Mobile technology and home broadband 2021. *Mob. Technol. Home Broadband* 1–26.
- Shoaib, M., Bosch, S., Durmaz Incel, O., Scholten, H., Havinga, P.J.M., 2014. Fusion of smartphone motion sensors for physical activity recognition. *Sensors (Switzerland)* 14. <https://doi.org/10.3390/s140610146>
- Smith, M., Hosking, J., Woodward, A., Witten, K., MacMillan, A., Field, A., Baas, P., Mackie, H., 2017. Systematic literature review of built environment effects on physical activity and active transport - an update and new findings on health equity. *Int. J. Behav. Nutr. Phys. Act.* 14. <https://doi.org/10.1186/s12966-017-0613-9>
- Stamatakis, E., Nnoaham, K., Foster, C., Scarborough, P., 2013. The Influence of Global Heating on Discretionary Physical Activity: An Important and Overlooked Consequence of Climate Change. *J. Phys. Act. Heal.* 10, 765–768. <https://doi.org/10.1123/jpah.10.6.765>
- Su, J.G., Jerrett, M., Beckerman, B., Wilhelm, M., Ghosh, J.K., Ritz, B.R., 2009. Predicting traffic-related air pollution in Los Angeles using a distance decay regression selection strategy. *Environ. Res.* 109, 657–670. <https://doi.org/10.1016/j.envres.2009.06.001>
- Su, J.G., Meng, Y.-Y., Chen, X., Molitor, J., Yue, D., Jerrett, M., 2020. Predicting differential improvements in annual pollutant concentrations and exposures for regulatory policy

- assessment. Environ. Int. 143, 105942.  
<https://doi.org/https://doi.org/10.1016/j.envint.2020.105942>
- Sun, F., Walton, D.B., Hall, A., 2015. A Hybrid Dynamical–Statistical Downscaling Technique. Part II: End-of-Century Warming Projections Predict a New Climate State in the Los Angeles Region. *J. Clim.* 28, 4618–4636. <https://doi.org/10.1175/JCLI-D-14-00197.1>
- Sydbom, A., Blomberg, A., Parnia, S., Stenfors, N., Sandström, T., Dahlén, S.-E., 2001. Health effects of diesel exhaust emissions. *Eur. Respir. J.* 17, 733 LP – 746.
- Thornton, M.M., Shrestha, R., Wei, Y., Thornton, P.E., Kao, S., Wilson, B.E., 2020. Daymet: Daily Surface Weather Data on a 1-km Grid for North America, Version 4. <https://doi.org/10.3334/ORNLDAAAC/1840>
- Trifan, A., Oliveira, M., Oliveira, J.L., 2019. Passive sensing of health outcomes through smartphones: Systematic review of current solutions and possible limitations. *JMIR mHealth uHealth* 7. <https://doi.org/10.2196/12649>
- Twohig-Bennett, C., Jones, A., 2018. The health benefits of the great outdoors: A systematic review and meta-analysis of greenspace exposure and health outcomes. *Environ. Res.* 166. <https://doi.org/10.1016/j.envres.2018.06.030>
- U.S. Department of Labor, 2021. AMERICAN TIME USE SURVEY — MAY TO DECEMBER 2019 AND 2020 RESULTS [WWW Document]. News Release, Bur. Labor Stat. URL [www.bls.gov/tus](http://www.bls.gov/tus) (accessed 6.1.22).
- US Census Bureau, 2020. U.S. Census Bureau QuickFacts: Los Angeles County, California [WWW Document]. URL <https://www.census.gov/quickfacts/losangelescountycalifornia> (accessed 11.10.20).
- US Census Bureau, 2018. American Community Survey 5-Year Data (2009-2018) [WWW Document]. URL <https://www.census.gov/data/developers/data-sets/acs-5year.html> (accessed 11.10.20).
- USDA NAIP GeoHub, 2022. National Agriculture Imagery Program - NAIP Hub Site [WWW Document]. URL <https://naip-usdaonline.hub.arcgis.com/> (accessed 6.1.22).
- van den Berg, A.E., Maas, J., Verheij, R.A., Groenewegen, P.P., 2010. Green space as a buffer between stressful life events and health. *Soc. Sci. Med.* 70. <https://doi.org/10.1016/j.socscimed.2010.01.002>
- Wolch, J.R., Byrne, J., Newell, J.P., 2014. Urban green space, public health, and environmental justice: The challenge of making cities “just green enough.” *Landsc. Urban Plan.* 125, 234–244. <https://doi.org/10.1016/j.landurbplan.2014.01.017>
- Wu, X., Nethery, R.C., Sabath, B.M., Braun, D., Dominici, F., 2020. Exposure to air pollution and

COVID-19 mortality in the United States. medRxiv.

Yu, Z., Bellander, T., Bergström, A., Dillner, J., Eneroth, K., Engardt, M., Georgelis, A., Kull, I., Ljungman, P., Pershagen, G., Stafoggia, M., Melén, E., Gruzieva, O., Group, B.C.-19 S., Almqvist, C., Andersson, N., Ballardini, N., Bergström, A., Björkander, S., Brodin, P., Castel, A., Ekström, S., Georgelis, A., Hammarström, L., Pan-Hammarström, Q., Hallberg, J., Jansson, C., Kere, M., Kull, I., Lauber, A., Lövquist, A., Melén, E., Mjösberg, J., Mogensen, I., Palmberg, L., Pershagen, G., Roxhed, N., Schwenk, J., 2022. Association of Short-term Air Pollution Exposure With SARS-CoV-2 Infection Among Young Adults in Sweden. *JAMA Netw. Open* 5, e228109–e228109. <https://doi.org/10.1001/JAMANETWORKOPEN.2022.8109>

Zeldovich, Y.B., 2015. 26. Oxidation of Nitrogen in Combustion and Explosions, in: *Selected Works of Yakov Borisovich Zeldovich*, Volume I. <https://doi.org/10.1515/9781400862979.404>

## CHAPTER 2: SPATIAL ANALYSIS OF COVID-19 AND TRAFFIC-RELATED AIR POLLUTION IN LOS ANGELES

(This chapter was published in *Environment International*, 2021, 153:106531. It has been updated to include a more recent literature review.)

### 2.1 INTRODUCTION

As of December 7<sup>th</sup>, 2021, more than 265 million people worldwide have been diagnosed with COVID-19, resulting in more than 5.2 million deaths (World Health Organization, 2021). Extensive investigation has been conducted on the etiology of COVID-19, yet researchers are still determining how exposure risk factors may influence COVID-19 incidence and mortality. Recent evidence from China, the United States, and Europe suggest that exposure to air pollution may play a role in COVID-19 incidence and deaths (Berg et al., 2021; Brandt et al., 2020; Coker et al., 2020; Huang et al., 2021; Li et al., 2020; Lippi et al., 2020; Travaglio et al., 2021; B. Wang et al., 2020; X. Wu et al., 2020; Yao et al., 2021; Zhang et al., 2020; Zhou et al., 2021; Zhu et al., 2020). These findings are consistent with prior research suggesting that air pollution, including traffic-related air pollution (TRAP), is associated with many respiratory morbidities (e.g., asthma, chronic pulmonary disease, lung cancer, and respiratory tract infections) (Bai et al., 2018; Dales et al., 2008; Franklin et al., 2015; Jerrett et al., 2008; Sydbom et al., 2001), hospitalizations (Neupane et al., 2010), all-cause mortality (Beelen et al., 2008; Jerrett et al., 2005b) and increased risk of respiratory viral infection (Ciencewicki and Jaspers, 2007; Wang et al., 2020). Nitrogen dioxide (NO<sub>2</sub>), a tracer of TRAP generated from tailpipe emissions (Quiros et al., 2013; Zeldovich, 2015), has been found to impair the function of alveolar macrophages and epithelial cells, thereby increasing the risk of lung infections (Neupane et al., 2010).

Other factors such as age, race/ethnicity, and other sociodemographic characteristics appear to increase risk for COVID-19 infection, severity, and associated death (Brandt et al., 2020). For example, compared to non-Hispanic whites, cumulative COVID-19 hospitalization rates for Black and Latinx populations are approximately 4.7 and 4.6 times higher in the U.S., respectively (Centers for Disease Control and Prevention, 2020). Black and Latinx U.S. populations are disproportionately exposed to SARS-CoV-2, as they are more likely to serve as essential workers (Martinez et al., 2020; Rogers et al., 2020) and to live in crowded conditions (Burr et al., 2010; Memken and Canabal, 1994). A higher prevalence of metabolic disorders (such as hypertension, diabetes, and obesity) in these populations likely contributes to more severe disease (Commodore-Mensah et al., 2018; Divens and Chatmon, 2019) and death, including those from COVID-19 (Du et al., 2020). In addition, minority populations are more likely to live in areas where there is greater air pollution (Ailshire and García, 2018; Collaco et al., 2020; Gaither et al., 2019).

Building on past research demonstrating an association between Severe Acute Respiratory Syndrome (SARS) and air pollution (Cui et al., 2003), Wu et al. (2020) reported associations between county-level COVID-19 mortality rates in 3,089 counties through June 2020 and long-term average (from years 2000 to 2016) PM<sub>2.5</sub> concentration across the United States. They reported that each 1 µg m<sup>-3</sup> increase in PM<sub>2.5</sub> concentration was associated with an 11% increase in COVID-19 mortality rate (95% CI: 6% - 17%). In another study of COVID-19 in 3,122 U.S. counties through July 2020, researchers found an increase in interquartile range (IQR) of 4.6 ppb of NO<sub>2</sub> to be associated with a 16.2% (95% CI: 8.7%, 24.0%) increase in mortality rate and an 11.3% (95% CI: 4.9%, 18.2%) increase in case-fatality rate (Liang et al., 2020b). In both U.S. studies, exposure estimates were based on concentrations at the county level and, therefore, could not account for variation in air pollution observable on a smaller scale within cities (Kulhánová et al., 2018; Wu et al., 2019). In addition, the quality and comparability of COVID-19

health outcome information may vary considerably across U.S. counties as reporting protocols may differ among jurisdictions at the local, state, and national levels (Bergman et al., 2020; Bialek et al., 2020), which may lead to case ascertainment bias.

LA became one of the only metropolitan cities globally to publicly report neighborhood-level COVID-19 cases in March 2020 and mortality in June 2020 (LACDPH, 2020). These data afforded the opportunity to conduct spatial modeling for a large population with a smaller geographical area neighborhood unit of analysis. These smaller geographic areas allow for more accurate pollution exposure estimates than the county-level studies above. LA has a wide range of air pollution exposure levels with which to investigate intra-urban relationships with COVID-19. Furthermore, because the Los Angeles County Department of Public Health (LACDPH) governs all health statistics, LA County is likely to have consistent health reporting practices. This diminishes the possibility of case ascertainment bias that may have been present in the national studies comparing among more than 3,000 counties.

Here, we aim to analyze the relationship between air pollution and COVID-19 case incidence, mortality, and case-fatality rates in neighborhoods of Los Angeles County, using high-resolution exposure models. We focus on  $\text{NO}_2$  because this gaseous pollutant serves as a marker for traffic pollution, which displays substantial intra-urban variation over small areas in Los Angeles and elsewhere (Su et al., 2020, 2009; Zeldovich, 2015). In California, where this study is situated, 62% of  $\text{NO}_x$  emissions come from mobile sources such as vehicle traffic (Almaraz et al., 2018).

## 2.2 MATERIAL AND METHODS

### 2.2.1 Setting

This study is situated in Los Angeles (LA) County. In 2019, LA County had a population size of 10,039,107 and was diverse in its racial, ethnic, and socioeconomic composition (U.S. Census Bureau, 2020). For example, 51% are White, 48% are Latinx, 15% are Asian, and 8.3% are Black. The median income of LA County is \$64,251 USD. LA County is spread across a large geographic area of 4,057 square miles or 10,508 square kilometers. The sprawling landscape induces high levels of travel by automobile and attendant traffic-related air pollution (TRAP) (Su et al., 2009). In addition, the presence of two major seaports and associated goods movement infrastructure creates additional emissions from diesel vehicles (Kozawa et al., 2009; Su et al., 2020, 2016). The first case of COVID-19 in California was identified on January 26<sup>th</sup>, 2020 (LACDPH, 2020; Los Angeles Times, 2020), and the first community-acquired case in the United States was confirmed in California on February 26<sup>th</sup>, 2020 (CADPH, 2020; Heinzerling et al., 2020).

### 2.2.2 Data sources

**Table 2.1** summarizes the data sources and variables used. Cumulative COVID-19 case and mortality counts for March 16<sup>th</sup> to February 23<sup>rd</sup>, 2021 were accessed from the Los Angeles County Department of Public Health (LACDPH) COVID-19 dashboard website. These outcome data were split into two time periods: a main study period from March 16<sup>th</sup> to September 8<sup>th</sup>, 2020; and a secondary period for sensitivity analyses from September 8<sup>th</sup>, 2020 to February 23<sup>rd</sup>, 2021. These data are reported at a neighborhood statistical area unit geography. LACDPH reports infectious disease data for 'Countywide Statistical Areas (CSAs)', used by many LA County agencies to report data to the County Board of Supervisors, and which include mixed areal classifications such as 'city', 'community', 'neighborhood', or 'unincorporated area' (Harris, 2020;

LACDPH, 2021). This study refers to CSAs as ‘neighborhoods’. Based on prior research (Su et al., 2020), a land-use regression model was used to produce an annual pollution surface of NO<sub>2</sub> across California at a spatial resolution of 30 m using data from 2016. This surface was used previously for another recent health study in Los Angeles (Wing et al., 2020). The land-use regression model had an out-of-sample cross-validation R<sup>2</sup> of 0.76. This average annual NO<sub>2</sub> surface was used to define the main exposure metric by neighborhood.

Potential covariates were identified *a priori* based on existing literature on risk factors for disease or severity of disease (including death) for COVID-19 (Myers et al., 2020), other pneumonic infectious diseases (Neupane et al., 2010), and previous studies on air pollution and COVID-19 (Liang et al., 2020; Wang et al., 2020). Demographic covariates, including age, race/ethnicity, median household income, and household owner occupancy, were downloaded from the U.S. Census Bureau’s American Community Survey (ACS) 5-year moving estimate for 2018 (U.S. Census Bureau, 2018). Population counts at the neighborhood level, and smoking and obesity prevalence at the census-tract level were downloaded from the LACDPH website (LACDPH, 2018). Population counts from LACDPH were compared to counts from the ACS to assess variable aggregation methods. Hospital and testing facility locations were acquired from the LA County’s GeoHub website for their potential association with case ascertainment (LAC, 2014). Residential building footprints were also downloaded from the LA County Geohub website to facilitate these demographic data aggregations (LAC, 2014).

We also considered hypertension and diabetes as health outcomes potentially associated with COVID-19 severity (Myers et al., 2020). These health outcomes were modeled in the U.S. Centers for Disease Control and Prevention’s (CDC) 500 Cities Project health dataset (Centers for Disease Control and Prevention, 2019). These covariates were included as sensitivity analyses due to incomplete spatial coverage.

Uncertainties in the testing regime raise questions about potential case-ascertainment

bias. As testing became more widely available, rates of testing likely changed from testing only suspected cases to people potentially exposed as a result of occupational or social interactions. This could have affected the case rate and subsequently the case-fatality rates. It is also possible that in the earlier stages of the pandemic, there was more undercounting of the deaths, which would have diminished over time as medical professionals learned how to more accurately identify deaths resulting from COVID-19.

To address the potential shifts in case-ascertainment, case-fatality, and mortality rates that could have occurred over time, we conducted further sensitivity analyses. Specifically, we extended our original study period which captured approximately the first six months of the pandemic (March 16<sup>th</sup> to September 8<sup>th</sup>, 2020), to the subsequent six months (September 8<sup>th</sup>, 2020 to February 23<sup>rd</sup>, 2021). Thus, we replicated the analysis for the subsequent 6-month period, which had nearly four times the incident cases (875,368 cases) as the first period (230,621 cases). In the latter period, the County changed the neighborhood definitions to exclude or combine about 13 neighborhoods, so the count of neighborhoods was less than in the original period (348 vs. 335). Consequently, the two data sets are not uniformly constructed, but they are quite similar.

### **2.2.3 Quantification of variables**

Very few spatial variables were available at the neighborhood geographies, as most environmental, health, and demographic areal data are published by postal ZIP code or census tract. Environmental Systems Research Institute's (ESRI) ArcGIS 10.7 (ESRI, 2020) was used to summarize NO<sub>2</sub> zonal mean by each of the N=348 neighborhoods ('neighborhood' statistical area geographies, as delineated by the LACDPH) in LA County. To account for misalignment in areal boundaries between COVID-19 case/mortality and selected covariates, all areal covariates were first reaggregated to residential building footprints (acquired from LA County's Geohub website (LAC, 2014)) and then reaggregated to neighborhoods by using counts per area density-based raster surfaces. This intermediate step was taken to minimize the effect of geographies with highly

variable population densities (e.g., a large neighborhood with few total residents). Hospital and testing facility areal densities were calculated using a 10-mile radius kernel density process – generating a raster surface describing the number of hospitals or facilities per sq km within 10 miles of each raster grid cell. History of hypertension and diabetes drawn from the 500 Cities Project covered only 61% (212 of 348) of neighborhoods; therefore, we imputed the global mean for the remaining 136 neighborhoods and report these results as sensitivity analyses.

#### **2.2.4 Statistical Modeling**

Extracted neighborhood NO<sub>2</sub> concentrations were modeled in relation to incident case rate (cases/population), mortality rate (deaths/population), and case-fatality rate (deaths/cases). NO<sub>2</sub> concentrations from neighborhoods were scaled to the interquartile range to aid in interpretation of model results (Liang et al., 2020b; Xiao Wu et al., 2020b). We used three different statistical models to assess sensitivity of our results to model specification: (1) zero-inflated Poisson, (2) zero-inflated negative binomial, and (3) Bayesian conditional autoregressive (CAR) zero-inflated Poisson models. To assess incident case rate, all models treated the count of COVID-19 cases in the neighborhoods as the dependent variable and the total population as the offset. These models were also run for mortality counts with the total population as the offset (mortality rate) and for mortality counts with the total number of COVID-19 cases as the offset (case-fatality rate). Zero-inflated models were selected to account for a high number of neighborhoods with zero counts of cases or deaths and often low total populations; without zero-inflation, these low-count areas could disproportionately influence the model results. We also employed a Bayesian zero-inflated Poisson model whose spatial random effects were assigned a CAR prior distribution to account for potential spatial autocorrelation between neighborhoods. This model incorporated a spatial adjacency matrix of first-order neighbors and employed flat priors.

All three models were run with and without adjustment for covariates. The final model included the following covariates: mean percent owner occupancy, mean median income, mean

percent above 65 years old, mean percent nonwhite; mean smoking prevalence, mean obesity prevalence, and mean hospital density per square mile within a 10-mile radius. Covariates selected for final model were identified *a priori*; however, in the event of highly correlated or colinear covariate pairs, the covariate with the highest bivariate association with the outcome was included. In all models, no covariates were found to be significant predictors of the zero-inflation component. We used R version 3.6.3 to run all statistical analyses (R Core Team, 2020).

## 2.3 RESULTS

The average area of the 348 LA County neighborhoods was 44.7 sq km (SD=171.8 sq km), with the largest being 1,144 sq km (Antelope Valley) in the northern exurban areas of the county and the smallest being 0.67 sq km (San Pasqual) in a more densely populated area near Pasadena, north of downtown LA. The annual mean NO<sub>2</sub> across the study region was 11.7 ppb (SD=7.3 ppb; range of 1.6 ppb to 31.3 ppb). Concentrations of NO<sub>2</sub> derived from the 2016 land-use regression surface are depicted in **Figure 2.1A**. The mean aggregated NO<sub>2</sub> across neighborhoods was 15.6 ppb (SD=6.0 ppb) with an interquartile range of 8.7 ppb. Between March 16<sup>th</sup> and September 8<sup>th</sup>, 2020, the LACDPH recorded 230,621 confirmed cases of COVID-19, and 5,653 deaths due to COVID-19 were observed. In a population of 10.0 million, this translated into a case rate of 2.2% (**Figure 2.1B**), a mortality rate of 0.054% (**Figure 2.1C**), and a case-fatality rate of 2.5% (**Figure 2.1D**). The period from September 8<sup>th</sup>, 2020 to February 23<sup>rd</sup>, 2021 included 875,368 cases and 13,344 deaths and was used as sensitivity analysis.

Between neighborhoods (N=348), the mean percent owner occupancy was 54.7% (SD=22.0%); mean median income was \$47,483 (SD = \$68,898); mean percent above 65 years old was 13.9% (SD=0.1%); mean percent nonwhite was 45.2% (SD= 20.1%); mean smoking prevalence was 12.7% (SD=2.6%); mean obesity prevalence was 23.7% (SD=7.4%); and the

mean hospital density per square mile within a 10-mile radius was  $1.2 \times 10^{-4}$  ( $SD=1.4 \times 10^{-4}$ ). The mean hypertension and diabetes prevalence were 18.7% ( $SD=9.6\%$ ), and 7.4% ( $SD=4.2\%$ ), respectively. Although median income was highly associated with the outcome in the crude model, it was highly correlated with owner occupancy ( $r = 0.89$ ); therefore, owner occupancy was selected for inclusion as it demonstrated a larger bivariate association with all outcomes.

Ordinary residuals from the zero-inflated Poisson and negative binomial models demonstrated significant spatial autocorrelation at the global (Moran's I p-value  $<0.001$ ) and local (Anselin hot-spots) levels; thus, we used a Bayesian zero-inflated Poisson model with a CAR prior on the random effects to account for spatial dependence of the residuals per neighborhood.

Crude and adjusted model results for (1) zero-inflated Poisson, (2) zero-inflated negative binomial, and (3) zero-inflated Poisson spatial models are shown in **Table 2.2**. In the adjusted zero-inflated Poisson model, we found that the incidence rate ratio (IRR) of  $NO_2$  was 1.31 (95% CI: 1.29, 1.33) for the case rate. That is, we found that an increase of 8.7 ppb (IQR) in mean annual  $NO_2$  (2016) was associated with a 31% increase in COVID-19 incident case rate. The adjusted zero-inflated negative binomial and spatial models demonstrated a smaller effect of 16% (95% CI: 2%, 32%) and 18% (Credible Interval – CrI: 10%, 32%) increase in case rate, respectively (**Table 2.2A**). Adjusted models reduced residual uncertainty compared to the crude model estimates for case rate. The adjusted Poisson, negative binomial, and spatial models all demonstrated an increase in COVID-19 mortality of 35% (95% CI: 23%, 48%), 44% (95% CI: 11%, 86%), and 60% (CrI: 37%, 88%), respectively, across the IQR exposure increment (**Table 2.2B**). Again, these adjusted models improved residual uncertainty compared to crude model estimates for mortality rate. Finally, adjusted Poisson and negative binomial models showed positive yet non-significant results for the association between  $NO_2$  and COVID-19 case-fatality; however, the spatial CAR model demonstrated that an IQR increase in mean annual  $NO_2$  was associated with a 31% (CrI: 10%, 65%) increase in case-fatality. Sensitivity analyses, which

included the addition of history of hypertension and diabetes in the models, had comparable results across all three models. In comparing the two time periods, before and after September 8<sup>th</sup>, 2020, we found that the results were largely consistent, despite very different case numbers, testing regimes, and improvements in classifying deaths. While some differences exist in the size of the effects, overall, the conclusions remain the same. The results of this sensitivity analysis give some assurance that the changes in testing, case ascertainment, and mortality classification over time are not having a substantial effect on the key conclusion that long-term air pollution exposure likely increases the risk of Covid-19 infection and death. Full model results, including incidence risk ratios for all covariates, are described in **Appendix A** for the main model, **Appendix B** for sensitivity analysis including hypertension and diabetes, and **Appendix C** for sensitivity analysis utilizing the period between September 8<sup>th</sup>, 2020 and February 23<sup>rd</sup>, 2021.

## **2.4 DISCUSSION AND CONCLUSION**

We found annual NO<sub>2</sub> to be associated with COVID-19 incidence and mortality in Los Angeles County neighborhoods while adjusting for selected confounders. These findings were consistent across statistical model specification, although risk estimates displayed some variation between models. In addition, we found in the CAR an association between NO<sub>2</sub> and COVID-19 case-fatality; other models also showed positive but insignificant associations. Covariates in the models largely had the expected sign of effect. Furthermore, our sensitivity analyses, which included the addition of hypertension and diabetes prevalence covariates, had a minimal impact on the effect size or interpretation of our model estimates for NO<sub>2</sub> and COVID-19 outcomes. Our sensitivity analysis involving a second, approximately 6-month time period, with slightly different outcome reporting (N=348 vs N=335) also demonstrated comparable results to the main model and study period.

Our findings are consistent with two previous studies demonstrating a relationship between air pollution and COVID-19 nationally at the county scale in the U.S. One study investigated the association between NO<sub>2</sub> and COVID-19, and they observed remarkably similar findings. Specifically, Liang et al. (2020) reported an increase of 4.6 ppb (IQR across all counties) NO<sub>2</sub> to be associated with a 16.2% (CI: 8.7%, 24.0%) increase in mortality rate and an 11.3% (CI: 4.9%, 18.2%) increase in case-fatality rate (Liang et al., 2020b). When we scaled to Liang et al.'s IQR of NO<sub>2</sub>, our models demonstrated similar results of 17.1% (CI: 11.3%, 23.2%), 21.3% (CI: 5.9%, 38.9%), and 30.1% (CI: 12.4%, 50.6%) increases in COVID-19 mortality rate for our zero-inflated Poisson, negative binomial, and CAR models, respectively. In comparison to the Wu et al. (2020) study, which observed that a 1 µg m<sup>-3</sup> increase in air pollutant PM<sub>2.5</sub> was associated with an 11% increase in mortality rate (Wu et al., 2020), we found an 8.7 ppb increase in another traffic-related air pollutant, NO<sub>2</sub>, to be associated with a 35 – 60% (range of three models; **Table 2.2**) increase in mortality rate. The Wu et al. study, however, did not report results scaled to the interquartile range of PM<sub>2.5</sub>, so we scaled their results to the IQR for PM<sub>2.5</sub> from the Liang et al. study (2.6 µg m<sup>-3</sup>), which uses a similar number of U.S. counties. This resulted in a highly comparable 31.2% increase in mortality for a 2.6 µg m<sup>-3</sup> increase in PM<sub>2.5</sub>. Although Wu et al., Liang et al., and the current research demonstrated similar effect sizes, there may be different biological effects of NO<sub>2</sub> and PM<sub>2.5</sub>.

The comparable effect size between our study and the Liang et al. study is notable given that the Liang et al. used large-area county-level geographies (3,122 U.S. counties), and we focused on small-area neighborhoods of LA. The two studies also utilized different data sources, covariates, and model types—with Liang et al. also controlling for multiple pollutants. Our confounders were either similarly associated with our outcomes, like those included in the Wu et al. and Liang et al.'s studies, or were found to be null, reinforcing the validity of our results based on a *priori* expectation. The larger effect size on mortality rate in our study compared to the other

two studies could be due to greater spatial variability resulting from using building-footprint covariate aggregation on smaller-area neighborhood geographies rather than using county-level data.

To our knowledge, only a handful of studies have undertaken small-area analysis of the association of COVID-19 and air pollution using spatial modeling techniques (Berg et al., 2021; Konstantinoudis et al., 2021; Travaglio et al., 2021). This study also reported associations with nitrogen dioxides at a sub-regional scale. In a study of 32,844 small areas in England, researchers also utilized Bayesian models with adjustments for confounding and spatial autocorrelation (Konstantinoudis et al., 2021). The study demonstrated a 0.5% (CrI: -0.2%, 1.2%) increase in COVID-19 mortality risk for a 1  $\mu\text{g m}^{-3}$  increase in long-term  $\text{NO}_2$  exposure (not scaled to our IQR). Although a smaller effect size, these results are comparable to those from our small-area spatial models. Smaller-area analyses likely reduce potential exposure measurement error and lead to more consistent ascertainment of cases and deaths than those using the larger county units—both of which likely result in more precise and reliable estimates of health effects from air pollution exposures. By utilizing Bayesian models with CAR priors, we also accounted for spatial autocorrelation or clustering between adjacent administratively defined neighborhoods. This addition is important as transmission for COVID-19 and other infectious diseases is likely to be clustered spatially due to respiratory community spread (see map of incidence in **Figure 2.1**).

Our study has several limitations. Most importantly, our study is limited by population-level counts of COVID-19 cases and deaths. These aggregate data, made publicly available by LACDPH, have facilitated this research but have also introduced some uncertainties. For example, it is difficult to determine how testing rates or the prevalence of asymptomatic cases, which may show significant neighborhood-level variation, could impact our results. These aggregate data, made publicly available by LACDPH, have facilitated this research but have also introduced some uncertainties. We are unable to determine data accuracy, specifically for the

earlier phases of the pandemic, when data collection protocols were still being defined. The number of neighborhoods reported by LACDPH has fluctuated, from 348 (in September 2020) to 335 (in February 2021) distinct areas. Our sensitivity analysis on a second time period (September 2020 to February 2021) including N=335 neighborhoods demonstrated similar results to our initial period (March 2020 to September 202), so these potential data quality issues appear to have minimal effect on the interpretation of our results. Ideally, with data access granted, future research would avoid aggregate-level data in favor of individual-level outcomes. Utilizing individual-level home locations of cases and deaths rather than neighborhood-level aggregate counts would greatly improve air pollution exposure attribution and allow for better ascertainment of potential confounders. In addition, we could not include daily or weekly observations to account for changes in case or mortality rate over time, but rather used cumulative counts for the study period. This was due to inconsistent case reporting and incomplete death reporting due to human subject concerns earlier in the pandemic. Deaths may have been undercounted, as death certificates and coroner reports may incorrectly attribute cause of death (Jewell et al., 2020; Quast and Andel, 2020). Future research may benefit from using excess mortality for comparison (Banerjee et al., 2020). Indicators of symptom severity from hospital, intensive care unit, and emergency room admittance data are more difficult to acquire, as they are not publicly available, but future analyses on outcomes of severity would allow for better understanding of the effect of NO<sub>2</sub> exposure on the progression of the disease.

This study is also limited by the use of land-use regression from 2016 to estimate long-term NO<sub>2</sub> exposure. In a study in of 1,237 census tracts in Colorado, researchers found a positive association between PM<sub>2.5</sub> and case rate and mortality, however, they also noted this statistically significant result was highly dependent on the origin of the PM<sub>2.5</sub> surface data—with many surfaces not producing significant results (Berg et al., 2021). Although additional data sources and years of land-use regression surfaces could be utilized to better describe long-term trends

and to conduct further sensitivity analyses, estimates of NO<sub>2</sub> in Los Angeles County in the years immediately preceding the pandemic are likely similar in their spatial pattern over such a short time span. Other covariate data included in these analyses were spatially misaligned. A strength of this study is our use of residential building footprints as an intermediate step in aggregating areal covariates. Although using these building footprints better accounts for population density patterns than more straightforward aggregation techniques (e.g., census-tract directly to neighborhood), the method may cause misalignment errors due to differences in building characteristics (e.g., height, unit size, etc.). Finally, our spatial models accounted for unexplained spatial variability in the between-neighborhood random effect, which suggests there may be additional covariates with a similar spatial pattern that we have not included in these analyses, and further investigation is necessary. While the CAR model accounts for this dependence in the statistical inference, we cannot rule out important missing confounders.

In summary, our findings imply a potentially large association between exposure to air pollution and population-level rates of COVID-19 cases and deaths. Our findings demonstrate comparable results to other recent literature, especially concerning the association of long-term NO<sub>2</sub> and COVID-19 mortality rate. Our small-area analyses, covariate aggregation methods using building footprints for accounting for population density variability, and utilization of spatial modeling (CAR model with spatial random effect) make novel contributions to the available literature. These findings are especially important for targeting interventions aimed at limiting the impact of COVID-19 in polluted communities.

In the U.S., more polluted communities often have lower incomes and higher proportions of Black and Latinx people. In addition, Black and Latinx people have higher rates of pre-existing conditions, potentially further exacerbating the risk of COVID-19 transmission and death (Clark et al., 2014; O'Neill et al., 2003). The elevated risk of case incidence and mortality observed in these populations might result from higher exposure to air pollution. As COVID-19 data reporting

improves and data access is given more readily to researchers, we will further refine these analyses to the individual-level in a spatial framework.

**Table 2.1.** Data sources and spatiotemporal dimensions for model of association between NO<sub>2</sub> and COVID-19 case, mortality, and case-fatality rates in Los Angeles County

<b>Data source</b>	<b>Attribute(s)</b>	<b>Spatial Dimension</b>	<b>Temporal Dimension<sup>t</sup></b>
<i>LACDPH</i> <sup>1</sup>	COVID-19 cases and COVID-19 deaths	Neighborhood statistical areas (polygon)	March 16 <sup>th</sup> – September 8 <sup>th</sup> , 2020
	Population*, smoking, and obesity		September 8 <sup>th</sup> , 2020 – February 23 <sup>rd</sup> , 2021 <sup>a</sup> 2019
<i>ACS</i> <sup>2</sup>	Age, median income, race/ethnicity, owner-occupancy status, and population*	Census tracts (polygon)	2018
<i>500 Cities Project</i>	Diabetes and hypertension	Census tracts (polygon)	2019
<i>LA County GeoHub</i>	Testing locations and hospital locations	Site location (point or polygon)	September 8 <sup>th</sup> , 2020
	Building footprints**		2014
<i>LUR</i> <sup>3</sup> <i>surface</i> (Su et al., 2020)	NO <sub>2</sub> (ppb)	California (raster; 30 m)	2016

\*LACDPH population used for regression modeling; ACS population used to validate aggregation methods.

\*\*building footprints used for data aggregation.

<sup>1</sup>LACDPH = Los Angeles County Department of Public Health.

<sup>2</sup>ACS = American Community Survey (U.S. Census Bureau).

<sup>3</sup>LUR = land-use regression.

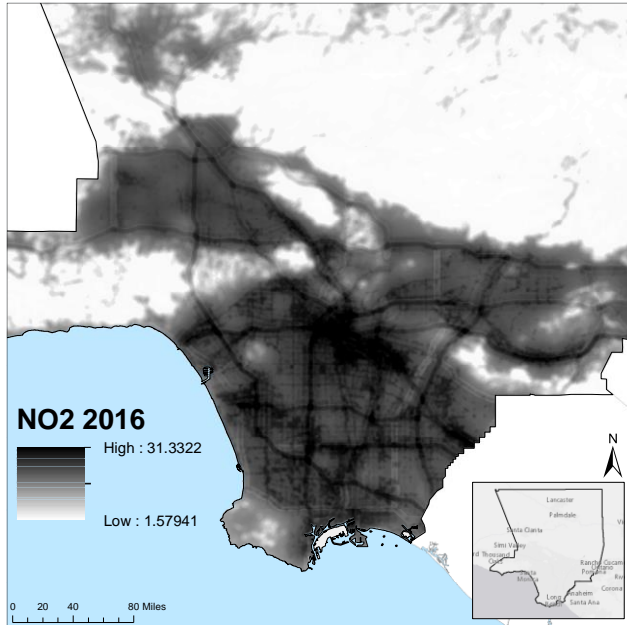
<sup>t</sup>Temporal dimension describes the range in time for which the data was recorded.

<sup>a</sup>Secondary time period used as sensitivity analysis in comparison to main study period of March 16<sup>th</sup> to September 8<sup>th</sup>, 2020

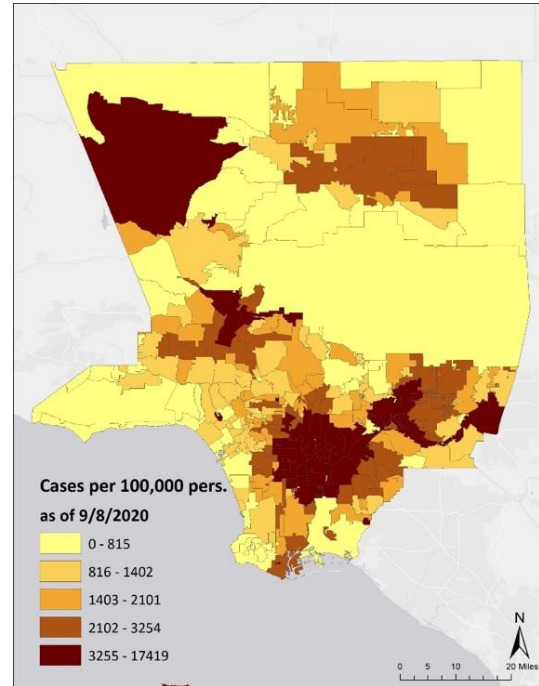
**Figure 2.1.** Maps of NO<sub>2</sub> and COVID-19 case, mortality, and case-fatality rates by neighborhood

**A.** NO<sub>2</sub> from land-use regression (LUR) model, 2016. (Map is zoomed in to demonstrate fine-resolution variability); **B.** COVID-19 Case rate (cases/population); **C.** Mortality rate (deaths/population); and **D.** Case-fatality rate (deaths/cases) for the period between March 16th and September 8th, 2020, depicted at the neighborhood level.

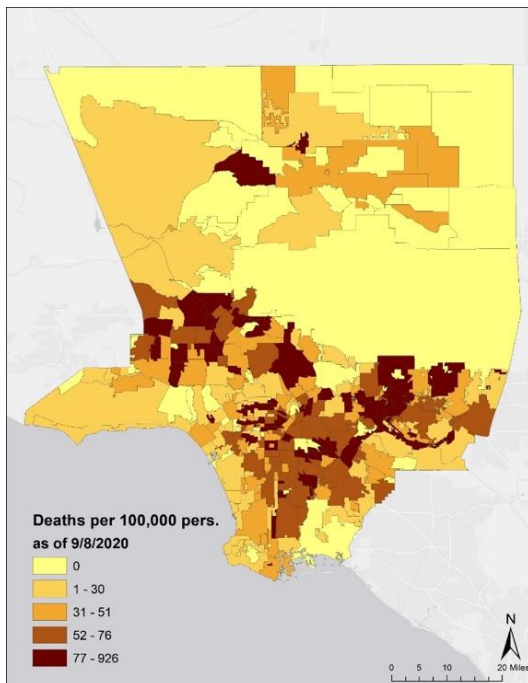
**A.**



**B.**



**C.**



**D.**

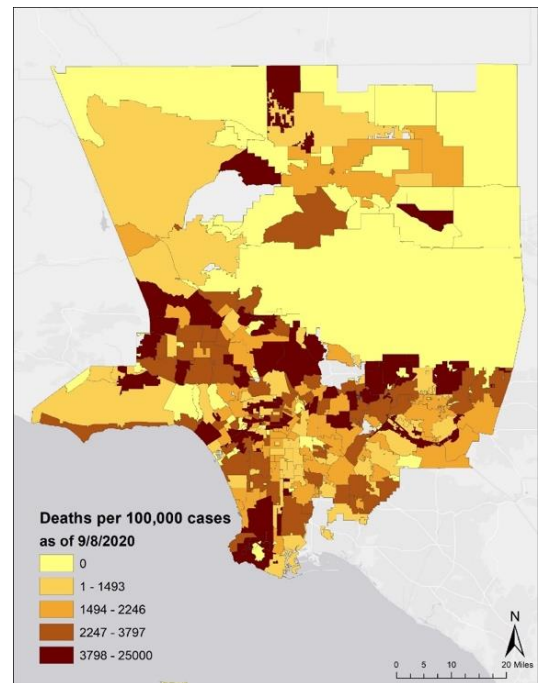


**Table 2.2.** Adjusted association of NO<sub>2</sub> and COVID-19 from three models

**A.** Case rate (cases/population); **B.** Mortality rate (deaths/population); and **C.** Case-fatality rate (deaths/cases) for Los Angeles County neighborhoods (N = 348) for the period between March 16<sup>th</sup> and September 8<sup>th</sup>, 2020. A sensitivity analysis was conducted to assess the inclusion of hypertension and diabetes as model covariates. A second sensitivity analysis assessed COVID-19 outcome data from a second time period between September 8<sup>th</sup>, 2020 and February 23<sup>rd</sup>, 2021 for N=335 neighborhoods.

Main model <sup>1</sup>	Zero-inflated Poisson				Zero-inflated negative binomial				CAR zero-inflated Poisson with spatial random effect				
	Crude		Adjusted		Crude		Adjusted		Crude		Adjusted		
	IRR	CI	IRR	CI	IRR	CI	IRR	CI	IRR	CI	IRR	CI	
<b>(n=348)</b>													
<b>A. Case rate</b>	1.82	(1.80, 1.84)	1.31	(1.29, 1.33)	1.47	(1.33, 1.62)	1.16	(1.02, 1.32)	1.77	(1.53, 2.09)	1.18	(1.10, 1.32)	
<b>B. Mortality rate</b>	1.72	(1.62, 1.83)	1.35	(1.23, 1.48)	1.77	(1.50, 2.08)	1.44	(1.11, 1.86)	1.94	(1.46, 2.58)	1.60	(1.37, 1.88)	
<b>C. Case-fatality rate</b>	0.96	(0.91, 1.01)	1.05	(0.96, 1.15)	1.07	(0.91, 1.25)	1.21	(0.97, 1.50)	1.13	(0.87, 1.42)	1.31	(1.10, 1.65)	
<b>Sensitivity Analysis:</b>	<b>Including hypertension &amp; diabetes<sup>2</sup> (n=348)</b>												
<b>A. Case rate</b>	1.82	(1.80, 1.84)	1.28	(1.26, 1.30)	1.47	(1.33, 1.62)	1.18	(1.04, 1.33)	1.77	(1.53, 2.09)	1.27	(1.14, 1.34)	
<b>B. Mortality rate</b>	1.72	(1.62, 1.83)	1.35	(1.23, 1.49)	1.77	(1.50, 2.08)	1.57	(1.23, 2.01)	1.94	(1.46, 2.58)	1.44	(1.13, 2.06)	
<b>C. Case-fatality rate</b>	0.96	(0.91, 1.01)	1.05	(0.96, 1.15)	1.07	(0.91, 1.25)	1.19	(0.96, 1.49)	1.13	(0.87, 1.42)	1.34	(1.13, 1.69)	
<b>Sensitivity Analysis:</b>	<b>Second time period<sup>3</sup> (n=335)</b>												
<b>A. Case rate</b>	1.66	(1.65, 1.67)	1.29	(1.28, 1.29)	1.22	(1.04, 1.42)	1.21	(1.01, 1.45)	1.38	(1.51, 1.66)	1.24	(1.10, 1.42)	
<b>B. Mortality rate</b>	1.72	(1.63, 1.81)	1.28	(1.21, 1.36)	1.82	(1.53, 2.18)	1.38	(1.14, 1.67)	1.88	(1.53, 2.35)	1.77	(1.34, 2.14)	
<b>C. Case-fatality rate</b>	1.04	(0.99, 1.09)	1.04	(0.98, 1.10)	1.10	(0.95, 1.26)	1.09	(0.94, 1.25)	1.10	(0.98, 1.24)	1.15	(1.00, 1.35)	

<sup>1</sup> All models controlled for owner-occupancy rate, percent population > 65 years of age, percent nonwhite, percent smokers, percent obese, and hospital density per sq mi within 10 miles. Full model results with covariates can be seen in Appendix A. COVID-19 outcome data was acquired from the Los Angeles County Department of Public Health (LACDPH).

<sup>2</sup> Model conducted for sensitivity analysis includes all covariates from main model plus percent hypertensive and percent diabetic derived from 500 Cities Project data. Hypertension and diabetes data covered 212 of N=348 neighborhoods (61% coverage). We imputed the global mean for the remaining 136 neighborhoods. Full model results from sensitivity analysis can be seen in Appendix B.

<sup>3</sup> Model conducted for sensitivity analyses includes all covariates from main model. COVID-19 outcome data acquired from the Los Angeles County Department of Public Health (LACDPH)

## 2.5 Appendix A. Adjusted association of NO<sub>2</sub> and COVID-19 from three models for the period between March 16<sup>th</sup> and September 8<sup>th</sup>, 2020

A. Case rate (cases/population); B. Mortality rate (deaths/population); and C. Case-fatality rate (deaths/cases) for Los Angeles County neighborhoods (N = 348) for the period between March 16<sup>th</sup> and September 8<sup>th</sup>, 2020. NO<sub>2</sub> was scaled by its interquartile range for interpretation purposes; other covariates were not scaled

A. Case rate	Zero-inflated Poisson		Zero-inflated negative binomial		CAR zero-inflated Poisson with spatial random effect	
	IRR	CI	IRR	CI	IRR	CrI
NO <sub>2</sub> IQR	1.307	(1.288, 1.327)	1.161	(1.024, 1.316)	1.180	(1.098, 1.316)
Owner occupancy (%)	0.996	(0.996, 0.997)	0.996	(0.992, 0.999)	0.998	(0.996, 0.999)
> 65 years (%)	0.977	(0.976, 0.978)	0.956	(0.942, 0.969)	0.965	(0.951, 0.989)
Nonwhite (%)	0.995	(0.995, 0.996)	1.001	(0.997, 1.005)	0.994	(0.991, 0.997)
Smokers (%)	1.020	(1.018, 1.022)	0.992	(0.966, 1.018)	1.033	(1.009, 1.073)
Obese (%)	1.040	(1.039, 1.041)	1.033	(1.023, 1.042)	1.038	(1.035, 1.045)
Hospital density	1.123	(1.118, 1.129)	1.036	(0.966, 1.111)	1.189	(1.149, 1.232)

B. Mortality rate	Zero-inflated Poisson		Zero-inflated negative binomial		CAR zero-inflated Poisson with spatial random effect	
	IRR	CI	IRR	CI	IRR	CrI
NO <sub>2</sub> IQR	1.347	(1.225, 1.481)	1.438	(1.114, 1.857)	1.597	(1.367, 1.879)
Owner occupancy (%)	0.989	(0.986, 0.991)	0.986	(0.979, 0.993)	0.987	(0.980, 0.991)
> 65 years (%)	1.035	(1.027, 1.044)	1.040	(1.014, 1.067)	1.034	(1.012, 1.065)
Nonwhite (%)	0.997	(0.995, 0.999)	0.996	(0.991, 1.002)	0.997	(0.992, 1.002)
Smokers (%)	1.037	(1.024, 1.050)	1.049	(1.005, 1.094)	1.033	(0.981, 1.081)
Obese (%)	1.019	(1.014, 1.024)	1.025	(1.010, 1.040)	1.025	(1.009, 1.041)
Hospital density	1.061	(1.027, 1.096)	1.014	(0.902, 1.140)	1.090	(0.961, 1.289)

C. Case-fatality rate	Zero-inflated Poisson		Zero-inflated negative binomial		CAR zero-inflated Poisson with spatial random effect	
	IRR	CI	IRR	CI	IRR	CrI
NO <sub>2</sub> IQR	1.049	(0.959, 1.148)	1.207	(0.969, 1.504)	1.308	(1.100, 1.650)
Owner occupancy (%)	0.991	(0.989, 0.994)	0.993	(0.987, 0.998)	0.994	(0.989, 1.000)
> 65 years (%)	1.070	(1.061, 1.080)	1.059	(1.038, 1.080)	1.064	(1.040, 1.086)
Nonwhite (%)	1.001	(0.999, 1.003)	0.998	(0.993, 1.003)	0.998	(0.994, 1.002)
Smokers (%)	1.001	(0.997, 1.022)	1.039	(1.001, 1.079)	1.037	(0.994, 1.070)
Obese (%)	0.983	(0.977, 0.988)	0.985	(0.974, 0.997)	0.990	(0.978, 1.001)
Hospital density	0.954	(0.924, 0.985)	0.927	(0.840, 1.023)	0.979	(0.868, 1.100)

**2.6 Appendix B.** Adjusted association of NO<sub>2</sub> and COVID-19 from three models for the period between March 16<sup>th</sup> and September 8<sup>th</sup>, 2020 – sensitivity analyses including hypertension and diabetes covariates

Model conducted for sensitivity analyses – including main model (Appendix A) covariates with the addition of hypertension and diabetes derived from the 500 Cities Project dataset. Hypertension and diabetes data covered 212 of N=348 (61% coverage) neighborhoods. We imputed the global mean for the remaining 136 neighborhoods. This table shows the adjusted association of NO<sub>2</sub> (scaled by interquartile range: 8.7 ppb) and COVID-19 from three models: A. Case rate (cases/population); B. Mortality rate (deaths/population); and C. Case-fatality rate (deaths/cases) for Los Angeles County neighborhoods (N = 348) for the period between March 16<sup>th</sup> and September 8<sup>th</sup>, 2020. NO<sub>2</sub> was scaled by its interquartile range for interpretation purposes; other covariates were not scaled.

<b>A. Case rate</b>	Zero-inflated Poisson		Zero-inflated negative binomial		CAR zero-inflated Poisson with spatial random effect	
	IRR	CI	IRR	CI	IRR	CrI
NO <sub>2</sub> IQR	1.280	(1.261, 1.299)	1.175	(1.037, 1.332)	1.272	(1.143, 1.344)
Owner occupancy (%)	0.999	(0.998, 0.999)	0.996	(0.992, 1.000)	1.000	(0.999, 1.001)
> 65 years (%)	0.974	(0.973, 0.976)	0.955	(0.942, 0.969)	0.962	(0.951, 0.972)
Nonwhite (%)	0.994	(0.994, 0.995)	1.000	(0.996, 1.004)	1.004	(1.003, 1.006)
Smokers (%)	1.014	(1.012, 1.016)	0.992	(0.965, 1.018)	1.005	(0.993, 1.020)
Obese (%)	1.034	(1.033, 1.035)	1.030	(1.021, 1.040)	1.023	(1.014, 1.032)
Hospital density	1.109	(1.103, 1.115)	1.028	(0.957, 1.103)	1.046	(1.005, 1.119)
Hypertensive (%)	0.981	(0.980, 0.983)	0.982	(0.967, 0.998)	0.978	(0.974, 0.983)
Diabetic (%)	1.073	(1.069, 1.077)	1.044	(1.005, 1.084)	1.060	(1.047, 1.077)

<b>A. Mortality rate</b>	Zero-inflated Poisson		Zero-inflated negative binomial		CAR zero-inflated Poisson with spatial random effect	
	IRR	CI	IRR	CI	IRR	CrI
NO <sub>2</sub> IQR	1.354	(1.233, 1.487)	1.570	(1.226, 2.012)	1.441	(1.133, 2.058)
Owner occupancy (%)	0.991	(0.989, 0.994)	0.988	(0.982, 0.995)	0.989	(0.979, 0.996)
> 65 years (%)	1.032	(1.023, 1.040)	1.034	(1.008, 1.061)	1.027	(0.997, 1.059)
Nonwhite (%)	0.996	(0.994, 0.998)	0.995	(0.989, 1.001)	0.999	(0.993, 1.006)
Smokers (%)	1.033	(1.020, 1.047)	1.054	(1.010, 1.100)	1.027	(0.973, 1.076)
Obese (%)	1.012	(1.007, 1.017)	1.021	(1.006, 1.036)	1.021	(0.999, 1.046)
Hospital density	1.047	(1.012, 1.083)	1.000	(0.887, 1.127)	1.100	(0.897, 1.242)
Hypertensive (%)	0.983	(0.974, 0.991)	0.985	(0.959, 1.012)	0.992	(0.980, 1.019)
Diabetic (%)	1.071	(1.049, 1.094)	1.040	(0.975, 1.108)	1.028	(0.943, 1.070)

<b>A. Case-fatality rate</b>	Zero-inflated Poisson		Zero-inflated negative binomial		CAR zero-inflated Poisson with spatial random effect	
	IRR	CI	IRR	CI	IRR	CrI
NO <sub>2</sub> IQR	1.050	(0.959, 1.149)	1.194	(0.958, 1.489)	1.336	(1.127, 1.691)
Owner occupancy (%)	0.992	(0.989, 0.994)	0.991	(0.985, 0.997)	0.994	(0.988, 1.001)
> 65 years (%)	1.071	(1.061, 1.081)	1.062	(1.041, 1.084)	1.061	(1.042, 1.084)
Nonwhite (%)	1.001	(0.999, 1.003)	0.999	(0.994, 1.004)	0.998	(0.991, 1.003)
Smokers (%)	1.007	(0.994, 1.020)	1.040	(1.002, 1.080)	1.046	(0.996, 1.105)
Obese (%)	0.983	(0.978, 0.988)	0.987	(0.975, 0.999)	0.992	(0.981, 1.002)
Hospital density	0.957	(0.927, 0.989)	0.935	(0.845, 1.034)	0.957	(0.858, 1.047)
Hypertensive (%)	1.003	(0.994, 1.012)	0.998	(0.975, 1.022)	1.010	(0.998, 1.023)
Diabetic (%)	1.001	(0.980, 1.021)	0.987	(0.932, 1.045)	0.966	(0.939, 0.999)

## 2.7 Appendix C. Adjusted association of NO<sub>2</sub> and COVID-19 from three models for the period between September 8<sup>th</sup>, 2020 and February 23<sup>rd</sup>, 2021

Model conducted for sensitivity analyses using secondary time period. Adjusted association of NO<sub>2</sub> (scaled by interquartile range: 8.7 ppb) and COVID-19 from three models: A. Case rate (cases/population); B. Mortality rate (deaths/population); and C. Case-fatality rate (deaths/cases) for Los Angeles County neighborhoods (N = 335) for the period between September 8<sup>th</sup>, 2020 and February 23<sup>rd</sup>, 2021. NO<sub>2</sub> was scaled by its interquartile range for interpretation purposes; other covariates were not scaled.

<b>A. Case rate</b>	Zero-inflated Poisson		Zero-inflated negative binomial		CAR zero-inflated Poisson with spatial random effect	
	IRR	CI	IRR	CI	IRR	CrI
NO <sub>2</sub> IQR	1.285	(1.276, 1.294)	1.212	(1.017, 1.445)	1.245	(1.101, 1.422)
Owner occupancy (%)	1.000	(0.999, 1.000)	0.996	(0.991, 1.001)	0.996	(0.995, 0.999)
> 65 years (%)	0.985	(0.985, 0.986)	0.940	(0.923, 0.958)	0.990	(0.984, 0.995)
Nonwhite (%)	0.995	(0.995, 0.995)	0.990	(0.985, 0.995)	0.991	(0.990, 0.994)
Smokers (%)	1.042	(1.041, 1.043)	1.028	(0.990, 1.068)	1.040	(1.032, 1.048)
Obese (%)	1.033	(1.033, 1.034)	1.035	(1.022, 1.049)	1.039	(1.035, 1.044)
Hospital density	1.092	(1.089, 1.095)	0.885	(0.803, 0.974)	1.220	(1.176, 1.244)

<b>B. Mortality rate</b>	Zero-inflated Poisson		Zero-inflated negative binomial		CAR zero-inflated Poisson with spatial random effect	
	IRR	CI	IRR	CI	IRR	CrI
NO <sub>2</sub> IQR	1.280	(1.206, 1.358)	1.377	(1.135, 1.671)	1.767	(1.339, 2.141)
Owner occupancy (%)	0.997	(0.995, 0.998)	0.999	(0.993, 1.004)	1.000	(0.996, 1.008)
> 65 years (%)	1.025	(1.019, 1.030)	0.980	(0.960, 1.002)	1.002	(0.980, 1.023)
Nonwhite (%)	1.000	(0.999, 1.001)	1.002	(0.997, 1.006)	1.003	(0.999, 1.007)
Smokers (%)	1.043	(1.035, 1.052)	1.040	(1.005, 1.076)	1.023	(0.991, 1.054)
Obese (%)	1.020	(1.017, 1.023)	1.015	(1.004, 1.027)	1.020	(1.006, 1.037)
Hospital density	1.100	(1.076, 1.124)	1.018	(0.929, 1.116)	1.074	(0.984, 1.142)

<b>C. Case-fatality rate</b>	Zero-inflated Poisson		Zero-inflated negative binomial		CAR zero-inflated Poisson with spatial random effect	
	IRR	CI	IRR	CI	IRR	CrI
NO <sub>2</sub> IQR	1.036	(0.977, 1.098)	1.087	(0.944, 1.251)	1.154	(1.004, 1.348)
Owner occupancy (%)	0.996	(0.995, 0.998)	0.999	(0.995, 1.003)	0.999	(0.996, 1.003)
> 65 years (%)	1.053	(1.047, 1.059)	1.037	(1.022, 1.052)	1.035	(1.018, 1.052)
Nonwhite (%)	1.005	(1.003, 1.006)	1.003	(1.000, 1.007)	1.004	(1.002, 1.007)
Smokers (%)	1.003	(0.995, 1.011)	1.008	(0.983, 1.032)	0.999	(0.977, 1.020)
Obese (%)	0.991	(0.988, 0.995)	0.991	(0.984, 0.999)	0.992	(0.985, 1.001)
Hospital density	1.011	(0.990, 1.033)	1.022	(0.960, 1.087)	1.038	(0.967, 1.105)

## 2.8 REFERENCES FOR CHAPTER 2

- Abel, M., Hannon, J., Mullineaux, D., Beighle, A., 2011. Determination of step rate thresholds corresponding to physical activity intensity classifications in adults. *J. Phys. Act. Heal.* 8, 45–51. <https://doi.org/10.1123/JPAH.8.1.45>
- Actigraph Corp, 2019. What's the difference among the Cut Points available in ActiLife? [WWW Document]. URL <https://actigraphcorp.my.site.com/support/s/article/What-s-the-difference-among-the-Cut-Points-available-in-ActiLife> (accessed 5.2.22).
- Ailshire, J., García, C., 2018. Unequal places: The impacts of socioeconomic and race/ethnic differences in neighborhoods. *Generations* 42.
- Alaimo, P., Loro, D., Mingione, M., Lipsitt, J., Jerrett, M., Banerjee, S., 2021. Bayesian Hierarchical Modeling and Analysis for Physical Activity Trajectories Using Actigraph Data. arxiv Pre-Print, 1–36. <https://doi.org/https://arxiv.org/abs/2101.01624>
- Almanza, E., Jerrett, M., Dunton, G., Seto, E., Ann Pentz, M., 2012. A study of community design, greenness, and physical activity in children using satellite, GPS and accelerometer data. *Health Place* 18, 46–54. <https://doi.org/10.1016/j.healthplace.2011.09.003>
- Almaraz, M., Bai, E., Wang, C., Trousdell, J., Conley, S., Faloona, I., Houlton, B.Z., 2018. Agriculture is a major source of NO<sub>x</sub> pollution in California. *Sci. Adv.* 4. <https://doi.org/10.1126/sciadv.aao3477>
- Alvarado, K., Hewitt, A., 2017. Bruin Bike Share now reaches from Santa Monica to West Hollywood | UCLA [WWW Document]. UCLA Newsroom. URL <https://newsroom.ucla.edu/stories/bruin-bike-share-now-reaches-from-santa-monica-to-west-hollywood> (accessed 5.2.22).
- Amoly, E., Dadvand, P., Forn, J., López-Vicente, M., Basagaña, X., Julvez, J., Alvarez-Pedrerol, M., Nieuwenhuijsen, M.J., Sunyer, J., 2015. Green and blue spaces and behavioral development in barcelona schoolchildren: The BREATHE project. *Environ. Health Perspect.* 122. <https://doi.org/10.1289/ehp.1408215>
- Anderson, T.K., 2009. Kernel density estimation and K-means clustering to profile road accident hotspots. *Accid. Anal. Prev.* 41. <https://doi.org/10.1016/j.aap.2008.12.014>
- Apte, J.S., Messier, K.P., Gani, S., Brauer, M., Kirchstetter, T.W., Lunden, M.M., Marshall, J.D., Portier, C.J., Vermeulen, R.C.H., Hamburg, S.P., 2017. High-Resolution Air Pollution Mapping with Google Street View Cars: Exploiting Big Data. *Environ. Sci. Technol.* 51. <https://doi.org/10.1021/acs.est.7b00891>
- Auchincloss, A.H., Diez Roux, A. V, Mujahid, M.S., Shen, M., Bertoni, A.G., Carnethon, M.R.,

2009. Neighborhood resources for physical activity and healthy foods and incidence of type 2 diabetes mellitus: the Multi-Ethnic study of Atherosclerosis. *Arch. Intern. Med.* 169, 1698–1704. <https://doi.org/10.1001/archinternmed.2009.302>
- Avila-Palencia, I., Int Panis, L., Dons, E., Gaupp-Berghausen, M., Raser, E., Götschi, T., Gerike, R., Brand, C., de Nazelle, A., Orjuela, J.P., Anaya-Boig, E., Stigell, E., Kahlmeier, S., Iacorossi, F., Nieuwenhuijsen, M.J., 2018. The effects of transport mode use on self-perceived health, mental health, and social contact measures: A cross-sectional and longitudinal study. *Environ. Int.* 120. <https://doi.org/10.1016/j.envint.2018.08.002>
- Aybar, C., Wu, Q., Bautista, L., Yali, R., Barja, A., 2020. rgee: An R package for interacting with Google Earth Engine. *J. Open Source Softw.*
- Bai, L., Chen, H., Hatzopoulou, M., Jerrett, M., Kwong, J.C., Burnett, R.T., Van Donkelaar, A., Copes, R., Martin, R. V., Van Ryswyk, K., Lu, H., Kopp, A., Weichenthal, S., 2018. Exposure to ambient ultrafine particles and nitrogen dioxide and incident hypertension and diabetes. *Epidemiology* 29. <https://doi.org/10.1097/EDE.0000000000000798>
- Bakrania, K., Edwardson, C.L., Khunti, K., Henson, J., Stamatakis, E., Hamer, M., Davies, M.J., Yates, T., 2017. Associations of objectively measured moderate-to-vigorous-intensity physical activity and sedentary time with all-cause mortality in a population of adults at high risk of type 2 diabetes mellitus. *Prev. Med. Reports* 5, 285–288. <https://doi.org/10.1016/j.pmedr.2017.01.013>
- Banerjee, A., Pasea, L., Harris, S., Gonzalez-Izquierdo, A., Torralbo, A., Shallcross, L., Noursadeghi, M., Pillay, D., Sebire, N., Holmes, C., Pagel, C., Wong, W.K., Langenberg, C., Williams, B., Denaxas, S., Hemingway, H., 2020. Estimating excess 1-year mortality associated with the COVID-19 pandemic according to underlying conditions and age: a population-based cohort study. *Lancet* 395. [https://doi.org/10.1016/S0140-6736\(20\)30854-0](https://doi.org/10.1016/S0140-6736(20)30854-0)
- Bates, D., Mächler, M., Bolker, B., Walker, S., 2015. Fitting Linear Mixed-Effects Models Using {lme4}. *J. Stat. Softw.* 67, 1–48. <https://doi.org/10.18637/jss.v067.i01>
- Beekhuizen, J., Kromhout, H., Huss, A., Vermeulen, R., 2013. Performance of GPS-devices for environmental exposure assessment. *J. Expo. Sci. Environ. Epidemiol.* 23. <https://doi.org/10.1038/jes.2012.81>
- Beelen, R., Hoek, G., van den Brandt, P.A., Goldbohm, R.A., Fischer, P., Schouten, L.J., Jerrett, M., Hughes, E., Armstrong, B., Brunekreef, B., 2008. Long-term effects of traffic-related air pollution on mortality in a Dutch cohort (NLCS-AIR study). *Environ. Health Perspect.* 116, 196–202. <https://doi.org/10.1289/ehp.10767>

- Benzinger, T.H., 1959. ON PHYSICAL HEAT REGULATION AND THE SENSE OF TEMPERATURE IN MAN. *Proc. Natl. Acad. Sci.* 45, 645. <https://doi.org/10.1073/pnas.45.4.645>
- Berg, K., Romer Present, P., Richardson, K., 2021. Long-term air pollution and other risk factors associated with COVID-19 at the census tract level in Colorado. *Environ. Pollut.* 287. [https://doi.org/10.1016/J.ENVPOL.2021.117584/LONG\\_TERM\\_AIR\\_POLLUTION\\_AND\\_OTHER\\_RISK\\_FACTORS\\_ASSOCIATED\\_WITH\\_COVID\\_19\\_AT\\_THE\\_CENSUS\\_TRACT\\_LEVEL\\_IN\\_COLORADO.PDF](https://doi.org/10.1016/J.ENVPOL.2021.117584/LONG_TERM_AIR_POLLUTION_AND_OTHER_RISK_FACTORS_ASSOCIATED_WITH_COVID_19_AT_THE_CENSUS_TRACT_LEVEL_IN_COLORADO.PDF)
- Bergman, A., Sella, Y., Agre, P., Casadevall, A., 2020. Oscillations in U.S. COVID-19 Incidence and Mortality Data Reflect Diagnostic and Reporting Factors. *mSystems* 5. <https://doi.org/10.1128/msystems.00544-20>
- Bialek, S., Bowen, V., Chow, N., Curns, A., Gierke, R., Hall, A., Hughes, M., Pilishvili, T., Ritchey, M., Roguski, K., Silk, B., Skoff, T., Sundararaman, P., Ussery, E., Vasser, M., Whitham, H., Wen, J., 2020. Geographic Differences in COVID-19 Cases, Deaths, and Incidence — United States, February 12–April 7, 2020. *MMWR. Morb. Mortal. Wkly. Rep.* 69, 465–471. <https://doi.org/10.15585/mmwr.mm6915e4>
- Bivand, R., Keitt, T., Rowlingson, B., 2021. rgdal: Bindings for the “Geospatial” Data Abstraction Library.
- Boakye, K.A., Amram, O., Schuna, J.M., Duncan, G.E., Hystad, P., 2021. GPS-based built environment measures associated with adult physical activity. *Heal. Place* 70. <https://doi.org/10.1016/j.healthplace.2021.102602>
- Bowler, D.E., Buyung-Ali, L., Knight, T.M., Pullin, A.S., 2010a. Urban greening to cool towns and cities: A systematic review of the empirical evidence. *Landsc. Urban Plan.* <https://doi.org/10.1016/j.landurbplan.2010.05.006>
- Bowler, D.E., Buyung-Ali, L.M., Knight, T.M., Pullin, A.S., 2010b. A systematic review of evidence for the added benefits to health of exposure to natural environments. *BMC Public Health* 10. <https://doi.org/10.1186/1471-2458-10-456>
- Brandt, E.B., Beck, A.F., Mersha, T.B., 2020. Air pollution, racial disparities, and COVID-19 mortality. *J. Allergy Clin. Immunol.* <https://doi.org/10.1016/j.jaci.2020.04.035>
- Branion-Calles, M., Götschi, T., Nelson, T., Anaya-Boig, E., Avila-Palencia, I., Castro, A., Cole-Hunter, T., de Nazelle, A., Dons, E., Gaupp-Berghausen, M., Gerike, R., Int Panis, L., Kahlmeier, S., Nieuwenhuijsen, M., Rojas-Rueda, D., Winters, M., 2020. Cyclist crash rates and risk factors in a prospective cohort in seven European cities. *Accid. Anal. Prev.* 141. <https://doi.org/10.1016/j.aap.2020.105540>

- Brooke Anderson, G., Bell, M.L., Peng, R.D., 2013. Methods to calculate the heat index as an exposure metric in environmental health research. *Environ. Health Perspect.* <https://doi.org/10.1289/ehp.1206273>
- Bui, R., Buliung, R.N., Remmel, T.K., 2012. aspace: A collection of functions for estimating centrographic statistics and computational geometries for spatial point patterns.
- Burr, J.A., Mutchler, J.E., Gerst, K., 2010. Patterns of residential crowding among Hispanics in later life: immigration, assimilation, and housing market factors. *J. Gerontol. B. Psychol. Sci. Soc. Sci.* 65, 772–782. <https://doi.org/10.1093/geronb/gbq069>
- CADPH, 2020. CDC Confirms Possible First Instance of COVID-19 Community Transmission in California [WWW Document]. URL <https://www.cdph.ca.gov/Programs/OPA/Pages/NR20-006.aspx> (accessed 11.10.20).
- Calenge, C., 2006. The package adehabitat for the R software: tool for the analysis of space and habitat use by animals. *Ecol. Modell.* 197, 1035.
- Caltrans, 2020. Highway Performance Monitoring System (HPMS) Data [WWW Document]. URL <https://dot.ca.gov/programs/research-innovation-system-information/highway-performance-monitoring-system> (accessed 5.2.22).
- Campello, R.J.G.B., Moulavi, D., Sander, J., 2013. Density-Based Clustering Based on Hierarchical Density Estimates.
- Case, M.A., Burwick, H.A., Volpp, K.G., Patel, M.S., 2015. Accuracy of Smartphone Applications and Wearable Devices for Tracking Physical Activity Data. *JAMA* 313, 625–626. <https://doi.org/10.1001/JAMA.2014.17841>
- Centers for Disease Control and Prevention, 2020. COVIDView: A Weekly Surveillance Summary of US. COVID-19 Activity [WWW Document]. URL <https://www.cdc.gov/coronavirus/2019-ncov/covid-data/pdf/covidview-07-24-2020.pdf> (accessed 10.30.20).
- Centers for Disease Control and Prevention, 2019. 500 Cities Project: Local data for better health | Home page | CDC [WWW Document]. URL <https://www.cdc.gov/500cities/> (accessed 11.10.20).
- Chaix, B., Méline, J., Duncan, S., Merrien, C., Karusisi, N., Perchoux, C., Lewin, A., Labadi, K., Kestens, Y., 2013. GPS tracking in neighborhood and health studies: A step forward for environmental exposure assessment, a step backward for causal inference? *Health Place* 21, 46–51. <https://doi.org/10.1016/j.healthplace.2013.01.003>
- Chan, C.B., Ryan, D.A.J., Tudor-Locke, C., 2006. Relationship between objective measures of physical activity and weather: A longitudinal study. *Int. J. Behav. Nutr. Phys. Act.* 3, 1–9. <https://doi.org/10.1186/1479-5868-3-21/FIGURES/2>

- Charreire, H., Casey, R., Salze, P., Simon, C., Chaix, B., Banos, A., Badariotti, D., Weber, C., Oppert, J.M., 2010. Measuring the food environment using geographical information systems: A methodological review. *Public Health Nutr.* <https://doi.org/10.1017/S1368980010000753>
- Chen, Y.-C., Dobra, A., 2017. Measuring Human Activity Spaces With Density Ranking Based on GPS Data 1–28.
- Chew, V., 1966. Confidence, Prediction, and Tolerance Regions for the Multivariate Normal Distribution. *J. Am. Stat. Assoc.* 61. <https://doi.org/10.1080/01621459.1966.10480892>
- Ciencewicki, J., Jaspers, I., 2007. Air Pollution and Respiratory Viral Infection. *Inhal. Toxicol.* 19, 1135–1146. <https://doi.org/10.1080/08958370701665434>
- Clark, L.P., Millet, D.B., Marshall, J.D., 2014. National patterns in environmental injustice and inequality: Outdoor NO<sub>2</sub> air pollution in the United States. *PLoS One* 9. <https://doi.org/10.1371/journal.pone.0094431>
- Coker, E.S., Cavalli, L., Fabrizi, E., Guastella, G., Lippo, E., Parisi, M.L., Pontarollo, N., Rizzati, M., Varacca, A., Vergalli, S., 2020. The Effects of Air Pollution on COVID-19 Related Mortality in Northern Italy. *Environ. Resour. Econ.* 76. <https://doi.org/10.1007/s10640-020-00486-1>
- Collaco, J.M., Morrow, M., Rice, J.L., McGrath-Morrow, S.A., 2020. Impact of road proximity on infants and children with bronchopulmonary dysplasia. *Pediatr. Pulmonol.* 55. <https://doi.org/10.1002/ppul.24594>
- Comodore-Mensah, Y., Selvin, E., Aboagye, J., Turkson-Ocran, R.A., Li, X., Himmelfarb, C.D., Ahima, R.S., Cooper, L.A., 2018. Hypertension, overweight/obesity, and diabetes among immigrants in the United States: An analysis of the 2010-2016 National Health Interview Survey. *BMC Public Health.* <https://doi.org/10.1186/s12889-018-5683-3>
- Cui, Y., Zhang, Z.-F., Froines, J., Zhao, J., Wang, H., Yu, S.-Z., Detels, R., 2003. Air pollution and case fatality of SARS in the People's Republic of China: an ecologic study. *Environ. Heal.* 2. <https://doi.org/10.1186/1476-069x-2-15>
- Dadvand, P., de Nazelle, A., Figueras, F., Basagaña, X., Su, J., Amoly, E., Jerrett, M., Vrijheid, M., Sunyer, J., Nieuwenhuijsen, M.J., 2012a. Green space, health inequality and pregnancy. *Environ. Int.* 40. <https://doi.org/10.1016/j.envint.2011.07.004>
- Dadvand, P., de Nazelle, A., Triguero-Mas, M., Schembari, A., Cirach, M., Amoly, E., Figueras, F., Basagaña, X., Ostro, B., Nieuwenhuijsen, M., 2012b. Surrounding greenness and exposure to air pollution during pregnancy: An analysis of personal monitoring data. *Environ. Health Perspect.* 120. <https://doi.org/10.1289/ehp.1104609>

- Dadvand, P., Villanueva, C.M., Font-Ribera, L., Martinez, D., Basagaña, X., Belmonte, J., Vrijheid, M., Gražulevičienė, R., Kogevinas, M., Nieuwenhuijsen, M.J., 2015. Risks and benefits of green spaces for children: A cross-sectional study of associations with sedentary behavior, obesity, asthma, and allergy. *Environ. Health Perspect.* 122. <https://doi.org/10.1289/ehp.1308038>
- Dales, R., Wheeler, A., Mahmud, M., Frescura, A.M., Smith-Doiron, M., Nethery, E., Liu, L., 2008. The Influence of Living Near Roadways on Spirometry and Exhaled Nitric Oxide in Elementary Schoolchildren. *Environ. Health Perspect.* 116, 1423–1427. <https://doi.org/10.1289/ehp.10943>
- Dance, J., 2018. Moves is shutting down. Here are alternatives. [WWW Document]. Medium.com. URL <https://joshdance.medium.com/moves-is-shutting-down-here-are-alternatives-8341aae695b4> (accessed 5.2.22).
- de Nazelle, A., Smeds, E., Anaya Boig, E., Wang, C., Sanchez, J., Dons, E., Kahlmeier, S., Iacorossi, F., Wegener, S., Nieuwenhuijsen, M., Rojas-Rueda, D., Avila-Palencia, I., Götschi, T., 2017. A Comparison between Literature Findings and Stakeholder Perspectives on Active Travel Promotion. *J. Transp. Heal.* 5. <https://doi.org/10.1016/j.jth.2017.05.216>
- Deeks, J.J., Dinnes, J., D'Amico, R., Sowden, A.J., Sakaravitch, C., Song, F., Petticrew, M., Altman, D.G., 2003. Evaluating non-randomised intervention studies. *Health Technol. Assess. (Rockv)*. <https://doi.org/10.3310/hta7270>
- Dempsey, D., Kelliher, F., 2018. *Industry Trends in Cloud Computing*. Springer International Publishing, Cham.
- Diaz, F., Freato, R., 2018. *Cloud Data Design, Orchestration, and Management Using Microsoft Azure: Master and Design a Solution Leveraging the Azure Data Platform*. Apress.
- Divens, L.L., Chatmon, B.N., 2019. Cardiovascular Disease Management in Minority Women: Special Considerations. *Crit. Care Nurs. Clin. North Am.* <https://doi.org/10.1016/j.cnc.2018.11.004>
- Dixon, J., Tredoux, C., Davies, G., Huck, J., Hocking, B., Sturgeon, B., Whyatt, D., Jarman, N., Bryan, D., 2020. Parallel lives: Intergroup contact, threat, and the segregation of everyday activity spaces. *J. Pers. Soc. Psychol.* 118. <https://doi.org/10.1037/pspi0000191>
- Dohrn, I.-M., Sjöström, M., Kwak, L., Oja, P., Hagströmer, M., 2018. Accelerometer-measured sedentary time and physical activity—A 15 year follow-up of mortality in a Swedish population-based cohort. *J. Sci. Med. Sport* 21, 702–707. <https://doi.org/10.1016/j.jsams.2017.10.035>
- Donaire-Gonzalez, D., de Nazelle, A., Seto, E., Mendez, M., Nieuwenhuijsen, M.J., Jerrett, M.,

2013. Comparison of Physical Activity Measures Using Mobile Phone-Based CalFit and Actigraph. *J. Med. Internet Res.* 15, e111. <https://doi.org/10.2196/jmir.2470>
- Dong, C., MacDonald, G., Okin, G.S., Gillespie, T.W., 2019. Quantifying drought sensitivity of mediterranean climate vegetation to recent warming: A case study in Southern California. *Remote Sens.* 11. <https://doi.org/10.3390/rs11242902>
- Dons, E., Götschi, T., Nieuwenhuijsen, M., De Nazelle, A., Anaya, E., Avila-Palencia, I., Brand, C., Cole-Hunter, T., Gaupp-Berghausen, M., Kahlmeier, S., Laeremans, M., Mueller, N., Orjuela, J.P., Raser, E., Rojas-Rueda, D., Standaert, A., Stigell, E., Uhlmann, T., Gerike, R., Int Panis, L., 2015. Physical Activity through Sustainable Transport Approaches (PASTA): protocol for a multi-centre, longitudinal study Energy balance-related behaviours. *BMC Public Health* 15. <https://doi.org/10.1186/s12889-015-2453-3>
- Du, Y., Lv, Y., Zha, W., Zhou, N., Hong, X., 2020. Association of Body mass index (BMI) with Critical COVID-19 and in-hospital Mortality: a dose-response meta-analysis. *Metabolism.* 154373. <https://doi.org/10.1016/j.metabol.2020.154373>
- Dunton, G.F., Almanza, E., Jerrett, M., Wolch, J., Pentz, M.A., 2014. Neighborhood park use by children: Use of accelerometry and global positioning systems. *Am. J. Prev. Med.* 46. <https://doi.org/10.1016/j.amepre.2013.10.009>
- Dzhambov, A., Hartig, T., Markevych, I., Tilov, B., Dimitrova, D., 2018. Urban residential greenspace and mental health in youth: Different approaches to testing multiple pathways yield different conclusions. *Environ. Res.* 160. <https://doi.org/10.1016/j.envres.2017.09.015>
- Eddelbuettel, D., 2018. CRAN Task View: High-Performance and Parallel Computing with R.
- Erdogan, S., Yilmaz, I., Baybura, T., Gullu, M., 2008. Geographical information systems aided traffic accident analysis system case study: city of Afyonkarahisar. *Accid. Anal. Prev.* 40. <https://doi.org/10.1016/j.aap.2007.05.004>
- ESRI, 2020. ArcGIS Desktop: Release 10. Redlands, CA: Environmental Systems Research Institute.
- Evenson, K.R., Catellier, D.J., Gill, K., Ondrak, K.S., McMurray, R.G., 2008. Calibration of two objective measures of physical activity for children. *J. Sports Sci.* 26. <https://doi.org/10.1080/02640410802334196>
- Evenson, K.R., Goto, M.M., Furberg, R.D., 2015. Systematic review of the validity and reliability of consumer-wearable activity trackers. *Int. J. Behav. Nutr. Phys. Act.* 12. <https://doi.org/10.1186/s12966-015-0314-1>
- Federal Highway Administration, 2019. FHWA Office of Highway Policy Information Fact Sheet: The 25 Most Traveled Route Locations by Annual Daily Traffic (AADT) [WWW Document].

- URL <https://www.fhwa.dot.gov/policyinformation/tables/02.cfm> (accessed 5.2.22).
- Federico, F., Rauser, C., Gold, M., 2017. 2017 Sustainable LA Grand Challenge Environmental Report Card for Los Angeles County Energy and Air Quality [WWW Document]. Univ. Calif. Escholarsh. URL <https://escholarship.org/uc/item/6xj45381> (accessed 5.2.22).
- Franklin, B.A., Brook, R., Arden Pope, C. 3rd, 2015. Air pollution and cardiovascular disease. *Curr. Probl. Cardiol.* 40, 207–238. <https://doi.org/10.1016/j.cpcardiol.2015.01.003>
- Freedson, P., Melanson, E., Sirard, J., 1998. Calibration of the Computer Science and Applications, Inc. accelerometer. *Med. Sci. Sport. Exerc.* 30.
- Fuertes, E., Markevych, I., Bowatte, G., Gruzieva, O., Gehring, U., Becker, A., Berdel, D., von Berg, A., Bergström, A., Brauer, M., Brunekreef, B., Brüske, I., Carlsten, C., Chan-Yeung, M., Dharmage, S.C., Hoffmann, B., Klümper, C., Koppelman, G.H., Kozyrskyj, A., Korek, M., Kull, I., Lodge, C., Lowe, A., MacIntyre, E., Pershagen, G., Standl, M., Sugiri, D., Wijga, A., Heinrich, J., 2016. Residential greenness is differentially associated with childhood allergic rhinitis and aeroallergen sensitization in seven birth cohorts. *Allergy Eur. J. Allergy Clin. Immunol.* 71. <https://doi.org/10.1111/all.12915>
- Gaither, C.J., Afrin, S., Garcia-Menendez, F., Odman, M.T., Huang, R., Goodrick, S., da Silva, A.R., 2019. African american exposure to prescribed fire smoke in Georgia, USA. *Int. J. Environ. Res. Public Health* 16. <https://doi.org/10.3390/ijerph16173079>
- Garcetti, E., 2019. L.A.'s Green New Deal: Sustainable City Plan 2019. Los Angeles.
- Gascon, M., Triguero-Mas, M., Martínez, D., Dadvand, P., Rojas-Rueda, D., Plasència, A., Nieuwenhuijsen, M.J., 2016. Residential green spaces and mortality: A systematic review. *Environ. Int.* 86, 60–67. <https://doi.org/10.1016/j.envint.2015.10.013>
- Gastin, P.B., Cayzer, C., Dwyer, D., Robertson, S., 2018. Validity of the ActiGraph GT3X+ and BodyMedia SenseWear Armband to estimate energy expenditure during physical activity and sport. *J. Sci. Med. Sport* 21, 291–295. <https://doi.org/10.1016/j.jsams.2017.07.022>
- Gerike, R., De Nazelle, A., Nieuwenhuijsen, M., Panis, L.I., Anaya, E., Avila-Palencia, I., Boschetti, F., Brand, C., Cole-Hunter, T., Dons, E., Eriksson, U., Gaupp-Berghausen, M., Kahlmeier, S., Laeremans, M., Mueller, N., Orjuela, J.P., Racioppi, F., Raser, E., Rojas-Rueda, D., Schweizer, C., Standaert, A., Uhlmann, T., Wegener, S., Götschi, T., 2016. Physical Activity through Sustainable Transport Approaches (PASTA): A study protocol for a multicentre project. *BMJ Open* 6. <https://doi.org/10.1136/bmjopen-2015-009924>
- Gething, P.W., Noor, A.M., Gikandi, P.W., Ogara, E.A.A., Hay, S.I., Nixon, M.S., Snow, R.W., Atkinson, P.M., 2006. Improving imperfect data from health management information systems in Africa using space-time geostatistics. *PLoS Med.* 3.

<https://doi.org/10.1371/journal.pmed.0030271>

- Glaeser, E.L., Kominers, S.D., Luca, M., Naik, N., 2018. BIG DATA AND BIG CITIES: THE PROMISES AND LIMITATIONS OF IMPROVED MEASURES OF URBAN LIFE. *Econ. Inq.* 56, 114–137. <https://doi.org/10.1111/ecin.12364>
- GlobalSat WorldCom Corporation, 2022a. BT-335 Bluetooth Data Logger User Manual [WWW Document]. URL <https://www.gpscentral.ca/products/usglobalsat/bt-335-user-manual.pdf> (accessed 5.9.22).
- GlobalSat WorldCom Corporation, 2022b. DG-500 GPS Data Logger Quick Start Guide [WWW Document]. URL [https://www.globalsat.com.tw/ftp/download/DG-500\\_QSG\\_ENG\\_V1.3\\_20170105.pdf](https://www.globalsat.com.tw/ftp/download/DG-500_QSG_ENG_V1.3_20170105.pdf) (accessed 5.9.22).
- Gong, L., Sato, H., Yamamoto, T., Miwa, T., Morikawa, T., 2015. Identification of activity stop locations in GPS trajectories by density-based clustering method combined with support vector machines. *J. Mod. Transp.* 23. <https://doi.org/10.1007/s40534-015-0079-x>
- Google Inc., 2022. Reducer Overview | Google Earth Engine [WWW Document]. URL [https://developers.google.com/earth-engine/guides/reducers\\_intro](https://developers.google.com/earth-engine/guides/reducers_intro) (accessed 5.6.22).
- Götschi, Thomas, de Nazelle, Audrey, Brand, Christian, Gerike, Regine, Alasya, B., Anaya, E., Avila-Palencia, I., Banister, D., Bartana, I., Benvenuti, F., Boschetti, F., Brand, C., Buekers, J., Carniel, L., Carrasco Turigas, G., Castro, A., Cianfano, M., Clark, A., Cole-Hunter, T., Copley, V., De Boever, P., de Nazelle, A., Dimajo, C., Dons, E., Duran, M., Eriksson, U., Franzen, H., Gaupp-Berghausen, M., Gerike, R., Girmenia, R., Götschi, T., Hartmann, F., Iacorossi, F., Int Panis, L., Kahlmeier, S., Khreis, H., Laeremans, M., Martinez, T., Meschik, M., Michelle, P., Muehlmann, P., Mueller, N., Nieuwenhuijsen, M., Nilsson, A., Nussio, F., Orjuela Mendoza, J.P., Pisanti, S., Porcel, J., Racioppi, F., Raser, E., Riegler, S., Robrecht, H., Rojas Rueda, D., Rothballer, C., Sanchez, J., Schaller, A., Schuthof, R., Schweizer, C., Sillero, A., Smidfeltrosqvist, L., Spezzano, G., Standaert, A., Stigell, E., Surace, M., Uhlmann, T., Vancluysen, K., Wegener, S., Wennberg, H., Willis, G., Witzell, J., Zeuschner, V., 2017. Towards a Comprehensive Conceptual Framework of Active Travel Behavior: a Review and Synthesis of Published Frameworks. *Curr. Environ. Heal. reports.* <https://doi.org/10.1007/s40572-017-0149-9>
- Graham, M., Shelton, T., 2013. Geography and the future of big data, big data and the future of geography. *Dialogues Hum. Geogr.* 3, 255–261. <https://doi.org/10.1177/2043820613513121>
- Gupta, A., Bherwani, H., Gautam, S., Anjum, S., Musugu, K., Kumar, N., Anshul, A., Kumar, R., 2021. Air pollution aggravating COVID-19 lethality? Exploration in Asian cities using statistical models. *Environ. Dev. Sustain.* 23. <https://doi.org/10.1007/s10668-020-00878-9>

- Hahsler, M., Piekenbrock, M., 2021. dbscan: Density Based Clustering of Applications with Noise (DBSCAN) and Related Algorithms.
- Hamada, S., Ohta, T., 2010. Seasonal variations in the cooling effect of urban green areas on surrounding urban areas. *Urban For. Urban Green.* 9, 15–24. <https://doi.org/10.1016/J.UFUG.2009.10.002>
- Harris, J.E., 2020. Understanding the Los Angeles County coronavirus epidemic: The critical role of intrahousehold transmission. medRxiv. <https://doi.org/10.1101/2020.10.11.20211045>
- Hayhoe, K., Cayan, D., Field, C.B., Frumhoff, P.C., Maurer, E.P., Miller, N.L., Moser, S.C., Schneider, S.H., Cahill, K.N., Cleland, E.E., Dale, L., Drapek, R., Hanemann, R.M., Kalkstein, L.S., Lenihan, J., Lunch, C.K., Neilson, R.P., Sheridan, S.C., Verville, J.H., 2004. Emissions pathways, climate change, and impacts on California. *Proc. Natl. Acad. Sci. U. S. A.* 101, 12422–12427. [https://doi.org/10.1073/PNAS.0404500101/SUPPL\\_FILE/04500FIG17.JPG](https://doi.org/10.1073/PNAS.0404500101/SUPPL_FILE/04500FIG17.JPG)
- Heinzerling, A., Stuckey, M.J., Scheuer, T., Xu, K., Perkins, K.M., Resseger, H., Magill, S., Verani, J.R., Jain, S., Acosta, M., Epton, E., 2020. Transmission of COVID-19 to Health Care Personnel During Exposures to a Hospitalized Patient — Solano County, California, February 2020. *MMWR. Morb. Mortal. Wkly. Rep.* 69. <https://doi.org/10.15585/mmwr.mm6915e5>
- Hekler, E.B., Buman, M.P., Grieco, L., Rosenberger, M., Winter, S.J., Haskell, W., King, A.C., 2015. Validation of Physical Activity Tracking via Android Smartphones Compared to ActiGraph Accelerometer: Laboratory-Based and Free-Living Validation Studies. *JMIR mHealth uHealth* 3, e36. <https://doi.org/10.2196/mhealth.3505>
- Higgs, G., Fry, R., Langford, M., 2012. Investigating the Implications of Using Alternative GIS-Based Techniques to Measure Accessibility to Green Space. *Environ. Plan. B Plan. Des.* 39, 326–343. <https://doi.org/10.1068/b37130>
- Hijmans, R.J., 2021. raster: Geographic Data Analysis and Modeling.
- Hirsch, Jana A, Winters, M., Clarke, P., McKay, H., 2014. Generating GPS activity spaces that shed light upon the mobility habits of older adults : a descriptive analysis 1–14.
- Hirsch, Jana A., Winters, M., Clarke, P., McKay, H., 2014. Generating GPS activity spaces that shed light upon the mobility habits of older adults: A descriptive analysis. *Int. J. Health Geogr.* 13, 1–14. <https://doi.org/10.1186/1476-072X-13-51>
- Ho, J.Y., Zijlema, W.L., Triguero-Mas, M., Donaire-Gonzalez, D., Valentín, A., Ballester, J., Chan, E.Y.Y., Goggins, W.B., Mo, P.K.H., Kruize, H., van den Berg, M., Gražuleviciene, R., Gidlow, C.J., Jerrett, M., Seto, E.Y.W., Barrera-Gómez, J., Nieuwenhuijsen, M.J., 2021. Does

- surrounding greenness moderate the relationship between apparent temperature and physical activity? Findings from the PHENOTYPE project. *Environ. Res.* 197, 110992. <https://doi.org/10.1016/J.ENVRES.2021.110992>
- Höchstmann, C., Knaier, R., Eymann, J., Hintermann, J., Infanger, D., Schmidt-Trucksäss, A., 2018. Validity of activity trackers, smartphones, and phone applications to measure steps in various walking conditions. *Scand. J. Med. Sci. Sport.* 28. <https://doi.org/10.1111/sms.13074>
- Holliday, K.M., Howard, A.G., Emch, M., Rodríguez, D.A., Evenson, K.R., 2017. Are buffers around home representative of physical activity spaces among adults? *Heal. Place* 45, 181–188. <https://doi.org/10.1016/j.healthplace.2017.03.013>
- Holt, J.B., Lo, C.P., Hodler, T.W., 2013. Dasymetric Estimation of Population Density and Areal Interpolation of Census Data. <http://dx.doi.org/10.1559/1523040041649407> 31, 103–121. <https://doi.org/10.1559/1523040041649407>
- Huang, G., Blangiardo, M., Brown, P.E., Pirani, M., 2021. Long-term exposure to air pollution and COVID-19 incidence: A multi-country study. *Spat. Spatiotemporal. Epidemiol.* 39, 100443. <https://doi.org/10.1016/J.SSTE.2021.100443>
- Humpel, N., 2002. Environmental factors associated with adults' participation in physical activity A review. *Am. J. Prev. Med.* 22, 188–199. [https://doi.org/10.1016/S0749-3797\(01\)00426-3](https://doi.org/10.1016/S0749-3797(01)00426-3)
- Imboden, M.T., Nelson, M.B., Kaminsky, L.A., Montoye, A.H., 2018. Comparison of four Fitbit and Jawbone activity monitors with a research-grade ActiGraph accelerometer for estimating physical activity and energy expenditure. *Br. J. Sports Med.* 52, 844–850. <https://doi.org/10.1136/bjsports-2016-096990>
- Jacobs, A., 2009. The pathologies of big data. *Queue* 7, 10–19. <https://doi.org/10.1145/1563821.1563874>
- Jerrett, M., Almanza, E., Davies, M., Wolch, J., Dunton, G., Spruitj-Metz, D., Ann Pentz, M., 2013a. Smart growth community design and physical activity in children. *Am. J. Prev. Med.* 45, 386–392. <https://doi.org/10.1016/j.amepre.2013.05.010>
- Jerrett, M., Almanza, E., Davies, M., Wolch, J., Dunton, G., Spruitj-Metz, D., Pentz, M.A., 2013b. Smart growth community design and physical activity in children. *Am. J. Prev. Med.* 45, 386–392. <https://doi.org/10.1016/j.amepre.2013.05.010>
- Jerrett, M., Arain, A., Kanaroglou, P., Beckerman, B., Potoglou, D., Sahuvaroglu, T., Morrison, J., Giovis, C., 2005a. A review and evaluation of intraurban air pollution exposure models. *J. Expo. Anal. Environ. Epidemiol.* <https://doi.org/10.1038/sj.jea.7500388>
- Jerrett, M., Burnett, R.T., Ma, R., Pope, C.A., Krewski, D., Newbold, K.B., Thurston, G., Shi, Y., Finkelstein, N., Calle, E.E., Thun, M.J., 2005b. Spatial Analysis of Air Pollution and Mortality

- in Los Angeles. *Epidemiology* 16, 727–736.  
<https://doi.org/10.1097/01.ede.0000181630.15826.7d>
- Jerrett, M., Shankardass, K., Berhane, K., Gauderman, W.J., Künzli, N., Avol, E., Gilliland, F., Lurmann, F., Molitor, J.N., Molitor, J.T., Thomas, D.C., Peters, J., McConnell, R., 2008. Traffic-related air pollution and asthma onset in children: A prospective cohort study with individual exposure measurement. *Environ. Health Perspect.* 116, 1433–1438.  
<https://doi.org/10.1289/ehp.10968>
- Jewell, N.P., Lewnard, J.A., Jewell, B.L., 2020. Caution Warranted: Using the Institute for Health Metrics and Evaluation Model for Predicting the Course of the COVID-19 Pandemic. *Ann. Intern. Med.* <https://doi.org/10.7326/M20-1565>
- Jia, P., Xue, H., Yin, L., Stein, A., Wang, M., Wang, Y., 2019. Spatial Technologies in Obesity Research: Current Applications and Future Promise. *Trends Endocrinol. Metab.* <https://doi.org/10.1016/j.tem.2018.12.003>
- Kaisler, S., Armour, F., Espinosa, J.A., Money, W., 2013. Big Data: Issues and Challenges Moving Forward, in: 2013 46th Hawaii International Conference on System Sciences. IEEE, Wailea, HI, USA, pp. 995–1004. <https://doi.org/10.1109/HICSS.2013.645>
- Kambatla, K., Kollias, G., Kumar, V., Grama, A., 2014. Trends in big data analytics. *J. Parallel Distrib. Comput.* 74, 2561–2573. <https://doi.org/10.1016/j.jpdc.2014.01.003>
- Kamel Boulos, M.N., Resch, B., Crowley, D.N., Breslin, J.G., Sohn, G., Burtner, R., Pike, W.A., Jezierski, E., Chuang, K.-Y., 2011. Crowdsourcing, citizen sensing and sensor web technologies for public and environmental health surveillance and crisis management: trends, OGC standards and application examples. *Int. J. Health Geogr.* 10, 67. <https://doi.org/10.1186/1476-072X-10-67>
- Kamruzzaman, M., Hine, J., 2012. Analysis of rural activity spaces and transport disadvantage using a multi-method approach. *Transp. Policy* 19, 105–120. <https://doi.org/10.1016/J.TRANPOL.2011.09.007>
- Keadle, S.K., Shiroma, E.J., Freedson, P.S., Lee, I.M., 2014. Impact of accelerometer data processing decisions on the sample size, wear time and physical activity level of a large cohort study. *BMC Public Health* 14. <https://doi.org/10.1186/1471-2458-14-1210>
- Kerr, G.H., Goldberg, D.L., Anenberg, S.C., 2021. COVID-19 pandemic reveals persistent disparities in nitrogen dioxide pollution. *Proc. Natl. Acad. Sci. U. S. A.* 118. <https://doi.org/10.1073/pnas.2022409118>
- Kerr, J., Duncan, S., Schipperjin, J., 2011. Using global positioning systems in health research: A practical approach to data collection and processing. *Am. J. Prev. Med.* 41.

<https://doi.org/10.1016/j.amepre.2011.07.017>

- Klompaker, J.O., Hoek, G., Bloemsma, L.D., Gehring, U., Strak, M., Wijga, A.H., van den Brink, C., Brunekreef, B., Lebret, E., Janssen, N.A.H., 2018. Green space definition affects associations of green space with overweight and physical activity. *Environ. Res.* 160, 531–540. <https://doi.org/10.1016/J.ENVRES.2017.10.027>
- Kong, F., Yin, H., James, P., Hutyra, L.R., He, H.S., 2014. Effects of spatial pattern of greenspace on urban cooling in a large metropolitan area of eastern China. *Landsc. Urban Plan.* 128, 35–47. <https://doi.org/10.1016/j.landurbplan.2014.04.018>
- Konstantinoudis, G., Padellini, T., Bennett, J., Davies, B., Ezzati, M., Blangiardo, M., 2021. Long-term exposure to air-pollution and COVID-19 mortality in England: A hierarchical spatial analysis. *Environ. Int.* 146. <https://doi.org/10.1016/J.ENVINT.2020.106316>
- Koo, T.K., Li, M.Y., 2016. A Guideline of Selecting and Reporting Intraclass Correlation Coefficients for Reliability Research. *J. Chiropr. Med.* 15. <https://doi.org/10.1016/j.jcm.2016.02.012>
- Kooiman, T.J.M., Dontje, M.L., Sprenger, S.R., Krijnen, W.P., van der Schans, C.P., de Groot, M., 2015. Reliability and validity of ten consumer activity trackers. *BMC Sports Sci. Med. Rehabil.* 7, 24. <https://doi.org/10.1186/s13102-015-0018-5>
- Korsiak, J., Tranmer, J., Leung, M., Borghese, M.M., Aronson, K.J., 2018. Actigraph measures of sleep among female hospital employees working day or alternating day and night shifts. *J. Sleep Res.* 27, e12579. <https://doi.org/10.1111/jsr.12579>
- Kozawa, K.H., Fruin, S.A., Winer, A.M., 2009. Near-road air pollution impacts of goods movement in communities adjacent to the Ports of Los Angeles and Long Beach. *Atmos. Environ.* 43. <https://doi.org/10.1016/j.atmosenv.2009.02.042>
- Ku, P.W., Steptoe, A., Liao, Y., Sun, W.J., Chen, L.J., 2018. Prospective relationship between objectively measured light physical activity and depressive symptoms in later life. *Int. J. Geriatr. Psychiatry* 33. <https://doi.org/10.1002/gps.4672>
- Kulhánová, I., Morelli, X., Le Tertre, A., Loomis, D., Charbotel, B., Medina, S., Ormsby, J.N., Lepeule, J., Slama, R., Soerjomataram, I., 2018. The fraction of lung cancer incidence attributable to fine particulate air pollution in France: Impact of spatial resolution of air pollution models. *Environ. Int.* <https://doi.org/10.1016/j.envint.2018.09.055>
- Künzli, N., Kaiser, R., Medina, S., Studnicka, M., Chanel, O., Filliger, P., Herry, M., Horak, F., Puybonnieux-Textier, V., Quénel, P., Schneider, J., Seethaler, R., Vergnaud, J.C., Sommer, H., 2000. Public-health impact of outdoor and traffic-related air pollution: A European assessment. *Lancet* 356. [https://doi.org/10.1016/S0140-6736\(00\)02653-2](https://doi.org/10.1016/S0140-6736(00)02653-2)

- Kuznetsova, A., Brockhoff, P.B., Christensen, R.H.B., 2017. {lmerTest} Package: Tests in Linear Mixed Effects Models. *J. Stat. Softw.* 82, 1–26. <https://doi.org/10.18637/jss.v082.i13>
- Kwan, M.P., 2012a. How GIS can help address the uncertain geographic context problem in social science research. *Ann. GIS* 18. <https://doi.org/10.1080/19475683.2012.727867>
- Kwan, M.P., 2012b. The Uncertain Geographic Context Problem. *Ann. Assoc. Am. Geogr.* 102, 958–968. <https://doi.org/10.1080/00045608.2012.687349>
- LAC, 2014. Countywide Building Outlines (2014) | County Of Los Angeles Enterprise GIS [WWW Document]. URL <https://egis-lacounty.hub.arcgis.com/datasets/countywide-building-outlines-2014> (accessed 11.1.20).
- LACDPH, 2021. Los Angeles County COVID-19 Dashboard - Data Dashboard - About [WWW Document]. URL [http://dashboard.publichealth.lacounty.gov/covid19\\_surveillance\\_dashboard/](http://dashboard.publichealth.lacounty.gov/covid19_surveillance_dashboard/) (accessed 2.25.21).
- LACDPH, 2020. COVID-19 Locations & Demographics - LA County Department of Public Health [WWW Document]. URL <http://publichealth.lacounty.gov/media/coronavirus/locations.htm> (accessed 11.10.20).
- LACDPH, 2018. Department of Public Health - Health Assessment Unit - Data Topics 2018 [WWW Document]. URL <http://publichealth.lacounty.gov/ha/LACHSDataTopics2018.htm> (accessed 11.10.20).
- Lachowycz, K., Jones, A.P., Page, A.S., Wheeler, B.W., Cooper, A.R., 2012. What can global positioning systems tell us about the contribution of different types of urban greenspace to children’s physical activity? *Health Place* 18, 586–594. <https://doi.org/10.1016/j.healthplace.2012.01.006>
- Lafortezza, R., Carrus, G., Sanesi, G., Davies, C., 2009. Benefits and well-being perceived by people visiting green spaces in periods of heat stress. *Urban For. Urban Green.* 8, 97–108. <https://doi.org/10.1016/j.ufug.2009.02.003>
- Lane, N., Miluzzo, E., Lu, H., Peebles, D., Choudhury, T., Campbell, A., 2010. A survey of mobile phone sensing. *IEEE Commun. Mag.* 48, 140–150. <https://doi.org/10.1109/MCOM.2010.5560598>
- Laurent, O., Wu, J., Li, L., Milesi, C., 2013. Green spaces and pregnancy outcomes in Southern California. *Heal. Place* 24. <https://doi.org/10.1016/j.healthplace.2013.09.016>
- Lee, J.H., Davis, A.W., Yoon, S.Y., Goulias, K.G., 2016. Activity space estimation with longitudinal observations of social media data. *Transportation (Amst).* 43. <https://doi.org/10.1007/s11116-016-9719-1>

- Lee, K., Kwan, M.P., 2018. Physical activity classification in free-living conditions using smartphone accelerometer data and exploration of predicted results. *Comput. Environ. Urban Syst.* 67. <https://doi.org/10.1016/j.compenvurbsys.2017.09.012>
- Lee, N.C., Voss, C., Frazer, A.D., Hirsch, J.A., McKay, H.A., Winters, M., 2016. Does activity space size influence physical activity levels of adolescents?-A GPS study of an urban environment. *Prev. Med. Reports* 3. <https://doi.org/10.1016/j.pmedr.2015.12.002>
- Leslie, E., Sugiyama, T., Ierodiaconou, D., Kremer, P., 2010. Perceived and objectively measured greenness of neighbourhoods: Are they measuring the same thing? *Landsc. Urban Plan.* 95. <https://doi.org/10.1016/j.landurbplan.2009.11.002>
- Li, H., Xu, X.L., Dai, D.W., Huang, Z.Y., Ma, Z., Guan, Y.J., 2020. Air pollution and temperature are associated with increased COVID-19 incidence: A time series study. *Int. J. Infect. Dis.* 97. <https://doi.org/10.1016/j.ijid.2020.05.076>
- Li, R., Tong, D., 2016. Constructing human activity spaces: A new approach incorporating complex urban activity-travel. *JTRG* 56, 23–35. <https://doi.org/10.1016/j.jtrangeo.2016.08.013>
- Li, S., Dragicevic, S., Castro, F.A., Sester, M., Winter, S., Coltekin, A., Pettit, C., Jiang, B., Haworth, J., Stein, A., Cheng, T., 2016. Geospatial big data handling theory and methods: A review and research challenges. *ISPRS J. Photogramm. Remote Sens.* 115, 119–133. <https://doi.org/10.1016/j.isprsjprs.2015.10.012>
- Li, X., Zhang, C., Li, W., Ricard, R., Meng, Q., Zhang, W., 2015. Assessing street-level urban greenery using Google Street View and a modified green view index. *Urban For. Urban Green.* 14. <https://doi.org/10.1016/j.ufug.2015.06.006>
- Liang, D., Shi, L., Zhao, J., Liu, P., Sarnat, J.A., Gao, S., Schwartz, J., Liu, Y., Ebel, S.T., Scovronick, N., Chang, H.H., 2020a. Urban Air Pollution May Enhance COVID-19 Case-Fatality and Mortality Rates in the United States. *Innov.* <https://doi.org/10.1016/j.xinn.2020.100047>
- Liang, D., Shi, L., Zhao, J., Liu, P., Schwartz, J., Gao, S., Sarnat, J., Liu, Y., Ebel, S., Scovronick, N., Chang, H.H., 2020b. Urban Air Pollution May Enhance COVID-19 Case-Fatality and Mortality Rates in the United States. *medRxiv Prepr. Serv. Heal. Sci.* <https://doi.org/10.1101/2020.05.04.20090746>
- Lippi, G., Sanchis-Gomar, F., Henry, B.M., 2020. Association between environmental pollution and prevalence of coronavirus disease 2019 (COVID-19) in Italy. <https://doi.org/10.1101/2020.04.22.20075986>
- Lipsitt, J., Chan-Golston, A.M., Liu, J., Su, J., Zhu, Y., Jerrett, M., 2021. Spatial analysis of COVID-

- 19 and traffic-related air pollution in Los Angeles. *Environ. Int.* <https://doi.org/10.1016/j.envint.2021.106531>
- Los Angeles County, 2018. LA County: Our County - Landscapes and Ecosystems [WWW Document]. Our Cty. Landscapes Ecosyst. Brief. URL [https://ourcountyla.lacounty.gov/wp-content/uploads/2018/10/Our-County-Landscapes-and-Ecosystems-Briefing\\_For-Web.pdf](https://ourcountyla.lacounty.gov/wp-content/uploads/2018/10/Our-County-Landscapes-and-Ecosystems-Briefing_For-Web.pdf) (accessed 5.2.22).
- Los Angeles County, 2012. County of Los Angeles: Bicycle Master Plan, Final Plan.
- Los Angeles Times, 2020. California confirms 2 cases of coronavirus in L.A., Orange counties - Los Angeles Times [WWW Document]. URL <https://www.latimes.com/california/story/2020-01-25/los-angeles-area-prepared-for-coronavirus> (accessed 11.10.20).
- Ma, X., Longley, I., Gao, J., Salmond, J., 2020. Assessing schoolchildren's exposure to air pollution during the daily commute - A systematic review. *Sci. Total Environ.* 737, 140389. <https://doi.org/10.1016/J.SCITOTENV.2020.140389>
- Macias, E., Suarez, A., Lloret, J., 2013. Mobile Sensing Systems. *Sensors* 13, 17292–17321. <https://doi.org/10.3390/s131217292>
- Martinez, D.A., Hinson, J.S., Klein, E.Y., Irvin, N.A., Saheed, M., Page, K.R., Levin, S.R., 2020. SARS-CoV-2 Positivity Rate for Latinos in the Baltimore–Washington, DC Region. *JAMA* 324, 392–395. <https://doi.org/10.1001/jama.2020.11374>
- Mayo Clinic, 2022. California COVID-19 Map: Tracking the Trends [WWW Document]. URL <https://www.mayoclinic.org/coronavirus-covid-19/map/california> (accessed 5.23.22).
- McCrorie, P.R., Fenton, C., Ellaway, A., 2014. Combining GPS, GIS, and accelerometry to explore the physical activity and environment relationship in children and young people - a review. *Int. J. Behav. Nutr. Phys. Act.* 11. <https://doi.org/10.1186/s12966-014-0093-0>
- McMorris, O., Villeneuve, P.J., Su, J., Jerrett, M., 2015. Urban greenness and physical activity in a national survey of Canadians. *Environ. Res.* 137, 94–100. <https://doi.org/10.1016/J.ENVRES.2014.11.010>
- Memken, J.A., Canabal, M.E., 1994. Housing tenure, structure, and crowding among Latino households. *J. Fam. Econ. Issues* 15, 349–365. <https://doi.org/10.1007/BF02353810>
- Microsoft, 2021. R developer's guide - R programming - Azure Architecture Center | Microsoft Docs [WWW Document]. URL <https://docs.microsoft.com/en-us/azure/architecture/data-guide/technology-choices/r-developers-guide> (accessed 5.2.22).
- Mooney, S.J., Pejaver, V., 2018. Big Data in Public Health: Terminology, Machine Learning, and Privacy. <https://doi.org/10.1146/annurev-publhealth-040617-014208> 39, 95–112. <https://doi.org/10.1146/ANNUREV-PUBLHEALTH-040617-014208>

- Mou, N., Yuan, R., Yang, T., Zhang, H., Tang, J., Makkonen, T., 2020. Exploring spatio-temporal changes of city inbound tourism flow: The case of Shanghai, China. *Tour. Manag.* 76. <https://doi.org/10.1016/j.tourman.2019.103955>
- Myers, L.C., Parodi, S.M., Escobar, G.J., Liu, V.X., 2020. Characteristics of Hospitalized Adults With COVID-19 in an Integrated Health Care System in California. *JAMA* 323, 2195–2198. <https://doi.org/10.1001/jama.2020.7202>
- NASA Earth Observatory, 2011. Measuring Vegetation (NDVI & EVI) [WWW Document]. URL [https://earthobservatory.nasa.gov/features/MeasuringVegetation/measuring\\_vegetation\\_2.php](https://earthobservatory.nasa.gov/features/MeasuringVegetation/measuring_vegetation_2.php) (accessed 5.9.22).
- Nazarian, N., Lee, J.K.W., 2021. Personal assessment of urban heat exposure: a systematic review. *Environ. Res. Lett.* 16, 033005. <https://doi.org/10.1088/1748-9326/ABD350>
- Nemati, E., Batteate, C., Jerrett, M., 2017. Opportunistic Environmental Sensing with Smartphones: a Critical Review of Current Literature and Applications. *Curr. Environ. Heal. reports* 4, 306–318. <https://doi.org/10.1007/s40572-017-0158-8>
- Neupane, B., Jerrett, M., Burnett, R.T., Marrie, T., Arain, A., Loeb, M., 2010. Long-term exposure to ambient air pollution and risk of hospitalization with community-acquired pneumonia in older adults. *Am. J. Respir. Crit. Care Med.* 181. <https://doi.org/10.1164/rccm.200901-0160OC>
- O'Neill, M.S., Jerrett, M., Kawachi, I., Levy, J.I., Cohen, A.J., Gouveia, N., Wilkinson, P., Fletcher, T., Cifuentes, L., Schwartz, J., Bateson, T.F., Cann, C., Dockery, D., Gold, D., Laden, F., London, S., Loomis, D., Speizer, F., Van den Eeden, S., Zanobetti, A., 2003. Health, wealth, and air pollution: Advancing theory and methods. *Environ. Health Perspect.* <https://doi.org/10.1289/ehp.6334>
- Oak Ridge National Laboratory, NASA, 2022. Daymet V4: Daily Surface Weather and Climatological Summaries [WWW Document]. URL <https://daymet.ornl.gov/> (accessed 5.15.22).
- Obradovich, N., Fowler, J.H., 2017. Climate change may alter human physical activity patterns. *Nat. Hum. Behav.* 2017 15 1, 1–7. <https://doi.org/10.1038/s41562-017-0097>
- Okabe, A., Satoh, T., Sugihara, K., 2009. A kernel density estimation method for networks, its computational method and a GIS-based tool. *Int. J. Geogr. Inf. Sci.* 23, 7–32. <https://doi.org/10.1080/13658810802475491>
- Oliveira, S., Andrade, H., Vaz, T., 2011. The cooling effect of green spaces as a contribution to the mitigation of urban heat: A case study in Lisbon. *Build. Environ.* 46, 2186–2194. <https://doi.org/10.1016/j.buildenv.2011.04.034>

- Olsen, J.R., Mitchell, R., McCrorie, P., Ellaway, A., 2019. Children's mobility and environmental exposures in urban landscapes: A cross-sectional study of 10–11 year old Scottish children. *Soc. Sci. Med.* 224, 11–22. <https://doi.org/10.1016/j.socscimed.2019.01.047>
- Pebesma, E., 2018. Simple Features for R: Standardized Support for Spatial Vector Data. *R J.* 10, 439–446. <https://doi.org/10.32614/RJ-2018-009>
- Perchoux, C., Chaix, B., Cummins, S., Kestens, Y., 2013a. Health & Place Conceptualization and measurement of environmental exposure in epidemiology : Accounting for activity space related to daily mobility. *Health Place* 21, 86–93. <https://doi.org/10.1016/j.healthplace.2013.01.005>
- Perchoux, C., Chaix, B., Cummins, S., Kestens, Y., 2013b. Conceptualization and measurement of environmental exposure in epidemiology: Accounting for activity space related to daily mobility. *Heal. Place* 21, 86–93. <https://doi.org/10.1016/j.healthplace.2013.01.005>
- Perrin, A., 2021. Mobile technology and home broadband 2021. *Mob. Technol. Home Broadband* 1–26.
- Pickering, T.A., Huh, J., Intille, S., Liao, Y., Pentz, M.A., Dunton, G.F., 2016. Physical activity and variation in momentary behavioral cognitions: An ecological momentary assessment study. *J. Phys. Act. Heal.* 13, 344–351. <https://doi.org/10.1123/jpah.2014-0547>
- Puyau, M.R., Adolph, A.L., Vohra, F.A., Butte, N.F., 2002. Validation and calibration of physical activity monitors in children. *Obes. Res.* 10. <https://doi.org/10.1038/oby.2002.24>
- Quast, T., Andel, R., 2020. Excess mortality and potential undercounting of COVID-19 deaths by demographic group in Ohio. *medRxiv* 2020.06.28.20141655. <https://doi.org/10.1101/2020.06.28.20141655>
- Quiros, D.C., Zhang, Q., Choi, W., He, M., Paulson, S.E., Winer, A.M., Wang, R., Zhu, Y., 2013. Air quality impacts of a scheduled 36-h closure of a major highway. *Atmos. Environ.* 67, 404–414. <https://doi.org/10.1016/j.atmosenv.2012.10.020>
- R Core Team, 2020. R: A language and environment for statistical computing. Vienna, Austria. R Foundation for Statistical Computing.
- Raser, E., Gaupp-Berghausen, M., Dons, E., Anaya-Boig, E., Avila-Palencia, I., Brand, C., Castro, A., Clark, A., Eriksson, U., Götschi, T., Int Panis, L., Kahlmeier, S., Laeremans, M., Mueller, N., Nieuwenhuijsen, M., Orjuela, J.P., Rojas-Rueda, D., Standaert, A., Stigell, E., Gerike, R., 2018. European cyclists' travel behavior: Differences and similarities between seven European (PASTA) cities. *J. Transp. Heal.* 9. <https://doi.org/10.1016/j.jth.2018.02.006>
- Reid, C.E., O'Neill, M.S., Gronlund, C.J., Brines, S.J., Brown, D.G., Diez-Roux, A. V., Schwartz, J., 2009. Mapping Community Determinants of Heat Vulnerability. *Environ. Health Perspect.*

- 117, 1730–1736. <https://doi.org/10.1289/ehp.0900683>
- Revelle, W., 2021. psych: Procedures for Psychological, Psychometric, and Personality Research.
- Rhys, H., 2020. Preventing overfitting with ridge regression, LASSO, and elastic net. *Mach. Learn. with R, tidyverse*, mlr 536.
- Roberts, H., Helbich, M., 2021. Multiple environmental exposures along daily mobility paths and depressive symptoms: A smartphone-based tracking study. *Environ. Int.* 156. <https://doi.org/10.1016/j.envint.2021.106635>
- Rogers, T.N., Rogers, C.R., VanSant-Webb, E., Gu, L.Y., Yan, B., Qeadan, F., 2020. Racial Disparities in COVID-19 Mortality Among Essential Workers in the United States. *World Med. Heal. Policy* 12. <https://doi.org/10.1002/wmh3.358>
- Salvaris, M., Dean, D., Tok, W.H., 2018. Microsoft AI Platform, in: Salvaris, M., Dean, D., Tok, W.H. (Eds.), *Deep Learning with Azure: Building and Deploying Artificial Intelligence Solutions on the Microsoft AI Platform*. Apress, Berkeley, CA, pp. 79–98.
- Sasaki, J.E., John, D., Freedson, P.S., 2011. Validation and comparison of ActiGraph activity monitors. *J. Sci. Med. Sport* 14, 411–416. <https://doi.org/10.1016/j.jsams.2011.04.003>
- Schmidberger, M., Morgan, M., Eddelbuettel, D., Yu, H., Tierney, L., Mansmann, U., 2009. State of the Art in Parallel Computing with R. *J. Stat. Softw.* 31. <https://doi.org/10.18637/jss.v031.i01>
- Schwalb-Willmann, J., Remelgado, R., Safi, K., Wegmann, M., 2020. moveVis: Animating movement trajectories in synchronicity with static or temporally dynamic environmental data in r. *Methods Ecol. Evol.* 11, 664–669. <https://doi.org/10.1111/2041-210X.13374>
- Shelley, J., Fairclough, S.J., Knowles, Z.R., Southern, K.W., McCormack, P., Dawson, E.A., Graves, L.E.F., Hanlon, C., 2018. A formative study exploring perceptions of physical activity and physical activity monitoring among children and young people with cystic fibrosis and health care professionals. *BMC Pediatr.* 18. <https://doi.org/10.1186/s12887-018-1301-x>
- Sherman, J.E., Spencer, J., Preisser, J.S., Gesler, W.M., Arcury, T.A., 2005. A suite of methods for representing activity space in a healthcare accessibility study. *Int. J. Health Geogr.* 4, 24. <https://doi.org/10.1186/1476-072X-4-24>
- Shih, P.C., Han, K., Poole, E.S., Rosson, M.B., Carroll, J.M., 2015. Use and Adoption Challenges of Wearable Activity Trackers. *iConference 2015 Proc.*
- Shin, J.C., Kwan, M.P., Grigsby-Toussaint, D.S., 2020. Do spatial boundaries matter for exploring the impact of community green spaces on health? *Int. J. Environ. Res. Public Health* 17, 1–17. <https://doi.org/10.3390/ijerph17207529>

- Shoaib, M., Bosch, S., Durmaz Incel, O., Scholten, H., Havinga, P.J.M., 2014. Fusion of smartphone motion sensors for physical activity recognition. *Sensors (Switzerland)* 14. <https://doi.org/10.3390/s140610146>
- Shrout, P.E., Fleiss, J.L., 1979. Intraclass correlations: Uses in assessing rater reliability. *Psychol. Bull.* 86. <https://doi.org/10.1037/0033-2909.86.2.420>
- Shyamasundar, R.K., 2018. Future of Computing Science. *Proc. Indian Natl. Sci. Acad.* 96. <https://doi.org/10.16943/ptinsa/2018/49341>
- Smith, M., Hosking, J., Woodward, A., Witten, K., MacMillan, A., Field, A., Baas, P., Mackie, H., 2017. Systematic literature review of built environment effects on physical activity and active transport - an update and new findings on health equity. *Int. J. Behav. Nutr. Phys. Act.* 14. <https://doi.org/10.1186/s12966-017-0613-9>
- Song, M.-L., Fisher, R., Wang, J.-L., Cui, L.-B., 2018. Environmental performance evaluation with big data: theories and methods. *Ann. Oper. Res.* 270, 459–472. <https://doi.org/10.1007/s10479-016-2158-8>
- Srivastava, A., 2021. COVID-19 and air pollution and meteorology-an intricate relationship: A review. *Chemosphere.* <https://doi.org/10.1016/j.chemosphere.2020.128297>
- Stamatakis, E., Nnoaham, K., Foster, C., Scarborough, P., 2013. The Influence of Global Heating on Discretionary Physical Activity: An Important and Overlooked Consequence of Climate Change. *J. Phys. Act. Heal.* 10, 765–768. <https://doi.org/10.1123/jpah.10.6.765>
- Steinhubl, S.R., Muse, E.D., Topol, E.J., 2015. The emerging field of mobile health. *Sci. Transl. Med.* 7, 283rv3-283rv3. <https://doi.org/10.1126/scitranslmed.aaa3487>
- Stone, B., Hess, J.J., Frumkin, H., 2010. Urban Form and Extreme Heat Events: Are Sprawling Cities More Vulnerable to Climate Change Than Compact Cities? *Environ. Health Perspect.* 118, 1425–1428. <https://doi.org/10.1289/ehp.0901879>
- Su, J.G., Dadvand, P., Nieuwenhuijsen, M.J., Bartoll, X., Jerrett, M., 2019. Associations of green space metrics with health and behavior outcomes at different buffer sizes and remote sensing sensor resolutions. *Environ. Int.* 126. <https://doi.org/10.1016/j.envint.2019.02.008>
- Su, J.G., Jerrett, M., Beckerman, B., Wilhelm, M., Ghosh, J.K., Ritz, B.R., 2009. Predicting traffic-related air pollution in Los Angeles using a distance decay regression selection strategy. *Environ. Res.* 109, 657–670. <https://doi.org/10.1016/j.envres.2009.06.001>
- Su, J.G., Meng, Y.-Y., Chen, X., Molitor, J., Yue, D., Jerrett, M., 2020. Predicting differential improvements in annual pollutant concentrations and exposures for regulatory policy assessment. *Environ. Int.* 143, 105942. <https://doi.org/10.1016/j.envint.2020.105942>

- Su, J.G., Meng, Y.Y., Pickett, M., Seto, E., Ritz, B., Jerrett, M., 2016. Identification of Effects of Regulatory Actions on Air Quality in Goods Movement Corridors in California. *Environ. Sci. Technol.* 50. <https://doi.org/10.1021/acs.est.6b00926>
- Sun, F., Walton, D.B., Hall, A., 2015. A Hybrid Dynamical–Statistical Downscaling Technique. Part II: End-of-Century Warming Projections Predict a New Climate State in the Los Angeles Region. *J. Clim.* 28, 4618–4636. <https://doi.org/10.1175/JCLI-D-14-00197.1>
- Swan, M., 2012. Sensor Mania! The Internet of Things, Wearable Computing, Objective Metrics, and the Quantified Self 2.0. *J. Sens. Actuator Networks* 1, 217–253. <https://doi.org/10.3390/jsan1030217>
- Sydbom, A., Blomberg, A., Parnia, S., Stenfors, N., Sandström, T., Dahlén, S.-E., 2001. Health effects of diesel exhaust emissions. *Eur. Respir. J.* 17, 733 LP – 746.
- Tang, J., Liu, F., Wang, Y., Wang, H., 2015. Uncovering urban human mobility from large scale taxi GPS data. *Phys. A Stat. Mech. its Appl.* 438. <https://doi.org/10.1016/j.physa.2015.06.032>
- Tate, E.B., Shah, A., Jones, M., Pentz, M.A., Liao, Y., Dunton, G., 2015. Toward a Better Understanding of the Link between Parent and Child Physical Activity Levels: The Moderating Role of Parental Encouragement. *J. Phys. Act. Heal.* 12, 1238–1244. <https://doi.org/10.1123/jpah.2014-0126>
- Thornton, M.M., Shrestha, R., Wei, Y., Thornton, P.E., Kao, S., Wilson, B.E., 2020. Daymet: Daily Surface Weather Data on a 1-km Grid for North America, Version 4. <https://doi.org/10.3334/ORNLDAAAC/1840>
- Travaglio, M., Yu, Y., Popovic, R., Selley, L., Leal, N.S., Martins, L.M., 2021. Links between air pollution and COVID-19 in England. *Environ. Pollut.* 268, 115859. <https://doi.org/10.1016/j.envpol.2020.115859>
- Tribby, C.P., Miller, H.J., Brown, B.B., Smith, K.R., Werner, C.M., 2017. Health & Place Geographic regions for assessing built environmental correlates with walking trips: A comparison using different metrics and model designs. *Health Place* 45, 1–9. <https://doi.org/10.1016/j.healthplace.2017.02.004>
- Trifan, A., Oliveira, M., Oliveira, J.L., 2019. Passive sensing of health outcomes through smartphones: Systematic review of current solutions and possible limitations. *JMIR mHealth uHealth* 7. <https://doi.org/10.2196/12649>
- Troped, P.J., Wilson, J.S., Matthews, C.E., Cromley, E.K., Melly, S.J., 2010. The Built Environment and Location-Based Physical Activity. *Am. J. Prev. Med.* 38, 429–438. <https://doi.org/10.1016/j.amepre.2009.12.032>

- Trost, S.G., Loprinzi, P.D., Moore, R., Pfeiffer, K.A., 2011. Comparison of accelerometer cut points for predicting activity intensity in youth. *Med. Sci. Sports Exerc.* 43. <https://doi.org/10.1249/MSS.0b013e318206476e>
- Tucker, J.M., Welk, G.J., Beyler, N.K., 2011. Physical activity in U.S. adults: Compliance with the physical activity guidelines for Americans. *Am. J. Prev. Med.* 40. <https://doi.org/10.1016/j.amepre.2010.12.016>
- Tucker, P., Gilliland, J., 2007. The effect of season and weather on physical activity: A systematic review. *Public Health* 121, 909–922. <https://doi.org/10.1016/j.puhe.2007.04.009>
- Twohig-Bennett, C., Jones, A., 2018. The health benefits of the great outdoors: A systematic review and meta-analysis of greenspace exposure and health outcomes. *Environ. Res.* 166. <https://doi.org/10.1016/j.envres.2018.06.030>
- U.S. Department of Labor, 2021. AMERICAN TIME USE SURVEY — MAY TO DECEMBER 2019 AND 2020 RESULTS [WWW Document]. News Release, Bur. Labor Stat. URL [www.bls.gov/tus](http://www.bls.gov/tus) (accessed 6.1.22).
- US Census Bureau, 2020. U.S. Census Bureau QuickFacts: Los Angeles County, California [WWW Document]. URL <https://www.census.gov/quickfacts/losangelescountycalifornia> (accessed 11.10.20).
- US Census Bureau, 2018. American Community Survey 5-Year Data (2009-2018) [WWW Document]. URL <https://www.census.gov/data/developers/data-sets/acs-5year.html> (accessed 11.10.20).
- USDA NAIP GeoHub, 2022. National Agriculture Imagery Program - NAIP Hub Site [WWW Document]. URL <https://naip-usdaonline.hub.arcgis.com/> (accessed 6.1.22).
- Ushey, K., Allaire, J.J., Tang, Y., 2021. reticulate: Interface to “Python.”
- Uyttendaele, N., 2015. How to speed up R code: an introduction. *arXiv1503.00855 [cs, stat]*.
- van den Berg, A.E., Maas, J., Verheij, R.A., Groenewegen, P.P., 2010. Green space as a buffer between stressful life events and health. *Soc. Sci. Med.* 70. <https://doi.org/10.1016/j.socscimed.2010.01.002>
- Varghese, B., Buyya, R., 2018. Next generation cloud computing: New trends and research directions. *Futur. Gener. Comput. Syst.* 79, 849–861. <https://doi.org/10.1016/j.future.2017.09.020>
- Vienneau, D., de Hoogh, K., Faeh, D., Kaufmann, M., Wunderli, J.M., Rösli, M., 2017. More than clean air and tranquillity: Residential green is independently associated with decreasing mortality. *Environ. Int.* 108. <https://doi.org/10.1016/j.envint.2017.08.012>
- Villeneuve, P.J., Jerrett, M., G. Su, J., Burnett, R.T., Chen, H., Wheeler, A.J., Goldberg, M.S.,

2012. A cohort study relating urban green space with mortality in Ontario, Canada. *Environ. Res.* 115, 51–58. <https://doi.org/10.1016/j.envres.2012.03.003>
- Wang, B., Chen, H., Chan, Y.L., Oliver, B.G., 2020. Is there an association between the level of ambient air pollution and COVID-19? *Am. J. Physiol. Lung Cell. Mol. Physiol.* <https://doi.org/10.1152/ajplung.00244.2020>
- Wang, B., Shi, W., Miao, Z., 2015. Confidence Analysis of Standard Deviation Ellipse and Its Extension into Higher Dimensional Euclidean Space. *PLoS One* 10, e0118537. <https://doi.org/10.1371/journal.pone.0118537>
- Wang, J., Kwan, M.P., Chai, Y., 2018. An innovative context-based crystal-growth activity space method for environmental exposure assessment: A study using GIS and GPS trajectory data collected in Chicago. *Int. J. Environ. Res. Public Health* 15. <https://doi.org/10.3390/ijerph15040703>
- Wang, Y., Kung, L., Byrd, T.A., 2018. Big data analytics: Understanding its capabilities and potential benefits for healthcare organizations. *Technol. Forecast. Soc. Change* 126, 3–13. <https://doi.org/10.1016/j.techfore.2015.12.019>
- Wang, Y., Wen, Y., Wang, Yue, Zhang, S., Zhang, K.M., Zheng, H., Xing, J., Wu, Y., Hao, J., 2020. Four-Month Changes in Air Quality during and after the COVID-19 Lockdown in Six Megacities in China. *Environ. Sci. Technol. Lett.* <https://doi.org/10.1021/acs.estlett.0c00605>
- Ward Thompson, C., Roe, J., Aspinall, P., Mitchell, R., Clow, A., Miller, D., 2012. More green space is linked to less stress in deprived communities: Evidence from salivary cortisol patterns. *Landsc. Urban Plan.* 105, 221–229. <https://doi.org/10.1016/j.landurbplan.2011.12.015>
- Wehener, S., Raser, E., Gaupp, M., Anata, E., De Nazelle, A., Eriksoon, U., Gerike, R., Horvath, I., Iacorossi, F., Int Panis, L., Kahlmeier, S., Nieuwenhuijsen, M., Mueller, N., Sanchez, J., Rothballer, C., 2017. Active Mobility, the New Health Trend in Smart Cities, or even More? REAL CORP.
- Wing, S.E., Larson, T. V., Hudda, N., Boonyarattaphan, S., Fruin, S., Ritz, B., 2020. Preterm birth among infants exposed to in utero ultrafine particles from aircraft emissions. *Environ. Health Perspect.* 128, 1–9. <https://doi.org/10.1289/EHP5732>
- Wolch, J.R., Byrne, J., Newell, J.P., 2014a. Urban green space, public health, and environmental justice: The challenge of making cities “just green enough.” *Landsc. Urban Plan.* 125, 234–244. <https://doi.org/10.1016/j.landurbplan.2014.01.017>
- Wolch, J.R., Byrne, J., Newell, J.P., 2014b. Urban green space, public health, and environmental justice: The challenge of making cities “just green enough.” *Landsc. Urban Plan.* 125, 234–

244. <https://doi.org/10.1016/j.landurbplan.2014.01.017>
- World Health Organization, 2022. Physical activity: Fact Sheet [WWW Document]. URL <https://www.who.int/news-room/fact-sheets/detail/physical-activity> (accessed 5.9.22).
- World Health Organization, 2021. WHO Coronavirus Disease (COVID-19) Dashboard | WHO Coronavirus Disease (COVID-19) Dashboard [WWW Document]. URL <https://covid19.who.int/> (accessed 11.2.20).
- Wu, C.Y.H., Zaitchik, B.F., Swarup, S., Gohlke, J.M., 2019. Influence of the Spatial Resolution of the Exposure Estimate in Determining the Association between Heat Waves and Adverse Health Outcomes. *Ann. Am. Assoc. Geogr.* 109. <https://doi.org/10.1080/24694452.2018.1511411>
- Wu, Xiao, Nethery, R.C., Sabath, B.M., Braun, D., Dominici, F., 2020a. Exposure to air pollution and COVID-19 mortality in the United States. medRxiv.
- Wu, Xiao, Nethery, R.C., Sabath, B.M., Braun, D., Dominici, F., 2020b. Exposure to air pollution and COVID-19 mortality in the United States: A nationwide cross-sectional study. medRxiv Prepr. *Serv. Heal. Sci.* <https://doi.org/10.1101/2020.04.05.20054502>
- Wu, X., Nethery, R.C., Sabath, M.B., Braun, D., Dominici, F., 2020. Air pollution and COVID-19 mortality in the United States: Strengths and limitations of an ecological regression analysis. *Sci. Adv.* 6, eabd4049. <https://doi.org/10.1126/sciadv.abd4049>
- Yang, D.H., Goerge, R., Mullner, R., 2006. Comparing GIS-based methods of measuring spatial accessibility to health services. *J. Med. Syst.* 30. <https://doi.org/10.1007/s10916-006-7400-5>
- Yao, Y., Pan, J., Liu, Z., Meng, X., Wang, Weidong, Kan, H., Wang, Weibing, 2021. Ambient nitrogen dioxide pollution and spreadability of COVID-19 in Chinese cities. *Ecotoxicol. Environ. Saf.* 208, 111421. <https://doi.org/10.1016/J.ECOENV.2020.111421>
- Yi, L., Wilson, J.P., Mason, T.B., Habre, R., Wang, S., Dunton, G.F., 2019. Methodologies for assessing contextual exposure to the built environment in physical activity studies: A systematic review. *Heal. Place.* <https://doi.org/10.1016/j.healthplace.2019.102226>
- Yu, Z., Bellander, T., Bergström, A., Dillner, J., Eneroth, K., Engardt, M., Georgelis, A., Kull, I., Ljungman, P., Pershagen, G., Stafoggia, M., Melén, E., Gruzieva, O., Group, B.C.-19 S., Almqvist, C., Andersson, N., Ballardini, N., Bergström, A., Björkander, S., Brodin, P., Castel, A., Ekström, S., Georgelis, A., Hammarström, L., Pan-Hammarström, Q., Hallberg, J., Jansson, C., Kere, M., Kull, I., Lauber, A., Lövquist, A., Melén, E., Mjösberg, J., Mogensen, I., Palmberg, L., Pershagen, G., Roxhed, N., Schwenk, J., 2022. Association of Short-term Air Pollution Exposure With SARS-CoV-2 Infection Among Young Adults in Sweden. *JAMA*

Netw. Open 5, e228109–e228109.  
<https://doi.org/10.1001/JAMANETWORKOPEN.2022.8109>

Zeldovich, Y.B., 2015. 26. Oxidation of Nitrogen in Combustion and Explosions, in: Selected Works of Yakov Borisovich Zeldovich, Volume I.  
<https://doi.org/10.1515/9781400862979.404>

Zenk, Shannon N, Schulz, A.J., Matthews, S.A., Odoms-young, A., Wilbur, J., Wegrzyn, L., Gibbs, K., Braunschweig, C., Stokes, C., 2011. Health & Place Activity space environment and dietary and physical activity behaviors: A pilot study. *Health Place* 17, 1150–1161.  
<https://doi.org/10.1016/j.healthplace.2011.05.001>

Zenk, Shannon N., Schulz, A.J., Matthews, S.A., Odoms-Young, A., Wilbur, J.E., Wegrzyn, L., Gibbs, K., Braunschweig, C., Stokes, C., 2011. Activity space environment and dietary and physical activity behaviors: A pilot study. *Heal. Place* 17, 1150–1161.  
<https://doi.org/10.1016/j.healthplace.2011.05.001>

Zhang, Z., Xue, T., Jin, X., 2020. Effects of meteorological conditions and air pollution on COVID-19 transmission: Evidence from 219 Chinese cities. *Sci. Total Environ.* 741.  
<https://doi.org/10.1016/j.scitotenv.2020.140244>

Zhao, P., Kwan, M.P., Zhou, S., 2018. The uncertain geographic context problem in the analysis of the relationships between obesity and the built environment in Guangzhou. *Int. J. Environ. Res. Public Health* 15. <https://doi.org/10.3390/ijerph15020308>

Zhou, X., Josey, K., Kamareddine, L., Caine, M.C., Liu, T., Mickley, L.J., Cooper, M., Dominici, F., 2021. Excess of COVID-19 cases and deaths due to fine particulate matter exposure during the 2020 wildfires in the United States. *Sci. Adv.* 7, 8789–8802.  
[https://doi.org/10.1126/SCIADV.ABI8789/SUPPL\\_FILE/SCIADV.ABI8789\\_SM.PDF](https://doi.org/10.1126/SCIADV.ABI8789/SUPPL_FILE/SCIADV.ABI8789_SM.PDF)

Zhu, Y., Xie, J., Huang, F., Cao, L., 2020. Association between short-term exposure to air pollution and COVID-19 infection: Evidence from China. *Sci. Total Environ.* 727.  
<https://doi.org/10.1016/j.scitotenv.2020.138704>

## **CHAPTER 3: PHYSICAL ACTIVITY SPACE METHODS FOR GREEN SPACE EXPOSURE**

### **ATTRIBUTION: A MULTI-METHOD COMPARISON STUDY**

#### **3.1 INTRODUCTION**

The quantification of spatial context is pivotal to research across many fields. In the field of exposure science, accurately describing the space around individuals and populations can lead to improved understanding of how the built and natural environments impact human health (Dixon et al., 2020; Hirsch et al., 2014; Jerrett et al., 2005a; Jia et al., 2019; Kwan, 2012a). The methods employed to measure and attribute spatial context have changed rapidly over the last few decades (Chen and Dobra, 2017; J. Wang et al., 2018; Yi et al., 2019). New technology advancements, such as those in mobile and remote sensing, have led to more precise descriptions of spatial context. In the study of physical activity, location tracking and accelerometry have provided opportunities and advancements towards better understanding of human activity (Dons et al., 2015; Ku et al., 2018; Lee and Kwan, 2018; Trifan et al., 2019). These advancements, however, have also created new hardware and software challenges.

Mobile sensing technologies are rapidly evolving, leading to increasing quantities of data (“big data”) available for physical activity and location-tracking research. In the past, geographic information system (GIS) analytics have primarily used GPS information on home or work location, sometimes augmented by self-reported information (Kwan, 2012b; Troped et al., 2010). Geospatial data of physical activity location and timing could only be collected from momentary sampling or with specific hardware (e.g., GPS device). These data render incomplete snapshots of someone’s overall activity and location pattern. More recent studies have used continuous data collection sensors (e.g. GlobalSat/Actigraph), but these are costly to collect and process and thus sample size is often restricted to less than 100 participants (Gastin et al., 2018; Imboden et al.,

2018; Sasaki et al., 2011; Shelley et al., 2018), and surveillance duration is often restricted to a week or less (Bakrania et al., 2017; Dohrn et al., 2018; Korsiak et al., 2018; Tate et al., 2015). Mobile-sensing research and innovation is exponentially expanding as mobile-sensing data are now widely used in academic research, government, and industry (Nemati et al., 2017; Steinhubl et al., 2015).

Now, other technologies gather geospatial data including by smartphones, wearable devices (such as Fitbits and smartwatches), and other sensors that are either wearable or kept near an individual. For example, 85% of adults in the U.S., 76% (median) of adults in countries with advanced economies, and 45% (median) of adults in countries with emerging economies now own a smartphone (Perrin, 2021). The average smartphone now includes GPS as well as an accelerometer, digital compass, gyroscope, various microphones, various cameras, and many other sensor-based hardwares (Nemati et al., 2017; Steinhubl et al., 2015).

Some researchers have designed their own physical activity tracking smartphone apps to take advantage of smartphone ownership. For example, the CalFit app, developed by researchers to allow for usability in larger population-based studies, was demonstrated to have a correlation coefficient of 0.932 when compared to gold-standard Actigraph accelerometers (Donaire-Gonzalez et al., 2013). However, given the cost of app design and maintenance, CalFit has not been widely adopted for research. Companies have developed smartphone apps that allow for crowd-sourced data collection by individuals, agencies, or academic researchers. Commercially available apps that collect, download, and aggregate these individually-collected data are now readily accessible from the Android and iOS app stores. Crowd-sourced (via smartphones) mobile sensing using these commercial apps may allow for continuous sampling in communities at a lower cost, generating much larger amounts of data to be analyzed (Nemati et al., 2017; Steinhubl et al., 2015). Researchers have begun to assess the validity and reliability of these consumer products (e.g. smartphone-based apps) in comparison to research-grade gold-standard

counterparts (e.g. ActiGraph - accelerometer; GlobalSat - GPS) (Evenson et al., 2015; Gastin et al., 2018; Imboden et al., 2018; Kooiman et al., 2015). Although there have been many systematic reviews of consumer-based activity tracking technologies, few have included both smartphone apps (e.g., MOVES) and stand-alone wearable devices (e.g. Actigraph, Fitbit, Jawbone, etc) (Donaire-Gonzalez et al., 2013; Hekler et al., 2015; Höchsmann et al., 2018). One example of a side-by-side study of apps (including of the MOVES app utilized in this study) and wearable devices was conducted in the Netherlands. Participants (n=56) were outfitted with 10 different consumer activity trackers including the MOVES app and were asked to walk on laboratory-setting treadmills and, or in 'free-living' conditions. The authors reported significant differences in steps and estimations of energy expenditure among the trackers but only 11 'free-living' participants used the MOVES smartphone app and they used them on a variety of smartphone models (Kooiman et al., 2015).

Researchers can access the backend components of these apps (application program interfaces, or APIs, made available by the commercial or open-source app developer) to continuously access or collect data on many individuals with less effort and lower cost compared to previous methods (Kamel Boulos et al., 2011; Lane et al., 2010; Macias et al., 2013; Nemati et al., 2017; Steinhubl et al., 2015; Swan, 2012). In a user study of 26 individuals outfitted with Fitbit activity trackers and followed for six weeks to assess usage ability, over 65% of participants failed to adhere to protocols for continuous wearing of the Fitbit. Many participants described barriers to proper usage such as annoyance (e.g., taking the device on and off), discomfort, and forgetting to wear or charge the device. A significant number of these participants preferred using smartphone apps instead of or in conjunction with the Fitbit (Shih et al., 2015). In addition, in the past, researchers would collect activity data over short periods of time, e.g., a week, which may not be generalizable to an individual's behavior over longer periods of time. However, with crowd-sourced activity and location data, researchers can define activity space continuously over longer

periods of time with minimal gap in coverage (Chen and Dobra, 2017; Hirsch et al., 2014; Holliday et al., 2017; Li and Tong, 2016; Perchoux et al., 2013a). Not having to generalize from smaller windows of data collection allows researchers to improve on past methods aimed at describing activity behavior.

The increased quantity of data, coupled with better computing capacity, allows for improved quantification of where and when individuals engage in physical activity, i.e., their physical activity space (PAS). The large quantities of data have resulted in improved statistical and analytic power; however the main bottleneck in the utility of this massive amount of data has been computer storage capacity and processing speed (Jacobs, 2009; Kaisler et al., 2013; Kambatla et al., 2014). In a systematic review of big data practices for healthcare, reviewers identified that the most significant scientific advancements are occurring in trend analysis, general data analytics, decision analytics, and predictive capability (Y. Wang et al., 2018). In a review of big data trends for urban environment research, reviewers identified the burgeoning analytic opportunities and “improved spatial granularity” of geospatial results (Glaeser et al., 2018). The combination of improved spatial detail and predictive capacity is essential for advancing analyses in environmental health.

Computing is improving due to cost reduction, faster processing chips, and new interconnected products and services such as cloud computing (Dempsey and Kelliher, 2018; Shyamasundar, 2018; Varghese and Buyya, 2018). Many for-profit companies now offer solutions that drastically improve storage capacity and utilize large datacenters with super computers for analysis. Some companies have even developed analytic platforms for improved processing power and speed. For example, Microsoft’s *Microsoft R (MRAN)*, designed to carry out matrix calculations and analytics, can run 500-times faster than traditional open source R (CRAN) (Diaz and Freato, 2018; Microsoft, 2021; Salvaris et al., 2018). New software and hardware continues to be developed. A few years ago, R would not allow for multi-core processing, but now there are

open-source library packages that allow or facilitate this and R Studio has parallel processing built into the user interface (Eddelbuettel, 2018; Schmidberger et al., 2009; Uyttendaele, 2015). GIS analytics have greatly benefitted from this improved processing power due to the inherently large amounts of data and rendering necessary (e.g., remote sensing has *always* been 'big data') (Graham and Shelton, 2013; Li et al., 2016; Song et al., 2018).

With the capacity to cheaply collect large amounts of continuous data coupled with advancements of hardware and processing capacity, activity space methods can be developed that better define activity patterns without having to generalize from small sample sizes, short spurts of data, or reduced data collection frequency (Chen and Dobra, 2017; Hirsch et al., 2014; Li and Tong, 2016; Perchoux et al., 2013a). Traditionally, due to a lack of continuously-collected data (e.g., big data from smartphone sensors), researchers would often oversimplify activity space, such as to a simple circular region (buffer) or a raster grid cell around the individual's geocoded home address. For example, in a study of 10-11 year old Scottish children (N=100), researchers aimed to assess how children's mobility was associated with environmental exposure and context (Olsen et al., 2019). The researchers, however, assigned exposure and context values based on 50-meter grids around the children's home—a major oversimplification, given that children venture beyond their home and that environmental context cannot logically be gridded (i.e., humans do not interact with their surroundings in perfect squares). In an assessment of how such oversimplifications affect physical activity research (Holliday et al., 2017), Holliday et al. compared the minutes of moderate-to-vigorous physical activity (MVPA) that participants (N=217) engaged in within simplified circular buffers with those that participants engaged in within a minimum convex polygon that incorporated repeatedly-collected GPS and activity data. They found that when comparing the circular buffer and convex polygon methods, the number of minutes of MVPA and where these minutes occurred differed by roughly four-fold. This implies that simplifications of activity space can drastically underestimate the variation in location and

amount of spatial-distributed activity (such as MVPA). Activities with energy expenditure similar to or more than a brisk walk are considered MVPA, and the World Health Organization recommends adults engage in at least 75 minutes of MVPA per week to receive related health benefits (World Health Organization, 2022).

In a different study of activity space methodologies, researchers collected GPS and activity data from 95 adults for 7 days each and assessed statistical difference of derived spatial metrics in three activity space approaches: (1) 95% ellipse; (2) minimum convex polygon (or convex hull); and (3) daily path areas (Hirsch et al., 2014). Their results showed significant correlation between each method, implying little effect in choice of approach. They acknowledge, however, that due to relatively low sample size (only 7-day collection windows per individual), their results may not be generalizable to other research, and other approaches utilizing larger sample sizes may be necessary (Hirsch et al., 2014). New methods, such as those that utilize big data acquired from smartphone sensing and from larger sample sizes, would provide better insight into activity spaces. Researchers in the Department of Statistics at the University of Washington have developed improved statistical approaches to defining activity space that utilize these larger continuous datasets. They assert that ranking kernel density surfaces (either by individual or time frame or both) may improve the inference of these activity space methods (Chen and Dobra, 2017).

Exposure to green space has been demonstrated to positively impact human health (Almanza et al., 2012; Bowler et al., 2010a; Wolch et al., 2014a). More research is needed, however, to better describe how to define and quantify green space exposure. In a major systematic review of physical activity and green space exposure, authors discussed the lack of consensus regarding green space exposure attribution methods, and pointed out the importance of improved quantification and evaluation of these methods for future research method selection (McCrorie et al., 2014). In this research, a comparison framework is provided to assess methods

for the quantification of green space exposure by physical activity space, using multiple activity and location data sources (i.e., smartphone, accelerometer, and personal GPS), multiple geospatial methods for describing activity space (i.e., home buffer, 95% ellipse, kernel density ranking, etc.), and multiple green space data sources. This framework is used to recommend approaches for future research decision regarding physical activity, activity space, and green space exposure attribution research—although this framework may also be applicable to other scientific endeavors involving repeated location tracking for the purposes of quantifying spatial context of individuals.

In the present study, we aim to determine if green space quantification for PASs—defined here as regions or polygons around the location of an individual engaged in moderate-to-vigorous physical activity (MVPA)—differs based on (1) the methods used to generate spatiotemporal MVPA data; (2) the spatial methods used to draw PASs; and (3) the time-period of green space data employed. For these comparisons, we mainly employ data acquired in the Physical Activity through Sustainable Transport Approaches in Los Angeles (PASTA-LA) study. This research is situated in Los Angeles (LA) County, a sprawling county of over 10,000 square km

## **3.2 METHODS**

### **3.2.1 Participants**

Participants were drawn from the PASTA-LA study, a study comparing active mobility before and after the October 2017 launch of the University of California, Los Angeles (UCLA) bike-sharing program (*Bruin Bike Share*) (Alvarado and Hewitt, 2017). The overall study aimed to assess the risks (e.g., air pollution exposure, traffic accidents) and benefits (e.g., physical activity, reduction of single-occupancy vehicle use) associated with the implementation of this bike-sharing program in the UCLA-Westwood area. Study protocols were largely derived in

collaboration with a larger PASTA study of seven cities in Europe (Avila-Palencia et al., 2018; Branion-Calles et al., 2020; de Nazelle et al., 2017; Dons et al., 2015; Gerike et al., 2016; Götschi et al., 2017; Raser et al., 2018; Wehener et al., 2017). For PASTA-LA, 440 participants were enrolled between Spring and Fall 2017 (see **Figure 3.1**). Participants were eligible if they lived or worked in the UCLA-Westwood areas, were over the age of 18, capable of physical activity, owned an Android or iPhone smartphone, and were willing to install the MOVES app on their smartphone. Participants included UCLA students, staff, and faculty as well as individuals living or working in the greater Westwood area. A subset of 163 participants volunteered to partake in a substudy, in which they wore research-grade GPS and Actigraph devices (GlobalSat BT-335 and DG-500 Global Positioning System (GPS) receivers; and Actigraph GT3X+ accelerometers) one week before and one week after the Bruin Bike Share launch.

Participants signed written consents. Human-subjects' approvals for PASTA-LA were maintained from the UCLA Institutional Review Boards (IRBs).

### **3.2.2 PASTA-LA data collection**

Enrollment took place between May and August 2017 and data collection ended in June 2018. Participation included activity tracking with the MOVES app and completion of six online questionnaires: a 40-minute baseline survey and two 20-minute follow-up surveys, before and after the Bruin Bike Share launch. Thus, all participants were required to install the MOVES smartphone app, commercially available (until July 31, 2018) on both Android and iPhone app stores, and to authorize their data to be sent via cellular or WIFI connection to a secure server. MOVES is a consumer-friendly, location and activity-tracking smartphone app that detected location, mode of transport and intensity of activity. MOVES outputs included tabular daily activity data, separated into 'events', where each event included: (1) a polyline route consisting of time-stamped GPS-coordinate nodes, (2) the total number of steps conducted along the route, and (3) a designation of one of three transport modes: "walking", "biking", and motor-vehicle "transport."

Steps and transport modes were determined by MOVES using unknown proprietary algorithms specific to the app. Data collection would pause or slow during periods of sedentary behavior (e.g., when inside a vehicle) and predictable behavior to reduce smartphone battery consumption. The time-stamped observations, therefore, ranged in frequency from seconds to hours. MOVES data were successfully collected on 404 of the 440 PASTA-LA participants, generating approximately 9 million time-stamped observations of location and activity information (**Figure 3.1**).

The participants who partook in the more detailed substudy, using research-grade devices, were required to visit the research office at UCLA to pick up and deposit their devices at the start and end of each collection week. The Actigraph accelerometer was worn on the wrist of the participant's choosing. Participants were asked to keep the GlobalSat GPS device within approximately one meter of their body. The Actigraph GT3X+ accelerometer is a tri-axial device that records 'counts' for all three axes of movement. The counts are proprietary and unitless, which is unique to Actigraph branded devices. The GlobalSat GPS BT-335 model has a positional horizontal accuracy of 10 meters (GlobalSat WorldCom Corporation, 2022a) and the DG-500 model has a positional horizontal accuracy of less than 2.5 meters (GlobalSat WorldCom Corporation, 2022b). After data collection, Actigraph's Actilife software version 6.13.3 was used to download the device data and convert the Actigraph vertical axis counts to number of steps per 10 second epoch (Actigraph Corp, 2019; Freedson et al., 1998; Keadle et al., 2014). GlobalSat's GPS Tools for Windows, proprietary for each model GPS unit (BT-335 and DG-500), were used to download GPS data. Actigraph counts for each of three accelerometer axes as well as derived step counts were combined with GPS data from the GlobalSat using linear interpolation based on the time-stamps from each device. The resulting dataset included 10-second interpolated GPS coordinates, interpolated step counts, and interpolated Actigraph 'counts' for all three axes (Alaimo et al., 2021).

Of 163 substudy participants, 123 collected Actigraph and GlobalSat data that could be interpolated, i.e., precisely overlapped in time. These 123 participants generated approximately 14 million observations of interpolated Actigraph accelerometer and GlobalSat GPS data (Actigraph+GPS).

### **3.2.3 Inclusion criteria and data cleaning**

Only observations occurring within LA County and between 7am and 10pm were included. (Participants were assumed asleep or inactive between 10pm and 7am.) MOVES and Actigraph+GPS data were cleaned by removing erroneous observations. For Actigraph+GPS, this was done in part previously where missingness was also assessed (Alaimo et al., 2021). Observations were automatically flagged for manual inspection if speeds above 50 m/s or accelerations above 10 m/s<sup>2</sup> were implied for a single observation or route segment (Kerr et al., 2011). Nine participants recorded routes that were removed upon visual inspection (e.g., due to major misalignments with transport networks). MOVES data were joined with Actigraph+GPS by day. Only MOVES data occurring on the same day as Actigraph+GPS data were included. After exclusion and cleaning, all 123 participants had at least one usable day of MOVES and Actigraph+GPS data for subsequent analyses.

The participants comprising this final data set averaged 33 years old (SD: 11; Range: 21 – 66) with 68.3% female, 32.5% White, 87.8% high school graduates, and 51.0% employed full-time. Their average body mass index (BMI) was 23.6 (SD: 4.0; Range: 9.2 – 35.5).

This final data set was used to demonstrate and evaluate the methods described below and was composed of 191,032 MOVES observations overlapping (by day) with 1,013,394 Actigraph+GPS observations across 275 unique days of data collection. For these 275 days, there was an average of 25.4 hours (SD: 20.1; Range: 0.2 – 106.4) of overlapping MOVES and Actigraph+GPS data across 1,125 person-days (Künzli et al., 2000). The average number of MOVES observations per person-day was 1,721, (SD: 1,384; Range: 2 – 6,285) while the average

number of Actigraph+GPS observations per person-day was 9,129 (SD: 7,252; Range: 85 – 38,303).

#### **3.2.4 Moderate-to-vigorous physical activity**

Equations that estimate metabolic equivalent of task (MET) from accelerometry data were employed to evaluate activity level. Observations of location and activity (MOVES or Actigraph+GPS) were categorized as sedentary-to-light physical activity or moderate-to-vigorous physical activity (MVPA). MET ratios of 0 to 3 were considered sedentary-to-light activity and ratios above 3 were considered MVPA (Tucker et al., 2011). The non-linear, step-rate classification equations (one equation for men, one for women) produced by a motorized-treadmill study of 9 men and 10 women (Abel et al., 2011) were used to categorize MVPA for MOVES and Actigraph+GPS step counts. In the case of MOVES, activity level was assumed to be homogenous for each 'event' or route (regardless of event duration) since step counts were reported as sums per event. For this reason, all observations along each route were assigned the same activity category. For comparison with the MOVES data, Actigraph+GPS vertical-axis counts were also converted to MET ratios using equations produced by a previous treadmill study of 25 men and 25 women (Freedson et al., 1998). Although Actigraph+GPS data included outputs from three axes, only the vertical axis was utilized for better comparison with step counts, which were also derived from the vertical axis of both smartphone (MOVES) and Actigraph accelerometer sensors. Three datasets were created: (1) MOVES data with MVPA derived from step rate (Abel et al., 2011); (2) Actigraph+GPS data with MVPA derived from step rate (Abel et al., 2011); and (3) Actigraph+GPS with MVPA derived from vertical-axis counts (Freedson et al., 1998). The resulting datasets included GPS-coordinate pairs, time stamps, and a binary activity level (0 = light-to-sedentary; 1 = MVPA). **Figure 3.2** and **Figure 3.3** visualize datasets (1) and (2), respectively.

### 3.2.5 Physical activity spaces

We operationally defined PAS as a region or polygon(s) where an individual engages in MVPA. The 1,125 person-days of location and activity data allowed for up to 1,125 MOVES PASs and up to 1,125 Actigraph+GPS PASs. Example PAS polygons can be seen in **Figure 3.4** and **Figure 3.5** for one partially simulated (to protect identifiable spatial information) person-day of collection. The methods used to draw PASs are as follows:

- 1. 250-meter location buffer and 2. 500-meter location buffer.** Locations categorized as MVPA were buffered by 250 meters and 500 meters. Euclidian distance-based buffers are commonly used to describe activity spaces and movement. Similarly referred to as “daily path areas” (Hirsch et al., 2014; N. C. Lee et al., 2016; Shannon N. Zenk et al., 2011) or “GPS trajectory buffers” (J. Wang et al., 2018) – these are also used to describe activity along routes. We selected the distances of 250 and 500 meters because they have been related to health and green space exposure science in the literature (Dzhambov et al., 2018; Su et al., 2019). This PAS method required a minimum of one observation of MVPA per person-day. **Figure 3.4** shows an example 250-meter location buffer PAS with both true-color NAIP imagery background and derived green space (NDVI) background (methods below).
- 3. Minimum convex polygon.** This PAS is a type of minimum bounding geometry often referred to as a “convex hull” and is very commonly employed in activity space research (Hirsch et al., 2014; J. H. Lee et al., 2016). It is the smallest convex shape that contains all observations—similar to wrapping a rubber band around a set of points. This PAS method required a minimum of three observations per person-day. **Figure 3.5** shows an example minimum convex polygon PAS.
- 4. 95% ‘directional distribution’ ellipse.** The standard deviation ellipse is commonly used to describe activity space (Hirsch et al., 2014; Sherman et al., 2005; Shannon N. Zenk et

al., 2011). We used two standard deviations to create a PAS ellipse that covered 95% of MVPA observations (Kamruzzaman and Hine, 2012; Zhao et al., 2018). This approach involved calculating the mean center, standard deviation, and angle of rotation of the array of locations (Chew, 1966; Wang et al., 2015). This PAS method required a minimum of five MVPA observations per person-day. **Figure 3.5** shows an example 95% ellipse PAS.

**3. Density-based spatial clustering applications (DBSCAN).** This approach uses machine-learning algorithms to bin points into either spatial clusters or 'noise'. DBSCAN is often used to assess patterns in trajectory data (e.g., routes) (Gong et al., 2015; Tang et al., 2015). Specifically, we used the process of ordering points to identify clustering structure (DBSCAN-OPTICS referred henceforth as DBSCAN). This process can detect clusters with variable spatial density (such as spatially-resolved MVPA data) (Rhys, 2020). DBSCAN allows for user-defined search radii when allocating points to clusters. We defined the search radius here as 500 meters. Clusters required a minimum of 6 observations. Raw cluster polygons were buffered by 5 meters for smoothing purposes, as this resulted in less error during green space extraction. The minimum number of MVPA observations for this method was 25. **Figure 3.5** shows an example DBSCAN PAS.

**4. Hierarchical DBSCAN (HDBSCAN).** This method is less commonly used but has been used for studying patterns in the location of individuals such as for identifying areas of high tourism (Mou et al., 2020). HDBSCAN is derived from DBSCAN methods, but instead of allowing for user-defined search radii, HDBSCAN assesses the full dataset of points to determine search radii automatically using spatially-constrained hierarchical machine learning (Campello et al., 2013). As with the DBSCAN method above, we required clusters to have a minimum of 6 observations and we buffered raw cluster

polygons by 5 meters for smoothing purposes. The minimum number of MVPA observations for this method was 25. **Figure 3.5** shows an example HDBSCAN PAS.

- 5. Kernel density ranking (KDR).** Kernel density is a very commonly used geospatial process for assessing the density of observations over a fixed Euclidean distance or search radius. It is regularly used for both transportation and health research (Anderson, 2009; Charreire et al., 2010; Erdogan et al., 2008; Okabe et al., 2009; J. Wang et al., 2018; Yang et al., 2006). Kernel density, however, may not sufficiently capture locations with low activity density. These low-density locations are potentially valuable for physical activity research (e.g., an arterial road traveled on only once by bike could be important for investigating PAS across a sparse dataset). Chen et al., have devised a method to generate ratio-based probability surfaces from GPS-based activity data (Chen and Dobra, 2017). Their method produces a raster surface with values between '0' and '1,' where '1' would imply a grid cell with a density at 100%, and where '0' would imply a grid cell with a density at 0%. Here we selected only grid cells greater than 0.9 to give areas where the top 10% of activity was expected to occur. A smoothing parameter of 0.01 was used. These areas of high activity were then converted to PAS polygons. The minimum number of MVPA observations for this method was 30. **Figure 3.5** shows an example KDR PAS.

Euclidian home buffers at 250 and 500 meters were also constructed for comparison, as these are commonly used to describe spatial context for individuals when repeated location and activity information is not available (Amoly et al., 2015; Dadvand et al., 2015; van den Berg et al., 2010). These circular home buffers were not considered physical activity spaces, as MVPA did not factor into this approach.

### 3.2.6 Green space exposure attribution

Multispectral four-band (red, green, blue, and infrared) satellite images produced by the National Agriculture Imagery Program (NAIP) of the U.S. Department of Agriculture (USDA) were used to estimate greenness of each PAS. The annual mosaiced images for 2018 were considered for use as the main result since they overlap in time with the PASTA-LA data collection period; 2016 mosaiced images were included for comparison. Both of these annual products are spatially resolved at 60 centimeters. This fine resolution makes the associated files very large (100s of gigabytes) and therefore challenging to access, download, or process. For this reason, the mosaics were accessed and processed on Google Earth Engine's cloud-based super-computing platform. The red and infrared bands of each mosaic were used to calculate the Normalized Difference Vegetation Index (NDVI). This index has been used to quantify greenness in many studies, including for activity space research (Dadvand et al., 2012a, 2012b; Leslie et al., 2010; McMorris et al., 2015; Vienneau et al., 2017). The index was calculated using the following band formula:  $[\text{Near Infrared} - \text{Red}] \div [\text{Near Infrared} + \text{Red}]$ . NDVI values range from -1 to 1 where values close to or below zero indicated no greenness (e.g., man-made objects, open water, etc.) and values closer to 1 indicated greener areas (NASA Earth Observatory, 2011). PAS polygons were used to extract the mean NDVI raster value for each region per person-day (up to 1,125) by using an areal "reducer" (Google Inc., 2022).

The above study procedures to quantify green space for each physical activity space are summarized in **Figure 3.6**.

To extract NDVI values for home-address buffers, separate protocols were devised to 'hide' participant home locations. A total of 10,000 fake addresses were generated and geocoded for the study area. The 123 addresses of the substudy participants were inserted into these 10,000 at random. 99 fake participant ID keys and one true participant ID key (that was kept secure) was included in the dataset of 10,123 addresses. After NDVI extraction, the true key was used to

determine which extractions belong to the participants. The methods for this anonymization protocol can be seen in **Figure 3.7**.

### **3.2.7 Comparison and evaluation**

All data sources used are shown in **Table 3.1**. This research utilized location information in the form of GPS coordinate pairs, physical activity information in the form of accelerometry outcomes from wearable devices, and green space surfaces derived from satellite imagery. These data are considered ‘big data.’ Other participant survey data were included to describe the sample (above).

In summary, 21 separate approaches to describe physical activity spaces were completed—7 PAS methods for each of 3 MVPA data sources (MOVES step counts, Actigraph+GPS step counts, and Actigraph+GPS vertical-axis counts). Sensitivity analyses were conducted on these 21 approaches by using data visualizations and intraclass correlation coefficients (ICCs). Specifically, ‘ICC3’ was used to compare extracted NDVI as these datasets were not sampled randomly so are not generalizable to a larger population, and the comparison group is fixed (Koo and Li, 2016; Shrout and Fleiss, 1979). Vertical-line plots were designed to visualize ICCs and the range of differences in NDVI across sensitivities. Bar plots were designed to demonstrate exclusion patterns by levels of activity, binned by quartiles of MVPA, where the 1<sup>st</sup> quartile represented person-days with the lowest amount of MVPA.

### **3.2.8 Software**

All analyses were conducted in R Studio version 1.2.5042 (R version 4.2.0). The *tidyverse* suite of R packages was used to clean data and convert counts to MVPA. Packages used to draw PASs included: *sf*, *sp*, *raster*, *rgdal*, *maptools*, *moveVIS*, *reticulate*, *aspace*, *adehabitatHR*, *dbscan*, and *density\_ranking* (Bivand et al., 2021; Bui et al., 2012; Calenge, 2006; Chen and Dobra, 2017; Hahsler and Piekenbrock, 2021; Hijmans, 2021; Pebesma, 2018; Schwalb-

Willmann et al., 2020; Ushey et al., 2021). Google Earth Engine was queried in R using the *rgee* package (Aybar et al., 2020). ICCs were calculated using the *psych* package (Revelle, 2021). Results visualization was conducted in R Studio, while mapping was completed in both R Studio and ESRI's ArcGIS Pro, version 2.8.6.

### 3.3 RESULTS

#### 3.3.1 Summary of 21 PAS methods

PASs are described in **Table 3.2**. The number of person-days where polygons were successfully drawn ranged widely across the 21 approaches—from 195 to 1,105 person-days (of 1,125 possible) for 44 to 122 participants (of 123 possible), respectively. The fewest number of PAS polygons were produced using kernel density ranking, applied to Actigraph+GPS data with MVPA derived from step-rate (Abel et al., 2011) and the largest number were generated by the 250-m and 500-m location buffers, drawn using Actigraph+GPS data with MVPA derived from vertical-axis counts (Freedson et al., 1998). In general, MOVES data resulted in fewer person-days of PASs than Actigraph+GPS for all seven PAS methods employed. With the exception of the DBSCAN and HDBSCAN PAS methods, step-count MVPA conversions (Abel et al., 2011) generated fewer person-days of PASs than vertical-axis conversions (Freedson et al., 1998).

The maximum duration of MVPA per person-day was 248.03 minutes and the minimum was 10 seconds (0.17 minutes; or one observation). DBSCAN, HDBSCAN, and kernel density ranking polygon-drawing methods, applied to MOVES data, utilized the highest average number of minutes of MVPA ( $M \pm SD = 33.81 \pm 24.77$ ) per person-day. These three PAS methods, however, utilized fewer person-days of data ( $n = 200$ ) than most other methods. 500-meter location buffer PASs, produced by Actigraph+GPS data with MVPA categorized from vertical-axis counts (Freedson et al., 1998), utilized the lowest average number of minutes of MVPA ( $M \pm SD =$

6.31±9.30) per person-day. This method and the analogous 250-meter location buffer method (produced by Actigraph+GPS data with MVPA categorized from vertical-axis counts (Freedson et al., 1998)), however, included the most person-days ( $n = 1,105$ ) of data.

**Figure 3.8** shows the proportion of person-days excluded for each of the other 19 methods when compared to the quartile distribution of person-day minutes of MVPA for these two methods (250-meter and 500-meter location buffers; Actigraph+GPS data; *Freedson* MVPA equation). Exclusion was skewed toward less active person-days, with more exclusion occurring for the 1<sup>st</sup> and 2<sup>nd</sup> quartiles of daily MVPA (minutes). In general, methods that utilized MOVES data had more exclusions across quartiles of daily MVPA (less active and more active person-days) than those that used Actigraph+GPS data. For Actigraph+GPS data, using step rate to categorize MVPA (Abel et al., 2011) resulted in a more even distribution of exclusion—i.e., a more similar proportion of exclusion across all quartiles of MVPA, than using vertical-axis counts (Freedson et al., 1998)—which resulted in more exclusions in the 1<sup>st</sup> and 2<sup>nd</sup> quartiles of MVPA. When applied to Actigraph+GPS data with MVPA categorized by vertical-axis counts (Freedson et al., 1998), DBSCAN, HDBSCAN, and kernel density ranking polygon methods excluded all person-days of data in the 1<sup>st</sup> and 2<sup>nd</sup> quartiles. This is due to the minimum number of MVPA observations per person-day (25 for DBSCAN, 25 for HDBSCAN, and 30 for kernel density ranking) needed to conduct these spatial processes.

Across all 21 methods, PASs ranged in size between 1.0 square-meter and 526.978 square-kilometers. There was no clear difference in PAS area between methods utilizing Actigraph+GPS data and those using MOVES data. For PAS methods utilizing Actigraph+GPS data, MVPA categorized with vertical-axis counts (Freedson et al., 1998) resulted in larger average PAS sizes (range = 0.039 – 10.491 square kilometers) than the MVPA categorized with step-rate (Abel et al., 2011) (range = 0.038 – 2.565 square kilometers). The 95% directional distribution ellipse PAS polygons, derived from Actigraph+GPS data with MVPA categorized by

vertical-axis counts (Freedson et al., 1998), averaged the largest area ( $M \pm SD = 10.791 \pm 45.622$  square kilometers), whereas HDBSCAN polygons, derived from Actigraph+GPS data with MVPA categorized by step-count (Abel et al., 2011), averaged the smallest area ( $M \pm SD = 0.038 \pm 0.084$  square kilometers).

### 3.3.2 Quantification of green space for 21 PAS methods

**Table 3.3** presents the NDVI areal means for 2016 and 2018 for each person-day using the 21 PAS methods. Across all methods applied to 2018 imagery, the lowest NDVI for a PAS was 0.119 (e.g., man-made object, not green) and the highest was 0.530 (moderately green). For 2016 imagery, the lowest NDVI for a PAS was -0.076 and the highest was 0.432. The 500-m location buffer PASs, derived from MOVES data, generated the highest average NDVI per person-day for both 2018 ( $M \pm SD = 0.063 \pm 0.063$ ) and 2016 ( $M \pm SD = 0.073 \pm 0.050$ ). Kernel density ranking PASs, derived from Actigraph+GPS data with MVPA categorized using step-count (Abel et al., 2011), generated the lowest average NDVI per person-day for both 2018 ( $M \pm SD = 0.025 \pm 0.076$ ) and 2016 ( $M \pm SD = 0.037 \pm 0.057$ ). **Table 3.4** shows the NDVI areal means for 250-m home buffer (2018:  $M \pm SD = 0.026 \pm 0.061$ ; 2016:  $M \pm SD = 0.038 \pm 0.053$ ) and 500-m home buffer (2018:  $M \pm SD = 0.043 \pm 0.064$ ; 2016:  $M \pm SD = 0.052 \pm 0.041$ ) extractions. These are not PASs but are used for comparison to the PAS methods.

Intraclass correlation coefficients (ICC3s) were used to compare methods for assigning NDVI values to PASs. The comparisons are depicted in **Figures 3.9–3.11** and **Tables 3.5–3.7**. Actigraph+GPS and MOVES data with MVPA categorized using step count (Abel et al., 2011), and Actigraph+GPS data with MVPA categorized using vertical-axis counts (Freedson et al., 1998), were used to compare difference in results due to choice in imagery year (2018 vs. 2016). ICCs between 0.83 and 0.88 were observed when comparing 2018 and 2016 NDVI defined using Actigraph+GPS data categorized by vertical-axis count (Freedson et al., 1998) (**Table 3.6**). The

maximum difference between 2018 and 2016 NDVI was found when kernel density ranking was used (difference was 0.35). ICCs between 0.83 and 0.89 were observed when comparing 2018 and 2016 NDVI defined using Actigraph+GPS data categorized by step-rate (Abel et al., 2011). The maximum difference between 2018 and 2016 NDVI was found when kernel density ranking was used (difference was 0.15). ICCs between 0.90 and 0.93 were observed when comparing 2018 and 2016 NDVI defined using MOVES data categorized by step-rate (Abel et al., 2011). The maximum difference between 2018 and 2016 NDVI was observed when minimum convex polygon was used (difference was 0.16).

NDVI values for each PAS polygon method were compared to the NDVI values extracted from 250-meter home buffers (not a PAS) (**Table 3.7**). We found low ICCs (0.06 to 0.31) between home buffers and PAS methods that used Actigraph+GPS with MVPA categorized by vertical-axis count (Freedson et al., 1998), indicating that home buffers may not be comparable for NDVI greenspace attribution in the context of physical activity. The maximum NDVI difference was 0.51, using minimum convex polygon. This was also true for comparisons between home buffers and PAS methods for Actigraph+GPS with MVPA categorized by step-rate (Abel et al., 2011), where we found low ICCs (0.09 to 0.23) as well where the maximum NDVI difference was 0.45, again using minimum convex polygon. Similarly, we observed low ICCs (0.06 and 0.15) between home buffers and PAS methods using MOVES and MVPA categorized by step-rate (Abel et al., 2011), with a maximum NDVI difference of 0.34 using minimum convex polygon.

The extracted values of NDVI from MOVES and Actigraph+GPS were compared across the seven PAS polygon methods (**Figure 3.8**). We found moderate-to-high correlations between Actigraph+GPS-*Freedson* and Actigraph+GPS-*Abel* as indicated by ICCs between 0.54 and 0.80. The maximum NDVI difference of 0.32 was observed for the 95% directional distribution ellipse. We found somewhat more moderate correlations between Actigraph+GPS-*Abel* and MOVES-*Abel* as indicated by ICCs between 0.41 and 0.61. The maximum NDVI difference of 0.32 was

observed for the 95% directional distribution ellipse. Finally, we found the lowest, but still moderate, correlations between *Actigraph+GPS-Freedson* and *MOVES-Abel* as indicated by ICCs between 0.30 and 0.59. The maximum NDVI difference of 0.32 was observed for the minimum convex polygon.

### 3.4 DISCUSSION

This study evaluated 21 approaches to defining physical activity spaces for use in quantifying green space, with activity and location tracking derived from the MOVES smartphone app and Actigraph accelerometers combined with GlobalSat GPS units (*Actigraph+GPS*), physical activity level (sedentary-to-light and MVPA) categorized using two equations (Abel et al., 2011; Freedson et al., 1998), and the shape and location of the spaces with the most physical activity (PASs) defined by seven geospatial methods for drawing polygons around highly active regions. Green space (NDVI) was quantified by extracting satellite data by each PAS for two separate years, 2018 and 2016. We found that MOVES data resulted in fewer completed PASs for the study population than *Actigraph+GPS* but these PASs utilized more minutes of MVPA on average. NDVI values extracted by PAS demonstrated high correlation between 2018 and 2016 NAIP imagery for all seven PAS methods, exhibited low correlation and large mean difference between PAS methods and home buffers, and showed a wide range in correlation between *Actigraph+GPS* and MOVES data across the PAS methods.

Our results showing that the MOVES app recorded fewer observations but higher estimated activity levels than *Actigraph+GPS* is consistent with the Dutch study of 56 free-living participants observed for a single workday (Kooiman et al., 2015). When the authors compared MOVES activity data to the “gold-standard” ActivPAL accelerometer (similar to Actigraph), MOVES data produced a high correlation with the “gold-standard” ActivPAL but with a large confidence interval (ICC = 0.80; CI = 0.05 – 0.99). As the authors noted, a limitation of this study

was only 11 of 56 free-living participants produced valid MOVES data, and this low sample size could lead to the large interval. In a similar study of 14 participants, researchers found MOVES to underestimate steps by 6.7% on average for Android smartphone users and overestimate steps by 6.2% for iPhone users (Case et al., 2015). Given the PASTA-LA participant sample included both iPhone and Android users, the results of these two studies could help explain the high number of excluded person-days of MOVES data (fewer minutes of MVPA potentially observed from Android users) while simultaneously having more minutes of MVPA (from iPhone users) for the person-days included. Furthermore, we have shown that once MOVES data is used to produce PASs, subsequent NDVI extracted is moderately correlated to NDVI extracted from Actigraph+GPS. Although MOVES data includes a large degree of uncertainty and possible imprecision due to its proprietary nature, it also allows for the collection of more tracking data over longer periods of time due to being a smartphone app (participants likely own smartphones). Due to the ability to collect more data for less cost, the difference in reliability may be less consequential for certain study designs.

Other studies also found that methods used to draw activity spaces demonstrated a wide range in coverage (size). Wang et al. used GPS tracking data from four individuals (sampled from  $n = 31$ ) to compare activity spaces constructed using 200-meter location buffers, standard deviation ellipses (including both 63% ellipses—1 standard deviation; and 95% ellipses—2 standard deviations), minimum convex polygons, kernel densities, and a new “context-based crystal-growth” (CCG) method (J. Wang et al., 2018). They found that their activity space methods averaged from 12.65 (CCG) to 70.08 km<sup>2</sup> (minimum convex polygon) in size, with the smallest individual activity space being 0.037 km<sup>2</sup> (63% ellipse) and the largest being 156.48 km<sup>2</sup> (95% ellipse). In the present study—with a much larger sample size of 123 participants—minimum convex polygons, specifically using Actigraph+GPS data with MVPA categorized by vertical-axis counts (Freedson et al., 1998), also generated the largest average sizes. Given that we used

*only* locations where MVPA is observed (PASs), rather than all locations (activity spaces) as in Wang et al., we would expect our PASs polygons to be smaller in size. Although our PASs had smaller average sizes, we did have some PASs with larger sizes—the largest being 526.98 km<sup>2</sup> (minimum convex polygon using Actigraph+GPS data, with MVPA categorized by vertical-axis counts (Freedson et al., 1998)).

Green space extracted by home location was poorly correlated with green space extracted by 21 PAS methods (**Table 3.6**), suggesting a potential of misclassification of green space using home buffers. Although many studies have quantified green space exposure using NDVI extraction, the majority of these studies utilize the home location (Amoly et al., 2015; Dadvand et al., 2015, 2012b; Dzhambov et al., 2018; Fuertes et al., 2016; Klompmaker et al., 2018; Laurent et al., 2013), or in some cases GPS location buffers (Almanza et al., 2012; Boakye et al., 2021; Roberts and Helbich, 2021), to extract mean NDVI values. In a study of 217 adults, Holliday et al. found that when using 0.5-mile buffers around the home (approximately 800 m), 60% of MVPA time occurred outside the buffer (Holliday et al., 2017). Holliday et. al. cautions against using home buffers as physical activity spaces—a recommendation that matches the present study findings, which further this understanding using extracted context (green space, NDVI).

Compared to other methods choices made in the present study, the choice between 2016 and 2018 NDVI (for green space exposure attribution) had the least impact on NDVI mean values extracted by PAS and were highly correlated (**Table 3.5**). In a study examining change in NDVI from 2000 to 2017 for Southern California, researchers found developed (urban) land areas to have the least annual change in vegetation (greenness) compared to other areas such as woodlands and grasslands (Dong et al., 2019). This is likely due to the impervious surfaces observed in urban areas, and the fact that these regions therefore have less areas where vegetation can fluctuate or grow. Furthermore, given the imagery used in this study are annual means of NDVI, it is unlikely that significant changes in vegetation would be observed.

The present study has a number of strengths and some limitations. It was one of very few studies that compared geospatial methodologies for defining physical activity space. It is the only study that has compared these multiple PAS approaches for quantifying green space exposure at locations of high physical activity (MVPA). Actigraph and other contemporary accelerometers can utilize tri-axial counts to more precisely categorize MVPA; however, this investigation uses step-rate (Abel et al., 2011) and vertical-axis counts (Freedson et al., 1998) to compare MOVES and Actigraph. Although a large amount of possible location and activity tracking data were excluded here (from 440 to 123), internal validity was retained (Deeks et al., 2003), and other studies have excluded similar amounts of analogous data (Jerrett et al., 2013a). Many of the PAS methods required a minimum number of MVPA observations (e.g., kernel density ranking requires a minimum of 30 point-locations of MVPA) to complete. This resulted in fewer PASs for certain methods (n=44 to 122; 195 to 1105 person-days of PASs, respectively). This suggests that certain PAS polygon methods may be better suited for research on more active populations (e.g., DBSCAN, kernel density ranking), whereas others may be better suited for less active populations (e.g., 250-m and 500-m location buffers, minimum convex polygon).

The methods described in this study for NDVI could be used to extract other context variables, besides green space, such as other satellite images, other raster data, and vector data. These methods are useful for public health research but could also be utilized for other contexts in which there is an interest in understanding where people engage in physical activity, such as for urban planning and marketing. A strength of this study lies in the low computing time needed to quantify high resolution imagery (in this study, NDVI) for large amounts of location and activity data, by using a singular open-source software platform (i.e., R Studio with r-based Google Earth Engine queries). Although MOVES is no longer commercially available (the app was purchased by Facebook, Inc. on July 31<sup>st</sup>, 2018 (Dance, 2018), one month after PASTA-LA data collection phase completed), other analogous activity-tracking smartphone apps could be used to crowd-

source and automate these methods. Many apps have already been developed and released for consumer use (e.g., the Arc App available for iOS, the Aware Framework available for Android, or the Gyroscope app available on both platforms) and, in the future, can be evaluated for quantifying spatial context of human activity.

### **3.5 CONCLUSION**

Quantifying spatial context is important for public health research, as it allows for better understanding of the built and natural environments. In the case of physical activity, it may be important to quantify green space as it has been shown to affect the location and amount of active behavior. Many geospatial methods exist for attributing green space exposure to individuals based on location and activity; however, there is not yet consensus on best practices. The results of this comparative study on physical activity spaces may inform future environmental study on active behavior, allowing researchers to craft methods and protocols more appropriate for a given research question or study population or as constrained by available resources.

**Table 3.1.** Data sources utilized for the assessment of green-space exposure attribution by physical activity space (PAS)

Data source	Attribute(s)	Spatial Dimension	Epoch of Collection	Collection Period
<i>Actigraph GT3x+ (PASTA-LA)</i>	Steps, counts*, date-time	-	10 seconds	May 2017-May 2018
<i>GlobalSat DG-500 (PASTA-LA)</i>	GPS coordinates, date-time	Point (accuracy 10-meters meters; <2.5 meters)	15 seconds	May 2017-May 2018
<i>MOVES smartphone app (PASTA-LA)</i>	Steps, mode of transport, GPS coordinates, date-time	Point (variable accuracy)	Variable**	May 2017-May 2018
<i>Online Questionnaire (PASTA-LA)</i>	Age, sex, ethnicity, BMI, educational attainment, job status, home address, work address	-	-	May 2017-May 2018
<i>USDA NAIP*** (via Google Earth Engine)</i>	Multispectral (4-band: red, green, blue, infrared) image	60 cm	Annual	2016, 2018

\* 'Counts' are a proprietary unitless metric unique to Actigraph-branded accelerometers.

\*\* MOVES collection epoch is variable based on the detection of bout of inactive or predictable behavior – during these periods, the app would shut off to preserve battery.

\*\*\*U.S. Department of Agriculture, National Agriculture Imagery Program, National Agriculture Imagery Program; accessed via Google Earth Engine

**Table 3.2.** Participant demographics and tracking data sample size

Variable		Mean	Standard Deviation	Range
Participant Background	Age (years)	33.3	11.0	21 – 66
	Gender <sup>a</sup>	0.317	0.467	0 – 1
	Ethnicity <sup>b</sup>	0.325	0.470	0 – 1
	Education <sup>c</sup>	0.878	0.329	0 – 1
	Job Status <sup>d</sup>	0.510	0.500	0 – 1
	BMI	23.6	3.95	9.3 – 35.5
Activity Tracking	Hours*	25.4	20.1	0.23 – 106.4
	Observations** (Actigraph+GPS)	9,129	7,252	85 – 38,303
	Observations** (MOVES app)	1,721	1,384	2 – 6,285

**Table 3.3.** Description of sample, minutes of MVPA included, and size of PAS polygons from activity and location data, for 21 methods

PAS Method	Data Source	MVPA Formula	N	N Person-Days	Daily MVPA (mins)		PAS Area (km <sup>2</sup> )	
					M±SD	Median (Range)	M±SD	Median(Range)
250-m Location Buffer	Act+GPS	<i>Freedson</i>	122	1105	6.36±9.56	3.00 (0.17, 86.20)	0.658±0.476	0.554(0.196, 3.860)
	Act+GPS	<i>Abel</i>	119	828	7.55±8.48	4.83(0.17, 62.31)	0.646±0.449	0.559(0.196, 6.271)
	MOVES	<i>Abel</i>	105	613	19.30±22.63	12.75(0.52, 248.03)	0.739±0.588	0.584(0.196, 5.695)
500-m Location Buffer	Act+GPS	<i>Freedson</i>	122	1105	6.31±9.30	3.00(0.17, 70.00)	1.973±1.177	1.771(0.785, 9.291)
	Act+GPS	<i>Abel</i>	119	828	7.55±8.48	4.83(0.17, 62.31)	1.788±1.030	1.652(0.785, 15.140)
	MOVES	<i>Abel</i>	105	613	19.33±22.63	12.75(0.52, 248.03)	1.900±1.166	1.655(0.785, 10.843)
Minimum Convex Polygon	Act+GPS	<i>Freedson</i>	120	894	7.48±9.42	4.00(0.83, 65.72)	9.274±39.432	0.026(1.0m <sup>2</sup> , 526.978)
	Act+GPS	<i>Abel</i>	115	710	8.71±8.59	6.01(0.83, 62.31)	1.908±10.496	0.014(1.0m <sup>2</sup> , 211.279)
	MOVES	<i>Abel</i>	101	550	20.09±21.84	14.46(1.23, 248.03)	0.990±3.369	0.103(128.9m <sup>2</sup> , 38.243)
95% Ellipse	Act+GPS	<i>Freedson</i>	119	869	7.65±9.50	4.33(0.83, 65.72)	10.791±45.622	0.276(11.0m <sup>2</sup> , 520.075)
	Act+GPS	<i>Abel</i>	113	703	8.78±8.61	6.01(0.83, 62.31)	2.565±16.916	0.116(10.0m <sup>2</sup> , 257.501)
	MOVES	<i>Abel</i>	101	549	20.09±21.84	14.47(1.23, 248.03)	1.106±3.985	0.111(279.1m <sup>2</sup> , 47.354)
DBSCAN - Optics	Act+GPS	<i>Freedson</i>	90	389	14.10±11.12	9.83(5.23, 65.72)	1.061±9.038	0.018(25.0m <sup>2</sup> , 151.70)
	Act+GPS	<i>Abel</i>	93	403	13.50±8.74	10.67(5.02, 62.31)	0.186±1.675	0.009(25.0m <sup>2</sup> , 23.387)
	MOVES	<i>Abel</i>	61	200	33.81±24.77	26.73(10.50, 159.63)	0.657±0.158	0.020(152.4m <sup>2</sup> , 1.610)
HDBSCAN	Act+GPS	<i>Freedson</i>	90	388	14.10±11.12	9.83(5.23, 65.72)	0.039±0.170	0.009(25.0m <sup>2</sup> , 2.346)
	Act+GPS	<i>Abel</i>	93	402	13.50±8.74	10.75(5.02, 65.72)	0.038±0.084	0.018(25.0m <sup>2</sup> , 0.877)
	MOVES	<i>Abel</i>	61	200	33.81±24.77	26.73(10.50, 159.63)	0.076±0.181	0.030(967.2m <sup>2</sup> , 1.638)
Kernel Density Ranking	Act+GPS	<i>Freedson</i>	90	389	14.10±11.12	9.83(5.23, 65.72)	1.494±2.504	0.228(5.5m <sup>2</sup> , 21.492)
	Act+GPS	<i>Abel</i>	44	195	13.79±9.13	10.83(5.02, 65.72)	0.773±2.133	0.075(50.4m <sup>2</sup> , 19.619)
	MOVES	<i>Abel</i>	61	200	33.81±24.77	26.73(10.50, 159.63)	0.309±0.759	0.065(0.002, 7.033)

**Table 3.4:** Green space (areal mean NDVI derived from NAIP imagery) values attributed to PASs for 21 methods

PAS Method	Data Source	MVPA Formula	N	N Person-Days	2018 NDVI		2016 NDVI	
					M±SD	Median (Range)	M±SD	Median(Range)
250-m Location Buffer	Act+GPS	<i>Freedson</i>	122	1105	0.027±0.061	0.020(-0.138, 0.239)	0.044±0.047	0.038(-0.142, 0.261)
	Act+GPS	<i>Abel</i>	119	828	0.029±0.067	0.020(-0.140, 0.287)	0.047±0.051	0.042(-0.103, 0.276)
	MOVES	<i>Abel</i>	105	613	0.039±0.066	0.030(-0.157, 0.269)	0.054±0.054	0.048(-0.161, 0.274)
500-m Location Buffer	Act+GPS	<i>Freedson</i>	122	1105	0.045±0.060	0.039(-0.132, 0.234)	0.059±0.046	0.052(-0.097, 0.249)
	Act+GPS	<i>Abel</i>	119	828	0.051±0.064	0.048(-0.159, 0.301)	0.065±0.048	0.064(-0.088, 0.273)
	MOVES	<i>Abel</i>	105	613	0.063±0.063	0.062(-0.196, 0.267)	0.073±0.050	0.073(-0.088, 0.269)
Minimum Convex Polygon	Act+GPS	<i>Freedson</i>	120	894	0.033±0.077	0.025(-0.195, 0.504)	0.046±0.059	0.039(-0.139, 0.378)
	Act+GPS	<i>Abel</i>	115	710	0.032±0.088	0.023(-0.228, 0.409)	0.047±0.068	0.036(-0.128, 0.381)
	MOVES	<i>Abel</i>	101	550	0.030±0.082	0.026(-0.211, 0.312)	0.045±0.062	0.039(-0.103, 0.301)
95% Ellipse	Act+GPS	<i>Freedson</i>	119	869	0.039±0.076	0.040(-0.216, 0.530)	0.053±0.056	0.048(-0.137, 0.303)
	Act+GPS	<i>Abel</i>	113	703	0.037±0.087	0.031(-0.222, 0.396)	0.051±0.067	0.041(-0.118, 0.352)
	MOVES	<i>Abel</i>	101	549	0.033±0.079	0.034(-0.201, 0.271)	0.047±0.059	0.046(-0.108, 0.281)
DBSCAN-Optics	Act+GPS	<i>Freedson</i>	90	389	0.035±0.091	0.025(-0.202, 0.392)	0.049±0.070	0.043(-0.103, 0.432)
	Act+GPS	<i>Abel</i>	93	403	0.036±0.098	0.024(-0.222, 0.329)	0.051±0.074	0.042(-0.145, 0.312)
	MOVES	<i>Abel</i>	61	200	0.044±0.086	0.032(-0.137, 0.331)	0.054±0.065	0.039(-0.090, 0.295)
HDBSCAN	Act+GPS	<i>Freedson</i>	90	388	0.037±0.090	0.027(-0.169, 0.333)	0.050±0.072	0.047(-0.121, 0.373)
	Act+GPS	<i>Abel</i>	93	402	0.038±0.091	0.030(-0.149, 0.298)	0.051±0.070	0.038(-0.118, 0.249)
	MOVES	<i>Abel</i>	61	200	0.033±0.079	0.028(-0.119, 0.227)	0.046±0.060	0.035(-0.095, 0.202)
Kernel Density Ranking	Act+GPS	<i>Freedson</i>	90	389	0.043±0.083	0.040(-0.261, 0.371)	0.053±0.061	0.049 (-0.099,0.298)
	Act+GPS	<i>Abel</i>	44	195	0.025±0.076	0.015(-0.139, 0.300)	0.037±0.057	0.022(-0.076, 0.298)
	MOVES	<i>Abel</i>	61	200	0.037±0.084	0.033(-0.144, 0.264)	0.049±0.064	0.038(-0.097, 0.304)

**Table 3.5.** Green space (areal mean NDVI derived from NAIP imagery) values attributed to home address buffers

Method	2018 NDVI		2016 NDVI	
	M±SD	Median (Range)	M±SD	Median(Range)
250-m Home Buffer	0.026±0.061	0.011(-0.076, 0.175)	0.038±0.053	0.027(-0.057, 0.180)
500-m Home Buffer	0.043±0.064	0.030(-0.056, 0.196)	0.052±0.054	0.041(-0.036, 0.181)

**Table 3.6.** Comparison of 2018 versus 2016 extracted NDVI values for seven PAS methods

Comparison of 2018 versus 2016 extracted NDVI values; extracted by seven PAS polygon methods using Actigraph+GPS (**TOP**) and MOVES (**BOTTOM**) datasets with MVPA categorized by step count (Abel et al., 2011). Intraclass correlation coefficients (ICC3) are used to compare.

<b>Method (Actigraph+GPS-Freedson)</b>	Mean Difference	Min. Difference	Max. Difference	ICC3
250-m Location Buffer	-0.019	-0.147	0.118	0.867
500-m Location Buffer	-0.015	-0.137	0.109	0.878
Minimum Convex Polygon	-0.015	-0.260	0.160	0.875
95% Directional Distribution Ellipse	-0.014	-0.173	0.246	0.867
HDBSCAN	-0.016	-0.275	0.307	0.844
DBSCAN - OPTICS	-0.014	-0.196	0.265	0.871
Kernel Density Ranking	-0.011	-0.165	0.352	0.830

<b>Method (Actigraph+GPS-Abel)</b>	Mean Difference	Min. Difference	Max. Difference	ICC3
250-m Location Buffer	-0.020	-0.146	0.137	0.874
500-m Location Buffer	-0.016	-0.136	0.139	0.877
Minimum Convex Polygon	-0.017	-0.275	0.130	0.879
95% Directional Distribution Ellipse	-0.016	-0.253	0.146	0.875
HDBSCAN	-0.018	-0.308	0.182	0.864
DBSCAN - OPTICS	-0.015	-0.179	0.117	0.888
Kernel Density Ranking	-0.014	-0.200	0.150	0.828

<b>Method (MOVES app-Abel)</b>	Mean Difference	Min. Difference	Max. Difference	ICC3
250-m Location Buffer	-0.014	-0.196	0.130	0.932
500-m Location Buffer	-0.010	-0.187	0.127	0.924
Minimum Convex Polygon	-0.014	-0.231	0.161	0.909
95% Directional Distribution Ellipse	-0.014	-0.214	0.148	0.908
HDBSCAN	-0.011	-0.138	0.096	0.913
DBSCAN - OPTICS	-0.014	-0.101	0.085	0.920
Kernel Density Ranking	-0.012	-0.147	0.126	0.897

**Table 3.7:** Comparison of NDVI extracted from 250-meter home address buffers versus NDVI extracted from seven PAS methods

Comparison of NDVI extracted from 250-meter home address buffers versus NDVI extracted from seven PAS methods using Actigraph+GPS and MOVES datasets with MVPA categorized by step count (Abel et al., 2011). Intraclass correlation coefficients (ICC3) are used to compare.

<b>Method (Actigraph+GPS-Freedson)</b>	Mean Difference	Min. Difference	Max. Difference	ICC3
250-m Location Buffer	0.005	-0.227	0.271	0.290
500-m Location Buffer	0.022	-0.215	0.283	0.305
Minimum Convex Polygon	0.008	-0.297	0.507	0.062
95% Directional Distribution Ellipse	0.014	-0.306	0.483	0.095
HDBSCAN	0.006	-0.328	0.329	0.128
DBSCAN - OPTICS	0.009	-0.249	0.320	0.155
90th Percentile Kernel Density Ranking	0.015	-0.251	0.335	0.165

<b>Method (Actigraph+GPS-Abel)</b>	Mean Difference	Min. Difference	Max. Difference	ICC3
250-m Location Buffer	-0.001	-0.214	0.303	0.229
500-m Location Buffer	0.021	-0.225	0.317	0.219
Minimum Convex Polygon	-0.001	-0.252	0.454	0.120
95% Directional Distribution Ellipse	0.003	-0.264	0.364	0.099
HDBSCAN	-0.009	-0.290	0.323	0.111
DBSCAN - OPTICS	-0.009	-0.263	0.304	0.104
90th Percentile Kernel Density Ranking	-0.023	-0.234	0.312	0.090

<b>Method (MOVES app-Abel)</b>	Mean Difference	Min. Difference	Max. Difference	ICC3
250-m Location Buffer	0.015	-0.232	0.251	0.150
500-m Location Buffer	0.038	-0.236	0.279	0.152
Minimum Convex Polygon	0.005	-0.247	0.329	0.098
95% Directional Distribution Ellipse	0.007	-0.229	0.266	0.065
HDBSCAN	0.012	-0.241	0.336	0.101
DBSCAN - OPTICS	0.001	-0.223	0.302	0.062
90th Percentile Kernel Density Ranking	0.004	-0.249	0.290	0.138

**Table 3.8:** Comparison of NDVI extracted from MOVES versus Actigraph+GPS (using step-count MVPA conversion—Abel 2011) for seven PAS methods

<b>Comparing Methods:</b>				
<b>Actigraph+GPS-Freedson</b>	Mean	Min.	Max.	
<b>Actigraph+GPS-Abel</b>	Difference	Difference	Difference	ICC3
250-m Location Buffer	0.004	-0.189	0.249	0.779
500-m Location Buffer	0.002	-0.222	0.251	0.802
Minimum Convex Polygon	0.001	-0.350	0.286	0.554
95% Directional Distribution Ellipse	0.005	-0.267	0.315	0.543
HDBSCAN	0.001	-0.240	0.274	0.605
DBSCAN - OPTICS	-0.010	-0.262	0.231	0.624
Kernel Density Ranking	0.016	-0.130	0.257	0.753

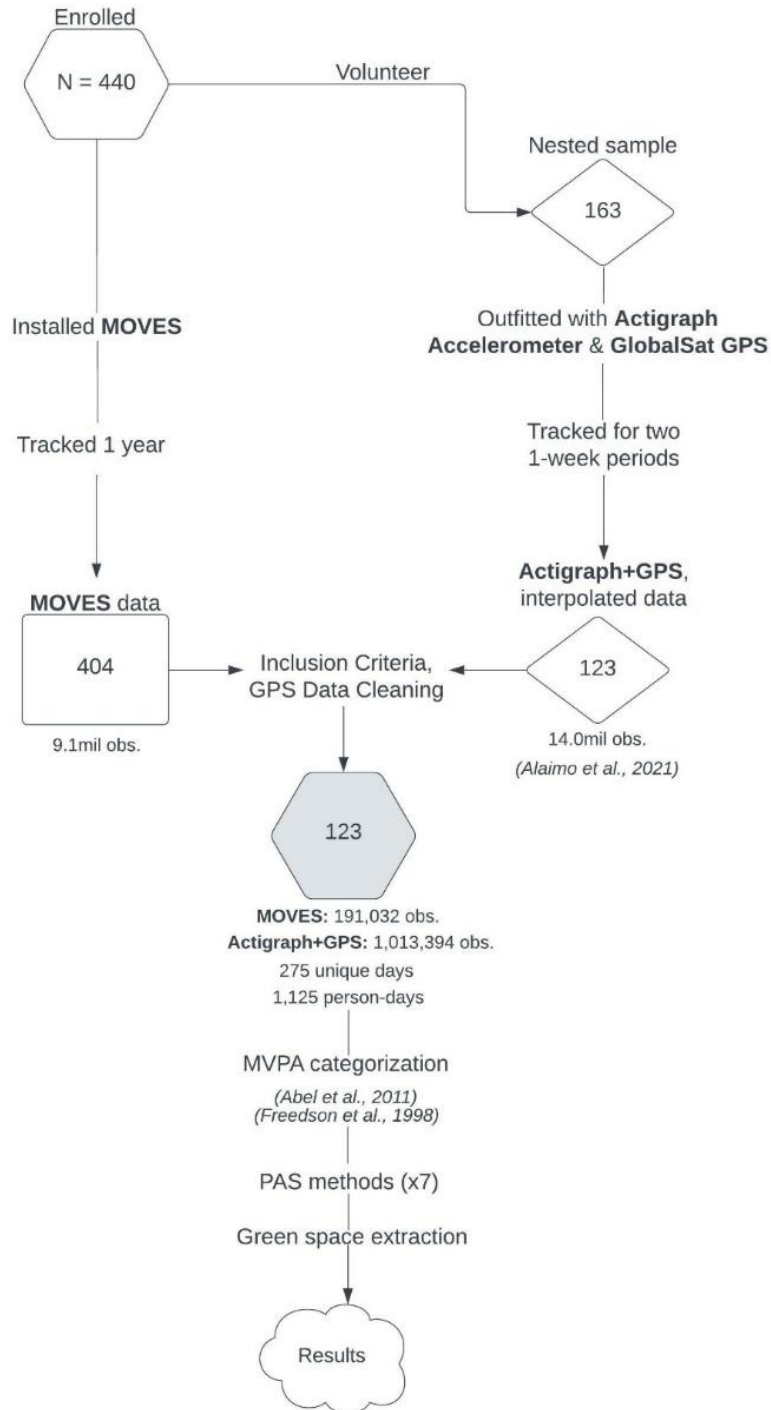
<b>Comparing Methods:</b>				
<b>Actigraph+GPS-Abel</b>	Mean	Min.	Max.	
<b>MOVES app-Abel</b>	Difference	Difference	Difference	ICC3
250-m Location Buffer	-0.012	-0.287	0.265	0.594
500-m Location Buffer	-0.013	-0.283	0.292	0.548
Minimum Convex Polygon	0.003	-0.296	0.318	0.411
95% Directional Distribution Ellipse	0.002	-0.308	0.324	0.484
HDBSCAN	-0.008	-0.355	0.288	0.469
DBSCAN - OPTICS	0.007	-0.353	0.193	0.495
Kernel Density Ranking	-0.010	-0.229	0.176	0.616

<b>Comparing Methods:</b>				
<b>Actigraph+GPS-Freedson</b>	Mean	Min.	Max.	
<b>MOVES app-Abel</b>	Difference	Difference	Difference	ICC3
250-m Location Buffer	-0.010	-0.304	0.231	0.534
500-m Location Buffer	-0.014	-0.300	0.253	0.493
Minimum Convex Polygon	-0.003	-0.295	0.319	0.300
95% Directional Distribution Ellipse	0.004	-0.310	0.266	0.333
HDBSCAN	-0.016	-0.319	0.235	0.536
DBSCAN - OPTICS	0.008	-0.372	0.304	0.385
Kernel Density Ranking	0.002	-0.259	0.169	0.594

**Figure 3.1.** Flow chart of participant sample utilized for analyses

Flow chart of PASTA-LA participants used to generate sample (in grey) utilized for the assessment of green space exposure attribution by physical activity space (PAS).



**Figure 3.2.** Map of participant activity and location data from MOVES app

MOVES data for n=123 participants after data cleaning and exclusions. Zoomed area shown (**RIGHT**) for more detail. Physical activity is categorized using step-rate conversions (Abel et al., 2011).

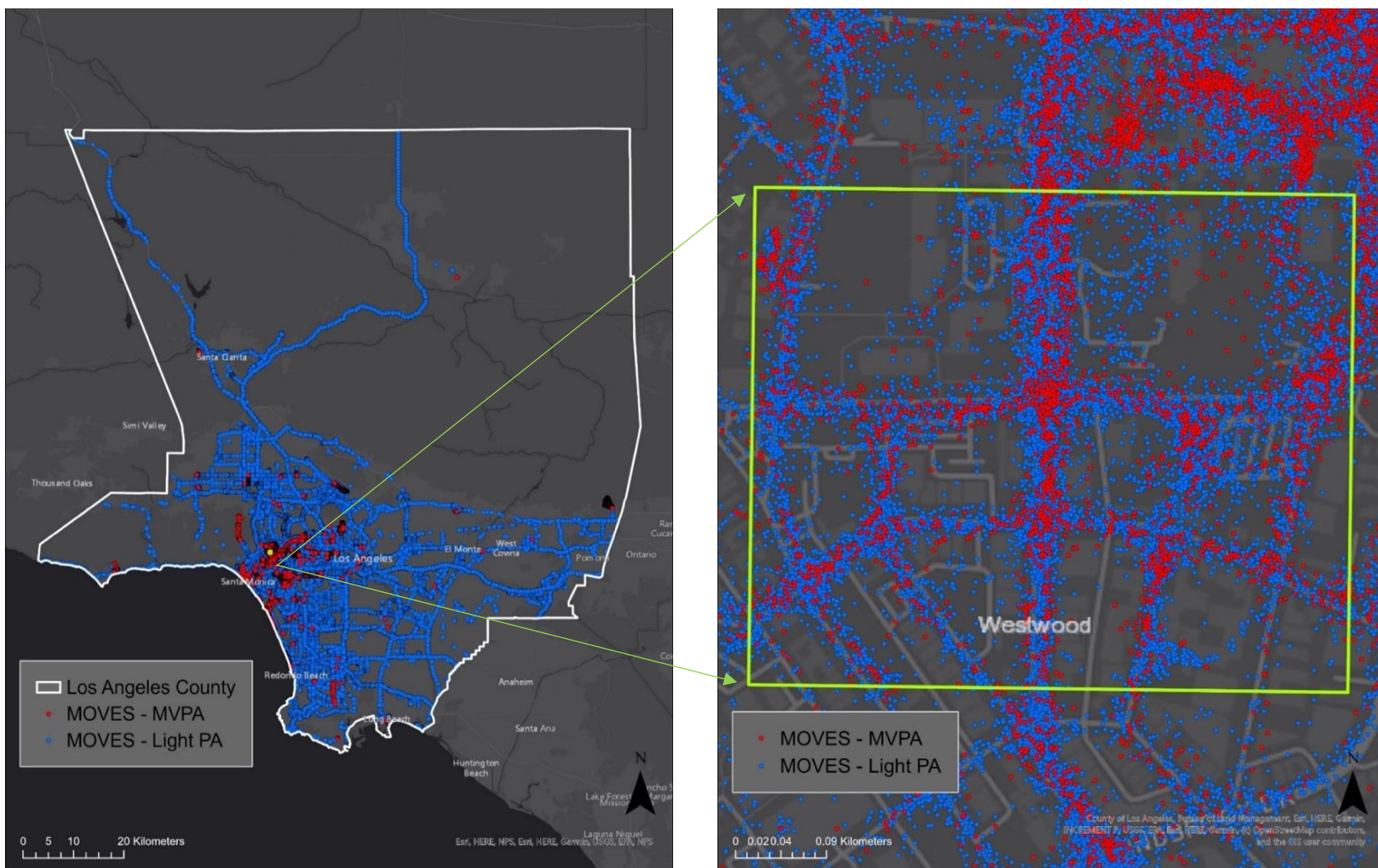


**Figure 3.3.** Map of participant activity and location data from Actigraph+GPS

Actigraph+GPS data for n = 123 participants, after data cleaning and exclusions. Zoomed area shown (**RIGHT**) for more detail. Physical activity is categorized using step-rate conversions (Abel et al., 2011)

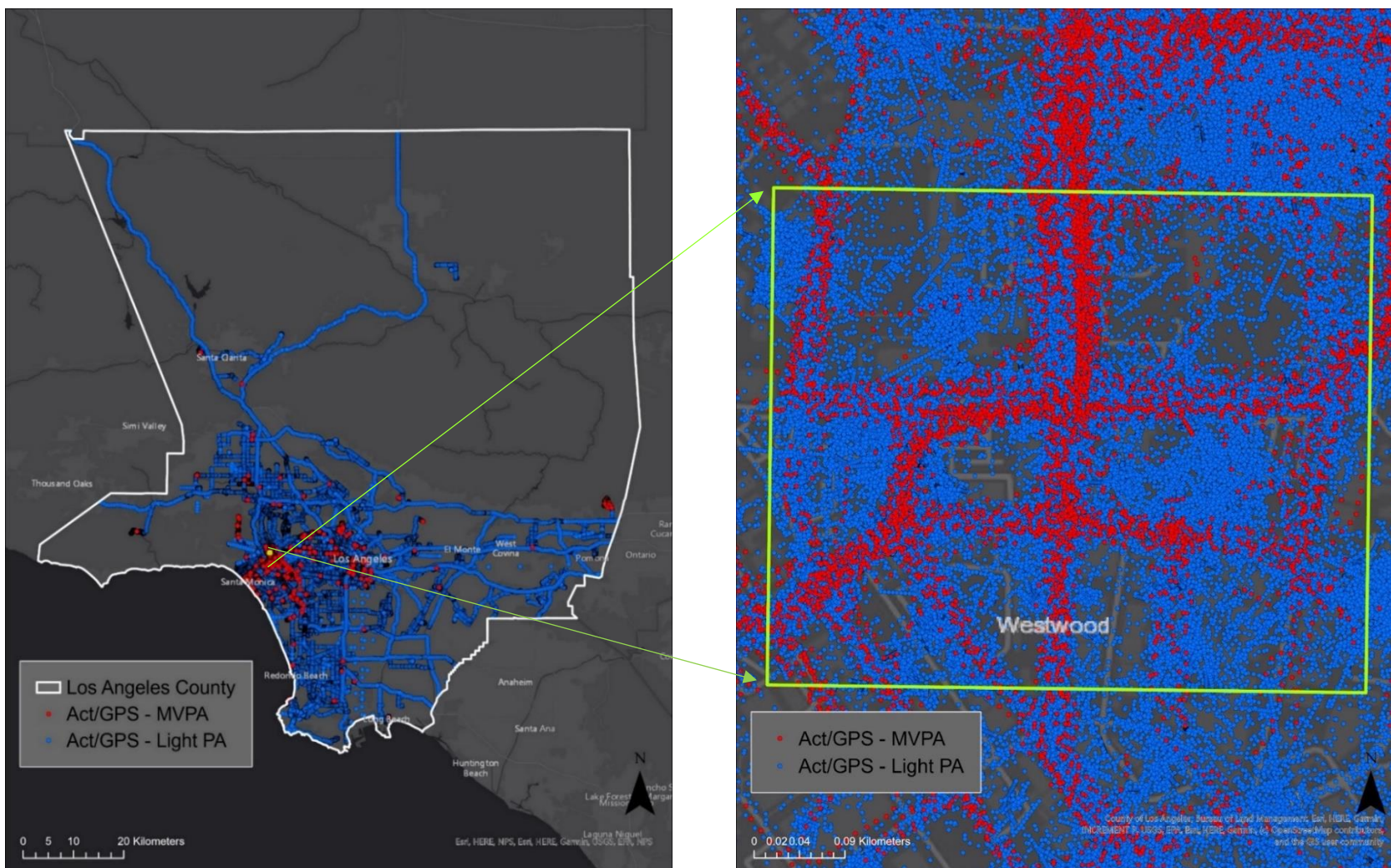


**Figure 3.4.** Map example of 250-meter location buffer PAS with true-color satellite image and NDVI

Example of 250-meter location buffer PAS for one person-day of partially simulated location and activity data. True color background from 60-cm resolution, 2018 NAIP imagery (**LEFT**); and derived green space (NDVI) background (**RIGHT**).

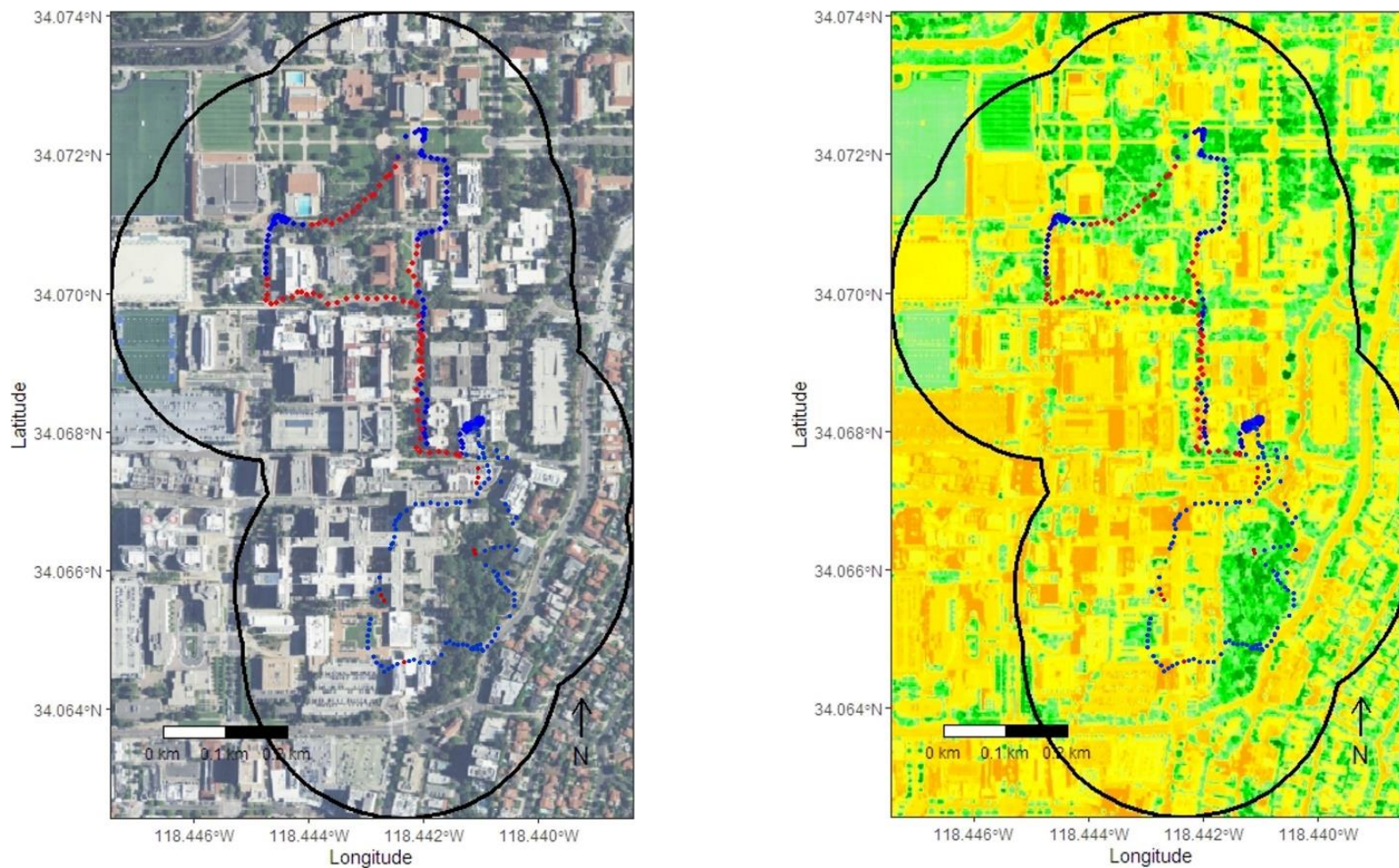


**Figure 3.5.** Map examples of PAS polygons with NDVI

Example six PAS polygons for one person-day of partially simulated location and activity data. 500-meter location buffer PAS is not depicted. True color background from 60-cm resolution, 2018 NAIP imagery (**LEFT**); and derived green space (NDVI) background (**RIGHT**).

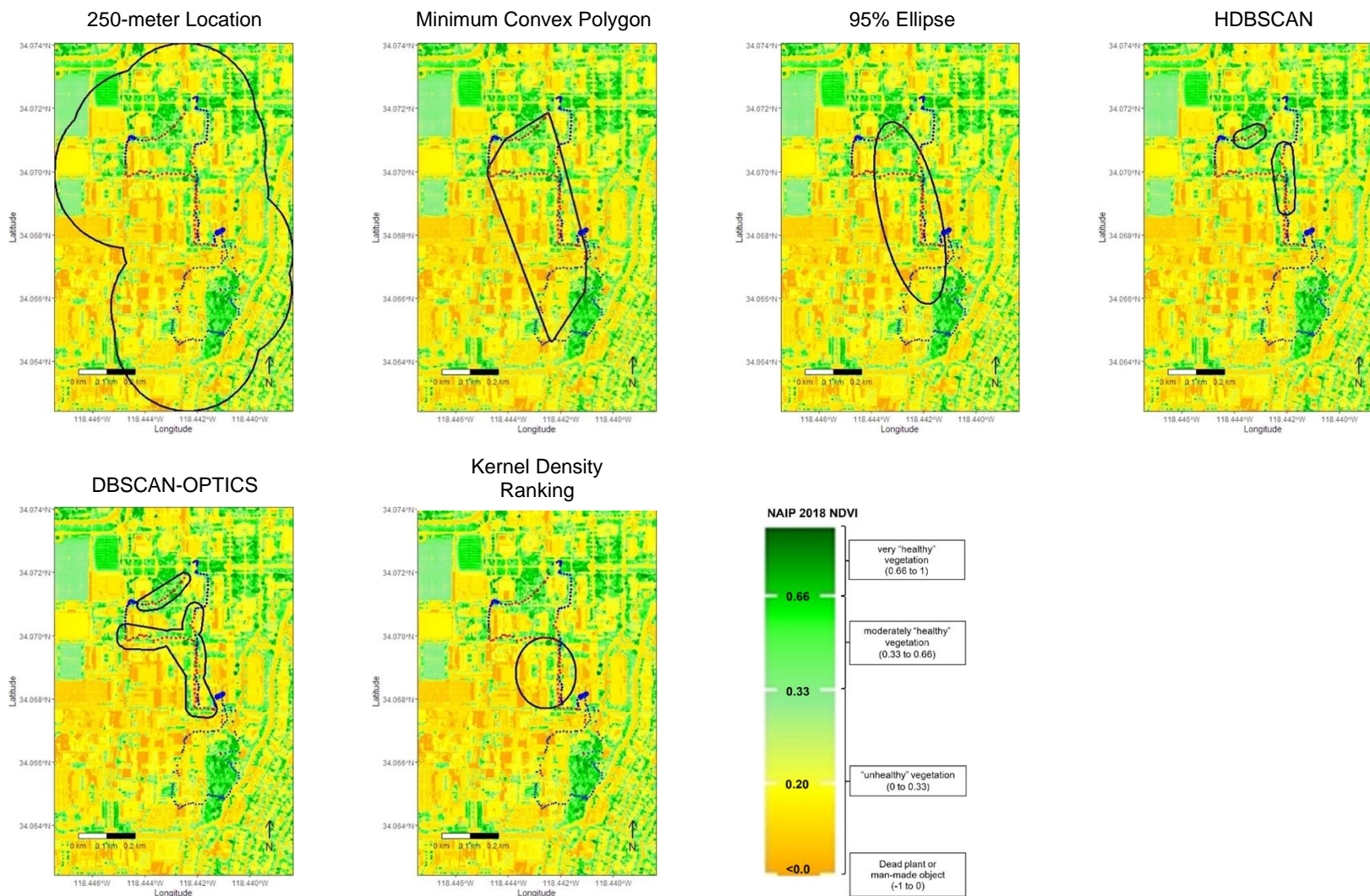


**Figure 3.6.** Overview of study procedures used to quantify green space exposure by PASs, including major software and software packages utilized

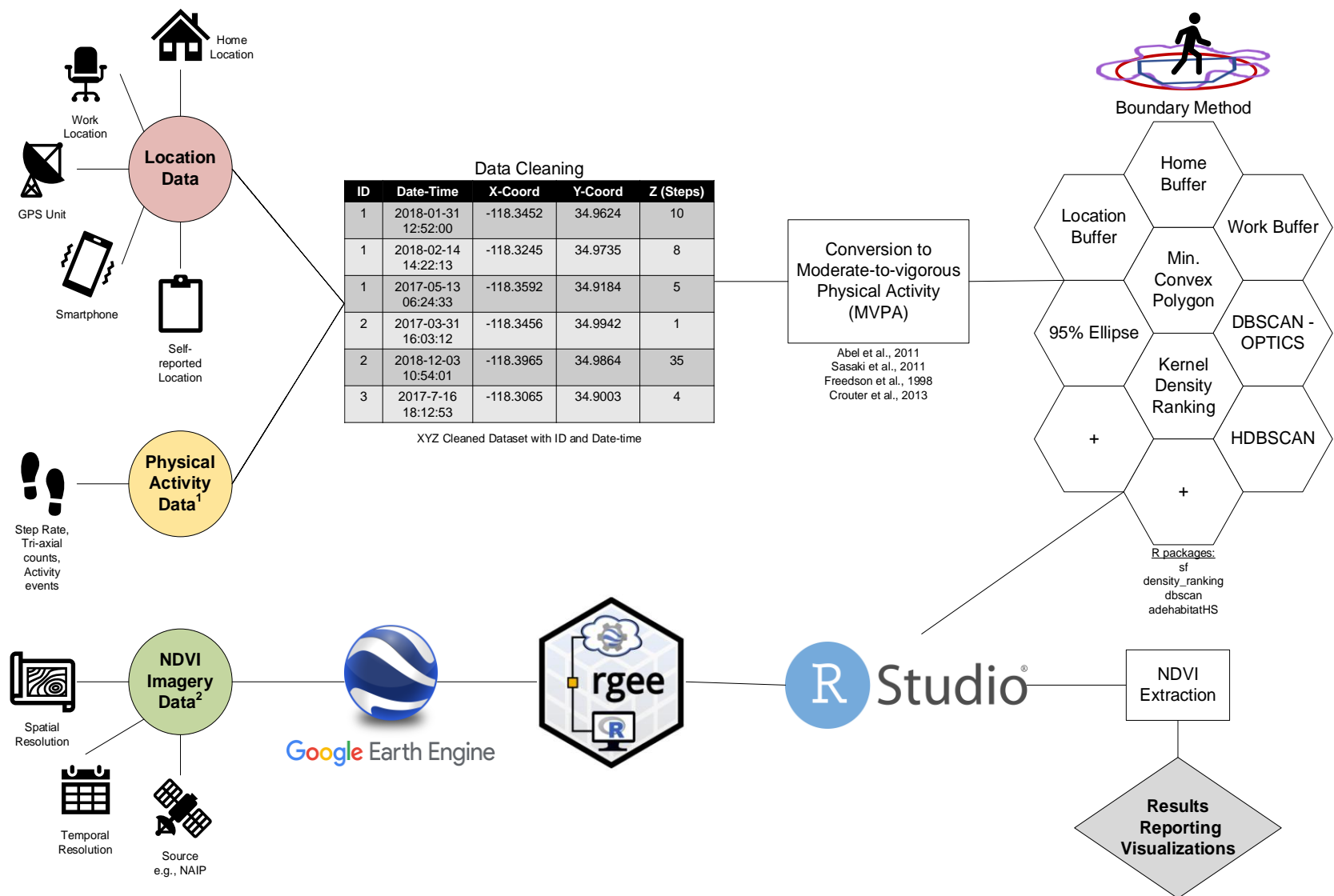


**Figure 3.7.** Flow chart of methods to extract green space (mean NDVI) from home location buffers while anonymizing data for cloud computing

These methods were specifically designed to help anonymize (in a random sample of 10,000) participant home locations (n = 163) when analyzed using cloud computing (Google Earth Engine). Other personally identifying information was removed from home-location data prior to analysis.

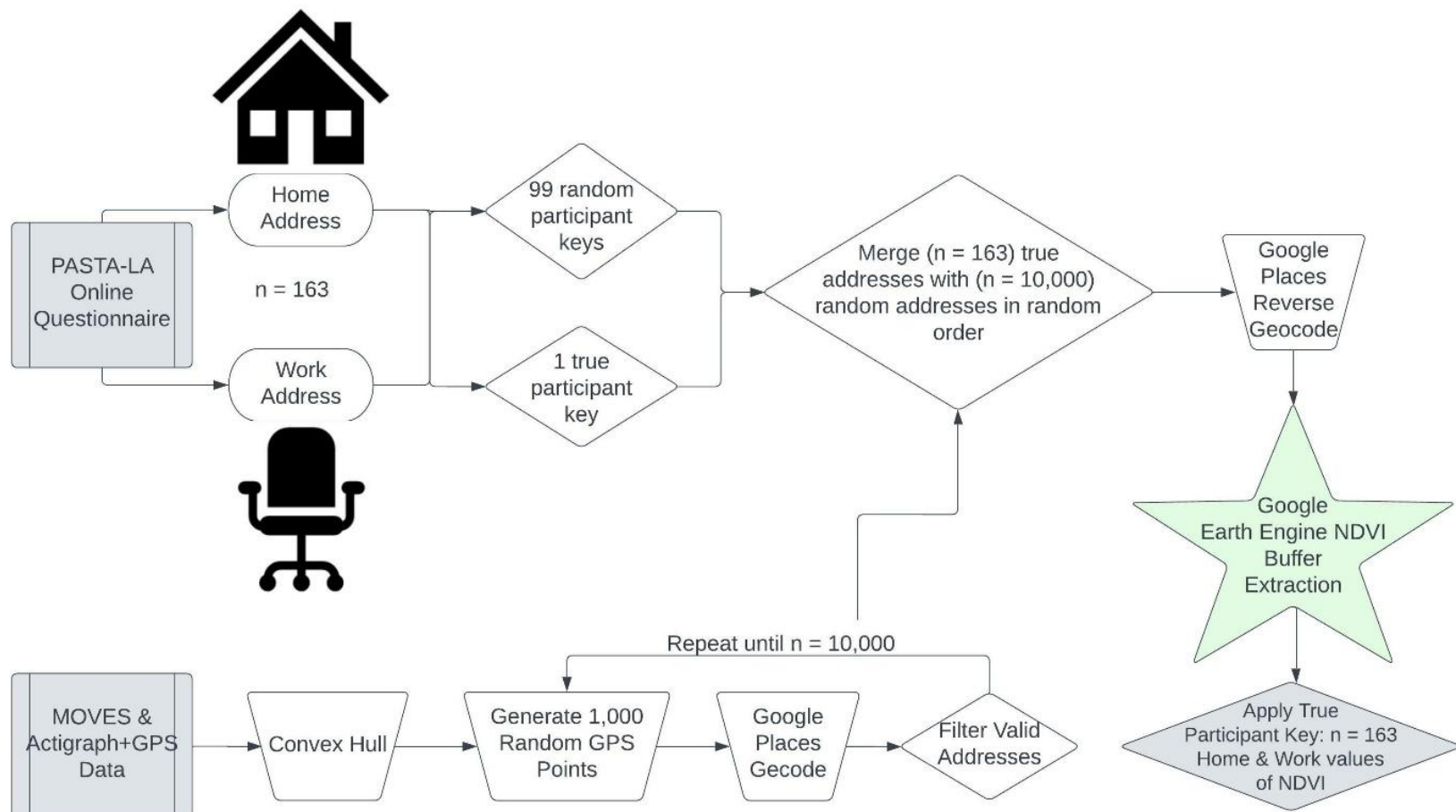


**Figure 3.8.** Proportion of person-days of observation excluded for each of 21 methods

Proportion excluded is compared with the quartile distribution of minutes MVPA per person-day for the 250-meter location buffer PAS, generated from Actigraph+GPS data with MVPA categorized using vertical-axis counts (Freedson et al., 1998). This method was selected for comparison due to having the least number of excluded person-days (n = 1,105).

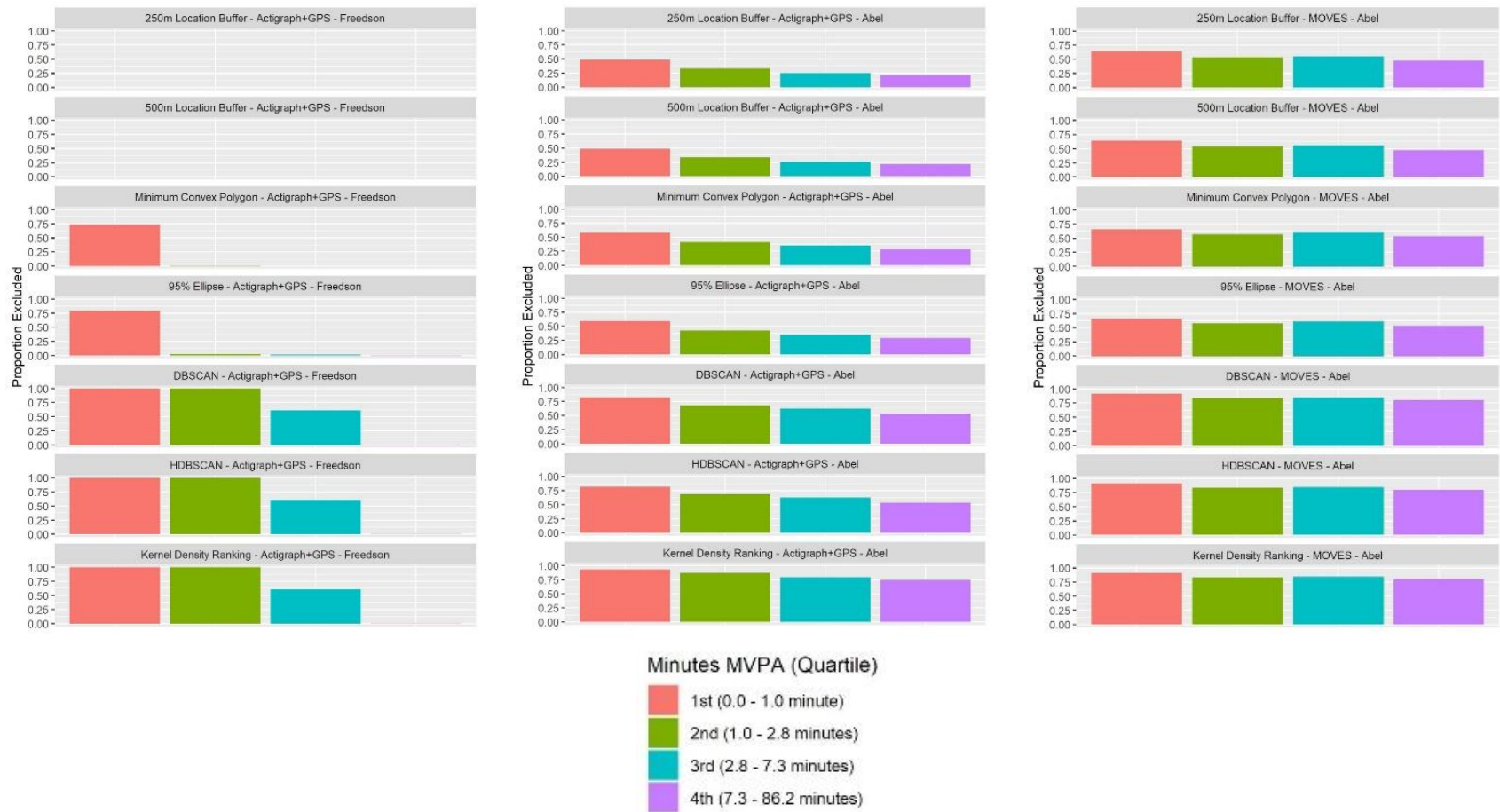


**Figure 3.9.** Comparison of 2018 versus 2016 extracted NDVI values for 7 PAS methods

Extracted by seven PAS polygon methods using Actigraph+GPS and MOVES datasets with MVPA categorized by step count (Abel et al., 2011). Top of each line depicts maximum NDVI difference, bottom of each line depicts minimum NDVI difference, and location of colored circle depicts mean NDVI difference for each method.

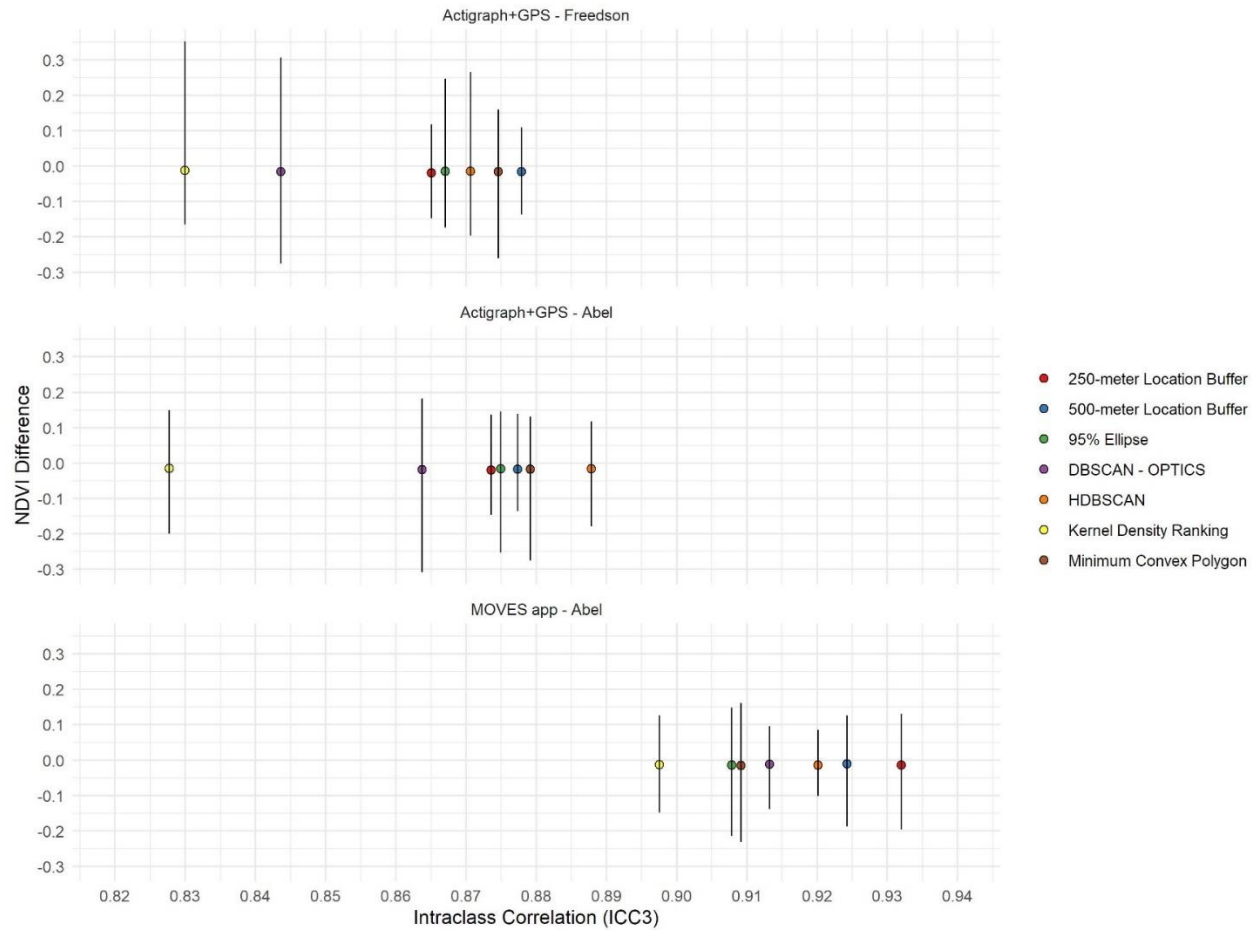


**Figure 3.10.** Comparison of NDVI extracted using 7 PAS methods versus NDVI extracted using 250-meter home address buffers

Comparison includes seven PAS polygon methods using Actigraph+GPS and MOVES datasets with MVPA categorized by step count (Abel et al., 2011). Top of each line depicts maximum NDVI difference, bottom of each line depicts minimum NDVI difference, and location of colored circle depicts mean NDVI difference for each method.

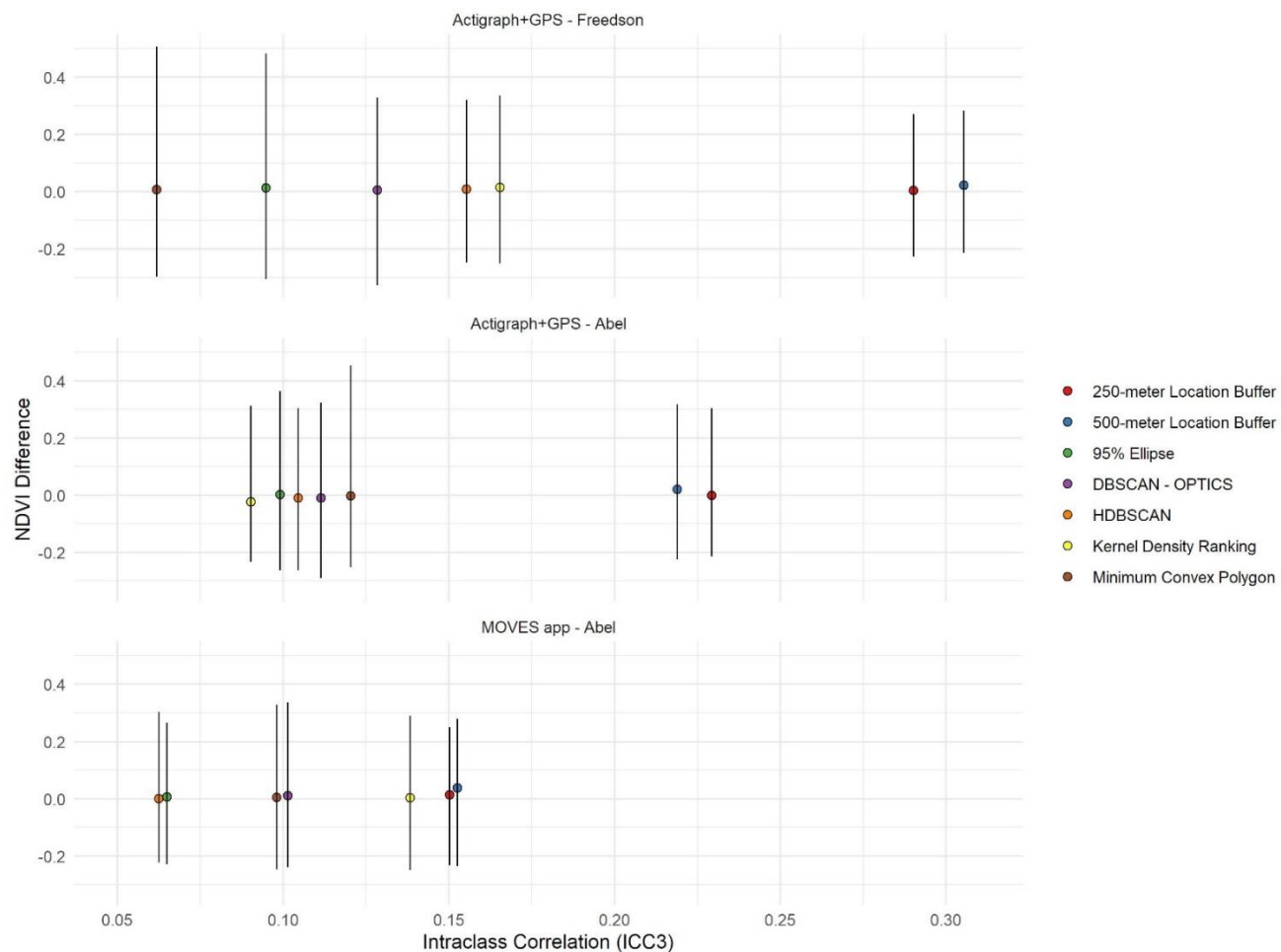
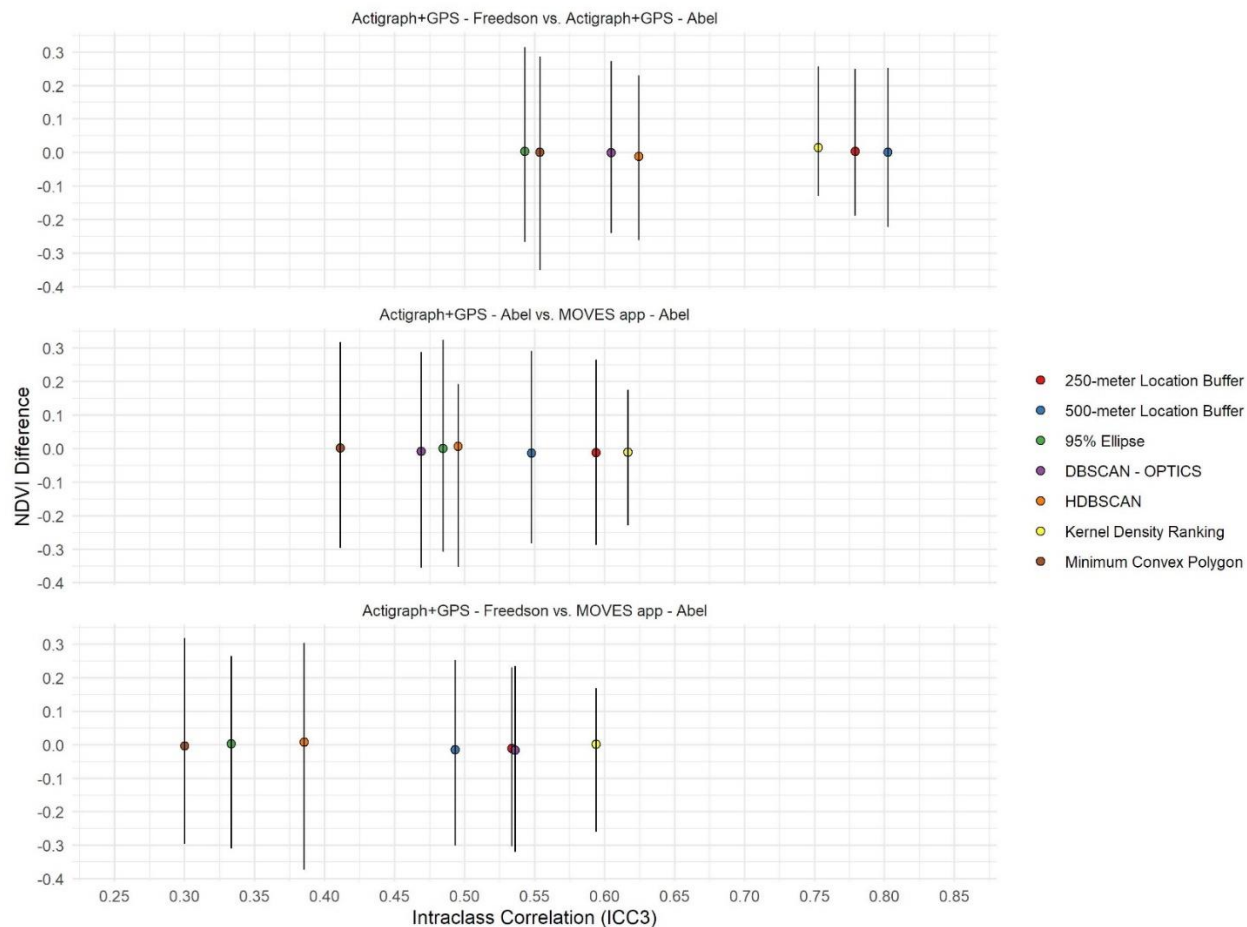


**Figure 3.11.** Comparison of NDVI extracted from MOVES-based PASs versus NDVI extracted from Actigraph+GPS-based PASs for seven PAS methods utilizing MVPA categorized by step-rate (Abel et al., 2011)

Top of each line depicts maximum NDVI difference, bottom of each line depicts minimum NDVI difference, and location of colored circle depicts mean NDVI difference for each method.



### 3.6 REFERENCES FOR CHAPTER 3

- Abel, M., Hannon, J., Mullineaux, D., Beighle, A., 2011. Determination of step rate thresholds corresponding to physical activity intensity classifications in adults. *J. Phys. Act. Heal.* 8, 45–51. <https://doi.org/10.1123/JPAH.8.1.45>
- Actigraph Corp, 2019. What's the difference among the Cut Points available in ActiLife? [WWW Document]. URL <https://actigraphcorp.my.site.com/support/s/article/What-s-the-difference-among-the-Cut-Points-available-in-ActiLife> (accessed 5.2.22).
- Ailshire, J., García, C., 2018. Unequal places: The impacts of socioeconomic and race/ethnic differences in neighborhoods. *Generations* 42.
- Alaimo, P., Loro, D., Mingione, M., Lipsitt, J., Jerrett, M., Banerjee, S., 2021. Bayesian Hierarchical Modeling and Analysis for Physical Activity Trajectories Using Actigraph Data. arxiv Pre-Print, 1–36. <https://doi.org/https://arxiv.org/abs/2101.01624>
- Almanza, E., Jerrett, M., Dunton, G., Seto, E., Ann Pentz, M., 2012. A study of community design, greenness, and physical activity in children using satellite, GPS and accelerometer data. *Health Place* 18, 46–54. <https://doi.org/10.1016/j.healthplace.2011.09.003>
- Almaraz, M., Bai, E., Wang, C., Trousdell, J., Conley, S., Faloon, I., Houlton, B.Z., 2018. Agriculture is a major source of NO<sub>x</sub> pollution in California. *Sci. Adv.* 4. <https://doi.org/10.1126/sciadv.aao3477>
- Alvarado, K., Hewitt, A., 2017. Bruin Bike Share now reaches from Santa Monica to West Hollywood | UCLA [WWW Document]. UCLA Newsroom. URL <https://newsroom.ucla.edu/stories/bruin-bike-share-now-reaches-from-santa-monica-to-west-hollywood> (accessed 5.2.22).
- Amoly, E., Dadvand, P., Forn, J., López-Vicente, M., Basagaña, X., Julvez, J., Alvarez-Pedrerol, M., Nieuwenhuijsen, M.J., Sunyer, J., 2015. Green and blue spaces and behavioral development in barcelona schoolchildren: The BREATHE project. *Environ. Health Perspect.* 122. <https://doi.org/10.1289/ehp.1408215>
- Anderson, T.K., 2009. Kernel density estimation and K-means clustering to profile road accident hotspots. *Accid. Anal. Prev.* 41. <https://doi.org/10.1016/j.aap.2008.12.014>
- Apte, J.S., Messier, K.P., Gani, S., Brauer, M., Kirchstetter, T.W., Lunden, M.M., Marshall, J.D., Portier, C.J., Vermeulen, R.C.H., Hamburg, S.P., 2017. High-Resolution Air Pollution Mapping with Google Street View Cars: Exploiting Big Data. *Environ. Sci. Technol.* 51. <https://doi.org/10.1021/acs.est.7b00891>

- Auchincloss, A.H., Diez Roux, A. V, Mujahid, M.S., Shen, M., Bertoni, A.G., Carnethon, M.R., 2009. Neighborhood resources for physical activity and healthy foods and incidence of type 2 diabetes mellitus: the Multi-Ethnic study of Atherosclerosis. *Arch. Intern. Med.* 169, 1698–1704. <https://doi.org/10.1001/archinternmed.2009.302>
- Avila-Palencia, I., Int Panis, L., Dons, E., Gaupp-Berghausen, M., Raser, E., Götschi, T., Gerike, R., Brand, C., de Nazelle, A., Orjuela, J.P., Anaya-Boig, E., Stigell, E., Kahlmeier, S., Iacorossi, F., Nieuwenhuijsen, M.J., 2018. The effects of transport mode use on self-perceived health, mental health, and social contact measures: A cross-sectional and longitudinal study. *Environ. Int.* 120. <https://doi.org/10.1016/j.envint.2018.08.002>
- Aybar, C., Wu, Q., Bautista, L., Yali, R., Barja, A., 2020. rgee: An R package for interacting with Google Earth Engine. *J. Open Source Softw.*
- Bai, L., Chen, H., Hatzopoulou, M., Jerrett, M., Kwong, J.C., Burnett, R.T., Van Donkelaar, A., Copes, R., Martin, R. V., Van Ryswyk, K., Lu, H., Kopp, A., Weichenthal, S., 2018. Exposure to ambient ultrafine particles and nitrogen dioxide and incident hypertension and diabetes. *Epidemiology* 29. <https://doi.org/10.1097/EDE.0000000000000798>
- Bakrania, K., Edwardson, C.L., Khunti, K., Henson, J., Stamatakis, E., Hamer, M., Davies, M.J., Yates, T., 2017. Associations of objectively measured moderate-to-vigorous-intensity physical activity and sedentary time with all-cause mortality in a population of adults at high risk of type 2 diabetes mellitus. *Prev. Med. Reports* 5, 285–288. <https://doi.org/10.1016/j.pmedr.2017.01.013>
- Banerjee, A., Pasea, L., Harris, S., Gonzalez-Izquierdo, A., Torralbo, A., Shallcross, L., Noursadeghi, M., Pillay, D., Sebire, N., Holmes, C., Pagel, C., Wong, W.K., Langenberg, C., Williams, B., Denaxas, S., Hemingway, H., 2020. Estimating excess 1-year mortality associated with the COVID-19 pandemic according to underlying conditions and age: a population-based cohort study. *Lancet* 395. [https://doi.org/10.1016/S0140-6736\(20\)30854-0](https://doi.org/10.1016/S0140-6736(20)30854-0)
- Bates, D., Mächler, M., Bolker, B., Walker, S., 2015. Fitting Linear Mixed-Effects Models Using {lme4}. *J. Stat. Softw.* 67, 1–48. <https://doi.org/10.18637/jss.v067.i01>
- Beekhuizen, J., Kromhout, H., Huss, A., Vermeulen, R., 2013. Performance of GPS-devices for environmental exposure assessment. *J. Expo. Sci. Environ. Epidemiol.* 23. <https://doi.org/10.1038/jes.2012.81>
- Beelen, R., Hoek, G., van den Brandt, P.A., Goldbohm, R.A., Fischer, P., Schouten, L.J., Jerrett, M., Hughes, E., Armstrong, B., Brunekreef, B., 2008. Long-term effects of traffic-related air pollution on mortality in a Dutch cohort (NLCS-AIR study). *Environ. Health Perspect.* 116,

- 196–202. <https://doi.org/10.1289/ehp.10767>
- Benzinger, T.H., 1959. ON PHYSICAL HEAT REGULATION AND THE SENSE OF TEMPERATURE IN MAN. *Proc. Natl. Acad. Sci.* 45, 645. <https://doi.org/10.1073/pnas.45.4.645>
- Berg, K., Romer Present, P., Richardson, K., 2021. Long-term air pollution and other risk factors associated with COVID-19 at the census tract level in Colorado. *Environ. Pollut.* 287. [https://doi.org/10.1016/J.ENVPOL.2021.117584/LONG\\_TERM\\_AIR\\_POLLUTION\\_AND\\_OTHER\\_RISK\\_FACTORS\\_ASSOCIATED\\_WITH\\_COVID\\_19\\_AT\\_THE\\_CENSUS\\_TRACT\\_LEVEL\\_IN\\_COLORADO.PDF](https://doi.org/10.1016/J.ENVPOL.2021.117584/LONG_TERM_AIR_POLLUTION_AND_OTHER_RISK_FACTORS_ASSOCIATED_WITH_COVID_19_AT_THE_CENSUS_TRACT_LEVEL_IN_COLORADO.PDF)
- Bergman, A., Sella, Y., Agre, P., Casadevall, A., 2020. Oscillations in U.S. COVID-19 Incidence and Mortality Data Reflect Diagnostic and Reporting Factors. *mSystems* 5. <https://doi.org/10.1128/msystems.00544-20>
- Bialek, S., Bowen, V., Chow, N., Curns, A., Gierke, R., Hall, A., Hughes, M., Pilishvili, T., Ritchey, M., Roguski, K., Silk, B., Skoff, T., Sundararaman, P., Ussery, E., Vasser, M., Whitham, H., Wen, J., 2020. Geographic Differences in COVID-19 Cases, Deaths, and Incidence — United States, February 12–April 7, 2020. *MMWR. Morb. Mortal. Wkly. Rep.* 69, 465–471. <https://doi.org/10.15585/mmwr.mm6915e4>
- Bivand, R., Keitt, T., Rowlingson, B., 2021. rgdal: Bindings for the “Geospatial” Data Abstraction Library.
- Boakye, K.A., Amram, O., Schuna, J.M., Duncan, G.E., Hystad, P., 2021. GPS-based built environment measures associated with adult physical activity. *Heal. Place* 70. <https://doi.org/10.1016/j.healthplace.2021.102602>
- Bowler, D.E., Buyung-Ali, L., Knight, T.M., Pullin, A.S., 2010a. Urban greening to cool towns and cities: A systematic review of the empirical evidence. *Landsc. Urban Plan.* <https://doi.org/10.1016/j.landurbplan.2010.05.006>
- Bowler, D.E., Buyung-Ali, L.M., Knight, T.M., Pullin, A.S., 2010b. A systematic review of evidence for the added benefits to health of exposure to natural environments. *BMC Public Health* 10. <https://doi.org/10.1186/1471-2458-10-456>
- Brandt, E.B., Beck, A.F., Mersha, T.B., 2020. Air pollution, racial disparities, and COVID-19 mortality. *J. Allergy Clin. Immunol.* <https://doi.org/10.1016/j.jaci.2020.04.035>
- Branion-Calles, M., Götschi, T., Nelson, T., Anaya-Boig, E., Avila-Palencia, I., Castro, A., Cole-Hunter, T., de Nazelle, A., Dons, E., Gaupp-Berghausen, M., Gerike, R., Int Panis, L., Kahlmeier, S., Nieuwenhuijsen, M., Rojas-Rueda, D., Winters, M., 2020. Cyclist crash rates and risk factors in a prospective cohort in seven European cities. *Accid. Anal. Prev.* 141.

- <https://doi.org/10.1016/j.aap.2020.105540>
- Brooke Anderson, G., Bell, M.L., Peng, R.D., 2013. Methods to calculate the heat index as an exposure metric in environmental health research. *Environ. Health Perspect.* <https://doi.org/10.1289/ehp.1206273>
- Bui, R., Buliung, R.N., Remmel, T.K., 2012. aspace: A collection of functions for estimating centrographic statistics and computational geometries for spatial point patterns.
- Burr, J.A., Mutchler, J.E., Gerst, K., 2010. Patterns of residential crowding among Hispanics in later life: immigration, assimilation, and housing market factors. *J. Gerontol. B. Psychol. Sci. Soc. Sci.* 65, 772–782. <https://doi.org/10.1093/geronb/gbq069>
- CADPH, 2020. CDC Confirms Possible First Instance of COVID-19 Community Transmission in California [WWW Document]. URL <https://www.cdph.ca.gov/Programs/OPA/Pages/NR20-006.aspx> (accessed 11.10.20).
- Calenge, C., 2006. The package adehabitat for the R software: tool for the analysis of space and habitat use by animals. *Ecol. Modell.* 197, 1035.
- Caltrans, 2020. Highway Performance Monitoring System (HPMS) Data [WWW Document]. URL <https://dot.ca.gov/programs/research-innovation-system-information/highway-performance-monitoring-system> (accessed 5.2.22).
- Campello, R.J.G.B., Moulavi, D., Sander, J., 2013. Density-Based Clustering Based on Hierarchical Density Estimates.
- Case, M.A., Burwick, H.A., Volpp, K.G., Patel, M.S., 2015. Accuracy of Smartphone Applications and Wearable Devices for Tracking Physical Activity Data. *JAMA* 313, 625–626. <https://doi.org/10.1001/JAMA.2014.17841>
- Centers for Disease Control and Prevention, 2020. COVIDView: A Weekly Surveillance Summary of US. COVID-19 Activity [WWW Document]. URL <https://www.cdc.gov/coronavirus/2019-ncov/covid-data/pdf/covidview-07-24-2020.pdf> (accessed 10.30.20).
- Centers for Disease Control and Prevention, 2019. 500 Cities Project: Local data for better health | Home page | CDC [WWW Document]. URL <https://www.cdc.gov/500cities/> (accessed 11.10.20).
- Chaix, B., Méline, J., Duncan, S., Merrien, C., Karusisi, N., Perchoux, C., Lewin, A., Labadi, K., Kestens, Y., 2013. GPS tracking in neighborhood and health studies: A step forward for environmental exposure assessment, a step backward for causal inference? *Health Place* 21, 46–51. <https://doi.org/10.1016/j.healthplace.2013.01.003>
- Chan, C.B., Ryan, D.A.J., Tudor-Locke, C., 2006. Relationship between objective measures of physical activity and weather: A longitudinal study. *Int. J. Behav. Nutr. Phys. Act.* 3, 1–9.

- <https://doi.org/10.1186/1479-5868-3-21/FIGURES/2>
- Charreire, H., Casey, R., Salze, P., Simon, C., Chaix, B., Banos, A., Badariotti, D., Weber, C., Oppert, J.M., 2010. Measuring the food environment using geographical information systems: A methodological review. *Public Health Nutr.* <https://doi.org/10.1017/S1368980010000753>
- Chen, Y.-C., Dobra, A., 2017. Measuring Human Activity Spaces With Density Ranking Based on GPS Data 1–28.
- Chew, V., 1966. Confidence, Prediction, and Tolerance Regions for the Multivariate Normal Distribution. *J. Am. Stat. Assoc.* 61. <https://doi.org/10.1080/01621459.1966.10480892>
- Ciencewicki, J., Jaspers, I., 2007. Air Pollution and Respiratory Viral Infection. *Inhal. Toxicol.* 19, 1135–1146. <https://doi.org/10.1080/08958370701665434>
- Clark, L.P., Millet, D.B., Marshall, J.D., 2014. National patterns in environmental injustice and inequality: Outdoor NO<sub>2</sub> air pollution in the United States. *PLoS One* 9. <https://doi.org/10.1371/journal.pone.0094431>
- Coker, E.S., Cavalli, L., Fabrizi, E., Guastella, G., Lippo, E., Parisi, M.L., Pontarollo, N., Rizzati, M., Varacca, A., Vergalli, S., 2020. The Effects of Air Pollution on COVID-19 Related Mortality in Northern Italy. *Environ. Resour. Econ.* 76. <https://doi.org/10.1007/s10640-020-00486-1>
- Collaco, J.M., Morrow, M., Rice, J.L., McGrath-Morrow, S.A., 2020. Impact of road proximity on infants and children with bronchopulmonary dysplasia. *Pediatr. Pulmonol.* 55. <https://doi.org/10.1002/ppul.24594>
- Comodore-Mensah, Y., Selvin, E., Aboagye, J., Turkson-Ocran, R.A., Li, X., Himmelfarb, C.D., Ahima, R.S., Cooper, L.A., 2018. Hypertension, overweight/obesity, and diabetes among immigrants in the United States: An analysis of the 2010-2016 National Health Interview Survey. *BMC Public Health.* <https://doi.org/10.1186/s12889-018-5683-3>
- Cui, Y., Zhang, Z.-F., Froines, J., Zhao, J., Wang, H., Yu, S.-Z., Detels, R., 2003. Air pollution and case fatality of SARS in the People's Republic of China: an ecologic study. *Environ. Heal.* 2. <https://doi.org/10.1186/1476-069x-2-15>
- Dadvand, P., de Nazelle, A., Figueras, F., Basagaña, X., Su, J., Amoly, E., Jerrett, M., Vrijheid, M., Sunyer, J., Nieuwenhuijsen, M.J., 2012a. Green space, health inequality and pregnancy. *Environ. Int.* 40. <https://doi.org/10.1016/j.envint.2011.07.004>
- Dadvand, P., de Nazelle, A., Triguero-Mas, M., Schembari, A., Cirach, M., Amoly, E., Figueras, F., Basagaña, X., Ostro, B., Nieuwenhuijsen, M., 2012b. Surrounding greenness and exposure to air pollution during pregnancy: An analysis of personal monitoring data. *Environ.*

- Health Perspect. 120. <https://doi.org/10.1289/ehp.1104609>
- Dadvand, P., Villanueva, C.M., Font-Ribera, L., Martinez, D., Basagaña, X., Belmonte, J., Vrijheid, M., Gražulevičienė, R., Kogevinas, M., Nieuwenhuijsen, M.J., 2015. Risks and benefits of green spaces for children: A cross-sectional study of associations with sedentary behavior, obesity, asthma, and allergy. *Environ. Health Perspect.* 122. <https://doi.org/10.1289/ehp.1308038>
- Dales, R., Wheeler, A., Mahmud, M., Frescura, A.M., Smith-Doiron, M., Nethery, E., Liu, L., 2008. The Influence of Living Near Roadways on Spirometry and Exhaled Nitric Oxide in Elementary Schoolchildren. *Environ. Health Perspect.* 116, 1423–1427. <https://doi.org/10.1289/ehp.10943>
- Dance, J., 2018. Moves is shutting down. Here are alternatives. [WWW Document]. Medium.com. URL <https://joshdance.medium.com/moves-is-shutting-down-here-are-alternatives-8341aae695b4> (accessed 5.2.22).
- de Nazelle, A., Smeds, E., Anaya Boig, E., Wang, C., Sanchez, J., Dons, E., Kahlmeier, S., Iacorossi, F., Wegener, S., Nieuwenhuijsen, M., Rojas-Rueda, D., Avila-Palencia, I., Götschi, T., 2017. A Comparison between Literature Findings and Stakeholder Perspectives on Active Travel Promotion. *J. Transp. Heal.* 5. <https://doi.org/10.1016/j.jth.2017.05.216>
- Deeks, J.J., Dinnes, J., D'Amico, R., Sowden, A.J., Sakarovitch, C., Song, F., Petticrew, M., Altman, D.G., 2003. Evaluating non-randomised intervention studies. *Health Technol. Assess. (Rockv)*. <https://doi.org/10.3310/hta7270>
- Dempsey, D., Kelliher, F., 2018. *Industry Trends in Cloud Computing*. Springer International Publishing, Cham.
- Diaz, F., Freato, R., 2018. *Cloud Data Design, Orchestration, and Management Using Microsoft Azure: Master and Design a Solution Leveraging the Azure Data Platform*. Apress.
- Divens, L.L., Chatmon, B.N., 2019. Cardiovascular Disease Management in Minority Women: Special Considerations. *Crit. Care Nurs. Clin. North Am.* <https://doi.org/10.1016/j.cnc.2018.11.004>
- Dixon, J., Tredoux, C., Davies, G., Huck, J., Hocking, B., Sturgeon, B., Whyatt, D., Jarman, N., Bryan, D., 2020. Parallel lives: Intergroup contact, threat, and the segregation of everyday activity spaces. *J. Pers. Soc. Psychol.* 118. <https://doi.org/10.1037/pspi0000191>
- Dohrn, I.-M., Sjöström, M., Kwak, L., Oja, P., Hagströmer, M., 2018. Accelerometer-measured sedentary time and physical activity—A 15 year follow-up of mortality in a Swedish population-based cohort. *J. Sci. Med. Sport* 21, 702–707. <https://doi.org/10.1016/j.jsams.2017.10.035>

- Donaire-Gonzalez, D., de Nazelle, A., Seto, E., Mendez, M., Nieuwenhuijsen, M.J., Jerrett, M., 2013. Comparison of Physical Activity Measures Using Mobile Phone-Based CalFit and Actigraph. *J. Med. Internet Res.* 15, e111. <https://doi.org/10.2196/jmir.2470>
- Dong, C., MacDonald, G., Okin, G.S., Gillespie, T.W., 2019. Quantifying drought sensitivity of mediterranean climate vegetation to recent warming: A case study in Southern California. *Remote Sens.* 11. <https://doi.org/10.3390/rs11242902>
- Dons, E., Götschi, T., Nieuwenhuijsen, M., De Nazelle, A., Anaya, E., Avila-Palencia, I., Brand, C., Cole-Hunter, T., Gaupp-Berghausen, M., Kahlmeier, S., Laeremans, M., Mueller, N., Orjuela, J.P., Raser, E., Rojas-Rueda, D., Standaert, A., Stigell, E., Uhlmann, T., Gerike, R., Int Panis, L., 2015. Physical Activity through Sustainable Transport Approaches (PASTA): protocol for a multi-centre, longitudinal study Energy balance-related behaviours. *BMC Public Health* 15. <https://doi.org/10.1186/s12889-015-2453-3>
- Du, Y., Lv, Y., Zha, W., Zhou, N., Hong, X., 2020. Association of Body mass index (BMI) with Critical COVID-19 and in-hospital Mortality: a dose-response meta-analysis. *Metabolism.* 154373. <https://doi.org/10.1016/j.metabol.2020.154373>
- Dunton, G.F., Almanza, E., Jerrett, M., Wolch, J., Pentz, M.A., 2014. Neighborhood park use by children: Use of accelerometry and global positioning systems. *Am. J. Prev. Med.* 46. <https://doi.org/10.1016/j.amepre.2013.10.009>
- Dzhambov, A., Hartig, T., Markevych, I., Tilov, B., Dimitrova, D., 2018. Urban residential greenspace and mental health in youth: Different approaches to testing multiple pathways yield different conclusions. *Environ. Res.* 160. <https://doi.org/10.1016/j.envres.2017.09.015>
- Eddelbuettel, D., 2018. CRAN Task View: High-Performance and Parallel Computing with R.
- Erdogan, S., Yilmaz, I., Baybura, T., Gullu, M., 2008. Geographical information systems aided traffic accident analysis system case study: city of Afyonkarahisar. *Accid. Anal. Prev.* 40. <https://doi.org/10.1016/j.aap.2007.05.004>
- ESRI, 2020. ArcGIS Desktop: Release 10. Redlands, CA: Environmental Systems Research Institute.
- Evenson, K.R., Catellier, D.J., Gill, K., Ondrak, K.S., McMurray, R.G., 2008. Calibration of two objective measures of physical activity for children. *J. Sports Sci.* 26. <https://doi.org/10.1080/02640410802334196>
- Evenson, K.R., Goto, M.M., Furberg, R.D., 2015. Systematic review of the validity and reliability of consumer-wearable activity trackers. *Int. J. Behav. Nutr. Phys. Act.* 12. <https://doi.org/10.1186/s12966-015-0314-1>
- Federal Highway Administration, 2019. FHWA Office of Highway Policy Information Fact Sheet:

- The 25 Most Traveled Route Locations by Annual Daily Traffic (AADT) [WWW Document]. URL <https://www.fhwa.dot.gov/policyinformation/tables/02.cfm> (accessed 5.2.22).
- Federico, F., Rauser, C., Gold, M., 2017. 2017 Sustainable LA Grand Challenge Environmental Report Card for Los Angeles County Energy and Air Quality [WWW Document]. Univ. Calif. Escholarsh. URL <https://escholarship.org/uc/item/6xj45381> (accessed 5.2.22).
- Franklin, B.A., Brook, R., Arden Pope, C. 3rd, 2015. Air pollution and cardiovascular disease. *Curr. Probl. Cardiol.* 40, 207–238. <https://doi.org/10.1016/j.cpcardiol.2015.01.003>
- Freedson, P., Melanson, E., Sirard, J., 1998. Calibration of the Computer Science and Applications, Inc. accelerometer. *Med. Sci. Sport. Exerc.* 30.
- Fuertes, E., Markevych, I., Bowatte, G., Gruzjeva, O., Gehring, U., Becker, A., Berdel, D., von Berg, A., Bergström, A., Brauer, M., Brunekreef, B., Brüske, I., Carlsten, C., Chan-Yeung, M., Dharmage, S.C., Hoffmann, B., Klümper, C., Koppelman, G.H., Kozyrskyj, A., Korek, M., Kull, I., Lodge, C., Lowe, A., MacIntyre, E., Pershagen, G., Standl, M., Sugiri, D., Wijga, A., Heinrich, J., 2016. Residential greenness is differentially associated with childhood allergic rhinitis and aeroallergen sensitization in seven birth cohorts. *Allergy Eur. J. Allergy Clin. Immunol.* 71. <https://doi.org/10.1111/all.12915>
- Gaither, C.J., Afrin, S., Garcia-Menendez, F., Odman, M.T., Huang, R., Goodrick, S., da Silva, A.R., 2019. African american exposure to prescribed fire smoke in Georgia, USA. *Int. J. Environ. Res. Public Health* 16. <https://doi.org/10.3390/ijerph16173079>
- Garcetti, E., 2019. L.A.'s Green New Deal: Sustainable City Plan 2019. Los Angeles.
- Gascon, M., Triguero-Mas, M., Martínez, D., Dadvand, P., Rojas-Rueda, D., Plasència, A., Nieuwenhuijsen, M.J., 2016. Residential green spaces and mortality: A systematic review. *Environ. Int.* 86, 60–67. <https://doi.org/10.1016/j.envint.2015.10.013>
- Gastin, P.B., Cayzer, C., Dwyer, D., Robertson, S., 2018. Validity of the ActiGraph GT3X+ and BodyMedia SenseWear Armband to estimate energy expenditure during physical activity and sport. *J. Sci. Med. Sport* 21, 291–295. <https://doi.org/10.1016/j.jsams.2017.07.022>
- Gerike, R., De Nazelle, A., Nieuwenhuijsen, M., Panis, L.I., Anaya, E., Avila-Palencia, I., Boschetti, F., Brand, C., Cole-Hunter, T., Dons, E., Eriksson, U., Gaupp-Berghausen, M., Kahlmeier, S., Laeremans, M., Mueller, N., Orjuela, J.P., Racioppi, F., Raser, E., Rojas-Rueda, D., Schweizer, C., Standaert, A., Uhlmann, T., Wegener, S., Götschi, T., 2016. Physical Activity through Sustainable Transport Approaches (PASTA): A study protocol for a multicentre project. *BMJ Open* 6. <https://doi.org/10.1136/bmjopen-2015-009924>
- Gething, P.W., Noor, A.M., Gikandi, P.W., Ogara, E.A.A., Hay, S.I., Nixon, M.S., Snow, R.W., Atkinson, P.M., 2006. Improving imperfect data from health management information

- systems in Africa using space-time geostatistics. *PLoS Med.* 3. <https://doi.org/10.1371/journal.pmed.0030271>
- Glaeser, E.L., Kominers, S.D., Luca, M., Naik, N., 2018. BIG DATA AND BIG CITIES: THE PROMISES AND LIMITATIONS OF IMPROVED MEASURES OF URBAN LIFE. *Econ. Inq.* 56, 114–137. <https://doi.org/10.1111/ecin.12364>
- GlobalSat WorldCom Corporation, 2022a. BT-335 Bluetooth Data Logger User Manual [WWW Document]. URL <https://www.gpscentral.ca/products/usglobalsat/bt-335-user-manual.pdf> (accessed 5.9.22).
- GlobalSat WorldCom Corporation, 2022b. DG-500 GPS Data Logger Quick Start Guide [WWW Document]. URL [https://www.globalsat.com.tw/ftp/download/DG-500\\_QSG\\_ENG\\_V1.3\\_20170105.pdf](https://www.globalsat.com.tw/ftp/download/DG-500_QSG_ENG_V1.3_20170105.pdf) (accessed 5.9.22).
- Gong, L., Sato, H., Yamamoto, T., Miwa, T., Morikawa, T., 2015. Identification of activity stop locations in GPS trajectories by density-based clustering method combined with support vector machines. *J. Mod. Transp.* 23. <https://doi.org/10.1007/s40534-015-0079-x>
- Google Inc., 2022. Reducer Overview | Google Earth Engine [WWW Document]. URL [https://developers.google.com/earth-engine/guides/reducers\\_intro](https://developers.google.com/earth-engine/guides/reducers_intro) (accessed 5.6.22).
- Götschi, Thomas, de Nazelle, Audrey, Brand, Christian, Gerike, Regine, Alasya, B., Anaya, E., Avila-Palencia, I., Banister, D., Bartana, I., Benvenuti, F., Boschetti, F., Brand, C., Buekers, J., Carniel, L., Carrasco Turigas, G., Castro, A., Cianfano, M., Clark, A., Cole-Hunter, T., Copley, V., De Boever, P., de Nazelle, A., Dimajo, C., Dons, E., Duran, M., Eriksson, U., Franzen, H., Gaupp-Berghausen, M., Gerike, R., Girmenia, R., Götschi, T., Hartmann, F., Iacorossi, F., Int Panis, L., Kahlmeier, S., Khreis, H., Laeremans, M., Martinez, T., Meschik, M., Michelle, P., Muehlmann, P., Mueller, N., Nieuwenhuijsen, M., Nilsson, A., Nussio, F., Orjuela Mendoza, J.P., Pisanti, S., Porcel, J., Racioppi, F., Raser, E., Riegler, S., Robrecht, H., Rojas Rueda, D., Rothballer, C., Sanchez, J., Schaller, A., Schuthof, R., Schweizer, C., Sillero, A., Smidfeltrosqvist, L., Spezzano, G., Standaert, A., Stigell, E., Surace, M., Uhlmann, T., Vancluysen, K., Wegener, S., Wennberg, H., Willis, G., Witzell, J., Zeuschner, V., 2017. Towards a Comprehensive Conceptual Framework of Active Travel Behavior: a Review and Synthesis of Published Frameworks. *Curr. Environ. Heal. reports.* <https://doi.org/10.1007/s40572-017-0149-9>
- Graham, M., Shelton, T., 2013. Geography and the future of big data, big data and the future of geography. *Dialogues Hum. Geogr.* 3, 255–261. <https://doi.org/10.1177/2043820613513121>
- Gupta, A., Bherwani, H., Gautam, S., Anjum, S., Musugu, K., Kumar, N., Anshul, A., Kumar, R., 2021. Air pollution aggravating COVID-19 lethality? Exploration in Asian cities using

- statistical models. *Environ. Dev. Sustain.* 23. <https://doi.org/10.1007/s10668-020-00878-9>
- Hahsler, M., Piekenbrock, M., 2021. dbscan: Density Based Clustering of Applications with Noise (DBSCAN) and Related Algorithms.
- Hamada, S., Ohta, T., 2010. Seasonal variations in the cooling effect of urban green areas on surrounding urban areas. *Urban For. Urban Green.* 9, 15–24. <https://doi.org/10.1016/J.UFUG.2009.10.002>
- Harris, J.E., 2020. Understanding the Los Angeles County coronavirus epidemic: The critical role of intrahousehold transmission. *medRxiv.* <https://doi.org/10.1101/2020.10.11.20211045>
- Hayhoe, K., Cayan, D., Field, C.B., Frumhoff, P.C., Maurer, E.P., Miller, N.L., Moser, S.C., Schneider, S.H., Cahill, K.N., Cleland, E.E., Dale, L., Drapek, R., Hanemann, R.M., Kalkstein, L.S., Lenihan, J., Lunch, C.K., Neilson, R.P., Sheridan, S.C., Verville, J.H., 2004. Emissions pathways, climate change, and impacts on California. *Proc. Natl. Acad. Sci. U. S. A.* 101, 12422–12427. [https://doi.org/10.1073/PNAS.0404500101/SUPPL\\_FILE/04500FIG17.JPG](https://doi.org/10.1073/PNAS.0404500101/SUPPL_FILE/04500FIG17.JPG)
- Heinzerling, A., Stuckey, M.J., Scheuer, T., Xu, K., Perkins, K.M., Resseger, H., Magill, S., Verani, J.R., Jain, S., Acosta, M., Epton, E., 2020. Transmission of COVID-19 to Health Care Personnel During Exposures to a Hospitalized Patient — Solano County, California, February 2020. *MMWR. Morb. Mortal. Wkly. Rep.* 69. <https://doi.org/10.15585/mmwr.mm6915e5>
- Hekler, E.B., Buman, M.P., Grieco, L., Rosenberger, M., Winter, S.J., Haskell, W., King, A.C., 2015. Validation of Physical Activity Tracking via Android Smartphones Compared to ActiGraph Accelerometer: Laboratory-Based and Free-Living Validation Studies. *JMIR mHealth uHealth* 3, e36. <https://doi.org/10.2196/mhealth.3505>
- Higgs, G., Fry, R., Langford, M., 2012. Investigating the Implications of Using Alternative GIS-Based Techniques to Measure Accessibility to Green Space. *Environ. Plan. B Plan. Des.* 39, 326–343. <https://doi.org/10.1068/b37130>
- Hijmans, R.J., 2021. raster: Geographic Data Analysis and Modeling.
- Hirsch, Jana A, Winters, M., Clarke, P., McKay, H., 2014. Generating GPS activity spaces that shed light upon the mobility habits of older adults : a descriptive analysis 1–14.
- Hirsch, Jana A., Winters, M., Clarke, P., McKay, H., 2014. Generating GPS activity spaces that shed light upon the mobility habits of older adults: A descriptive analysis. *Int. J. Health Geogr.* 13, 1–14. <https://doi.org/10.1186/1476-072X-13-51>
- Ho, J.Y., Zijlema, W.L., Triguero-Mas, M., Donaire-Gonzalez, D., Valentín, A., Ballester, J., Chan, E.Y.Y., Goggins, W.B., Mo, P.K.H., Kruize, H., van den Berg, M., Gražulevičienė, R., Gidlow,

- C.J., Jerrett, M., Seto, E.Y.W., Barrera-Gómez, J., Nieuwenhuijsen, M.J., 2021. Does surrounding greenness moderate the relationship between apparent temperature and physical activity? Findings from the PHENOTYPE project. *Environ. Res.* 197, 110992. <https://doi.org/10.1016/J.ENVRES.2021.110992>
- Höchsmann, C., Knaier, R., Eymann, J., Hintermann, J., Infanger, D., Schmidt-Trucksäss, A., 2018. Validity of activity trackers, smartphones, and phone applications to measure steps in various walking conditions. *Scand. J. Med. Sci. Sport.* 28. <https://doi.org/10.1111/sms.13074>
- Holliday, K.M., Howard, A.G., Emch, M., Rodríguez, D.A., Evenson, K.R., 2017. Are buffers around home representative of physical activity spaces among adults? *Heal. Place* 45, 181–188. <https://doi.org/10.1016/j.healthplace.2017.03.013>
- Holt, J.B., Lo, C.P., Hodler, T.W., 2013. Dasymetric Estimation of Population Density and Areal Interpolation of Census Data. <http://dx.doi.org/10.1559/1523040041649407> 31, 103–121. <https://doi.org/10.1559/1523040041649407>
- Huang, G., Blangiardo, M., Brown, P.E., Pirani, M., 2021. Long-term exposure to air pollution and COVID-19 incidence: A multi-country study. *Spat. Spatiotemporal. Epidemiol.* 39, 100443. <https://doi.org/10.1016/J.SSTE.2021.100443>
- Humpel, N., 2002. Environmental factors associated with adults' participation in physical activity A review. *Am. J. Prev. Med.* 22, 188–199. [https://doi.org/10.1016/S0749-3797\(01\)00426-3](https://doi.org/10.1016/S0749-3797(01)00426-3)
- Imboden, M.T., Nelson, M.B., Kaminsky, L.A., Montoye, A.H., 2018. Comparison of four Fitbit and Jawbone activity monitors with a research-grade ActiGraph accelerometer for estimating physical activity and energy expenditure. *Br. J. Sports Med.* 52, 844–850. <https://doi.org/10.1136/bjsports-2016-096990>
- Jacobs, A., 2009. The pathologies of big data. *Queue* 7, 10–19. <https://doi.org/10.1145/1563821.1563874>
- Jerrett, M., Almanza, E., Davies, M., Wolch, J., Dunton, G., Spruitj-Metz, D., Ann Pentz, M., 2013a. Smart growth community design and physical activity in children. *Am. J. Prev. Med.* 45, 386–392. <https://doi.org/10.1016/j.amepre.2013.05.010>
- Jerrett, M., Almanza, E., Davies, M., Wolch, J., Dunton, G., Spruitj-Metz, D., Pentz, M.A., 2013b. Smart growth community design and physical activity in children. *Am. J. Prev. Med.* 45, 386–392. <https://doi.org/10.1016/j.amepre.2013.05.010>
- Jerrett, M., Arain, A., Kanaroglou, P., Beckerman, B., Potoglou, D., Sahuvaroglu, T., Morrison, J., Giovis, C., 2005a. A review and evaluation of intraurban air pollution exposure models. *J. Expo. Anal. Environ. Epidemiol.* <https://doi.org/10.1038/sj.jea.7500388>
- Jerrett, M., Burnett, R.T., Ma, R., Pope, C.A., Krewski, D., Newbold, K.B., Thurston, G., Shi, Y.,

- Finkelstein, N., Calle, E.E., Thun, M.J., 2005b. Spatial Analysis of Air Pollution and Mortality in Los Angeles. *Epidemiology* 16, 727–736. <https://doi.org/10.1097/01.ede.0000181630.15826.7d>
- Jerrett, M., Shankardass, K., Berhane, K., Gauderman, W.J., Künzli, N., Avol, E., Gilliland, F., Lurmann, F., Molitor, J.N., Molitor, J.T., Thomas, D.C., Peters, J., McConnell, R., 2008. Traffic-related air pollution and asthma onset in children: A prospective cohort study with individual exposure measurement. *Environ. Health Perspect.* 116, 1433–1438. <https://doi.org/10.1289/ehp.10968>
- Jewell, N.P., Lewnard, J.A., Jewell, B.L., 2020. Caution Warranted: Using the Institute for Health Metrics and Evaluation Model for Predicting the Course of the COVID-19 Pandemic. *Ann. Intern. Med.* <https://doi.org/10.7326/M20-1565>
- Jia, P., Xue, H., Yin, L., Stein, A., Wang, M., Wang, Y., 2019. Spatial Technologies in Obesity Research: Current Applications and Future Promise. *Trends Endocrinol. Metab.* <https://doi.org/10.1016/j.tem.2018.12.003>
- Kaisler, S., Armour, F., Espinosa, J.A., Money, W., 2013. Big Data: Issues and Challenges Moving Forward, in: 2013 46th Hawaii International Conference on System Sciences. IEEE, Wailea, HI, USA, pp. 995–1004. <https://doi.org/10.1109/HICSS.2013.645>
- Kambatla, K., Kollias, G., Kumar, V., Grama, A., 2014. Trends in big data analytics. *J. Parallel Distrib. Comput.* 74, 2561–2573. <https://doi.org/10.1016/j.jpdc.2014.01.003>
- Kamel Boulos, M.N., Resch, B., Crowley, D.N., Breslin, J.G., Sohn, G., Burtner, R., Pike, W.A., Jezierski, E., Chuang, K.-Y., 2011. Crowdsourcing, citizen sensing and sensor web technologies for public and environmental health surveillance and crisis management: trends, OGC standards and application examples. *Int. J. Health Geogr.* 10, 67. <https://doi.org/10.1186/1476-072X-10-67>
- Kamruzzaman, M., Hine, J., 2012. Analysis of rural activity spaces and transport disadvantage using a multi-method approach. *Transp. Policy* 19, 105–120. <https://doi.org/10.1016/J.TRANPOL.2011.09.007>
- Keadle, S.K., Shiroma, E.J., Freedson, P.S., Lee, I.M., 2014. Impact of accelerometer data processing decisions on the sample size, wear time and physical activity level of a large cohort study. *BMC Public Health* 14. <https://doi.org/10.1186/1471-2458-14-1210>
- Kerr, G.H., Goldberg, D.L., Anenberg, S.C., 2021. COVID-19 pandemic reveals persistent disparities in nitrogen dioxide pollution. *Proc. Natl. Acad. Sci. U. S. A.* 118. <https://doi.org/10.1073/pnas.2022409118>
- Kerr, J., Duncan, S., Schipperjin, J., 2011. Using global positioning systems in health research: A

- practical approach to data collection and processing. *Am. J. Prev. Med.* 41. <https://doi.org/10.1016/j.amepre.2011.07.017>
- Klompaker, J.O., Hoek, G., Bloemasma, L.D., Gehring, U., Strak, M., Wijga, A.H., van den Brink, C., Brunekreef, B., Lebret, E., Janssen, N.A.H., 2018. Green space definition affects associations of green space with overweight and physical activity. *Environ. Res.* 160, 531–540. <https://doi.org/10.1016/J.ENVRES.2017.10.027>
- Kong, F., Yin, H., James, P., Hutyra, L.R., He, H.S., 2014. Effects of spatial pattern of greenspace on urban cooling in a large metropolitan area of eastern China. *Landsc. Urban Plan.* 128, 35–47. <https://doi.org/10.1016/j.landurbplan.2014.04.018>
- Konstantinoudis, G., Padellini, T., Bennett, J., Davies, B., Ezzati, M., Blangiardo, M., 2021. Long-term exposure to air-pollution and COVID-19 mortality in England: A hierarchical spatial analysis. *Environ. Int.* 146. <https://doi.org/10.1016/J.ENVINT.2020.106316>
- Koo, T.K., Li, M.Y., 2016. A Guideline of Selecting and Reporting Intraclass Correlation Coefficients for Reliability Research. *J. Chiropr. Med.* 15. <https://doi.org/10.1016/j.jcm.2016.02.012>
- Kooiman, T.J.M., Dontje, M.L., Sprenger, S.R., Krijnen, W.P., van der Schans, C.P., de Groot, M., 2015. Reliability and validity of ten consumer activity trackers. *BMC Sports Sci. Med. Rehabil.* 7, 24. <https://doi.org/10.1186/s13102-015-0018-5>
- Korsiak, J., Tranmer, J., Leung, M., Borghese, M.M., Aronson, K.J., 2018. Actigraph measures of sleep among female hospital employees working day or alternating day and night shifts. *J. Sleep Res.* 27, e12579. <https://doi.org/10.1111/jsr.12579>
- Kozawa, K.H., Fruin, S.A., Winer, A.M., 2009. Near-road air pollution impacts of goods movement in communities adjacent to the Ports of Los Angeles and Long Beach. *Atmos. Environ.* 43. <https://doi.org/10.1016/j.atmosenv.2009.02.042>
- Ku, P.W., Steptoe, A., Liao, Y., Sun, W.J., Chen, L.J., 2018. Prospective relationship between objectively measured light physical activity and depressive symptoms in later life. *Int. J. Geriatr. Psychiatry* 33. <https://doi.org/10.1002/gps.4672>
- Kulhánová, I., Morelli, X., Le Tertre, A., Loomis, D., Charbotel, B., Medina, S., Ormsby, J.N., Lepeule, J., Slama, R., Soerjomataram, I., 2018. The fraction of lung cancer incidence attributable to fine particulate air pollution in France: Impact of spatial resolution of air pollution models. *Environ. Int.* <https://doi.org/10.1016/j.envint.2018.09.055>
- Künzli, N., Kaiser, R., Medina, S., Studnicka, M., Chanel, O., Filliger, P., Herry, M., Horak, F., Puybonnieux-Textier, V., Quénel, P., Schneider, J., Seethaler, R., Vergnaud, J.C., Sommer, H., 2000. Public-health impact of outdoor and traffic-related air pollution: A European

- assessment. *Lancet* 356. [https://doi.org/10.1016/S0140-6736\(00\)02653-2](https://doi.org/10.1016/S0140-6736(00)02653-2)
- Kuznetsova, A., Brockhoff, P.B., Christensen, R.H.B., 2017. {lmerTest} Package: Tests in Linear Mixed Effects Models. *J. Stat. Softw.* 82, 1–26. <https://doi.org/10.18637/jss.v082.i13>
- Kwan, M.P., 2012a. How GIS can help address the uncertain geographic context problem in social science research. *Ann. GIS* 18. <https://doi.org/10.1080/19475683.2012.727867>
- Kwan, M.P., 2012b. The Uncertain Geographic Context Problem. *Ann. Assoc. Am. Geogr.* 102, 958–968. <https://doi.org/10.1080/00045608.2012.687349>
- LAC, 2014. Countywide Building Outlines (2014) | County Of Los Angeles Enterprise GIS [WWW Document]. URL <https://egis-lacounty.hub.arcgis.com/datasets/countywide-building-outlines-2014> (accessed 11.1.20).
- LACDPH, 2021. Los Angeles County COVID-19 Dashboard - Data Dashboard - About [WWW Document]. URL [http://dashboard.publichealth.lacounty.gov/covid19\\_surveillance\\_dashboard/](http://dashboard.publichealth.lacounty.gov/covid19_surveillance_dashboard/) (accessed 2.25.21).
- LACDPH, 2020. COVID-19 Locations & Demographics - LA County Department of Public Health [WWW Document]. URL <http://publichealth.lacounty.gov/media/coronavirus/locations.htm> (accessed 11.10.20).
- LACDPH, 2018. Department of Public Health - Health Assessment Unit - Data Topics 2018 [WWW Document]. URL <http://publichealth.lacounty.gov/ha/LACHSDataTopics2018.htm> (accessed 11.10.20).
- Lachowycz, K., Jones, A.P., Page, A.S., Wheeler, B.W., Cooper, A.R., 2012. What can global positioning systems tell us about the contribution of different types of urban greenspace to children's physical activity? *Health Place* 18, 586–594. <https://doi.org/10.1016/j.healthplace.2012.01.006>
- Lafortezza, R., Carrus, G., Sanesi, G., Davies, C., 2009. Benefits and well-being perceived by people visiting green spaces in periods of heat stress. *Urban For. Urban Green.* 8, 97–108. <https://doi.org/10.1016/j.ufug.2009.02.003>
- Lane, N., Miluzzo, E., Lu, H., Peebles, D., Choudhury, T., Campbell, A., 2010. A survey of mobile phone sensing. *IEEE Commun. Mag.* 48, 140–150. <https://doi.org/10.1109/MCOM.2010.5560598>
- Laurent, O., Wu, J., Li, L., Milesi, C., 2013. Green spaces and pregnancy outcomes in Southern California. *Heal. Place* 24. <https://doi.org/10.1016/j.healthplace.2013.09.016>
- Lee, J.H., Davis, A.W., Yoon, S.Y., Goulias, K.G., 2016. Activity space estimation with longitudinal observations of social media data. *Transportation (Amst).* 43.

<https://doi.org/10.1007/s11116-016-9719-1>

- Lee, K., Kwan, M.P., 2018. Physical activity classification in free-living conditions using smartphone accelerometer data and exploration of predicted results. *Comput. Environ. Urban Syst.* 67. <https://doi.org/10.1016/j.compenvurbsys.2017.09.012>
- Lee, N.C., Voss, C., Frazer, A.D., Hirsch, J.A., McKay, H.A., Winters, M., 2016. Does activity space size influence physical activity levels of adolescents?-A GPS study of an urban environment. *Prev. Med. Reports* 3. <https://doi.org/10.1016/j.pmedr.2015.12.002>
- Leslie, E., Sugiyama, T., Ierodiaconou, D., Kremer, P., 2010. Perceived and objectively measured greenness of neighbourhoods: Are they measuring the same thing? *Landsc. Urban Plan.* 95. <https://doi.org/10.1016/j.landurbplan.2009.11.002>
- Li, H., Xu, X.L., Dai, D.W., Huang, Z.Y., Ma, Z., Guan, Y.J., 2020. Air pollution and temperature are associated with increased COVID-19 incidence: A time series study. *Int. J. Infect. Dis.* 97. <https://doi.org/10.1016/j.ijid.2020.05.076>
- Li, R., Tong, D., 2016. Constructing human activity spaces: A new approach incorporating complex urban activity-travel. *JTRG* 56, 23–35. <https://doi.org/10.1016/j.jtrangeo.2016.08.013>
- Li, S., Dragicevic, S., Castro, F.A., Sester, M., Winter, S., Coltekin, A., Pettit, C., Jiang, B., Haworth, J., Stein, A., Cheng, T., 2016. Geospatial big data handling theory and methods: A review and research challenges. *ISPRS J. Photogramm. Remote Sens.* 115, 119–133. <https://doi.org/10.1016/j.isprsjprs.2015.10.012>
- Li, X., Zhang, C., Li, W., Ricard, R., Meng, Q., Zhang, W., 2015. Assessing street-level urban greenery using Google Street View and a modified green view index. *Urban For. Urban Green.* 14. <https://doi.org/10.1016/j.ufug.2015.06.006>
- Liang, D., Shi, L., Zhao, J., Liu, P., Sarnat, J.A., Gao, S., Schwartz, J., Liu, Y., Ebelt, S.T., Scovronick, N., Chang, H.H., 2020a. Urban Air Pollution May Enhance COVID-19 Case-Fatality and Mortality Rates in the United States. *Innov.* <https://doi.org/10.1016/j.xinn.2020.100047>
- Liang, D., Shi, L., Zhao, J., Liu, P., Schwartz, J., Gao, S., Sarnat, J., Liu, Y., Ebelt, S., Scovronick, N., Chang, H.H., 2020b. Urban Air Pollution May Enhance COVID-19 Case-Fatality and Mortality Rates in the United States. *medRxiv Prepr. Serv. Heal. Sci.* <https://doi.org/10.1101/2020.05.04.20090746>
- Lippi, G., Sanchis-Gomar, F., Henry, B.M., 2020. Association between environmental pollution and prevalence of coronavirus disease 2019 (COVID-19) in Italy. <https://doi.org/10.1101/2020.04.22.20075986>

- Lipsitt, J., Chan-Golston, A.M., Liu, J., Su, J., Zhu, Y., Jerrett, M., 2021. Spatial analysis of COVID-19 and traffic-related air pollution in Los Angeles. *Environ. Int.* <https://doi.org/10.1016/j.envint.2021.106531>
- Los Angeles County, 2018. LA County: Our County - Landscapes and Ecosystems [WWW Document]. Our Cty. Landscapes Ecosyst. Brief. URL [https://ourcounty.lacounty.gov/wp-content/uploads/2018/10/Our-County-Landscapes-and-Ecosystems-Briefing\\_For-Web.pdf](https://ourcounty.lacounty.gov/wp-content/uploads/2018/10/Our-County-Landscapes-and-Ecosystems-Briefing_For-Web.pdf) (accessed 5.2.22).
- Los Angeles County, 2012. County of Los Angeles: Bicycle Master Plan, Final Plan.
- Los Angeles Times, 2020. California confirms 2 cases of coronavirus in L.A., Orange counties - Los Angeles Times [WWW Document]. URL <https://www.latimes.com/california/story/2020-01-25/los-angeles-area-prepared-for-coronavirus> (accessed 11.10.20).
- Ma, X., Longley, I., Gao, J., Salmond, J., 2020. Assessing schoolchildren's exposure to air pollution during the daily commute - A systematic review. *Sci. Total Environ.* 737, 140389. <https://doi.org/10.1016/J.SCITOTENV.2020.140389>
- Macias, E., Suarez, A., Lloret, J., 2013. Mobile Sensing Systems. *Sensors* 13, 17292–17321. <https://doi.org/10.3390/s131217292>
- Martinez, D.A., Hinson, J.S., Klein, E.Y., Irvin, N.A., Saheed, M., Page, K.R., Levin, S.R., 2020. SARS-CoV-2 Positivity Rate for Latinos in the Baltimore–Washington, DC Region. *JAMA* 324, 392–395. <https://doi.org/10.1001/jama.2020.11374>
- Mayo Clinic, 2022. California COVID-19 Map: Tracking the Trends [WWW Document]. URL <https://www.mayoclinic.org/coronavirus-covid-19/map/california> (accessed 5.23.22).
- McCrorie, P.R., Fenton, C., Ellaway, A., 2014. Combining GPS, GIS, and accelerometry to explore the physical activity and environment relationship in children and young people - a review. *Int. J. Behav. Nutr. Phys. Act.* 11. <https://doi.org/10.1186/s12966-014-0093-0>
- McMorris, O., Villeneuve, P.J., Su, J., Jerrett, M., 2015. Urban greenness and physical activity in a national survey of Canadians. *Environ. Res.* 137, 94–100. <https://doi.org/10.1016/J.ENVRES.2014.11.010>
- Memken, J.A., Canabal, M.E., 1994. Housing tenure, structure, and crowding among Latino households. *J. Fam. Econ. Issues* 15, 349–365. <https://doi.org/10.1007/BF02353810>
- Microsoft, 2021. R developer's guide - R programming - Azure Architecture Center | Microsoft Docs [WWW Document]. URL <https://docs.microsoft.com/en-us/azure/architecture/data-guide/technology-choices/r-developers-guide> (accessed 5.2.22).
- Mooney, S.J., Pejaver, V., 2018. Big Data in Public Health: Terminology, Machine Learning, and Privacy. <https://doi.org/10.1146/annurev-publhealth-040617-014208> 39, 95–112.

<https://doi.org/10.1146/ANNUREV-PUBLHEALTH-040617-014208>

- Mou, N., Yuan, R., Yang, T., Zhang, H., Tang, J., Makkonen, T., 2020. Exploring spatio-temporal changes of city inbound tourism flow: The case of Shanghai, China. *Tour. Manag.* 76. <https://doi.org/10.1016/j.tourman.2019.103955>
- Myers, L.C., Parodi, S.M., Escobar, G.J., Liu, V.X., 2020. Characteristics of Hospitalized Adults With COVID-19 in an Integrated Health Care System in California. *JAMA* 323, 2195–2198. <https://doi.org/10.1001/jama.2020.7202>
- NASA Earth Observatory, 2011. Measuring Vegetation (NDVI & EVI) [WWW Document]. URL [https://earthobservatory.nasa.gov/features/MeasuringVegetation/measuring\\_vegetation\\_2.php](https://earthobservatory.nasa.gov/features/MeasuringVegetation/measuring_vegetation_2.php) (accessed 5.9.22).
- Nazarian, N., Lee, J.K.W., 2021. Personal assessment of urban heat exposure: a systematic review. *Environ. Res. Lett.* 16, 033005. <https://doi.org/10.1088/1748-9326/ABD350>
- Nemati, E., Batteate, C., Jerrett, M., 2017. Opportunistic Environmental Sensing with Smartphones: a Critical Review of Current Literature and Applications. *Curr. Environ. Heal. reports* 4, 306–318. <https://doi.org/10.1007/s40572-017-0158-8>
- Neupane, B., Jerrett, M., Burnett, R.T., Marrie, T., Arain, A., Loeb, M., 2010. Long-term exposure to ambient air pollution and risk of hospitalization with community-acquired pneumonia in older adults. *Am. J. Respir. Crit. Care Med.* 181. <https://doi.org/10.1164/rccm.200901-0160OC>
- O'Neill, M.S., Jerrett, M., Kawachi, I., Levy, J.I., Cohen, A.J., Gouveia, N., Wilkinson, P., Fletcher, T., Cifuentes, L., Schwartz, J., Bateson, T.F., Cann, C., Dockery, D., Gold, D., Laden, F., London, S., Loomis, D., Speizer, F., Van den Eeden, S., Zanobetti, A., 2003. Health, wealth, and air pollution: Advancing theory and methods. *Environ. Health Perspect.* <https://doi.org/10.1289/ehp.6334>
- Oak Ridge National Laboratory, NASA, 2022. Daymet V4: Daily Surface Weather and Climatological Summaries [WWW Document]. URL <https://daymet.ornl.gov/> (accessed 5.15.22).
- Obradovich, N., Fowler, J.H., 2017. Climate change may alter human physical activity patterns. *Nat. Hum. Behav.* 2017 15 1, 1–7. <https://doi.org/10.1038/s41562-017-0097>
- Okabe, A., Satoh, T., Sugihara, K., 2009. A kernel density estimation method for networks, its computational method and a GIS-based tool. *Int. J. Geogr. Inf. Sci.* 23, 7–32. <https://doi.org/10.1080/13658810802475491>
- Oliveira, S., Andrade, H., Vaz, T., 2011. The cooling effect of green spaces as a contribution to the mitigation of urban heat: A case study in Lisbon. *Build. Environ.* 46, 2186–2194.

<https://doi.org/10.1016/j.buildenv.2011.04.034>

- Olsen, J.R., Mitchell, R., McCrorie, P., Ellaway, A., 2019. Children's mobility and environmental exposures in urban landscapes: A cross-sectional study of 10–11 year old Scottish children. *Soc. Sci. Med.* 224, 11–22. <https://doi.org/10.1016/j.socscimed.2019.01.047>
- Pebesma, E., 2018. Simple Features for R: Standardized Support for Spatial Vector Data. *R J.* 10, 439–446. <https://doi.org/10.32614/RJ-2018-009>
- Perchoux, C., Chaix, B., Cummins, S., Kestens, Y., 2013a. Health & Place Conceptualization and measurement of environmental exposure in epidemiology: Accounting for activity space related to daily mobility. *Health Place* 21, 86–93. <https://doi.org/10.1016/j.healthplace.2013.01.005>
- Perchoux, C., Chaix, B., Cummins, S., Kestens, Y., 2013b. Conceptualization and measurement of environmental exposure in epidemiology: Accounting for activity space related to daily mobility. *Heal. Place* 21, 86–93. <https://doi.org/10.1016/j.healthplace.2013.01.005>
- Perrin, A., 2021. Mobile technology and home broadband 2021. *Mob. Technol. Home Broadband* 1–26.
- Pickering, T.A., Huh, J., Intille, S., Liao, Y., Pentz, M.A., Dunton, G.F., 2016. Physical activity and variation in momentary behavioral cognitions: An ecological momentary assessment study. *J. Phys. Act. Heal.* 13, 344–351. <https://doi.org/10.1123/jpah.2014-0547>
- Puyau, M.R., Adolph, A.L., Vohra, F.A., Butte, N.F., 2002. Validation and calibration of physical activity monitors in children. *Obes. Res.* 10. <https://doi.org/10.1038/oby.2002.24>
- Quast, T., Andel, R., 2020. Excess mortality and potential undercounting of COVID-19 deaths by demographic group in Ohio. *medRxiv* 2020.06.28.20141655. <https://doi.org/10.1101/2020.06.28.20141655>
- Quiros, D.C., Zhang, Q., Choi, W., He, M., Paulson, S.E., Winer, A.M., Wang, R., Zhu, Y., 2013. Air quality impacts of a scheduled 36-h closure of a major highway. *Atmos. Environ.* 67, 404–414. <https://doi.org/10.1016/j.atmosenv.2012.10.020>
- R Core Team, 2020. R: A language and environment for statistical computing. Vienna, Austria. R Foundation for Statistical Computing.
- Raser, E., Gaupp-Berghausen, M., Dons, E., Anaya-Boig, E., Avila-Palencia, I., Brand, C., Castro, A., Clark, A., Eriksson, U., Götschi, T., Int Panis, L., Kahlmeier, S., Laeremans, M., Mueller, N., Nieuwenhuijsen, M., Orjuela, J.P., Rojas-Rueda, D., Standaert, A., Stigell, E., Gerike, R., 2018. European cyclists' travel behavior: Differences and similarities between seven European (PASTA) cities. *J. Transp. Heal.* 9. <https://doi.org/10.1016/j.jth.2018.02.006>
- Reid, C.E., O'Neill, M.S., Gronlund, C.J., Brines, S.J., Brown, D.G., Diez-Roux, A. V., Schwartz,

- J., 2009. Mapping Community Determinants of Heat Vulnerability. *Environ. Health Perspect.* 117, 1730–1736. <https://doi.org/10.1289/ehp.0900683>
- Revelle, W., 2021. *psych: Procedures for Psychological, Psychometric, and Personality Research.*
- Rhys, H., 2020. Preventing overfitting with ridge regression, LASSO, and elastic net. *Mach. Learn. with R, tidyverse, mlr* 536.
- Roberts, H., Helbich, M., 2021. Multiple environmental exposures along daily mobility paths and depressive symptoms: A smartphone-based tracking study. *Environ. Int.* 156. <https://doi.org/10.1016/j.envint.2021.106635>
- Rogers, T.N., Rogers, C.R., VanSant-Webb, E., Gu, L.Y., Yan, B., Qeadan, F., 2020. Racial Disparities in COVID-19 Mortality Among Essential Workers in the United States. *World Med. Heal. Policy* 12. <https://doi.org/10.1002/wmh3.358>
- Salvaris, M., Dean, D., Tok, W.H., 2018. Microsoft AI Platform, in: Salvaris, M., Dean, D., Tok, W.H. (Eds.), *Deep Learning with Azure: Building and Deploying Artificial Intelligence Solutions on the Microsoft AI Platform.* Apress, Berkeley, CA, pp. 79–98.
- Sasaki, J.E., John, D., Freedson, P.S., 2011. Validation and comparison of ActiGraph activity monitors. *J. Sci. Med. Sport* 14, 411–416. <https://doi.org/10.1016/j.jsams.2011.04.003>
- Schmidberger, M., Morgan, M., Eddelbuettel, D., Yu, H., Tierney, L., Mansmann, U., 2009. State of the Art in Parallel Computing with R. *J. Stat. Softw.* 31. <https://doi.org/10.18637/jss.v031.i01>
- Schwalb-Willmann, J., Remelgado, R., Safi, K., Wegmann, M., 2020. moveVis: Animating movement trajectories in synchronicity with static or temporally dynamic environmental data in r. *Methods Ecol. Evol.* 11, 664–669. <https://doi.org/10.1111/2041-210X.13374>
- Shelley, J., Fairclough, S.J., Knowles, Z.R., Southern, K.W., McCormack, P., Dawson, E.A., Graves, L.E.F., Hanlon, C., 2018. A formative study exploring perceptions of physical activity and physical activity monitoring among children and young people with cystic fibrosis and health care professionals. *BMC Pediatr.* 18. <https://doi.org/10.1186/s12887-018-1301-x>
- Sherman, J.E., Spencer, J., Preisser, J.S., Gesler, W.M., Arcury, T.A., 2005. A suite of methods for representing activity space in a healthcare accessibility study. *Int. J. Health Geogr.* 4, 24. <https://doi.org/10.1186/1476-072X-4-24>
- Shih, P.C., Han, K., Poole, E.S., Rosson, M.B., Carroll, J.M., 2015. Use and Adoption Challenges of Wearable Activity Trackers. *iConference 2015 Proc.*
- Shin, J.C., Kwan, M.P., Grigsby-Toussaint, D.S., 2020. Do spatial boundaries matter for exploring the impact of community green spaces on health? *Int. J. Environ. Res. Public Health* 17, 1–

17. <https://doi.org/10.3390/ijerph17207529>
- Shoaib, M., Bosch, S., Durmaz Incel, O., Scholten, H., Havinga, P.J.M., 2014. Fusion of smartphone motion sensors for physical activity recognition. *Sensors (Switzerland)* 14. <https://doi.org/10.3390/s140610146>
- Shrout, P.E., Fleiss, J.L., 1979. Intraclass correlations: Uses in assessing rater reliability. *Psychol. Bull.* 86. <https://doi.org/10.1037/0033-2909.86.2.420>
- Shyamasundar, R.K., 2018. Future of Computing Science. *Proc. Indian Natl. Sci. Acad.* 96. <https://doi.org/10.16943/ptinsa/2018/49341>
- Smith, M., Hosking, J., Woodward, A., Witten, K., MacMillan, A., Field, A., Baas, P., Mackie, H., 2017. Systematic literature review of built environment effects on physical activity and active transport - an update and new findings on health equity. *Int. J. Behav. Nutr. Phys. Act.* 14. <https://doi.org/10.1186/s12966-017-0613-9>
- Song, M.-L., Fisher, R., Wang, J.-L., Cui, L.-B., 2018. Environmental performance evaluation with big data: theories and methods. *Ann. Oper. Res.* 270, 459–472. <https://doi.org/10.1007/s10479-016-2158-8>
- Srivastava, A., 2021. COVID-19 and air pollution and meteorology-an intricate relationship: A review. *Chemosphere.* <https://doi.org/10.1016/j.chemosphere.2020.128297>
- Stamatakis, E., Nnoaham, K., Foster, C., Scarborough, P., 2013. The Influence of Global Heating on Discretionary Physical Activity: An Important and Overlooked Consequence of Climate Change. *J. Phys. Act. Heal.* 10, 765–768. <https://doi.org/10.1123/jpah.10.6.765>
- Steinhubl, S.R., Muse, E.D., Topol, E.J., 2015. The emerging field of mobile health. *Sci. Transl. Med.* 7, 283rv3-283rv3. <https://doi.org/10.1126/scitranslmed.aaa3487>
- Stone, B., Hess, J.J., Frumkin, H., 2010. Urban Form and Extreme Heat Events: Are Sprawling Cities More Vulnerable to Climate Change Than Compact Cities? *Environ. Health Perspect.* 118, 1425–1428. <https://doi.org/10.1289/ehp.0901879>
- Su, J.G., Dadvand, P., Nieuwenhuijsen, M.J., Bartoll, X., Jerrett, M., 2019. Associations of green space metrics with health and behavior outcomes at different buffer sizes and remote sensing sensor resolutions. *Environ. Int.* 126. <https://doi.org/10.1016/j.envint.2019.02.008>
- Su, J.G., Jerrett, M., Beckerman, B., Wilhelm, M., Ghosh, J.K., Ritz, B.R., 2009. Predicting traffic-related air pollution in Los Angeles using a distance decay regression selection strategy. *Environ. Res.* 109, 657–670. <https://doi.org/10.1016/j.envres.2009.06.001>
- Su, J.G., Meng, Y.-Y., Chen, X., Molitor, J., Yue, D., Jerrett, M., 2020. Predicting differential improvements in annual pollutant concentrations and exposures for regulatory policy assessment. *Environ. Int.* 143, 105942.

<https://doi.org/https://doi.org/10.1016/j.envint.2020.105942>

- Su, J.G., Meng, Y.Y., Pickett, M., Seto, E., Ritz, B., Jerrett, M., 2016. Identification of Effects of Regulatory Actions on Air Quality in Goods Movement Corridors in California. *Environ. Sci. Technol.* 50. <https://doi.org/10.1021/acs.est.6b00926>
- Sun, F., Walton, D.B., Hall, A., 2015. A Hybrid Dynamical–Statistical Downscaling Technique. Part II: End-of-Century Warming Projections Predict a New Climate State in the Los Angeles Region. *J. Clim.* 28, 4618–4636. <https://doi.org/10.1175/JCLI-D-14-00197.1>
- Swan, M., 2012. Sensor Mania! The Internet of Things, Wearable Computing, Objective Metrics, and the Quantified Self 2.0. *J. Sens. Actuator Networks* 1, 217–253. <https://doi.org/10.3390/jsan1030217>
- Sydbom, A., Blomberg, A., Parnia, S., Stenfors, N., Sandström, T., Dahlén, S.-E., 2001. Health effects of diesel exhaust emissions. *Eur. Respir. J.* 17, 733 LP – 746.
- Tang, J., Liu, F., Wang, Y., Wang, H., 2015. Uncovering urban human mobility from large scale taxi GPS data. *Phys. A Stat. Mech. its Appl.* 438. <https://doi.org/10.1016/j.physa.2015.06.032>
- Tate, E.B., Shah, A., Jones, M., Pentz, M.A., Liao, Y., Dunton, G., 2015. Toward a Better Understanding of the Link between Parent and Child Physical Activity Levels: The Moderating Role of Parental Encouragement. *J. Phys. Act. Heal.* 12, 1238–1244. <https://doi.org/10.1123/jpah.2014-0126>
- Thornton, M.M., Shrestha, R., Wei, Y., Thornton, P.E., Kao, S., Wilson, B.E., 2020. Daymet: Daily Surface Weather Data on a 1-km Grid for North America, Version 4. <https://doi.org/10.3334/ORNLDAAAC/1840>
- Travaglio, M., Yu, Y., Popovic, R., Selley, L., Leal, N.S., Martins, L.M., 2021. Links between air pollution and COVID-19 in England. *Environ. Pollut.* 268, 115859. <https://doi.org/10.1016/j.envpol.2020.115859>
- Tribby, C.P., Miller, H.J., Brown, B.B., Smith, K.R., Werner, C.M., 2017. Health & Place Geographic regions for assessing built environmental correlates with walking trips: A comparison using different metrics and model designs. *Health Place* 45, 1–9. <https://doi.org/10.1016/j.healthplace.2017.02.004>
- Trifan, A., Oliveira, M., Oliveira, J.L., 2019. Passive sensing of health outcomes through smartphones: Systematic review of current solutions and possible limitations. *JMIR mHealth uHealth* 7. <https://doi.org/10.2196/12649>
- Troped, P.J., Wilson, J.S., Matthews, C.E., Cromley, E.K., Melly, S.J., 2010. The Built Environment and Location-Based Physical Activity. *Am. J. Prev. Med.* 38, 429–438.

- <https://doi.org/10.1016/j.amepre.2009.12.032>
- Trost, S.G., Loprinzi, P.D., Moore, R., Pfeiffer, K.A., 2011. Comparison of accelerometer cut points for predicting activity intensity in youth. *Med. Sci. Sports Exerc.* 43. <https://doi.org/10.1249/MSS.0b013e318206476e>
- Tucker, J.M., Welk, G.J., Beyler, N.K., 2011. Physical activity in U.S. adults: Compliance with the physical activity guidelines for Americans. *Am. J. Prev. Med.* 40. <https://doi.org/10.1016/j.amepre.2010.12.016>
- Tucker, P., Gilliland, J., 2007. The effect of season and weather on physical activity: A systematic review. *Public Health* 121, 909–922. <https://doi.org/10.1016/j.puhe.2007.04.009>
- Twohig-Bennett, C., Jones, A., 2018. The health benefits of the great outdoors: A systematic review and meta-analysis of greenspace exposure and health outcomes. *Environ. Res.* 166. <https://doi.org/10.1016/j.envres.2018.06.030>
- U.S. Department of Labor, 2021. AMERICAN TIME USE SURVEY — MAY TO DECEMBER 2019 AND 2020 RESULTS [WWW Document]. News Release, Bur. Labor Stat. URL [www.bls.gov/tus](http://www.bls.gov/tus) (accessed 6.1.22).
- US Census Bureau, 2020. U.S. Census Bureau QuickFacts: Los Angeles County, California [WWW Document]. URL <https://www.census.gov/quickfacts/losangelescountycalifornia> (accessed 11.10.20).
- US Census Bureau, 2018. American Community Survey 5-Year Data (2009-2018) [WWW Document]. URL <https://www.census.gov/data/developers/data-sets/acs-5year.html> (accessed 11.10.20).
- USDA NAIP GeoHub, 2022. National Agriculture Imagery Program - NAIP Hub Site [WWW Document]. URL <https://naip-usdaonline.hub.arcgis.com/> (accessed 6.1.22).
- Ushey, K., Allaire, J.J., Tang, Y., 2021. reticulate: Interface to “Python.”
- Uyttendaele, N., 2015. How to speed up R code: an introduction. *arXiv1503.00855* [cs, stat].
- van den Berg, A.E., Maas, J., Verheij, R.A., Groenewegen, P.P., 2010. Green space as a buffer between stressful life events and health. *Soc. Sci. Med.* 70. <https://doi.org/10.1016/j.socscimed.2010.01.002>
- Varghese, B., Buyya, R., 2018. Next generation cloud computing: New trends and research directions. *Futur. Gener. Comput. Syst.* 79, 849–861. <https://doi.org/10.1016/j.future.2017.09.020>
- Vienneau, D., de Hoogh, K., Faeh, D., Kaufmann, M., Wunderli, J.M., Rösli, M., 2017. More than clean air and tranquillity: Residential green is independently associated with decreasing mortality. *Environ. Int.* 108. <https://doi.org/10.1016/j.envint.2017.08.012>

- Villeneuve, P.J., Jerrett, M., G. Su, J., Burnett, R.T., Chen, H., Wheeler, A.J., Goldberg, M.S., 2012. A cohort study relating urban green space with mortality in Ontario, Canada. *Environ. Res.* 115, 51–58. <https://doi.org/10.1016/j.envres.2012.03.003>
- Wang, B., Chen, H., Chan, Y.L., Oliver, B.G., 2020. Is there an association between the level of ambient air pollution and COVID-19? *Am. J. Physiol. Lung Cell. Mol. Physiol.* <https://doi.org/10.1152/ajplung.00244.2020>
- Wang, B., Shi, W., Miao, Z., 2015. Confidence Analysis of Standard Deviation Ellipse and Its Extension into Higher Dimensional Euclidean Space. *PLoS One* 10, e0118537. <https://doi.org/10.1371/journal.pone.0118537>
- Wang, J., Kwan, M.P., Chai, Y., 2018. An innovative context-based crystal-growth activity space method for environmental exposure assessment: A study using GIS and GPS trajectory data collected in Chicago. *Int. J. Environ. Res. Public Health* 15. <https://doi.org/10.3390/ijerph15040703>
- Wang, Y., Kung, L., Byrd, T.A., 2018. Big data analytics: Understanding its capabilities and potential benefits for healthcare organizations. *Technol. Forecast. Soc. Change* 126, 3–13. <https://doi.org/10.1016/j.techfore.2015.12.019>
- Wang, Y., Wen, Y., Wang, Yue, Zhang, S., Zhang, K.M., Zheng, H., Xing, J., Wu, Y., Hao, J., 2020. Four-Month Changes in Air Quality during and after the COVID-19 Lockdown in Six Megacities in China. *Environ. Sci. Technol. Lett.* <https://doi.org/10.1021/acs.estlett.0c00605>
- Ward Thompson, C., Roe, J., Aspinall, P., Mitchell, R., Clow, A., Miller, D., 2012. More green space is linked to less stress in deprived communities: Evidence from salivary cortisol patterns. *Landsc. Urban Plan.* 105, 221–229. <https://doi.org/10.1016/j.landurbplan.2011.12.015>
- Wehener, S., Raser, E., Gaupp, M., Anata, E., De Nazelle, A., Eriksoon, U., Gerike, R., Horvath, I., Iacorossi, F., Int Panis, L., Kahlmeier, S., Nieuwenhuijsen, M., Mueller, N., Sanchez, J., Rothballer, C., 2017. Active Mobility, the New Health Trend in Smart Cities, or even More? REAL CORP.
- Wing, S.E., Larson, T. V., Hudda, N., Boonyarattaphan, S., Fruin, S., Ritz, B., 2020. Preterm birth among infants exposed to in utero ultrafine particles from aircraft emissions. *Environ. Health Perspect.* 128, 1–9. <https://doi.org/10.1289/EHP5732>
- Wolch, J.R., Byrne, J., Newell, J.P., 2014a. Urban green space, public health, and environmental justice: The challenge of making cities “just green enough.” *Landsc. Urban Plan.* 125, 234–244. <https://doi.org/10.1016/j.landurbplan.2014.01.017>
- Wolch, J.R., Byrne, J., Newell, J.P., 2014b. Urban green space, public health, and environmental

- justice: The challenge of making cities “just green enough.” *Landsc. Urban Plan.* 125, 234–244. <https://doi.org/10.1016/j.landurbplan.2014.01.017>
- World Health Organization, 2022. Physical activity: Fact Sheet [WWW Document]. URL <https://www.who.int/news-room/fact-sheets/detail/physical-activity> (accessed 5.9.22).
- World Health Organization, 2021. WHO Coronavirus Disease (COVID-19) Dashboard | WHO Coronavirus Disease (COVID-19) Dashboard [WWW Document]. URL <https://covid19.who.int/> (accessed 11.2.20).
- Wu, C.Y.H., Zaitchik, B.F., Swarup, S., Gohlke, J.M., 2019. Influence of the Spatial Resolution of the Exposure Estimate in Determining the Association between Heat Waves and Adverse Health Outcomes. *Ann. Am. Assoc. Geogr.* 109. <https://doi.org/10.1080/24694452.2018.1511411>
- Wu, Xiao, Nethery, R.C., Sabath, B.M., Braun, D., Dominici, F., 2020a. Exposure to air pollution and COVID-19 mortality in the United States. *medRxiv*.
- Wu, Xiao, Nethery, R.C., Sabath, B.M., Braun, D., Dominici, F., 2020b. Exposure to air pollution and COVID-19 mortality in the United States: A nationwide cross-sectional study. *medRxiv Prepr. Serv. Heal. Sci.* <https://doi.org/10.1101/2020.04.05.20054502>
- Wu, X., Nethery, R.C., Sabath, M.B., Braun, D., Dominici, F., 2020. Air pollution and COVID-19 mortality in the United States: Strengths and limitations of an ecological regression analysis. *Sci. Adv.* 6, eabd4049. <https://doi.org/10.1126/sciadv.abd4049>
- Yang, D.H., Goerge, R., Mullner, R., 2006. Comparing GIS-based methods of measuring spatial accessibility to health services. *J. Med. Syst.* 30. <https://doi.org/10.1007/s10916-006-7400-5>
- Yao, Y., Pan, J., Liu, Z., Meng, X., Wang, Weidong, Kan, H., Wang, Weibing, 2021. Ambient nitrogen dioxide pollution and spreadability of COVID-19 in Chinese cities. *Ecotoxicol. Environ. Saf.* 208, 111421. <https://doi.org/10.1016/J.ECOENV.2020.111421>
- Yi, L., Wilson, J.P., Mason, T.B., Habre, R., Wang, S., Dunton, G.F., 2019. Methodologies for assessing contextual exposure to the built environment in physical activity studies: A systematic review. *Heal. Place.* <https://doi.org/10.1016/j.healthplace.2019.102226>
- Yu, Z., Bellander, T., Bergström, A., Dillner, J., Eneroth, K., Engardt, M., Georgelis, A., Kull, I., Ljungman, P., Pershagen, G., Stafoggia, M., Melén, E., Gruzieva, O., Group, B.C.-19 S., Almqvist, C., Andersson, N., Ballardini, N., Bergström, A., Björkander, S., Brodin, P., Castel, A., Ekström, S., Georgelis, A., Hammarström, L., Pan-Hammarström, Q., Hallberg, J., Jansson, C., Kere, M., Kull, I., Lauber, A., Lövquist, A., Melén, E., Mjösberg, J., Mogensen, I., Palmberg, L., Pershagen, G., Roxhed, N., Schwenk, J., 2022. Association of Short-term

- Air Pollution Exposure With SARS-CoV-2 Infection Among Young Adults in Sweden. *JAMA Netw. Open* 5, e228109–e228109. <https://doi.org/10.1001/JAMANETWORKOPEN.2022.8109>
- Zeldovich, Y.B., 2015. 26. Oxidation of Nitrogen in Combustion and Explosions, in: *Selected Works of Yakov Borisovich Zeldovich, Volume I*. <https://doi.org/10.1515/9781400862979.404>
- Zenk, Shannon N, Schulz, A.J., Matthews, S.A., Odoms-young, A., Wilbur, J., Wegrzyn, L., Gibbs, K., Braunschweig, C., Stokes, C., 2011. Health & Place Activity space environment and dietary and physical activity behaviors: A pilot study. *Health Place* 17, 1150–1161. <https://doi.org/10.1016/j.healthplace.2011.05.001>
- Zenk, Shannon N., Schulz, A.J., Matthews, S.A., Odoms-Young, A., Wilbur, J.E., Wegrzyn, L., Gibbs, K., Braunschweig, C., Stokes, C., 2011. Activity space environment and dietary and physical activity behaviors: A pilot study. *Heal. Place* 17, 1150–1161. <https://doi.org/10.1016/j.healthplace.2011.05.001>
- Zhang, Z., Xue, T., Jin, X., 2020. Effects of meteorological conditions and air pollution on COVID-19 transmission: Evidence from 219 Chinese cities. *Sci. Total Environ.* 741. <https://doi.org/10.1016/j.scitotenv.2020.140244>
- Zhao, P., Kwan, M.P., Zhou, S., 2018. The uncertain geographic context problem in the analysis of the relationships between obesity and the built environment in Guangzhou. *Int. J. Environ. Res. Public Health* 15. <https://doi.org/10.3390/ijerph15020308>
- Zhou, X., Josey, K., Kamareddine, L., Caine, M.C., Liu, T., Mickley, L.J., Cooper, M., Dominici, F., 2021. Excess of COVID-19 cases and deaths due to fine particulate matter exposure during the 2020 wildfires in the United States. *Sci. Adv.* 7, 8789–8802. [https://doi.org/10.1126/SCIADV.ABI8789/SUPPL\\_FILE/SCIADV.ABI8789\\_SM.PDF](https://doi.org/10.1126/SCIADV.ABI8789/SUPPL_FILE/SCIADV.ABI8789_SM.PDF)
- Zhu, Y., Xie, J., Huang, F., Cao, L., 2020. Association between short-term exposure to air pollution and COVID-19 infection: Evidence from China. *Sci. Total Environ.* 727. <https://doi.org/10.1016/j.scitotenv.2020.138704>

## **CHAPTER 4: HEAT, GREEN SPACE, AND PHYSICAL ACTIVITY IN LOS ANGELES: AN ACTIVITY SPACES APPROACH**

### **4.1 INTRODUCTION**

As a result of climate change, heatwaves in Southern California could rise as much as six to eight times in frequency by year 2100, with a concomitant increase in excess mortality (Hayhoe et al., 2004). Similarly, in Los Angeles, the number of days per year above 35°C (95° Fahrenheit) could increase from six (in 2015) to 54 (in 2100) (Sun et al., 2015). Exposure to extreme heat is well-known to have a negative impact on physical activity (Benzinger, 1959; Humpel, 2002; Stone et al., 2010; Tucker and Gilliland, 2007) and will likely compound the already observed low rates of physical activity in a large segment of the population (Stamatakis et al., 2013). Researchers have hypothesized that individuals will become more prone to acute health effects (such as heat stroke) due to immediate exposure to extreme heat while exercising and may reduce their overall amount of physical activity.

Although extreme heat exposure dampens outdoor physical activity, less-extreme warming may actually increase physical activity (Chan et al., 2006; Ho et al., 2021). In a study of 1.9 million U.S. survey respondents, researchers found that physical activity increased when temperatures warmed but stayed below 29°C (Obradovich and Fowler, 2017). The study region and population investigated may govern the ability for researchers to detect effects from both moderate increases and “extreme” increases in temperature due to differences in temperature distribution, adaptation, and environmental context (Ho et al., 2021).

Community vulnerability to heat is higher in areas with high amounts of impervious surface (e.g., concrete parking lots), and lower in areas of green space. This is due to the cooling effect of vegetation and the shade it provides (Kong et al., 2014; Oliveira et al., 2011; Reid et al., 2009), as well as benefits due to perceived improvements in well-being (Lafortezza et al., 2009). This

leads to a potential modifying effect of green space on heat and physical activity (Ho et al., 2021), but in quantitative analyses the ability to detect this phenomena may depend on how exposure to green space and temperature is attributed to individuals (Almanza et al., 2012; Chaix et al., 2013; Gascon et al., 2016; Higgs et al., 2012; Villeneuve et al., 2012; Wolch et al., 2014b). Circular home buffers have been frequently used to define total daily exposure to green space (Amoly et al., 2015; Dadvand et al., 2015; van den Berg et al., 2010) and even methods that utilize location-tracking data may oversimplify and misclassify environmental exposure due to spatiotemporal misalignment of underlying data (Beekhuizen et al., 2013; Chaix et al., 2013). Given that environmental data (e.g., green space and temperature) are collected at sparse point locations (e.g., weather stations) via remote sensing imagery (e.g., gridded data) or via areal aggregation (e.g., census tract polygons), the quantification of exposure may lead to outcomes that do not overlap closely in time or space. For example, in a study on the effects of green space exposure on stress, researchers defined green space exposure as the area of green space within the post-code (the lowest level of census data aggregation in the United Kingdom) of each participant's home address (Ward Thompson et al., 2012). This approach, however, could lead to a misclassification of daily exposure, as individuals likely do not remain within their post-code. Similarly, in another study, assessing the effect of urban green space on physical activity in children, researchers used park boundaries to describe green space exposure at each GPS location collected on participants; it is likely, however, that individuals are exposed to green space outside of a park (Lachowycz et al., 2012). In a systematic review of physical activity and green space exposure, McCrorie et al. discussed the lack of consensus regarding green space exposure attribution methods and suggested that future methods should combine contemporary "GPS, GIS, accelerometry and [survey]" data, and methods (McCrorie et al., 2014).

Similarly, heat exposure attribution methods often do not account for spatiotemporal misalignments between the location of individuals being studied and the heat data being utilized (Nazarian and Lee, 2021). For example, Chan et al. found an increase in temperature of 10 °C to

be associated with a 2.9% (CI: 0.4% to 5.4%) increase in physical activity (Chan et al., 2006) but heat exposure (raw temperature) was based on region-wide measurements of the entire Prince Edward Island (Canada) province, potentially leading to exposure misclassification due to participants engaging with only a relatively small portion of the province. In a study by Ho et al. of the relationship between temperature and physical activity (tracked by smartphones) and the effect modification by green space, temperature attribution was based on the nearest weather station and green space attribution was based on 30-meter gridded NDVI (Ho et al., 2021). Given the potential for spatial misalignment between these data and the location of individuals, it is possible that the relationship between temperature, green space, and physical activity was incorrectly quantified. Researchers have discussed new methods to incorporate activity spaces, combined with high-resolution imagery for better attribution of environmental exposures such as to green space and temperature (Chen and Dobra, 2017; Hirsch et al., 2014; Holliday et al., 2017; Li and Tong, 2016).

In the present study, we investigate the relationship of heat exposure on daily physical activity among participants in the Physical Activity through Sustainable Transport Approaches in Los Angeles (PASTA-LA) study. We further determine whether the association between heat exposure and physical activity is modified by proximal green space. We aim to determine how model results differ by: (1) accelerometry-based methods used to quantify activity level; and (2) geospatial methods used for attribution of heat and green space exposure. We utilize high-resolution and high-frequency data to better account for spatiotemporal misalignment.

## **4.2 METHODS**

### **4.2.1 Participants**

**Figure 4.1** outlines the participant selection and procedures. Participants were eligible to enroll in the PASTA-LA study if they worked or lived in the University of California at Los Angeles (UCLA)-Westwood areas, and were 18 years or older, able to engage in physical activity, owners

of an iPhone or Android smartphone, and willing to install the MOVES activity tracking app and share data through an internet connection with a secure server managed by PASTA-LA personnel. Participants were recruited using flyers, street canvassing, email listservs, and paid social media advertisements. Between May and August 2017, over 1,000 individuals were screened, and 440 were enrolled as study participants. A total of 163 participants volunteered to be in a substudy, in which participants were required to wear a research-grade accelerometer (Actigraph GT3X+) to measure activity and GPS device (GlobalSat BT-335 or DG-500) to measure location (Actigraph+GPS). Only the Actigraph+GPS data (not MOVES data) will be used in the current analysis.

Signed written consents were obtained from all participants. Participants were given cash gift cards and raffled prizes (e.g., iPads) upon completion of the study. PASTA-LA human-subjects' approvals were kept in accordance with the UCLA Institutional Review Boards (IRBs).

#### **4.2.2 Participant data collection**

Data collection began upon enrollment (between May and August 2017) and ended in June 2018. Participants were observed for a duration of three months to one year. This study utilizes tracking and survey data gathered in two data collection phases, one before and one after the launch of the UCLA *Bruin Bike Share* program. Online questionnaires and participant-tracking protocols were developed in collaboration from materials created by a larger PASTA study of seven cities in Europe (Avila-Palencia et al., 2018; Branion-Calles et al., 2020; Raser et al., 2018; Wehener et al., 2017). All data sources used in this study are shown in **Table 4.1**.

All 440 participants were asked to complete a baseline questionnaire (40 minutes) and two follow-up questionnaires (20 minutes each) before the launch of the *Bruin Bike Share* in October 2017; they were then asked to repeat these three questionnaires after the launch, for a total of six questionnaires completed.

The participants visited the study office to check out the Actigraph+GPS research-grade devices for the two one-week periods before and after the launch of the *Bruin Bike Share*. The Actigraph accelerometer was worn on a wrist of the participants choosing and the GlobalSat GPS was kept within a 1-meter proximity radius. The Actigraph was removed during sleep and bathing activities (handwashing, showering, etc.). The GlobalSat had to be charged every night by the participant using a supplied charging cable, while the Actigraph held a charge for the entire week-long observation period. The Actigraph GT3X+ outputs activity data in the form of proprietary acceleration counts from three directional axes (tri-axial counts). These counts are unitless and unique to Actigraph devices but are heavily used in physical activity tracking research, both in laboratory and free-living studies (Abel et al., 2011; Evenson et al., 2008; Freedson et al., 1998; Puyau et al., 2002; Trost et al., 2011). The proprietary counts can therefore be converted into measures of energy expenditure or other measures of activity level or type. GlobalSat DG-500 and BT-335 GPS units have a positional horizontal accuracy of less than 2.5 meters and 10 meters, respectively (GlobalSat WorldCom Corporation, 2022b, 2022a). GPS measurements were collected every 15 seconds. Accelerometer tracking data were downloaded using Actigraph's Actilife software version 6.13.3—the raw outputs included 10-second measures of steps and tri-axial counts (proprietary) (Actigraph Corp, 2019; Freedson et al., 1998; Keadle et al., 2014). GPS unit data were downloaded using GlobalSat's GPS Tools for Windows. Accelerometer and GPS data were combined using linear interpolation based on the time-stamps of each device, resulting in a dataset including GPS, tri-axial counts, and steps counted for each 10-second interpolated interval (Alaimo et al., 2021). A total of 123 of the 163 substudy participants collected accelerometry and GPS data using the Actigraph and GlobalSat devices that could be interpolated for subsequent analyses, generating 14.0 million 10-second observations (Actigraph+GPS).

### **4.2.3 Inclusion criteria and data cleaning**

Actigraph+GPS data were, in part, cleaned previously (Alaimo et al., 2021). Observations were restricted spatially to LA County, as this research focuses on physical activity patterns relative to the free-living, every-day environment of the study participants. All 123 participants lived inside LA County; observations outside the county were excluded from the sample. Participants were considered sleeping or inactive between the hours of 10pm and 7am and the corresponding observations were excluded. Actigraph+GPS were also cleaned by hand by flagging erroneous observations where speeds over 50 m/s or accelerations over 10 m/s<sup>2</sup> were calculated (Kerr et al., 2011), and then reviewing each flagged observation visually. Flagged review resulted in daily trajectories from nine routes (across nine individuals) being removed. After applying inclusion criteria and cleaning the data, 13.4 million observations were retained from 14.0 million across 123 participants.

### **4.2.4 Moderate-to-vigorous physical activity**

Activity data from Actigraph+GPS datasets was converted to metabolic equivalent of task (MET) ratios. This was done using equations derived from laboratory-based treadmill studies aimed at evaluating Actigraph accelerometers. Step counts from Actigraph+GPS were converted to METs using gender-specific non-linear equations from a study of nine men and 10 women (Abel et al., 2011). Vertical-axis counts from Actigraph+GPS were converted to METs using an equation from a study of 25 men and 25 women (Freedson et al., 1998). Observations with MET ratios above three were considered locations where individuals were engaged in moderate-to-vigorous physical activity (MVPA) (Tucker et al., 2011). Although Actigraph+GPS data included tri-axial measurements, only the vertical-axis counts were included for these analyses to allow for better comparison with MVPA derived from step counts, which is also derived from only the vertical-axis sensor. All 123 participants recorded at least one day with an observation categorized as MVPA. Across the 123 participants, there were 1,125 person-days where MVPA

was observed. These data were utilized as the main study sample for the methods described hereafter.

#### **4.2.5 Physical activity space**

Physical activity space (PAS) polygons were generated from location-based observations of MVPA. Two approaches to drawing PASs were utilized: the 500-meter location buffer and the minimum convex polygon. Both methods are commonly used in activity space research (Hirsch et al., 2014; J. H. Lee et al., 2016; N. C. Lee et al., 2016; Shannon N Zenk et al., 2011) and are considered a major improvement to using home locations as the spatial context for environmental exposure (Amoly et al., 2015; Dadvand et al., 2015; van den Berg et al., 2010). We selected 500-meter location buffers as the main method because this method is superior for describing context along routes and it is commonly used in the assessment of green space (Dzhambov et al., 2018; Su et al., 2019). We selected minimum convex polygons for comparison, as these polygons often include larger regions between observations or routes (J. Wang et al., 2018). 500-meter location buffers required a minimum of one observation of MVPA per person-day, while minimum convex polygons required a minimum of three observations. Physical activity spaces were generated in R Studio version 1.2.5042 (R version 4.2.0).

#### **4.2.6 Temperature attribution**

Daymet Version 4 (Oak Ridge National Laboratory and NASA, 2022) was utilized for attributing heat exposure. Daymet is a continuous 1,000-meter gridded climate summary product interpolated from ground-based weather observations. Areal mean daily maximum temperature was extracted for each PAS for each person-day of observation (of 1,125 person-days) as well as for the same calendar-day for the previous 20 years, previous 10 years, previous 30 days, and previous 15 days. Using these data, daily temperature deviations were calculated (e.g., 20-year temperature deviation = [daily max temperature] – [20-year average daily maximum temperature]) for each period (20-year, 10-year, 30-day, and 15-day). Raw daily maximum temperature was

highly correlated with all temperature deviations (correlations between 0.69 and 0.85), so daily maximum temperature was used as the main factor describing heat exposure; temperature deviations were excluded from subsequent modeling to avoid issues of collinearity and are not described here. Temperature data were accessed and extracted using Google Earth Engine via the *rgee* R package (Aybar et al., 2020).

#### **4.2.7 Green space attribution**

We used National Agriculture and Imagery Program (NAIP) multispectral images for 2018 to attribute green space exposure by PAS. NAIP produces these satellite products approximately once every two years; the year 2018 was used here as it included the most temporal overlap with the participant data. These 60-centimeter multispectral images include red, green, blue, and infrared bands for each mosaiced image. The Normalized Difference Vegetation Index (NDVI) from the red and infrared bands is defined as:  $[Near\ Infrared - Red] \div [Near\ Infrared + Red]$ . NDVI has a range between -1 and 1, where values closer to 1 are very green and values close to and below 0 are not green (i.e., man-made objects, open water, etc.) (NASA Earth Observatory, 2011). This index is commonly used to describe green space and has been used in other research involving activity space methods (Dadvand et al., 2012a, 2012b; Leslie et al., 2010; McMorris et al., 2015; Vienneau et al., 2017). Using the same extraction process utilized for the attribution of daily maximum temperature (from Daymet), PASs were used to extract areal mean NDVI for each PAS. Green space data were accessed and extracted using Google Earth Engine via the *rgee* R package (Aybar et al., 2020).

#### 4.2.8 Statistical modeling

Questionnaire and Actigraph+GPS data from the 123 PASTA-LA participants were used to investigate the relationship between heat exposure (daily maximum temperature deviation) and minutes of MVPA per day and the effect modification of this relationship by NDVI. We developed four discrete data sets employing location and activity data from Actigraph+GPS, identified locations where MVPA was observed by applying two literature-derived equations (*Freedson 1998* and *Abel 2011*), and employing two geospatial methods for defining PAS polygons (500-meter location buffer and minimum convex polygon) that were used to quantify heat (daily maximum temperature) and green space (NDVI) exposures.

A linear mixed-effect regression model (Bates et al., 2015) was utilized to assess the relationship between daily maximum temperature and minutes of MVPA per day. This model type is appropriate to account for within-participant variability, where daily observations are observed for each individual. MVPA (minutes) was  $\log_e$ -transformed due to right skewed data. Covariates were selected *a priori* based on the related literature and included: age (continuous), sex (male = 1; female = 0), ethnicity (white = 1; non-white = 0), high-school education attainment (completed high school = 1; did not complete = 0), job status (employed = 1; unemployed = 0), body mass index (BMI) (continuous in  $\text{kg}/\text{m}^2$ ), and NDVI (continuous). Demographic covariates were abstracted from PASTA-LA baseline questionnaires. For ease of interpretability, daily maximum temperature was scaled by its interquartile range (IQR) of  $7.2^\circ\text{C}$ ; NDVI was scaled by its IQR of 0.078; and age and BMI were converted to z-scores. Due to low observations in subcategories, ethnicity and education were dichotomized as noted above. All covariates were included in the final models except for job status, which was excluded due to high correlation with age ( $r = -0.65$ ) and being less predictive of model outcomes. A quadratic term for daily maximum temperature (scaled by IQR of  $7.2^\circ\text{C}$ ) was included for more flexible modeling of the relationship between temperature and  $\log_e$ -transformed MVPA, as the added curvature may allow for better inference at extreme ends of temperature (much hotter or much colder than normal). This quadratic term

was included *a priori* so as to capture differences, potentially opposite, between the effect of heat exposure and *extreme* heat exposure on physical activity and has been included in other studies of heat exposure and physical activity (Ho et al., 2021). To assess the modifying effect of green space on the association between heat exposure and physical activity, interactions between temperature and NDVI were also included *a priori* for both linear  $[(max.daily.temp)_{ij}X(NDVI)_{ij}]$  and quadratic temperature  $[(max.daily.temp.)^2_{ij}X(NDVI)_{ij}]$  terms. The linear interaction term and the quadratic interaction term were highly correlated ( $r = 0.90$ ) so only one was included. Since the quadratic interaction term improved model fit (using restricted maximum likelihood (REML) criterion at convergence (Bates et al., 2015)) more than the linear interaction term, the quadratic interaction term is included. The final model equation employed can be seen below:

$$\begin{aligned} \log(\mathbf{minutes\ MVPA})_{ij} = & \beta_0 + \beta_1(max.daily\ temp.)_{ij} + \beta_2(max.daily\ temp.)^2_{ij} + \\ & \beta_3(NDVI)_{ij} + \beta_4(age)_i + \beta_5(sex)_i + \beta_6(ethnicity)_i + \beta_7(high\ school)_i + \\ & \beta_8(BMI)_i + \beta_9(max.daily\ temp.)^2_{ij}X(NDVI)_{ij} + u_i + \varepsilon_{ij} \end{aligned}$$

where  $\log_e$ -transformed minutes of MVPA (per person-day) is indexed by  $i$  for the  $i$ -th individual using the identifying number assigned to each participant; and  $j$  for the  $j$ -th observation corresponding to the  $i$ -th individual. The random intercept here is defined as  $u_i$  and the error term is defined as  $\varepsilon_{ij}$ .

Model results are presented here as regression tables and as figures. The relationship between daily maximum temperature (scaled by IQR of 7.2°C) and  $\log_e$  daily MVPA is visualized in the figures by constructing point estimates and 95% confidence intervals at the observed means (modes for categorical variables) for each of the variables in the model using their regression coefficients and 10,000 simulated observations. We illustrate the effect modification of NDVI (scaled by IQR of 0.078) on the relationship between daily maximum temperature (scaled by IQR of 7.2°C) and MVPA by dichotomizing NDVI at the median and examining this relationship

within each segment. Model results derived from exposures attributed using 500-meter location buffer PASs applied to Actigraph+GPS data with MVPA categorized using vertical-axis counts (Freedson et al., 1998) was considered the main results, as this dataset is most comparable to those used by other studies (Jerrett et al., 2013b; Pickering et al., 2016), and because green space attributed with this PAS method showed high correlation ( $r > 0.8$ ; see **Dissertation Chapter 3**) between vertical-axis and step count MVPA methods.

In sensitivity analyses, we restrict sample size to only overlapping person-days between (1) the Actigraph+GPS vertical-axis count MVPA and the step-count MVPA datasets; and (2) the 500-meter location buffer and minimum convex polygon methods. We re-run models to assess how difference in exclusions may have influenced the model results.

R studio version 1.2.5042 (R version 4.2.0) was used for all statistical analyses. The *lme4* and *lmerTest* R packages were utilized for linear mixed-effect regression modeling (Bates et al., 2015; Kuznetsova et al., 2017).

### 4.3 RESULTS

Among the 123 participants, 68.3% were female, 32.5% were White, 87.8% graduated high school, and 51.0% were employed full-time. The participants had an average age of 33 years (SD: 11; Range 21 – 66) and an average BMI of 23.6 (SD: 4.0; Range 9.2 – 35.5). From these 123 participants, 1,125 person-days were assessed across 275 days. For this period, 13.4 million observations of location and activity from Actigraph+GPS were included where participants contributed an average of 13.21 days (SD: 4.01; Median: 14.78; Range: 4.30 – 29.00) of tracking data.

The 500-meter location buffer PASs derived from Actigraph+GPS observations and categorized as MVPA using vertical-axis accelerometry counts (Freedson et al., 1998) were used to quantify temperature and NDVI. MVPA categorization further restricted the 123-person (1,125

person-days) sample to 122 individuals (observed across 1,105 person-days on 275 unique days). A description of this final sample is shown in **Table 4.2**. Across these 1,105 person-days, participants engaged in an average of 6.31 (SD=9.30) minutes of MVPA per day; had an average physical activity space that was 1.97 (SD=1.18) square-kilometers in area; were exposed to average daily maximum temperatures of 25.5 °C (SD=5.4); and were exposed to green space with an average NDVI of 0.045 (SD=0.060).

Adjusted linear mixed-effect regression model results are shown in **Table 4.3**. Neither the linear term for daily maximum temperature (IRR=1.014; CI=0.602, 1.716) nor the quadratic term for daily maximum temperature (IRR=1.012; CI=0.940, 1.088) was associated with  $\log_e$  daily MVPA. Increased exposure to green space (scaled by NDVI IQR of 0.078) was found to be significantly associated with an increase in  $\log_e$  daily minutes of MVPA (IRR=1.117; CI=1.032, 1.210). Age (z-score years) was also significantly inversely associated with MVPA (IRR=0.861, CI = 0.778, 0.954) and men had higher MVPA than women (IRR = 0.693; CI = 0.564, 0.851). **Figure 4.1** illustrates model-predicted  $\log_e$  minutes of MVPA per day associated with daily maximum temperature (scaled by IQR of 7.2°C) (accounting for both the linear and quadratic terms). As shown, the adjusted model predicts an increase in MVPA with increasing daily maximum temperature across 10,000 simulated observations.

**Table 4.4** includes in the above model an interaction term between temperature (quadratic term of daily maximum temperature scaled by IQR of 7.2°C) and green space (NDVI scaled by IQR of 0.078). As in the model without the interaction term, we observe no association between the linear term for temperature (IRR=1.053; CI=0.623, 1.786) nor the quadratic term for temperature (IRR=1.001, CI=0.929, 1.078) and daily MVPA. The interaction term, however, was found to be marginally positively associated with daily MVPA (IRR=1.008; CI=0.996, 1.021). **Figure 4.2** illustrates the model-predicted MVPA (including quadratic interaction) associated with daily maximum temperature for the bottom half (< median NDVI) and top half (> median NDVI) of green space exposures, by person-day. With lower than the median green space exposure, we

observe an increase in physical activity up until 25.8°C (the median temperature) and then a slight decrease in activity with higher temperatures (**Figure 4.2: LEFT**). With greater than the median green space exposure, however, we observe little change in activity before 25.8°C but an increase in activity with higher temperatures (**Figure 2: RIGHT**).

We also compared the results of the main PAS method, utilizing 500-meter location buffer PASs, derived from observations with MVPA categorized using vertical-axis counts (Freedson et al., 1998), to the three other PAS methods: (1) 500-meter location buffer PASs, derived from observations with MVPA categorized using step counts (Abel et al., 2011); (2) minimum convex polygon PASs, derived from observations with MVPA categorized using vertical-axis counts (Freedson et al., 1998); and (3) minimum convex polygon PASs, derived from observations with MVPA categorized using step counts (Abel et al., 2011). Description of the sample produced by each method is shown in **Supplemental Table 1**. Adjusted linear mixed-effect regression model results for these three methods (and the main model) are displayed in **Supplemental Table 2**. **Supplemental Table 3** includes adjustment for the interaction between quadratic temperature and NDVI. As outlined in **Table 4.5**, there are key differences in the results depending on the method utilized. Only the model with exposures quantified using 500-meter location buffers, derived from observations with MVPA categorized using step counts (Abel et al., 2011), demonstrated an association ( $p < 0.1$ ) between the linear term for daily maximum temperature and MVPA. Both models using the 500-meter location buffers (vertical-axis count and step count) demonstrated positive associations between NDVI and daily MVPA, and a significant interaction between temperature (quadratic term) and green space on daily MVPA. None of the models using minimum convex polygons found any association between any of the main effects (temperature, temperature<sup>2</sup>, NDVI) or of the interaction (temperature<sup>2</sup> and NDVI) and daily MVPA. To better understand the differences among the models using the minimum convex polygon and the 500-meter location buffer PAS methods (both using the vertical-axis counts), we compare the prediction plots in **Supplemental Figures 1–2** (minimum convex polygon) with **Figures 1–2** (500-

meter location buffer). Although the regression models using minimum convex polygons do not produce significant associations (**Table 4.5**), the predicted trends are similar across both PAS methods, albeit attenuated for those using the minimum convex polygons. In sensitivity analyses restricting the models to overlapping person-days, we found that the results were largely unchanged with one notable exception; the association between the interaction (temperature<sup>2</sup> and NDVI) and MVPA using the minimum convex polygon PAS methods now became marginally significant as we had observed for the 500-meter location buffer methods (**Supplemental Tables 4–7** compared to **Supplemental Tables 2–3**).

#### **4.4 DISCUSSION**

This study evaluated the relationship between heat exposure (daily maximum temperature observed within an individual's daily physical activity space) and daily minutes of moderate-to-vigorous physical activity, using sensor-collected location and activity data from 123 individuals across 1,125 person-days. We compared our main model using 500-meter location buffer with MVPA categorized by vertical-axis counts (Freedson et al., 1998) with results to three other PAS-based approaches to quantifying spatiotemporal covariates (500-meter location buffer with step count and minimum convex polygon with vertical-axis count and with step count). We found that using the main model, NDVI but not heat exposure was associated with MVPA and NDVI modified the relationship of heat exposure and MVPA. Prediction plots indicated in the main effect model (accounting for the linear and quadratic terms) that there was a slight increase in activity with increasing temperatures and in the interaction model (accounting for the quadratic and quadratic interaction terms) that when the temperatures were hotter than normal, individuals with lower daily exposure to green space (< median NDVI) engaged in less MVPA whereas individuals with higher daily exposure to green space (> median NDVI) engaged in more MVPA. The other PAS-based

approaches showed similar findings between heat and physical activity and the effect modification of green space on this association.

Chan et al., using pedometers (single-axis accelerometer) to track participant activity, observed a 2.9% (CI: 0.4% to 5.4%) increase in steps per day for every 10°C increase in mean temperature (Chan et al., 2006) but no decrease in the amount of physical activity associated with more extreme heat exposure (i.e., heat waves, or temperature deviations closer to the warmer temperature right-tail of the distribution). In a study of 1.9 million U.S. survey respondents, researchers showed that increases in temperatures remaining below 29 degrees Celsius (°C) led to increased physical activity but that incident increases in temperature above 29°C were associated with reduced physical activity (Obradovich and Fowler, 2017). Prediction plots demonstrate comparable results to Chan et al., showing increases in MVPA with higher daily temperature deviation, but we do not detect a flip in this association for the warmest temperature deviations. Although we would expect physical activity to decrease at the highest temperatures, this was not observed in our sample possibly due to insufficient observations at more extreme temperatures. It is also possible, that due to the availability of outdoor recreational options in LA County, participants in our sample may have mitigated more extreme heat exposure by engaging with green spaces or other locations with cooling features (e.g., the beach). Since green spaces and shaded areas generate cooling, using PASs to attribute both green space and heat exposure may have led to exposure error (Hamada and Ohta, 2010; Ho et al., 2021).

The observed modifying effect of green space on the relationship between heat exposure and physical activity is consistent with the results of other studies, although there is minimal research on this subject. In a 2021 study of 352 adults living in cities in Spain, Holland, Lithuania, and the United Kingdom, Ho et al. (Ho et al., 2021) collected accelerometry and location data from a smartphone app (CalFit) and attributed green space exposure using NDVI extracted by 30-meter grid cell and temperature using the nearest local weather station. They showed that a 10°C increase in temperature resulted in a decrease in physical activity in the lowest quartile of

NDVI, an increase in physical activity in the 2<sup>nd</sup> and 3<sup>rd</sup> quartiles of NDVI (except in Holland where it decreased), and an increase in physical activity in the 4<sup>th</sup> quartile of NDVI in Spain and Lithuania but a decrease in Holland and the United Kingdom. In comparison, we showed a slight decrease in physical activity with increased heat exposure (approximately > median temperature of 25.8°C) for the bottom half of NDVI and an increase in physical activity with increased heat exposure for the top half of NDVI.

Our approach had some limitations. Although a large quantity of the original PASTA-LA location and activity tracking data (N = 440) were excluded for the present study (N = 123), internal validity was retained as we are modeling within-participant effects across person-days (Deeks et al., 2003) and other studies have excluded similar amounts of tracking data (Jerrett et al., 2013a). In addition, our methods may artificially increase the level of activity of the sample analyzed because the inclusion criteria and geospatial methods applied to the underlying location and activity data are more likely to exclude lower-MVPA person-days than higher-MVPA person-days. For this reason, it is possible our methods and results are more applicable for assessment and comparison of more active populations, such as athletes. We also employ only one metric for defining heat exposure (areal-mean daily maximum temperature) and one metric for defining green space exposure (areal-mean NDVI). More contemporary metrics for these outcomes, such as “heat indexes” for heat exposure (Brooke Anderson et al., 2013) and Google-Street-View “green view indexes” (Li et al., 2015) for green space exposure, could be used to determine how these metrics impact results.

Our study had a number of important strengths. While other studies have used only one method to define spatiotemporal covariates (MVPA, green space and heat exposure), we have examined the relationship between heat and physical activity with four different geospatial approaches. While Ho et al. (Ho et al., 2021) attributed green space from a 30-meter grid cell containing each observation, we used physical activity spaces to define the surrounding area of exposure. Similarly, Ho et al. attributed temperature using the nearest weather station

measurement, whereas we used continuous interpolated surfaces (Daymet V4) extracted by PAS. Our geospatial methods provide a potentially improved framework for combining these spatiotemporally misaligned covariate data where the use of activity space methodologies (PASs in this case) may improve quantification of surroundings and avoid exposure misclassification (Perchoux et al., 2013b). Furthermore, we have shown that although modeled associations may be attenuated by using different exposure quantification methods (i.e., 500-meter location buffer versus minimum convex polygon), the model-predicted outcomes follow similar trends—implying that choices in geospatial methods may matter less than the underlying data analyzed. Future research would benefit from similar analyses applied to other populations and regions. Our methods can provide a framework toward choosing methods for compiling datasets aimed at the assessment of physical activity, heat exposure, and green space.

#### **4.5 CONCLUSION**

This study found that increased heat exposure (defined as daily maximum temperature) was associated with increased physical activity (MVPA). In hotter than average temperatures, individuals with more green space in their surroundings were likely to engage in more MVPA, whereas individuals with less green space in their surroundings were likely to engage in slightly less MVPA. We evaluated multiple spatiotemporal approaches to attribute physical activity outcomes, heat exposure, and green space exposure, and found these results to be robust to the methods selected. The spatiotemporal methods employed improve upon other existing literature by introducing new activity space methods applied to high-resolution covariate information to account for misalignment of spatial covariates—a major limitation of previous research.

**Table 4.1:** Data sources utilized for the assessment of exposure to heat on physical activity

Data sources utilized for the assessment of exposure to heat (defined as daily maximum temperature) on daily minutes of MVPA; including covariates.

<b>Data source</b>	<b>Attribute(s)</b>	<b>Spatial Dimension</b>	<b>Epoch of Collection</b>	<b>Collection Period</b>
<i>Actigraph GT3x+ (PASTA-LA)</i>	Steps, counts*, date-time	-	10 seconds	May 2017-May 2018
<i>GlobalSat BT-335; DG-500 (PASTA-LA)</i>	GPS coordinates, date-time	Point (accuracy: 10-meters; <2.5 meters)	15 seconds	May 2017-May 2018
<i>Online Questionnaire (PASTA-LA)</i>	Age, sex, ethnicity, BMI, educational attainment, job status, home address, work address	-	-	May 2017-May 2018
<i>USDA NAIP** (via Google Earth Engine)</i>	Multispectral (4-band: red, green, blue, infrared) image	60 centimeters	Annual	2016, 2018
<i>NASA Daymet V4 (via Google Earth Engine)</i>	Daily maximum temperature (Celsius)	1,000 meters	Daily	May 2017-May 2018

\*'Counts' are a proprietary unitless metric unique to Actigraph-branded accelerometers.

\*\*U.S. Department of Agriculture, National Agriculture Imagery Program

**Table 4.2:** Description of sample for main model

Description of sample, minutes of MVPA per person-day, size of PAS polygons, daily maximum temperature, and areal mean NDVI (NAIP 2018) from activity and location data.

<b>PAS → 500-m Location Buffer</b>	
<b>MVPA conversion → Freedson et al., 1998</b>	
N	122
N Person-days	1105
Daily MVPA (mins)	
M±SD	6.31±9.30
Median (Range)	3.00(0.17, 70.00)
PAS area (km <sup>2</sup> )	
M±SD	1.973±1.177
Median (Range)	1.771(0.785, 9.291)
Daily max. temp. (°C)	
M±SD	25.5±5.4
Median (Range)	25.8(14.1, 42.2)
IQR	7.2
2018 NDVI	
M±SD	0.045±0.060
Median (Range)	0.039 (-0.132, 0.234)
IQR	0.078

**Table 4.3: Adjusted models of association for temperature and MVPA**

Adjusted models for the association of daily maximum temperature (scaled by IQR of 7.2°C) and log<sub>e</sub> daily minutes of MVPA.

<b>Actigraph+GPS:</b> Log MVPA by <b>Freedson 1998</b> (vertical-axis count)	N=122 (1,105 pers.-days)		
	500-meter Location Buffer		
	IRR	CI	
Daily maximum temperature <sup>a</sup>	1.014	0.602	1.716
Daily maximum temperature <sup>2</sup>	1.012	0.940	1.088
2018 NDVI <sup>b</sup>	1.117	1.032	1.210
Age (years) <sup>c</sup>	0.861	0.778	0.954
Sex <sup>d</sup>	0.693	0.564	0.851
BMI <sup>e</sup>	1.025	0.936	1.122
High school education <sup>f</sup>	0.977	0.719	1.327
Ethnicity <sup>g</sup>	1.061	0.862	1.305

<sup>a</sup>Daily maximum temperature scaled by interquartile range (IQR) of 7.2°C

<sup>b</sup>Areal mean 2018 NDVI by PAS, scaled by IQR of 0.078

<sup>c</sup>Z-score of age (continuous years)

<sup>d</sup>Female = 1; Male = 0

<sup>e</sup>Z-score of BMI (continuous kg/m<sup>2</sup>)

<sup>f</sup>Completed high school = 1; did not complete high school = 0

<sup>g</sup>White = 1; non-White = 0

**Table 4.4:** Adjusted models of association for temperature and MVPA, including interaction between temperature<sup>2</sup> and NDVI

Adjusted models of association between daily maximum temperature (scaled by IQR of 7.2°C) and log<sub>e</sub> daily minutes of MVPA, including interaction between quadratic temperature and NDVI (scaled by IQR of 0.078).

<b>Actigraph+GPS:</b> Log MVPA by <b>Freedson 1998</b> (vertical-axis count)	N=122 (1,105 pers.-days)		
	500-meter Location Buffer		
	IRR	CI	
Daily maximum temperature <sup>a</sup>	1.053	0.623	1.786
Daily maximum temperature <sup>2</sup>	1.001	0.929	1.078
2018 NDVI <sup>b</sup>	0.999	0.832	1.204
Age (years) <sup>c</sup>	0.858	0.775	0.951
Sex <sup>d</sup>	0.693	0.564	0.851
BMI <sup>e</sup>	1.024	0.936	1.121
High school education <sup>f</sup>	0.976	0.718	1.326
Ethnicity <sup>g</sup>	1.059	0.860	1.303
Max. daily temp. <sup>2</sup> X 2018 NDVI	1.008	0.996	1.021

<sup>a</sup>Daily maximum temperature scaled by interquartile range (IQR) of 7.2°C

<sup>b</sup>Areal mean 2018 NDVI by PAS, scaled by IQR of 0.078

<sup>c</sup>Z-score of age (continuous years)

<sup>d</sup>Female = 1; Male = 0

<sup>e</sup>Z-score of BMI (continuous kg/m<sup>2</sup>)

<sup>f</sup>Completed high school = 1; did not complete high school = 0

<sup>g</sup>White = 1; non-White = 0

**Table 4.5:** Comparison of model results for four methods

Table of model results for the association between daily maximum temperature (scaled by IQR of 7.2°C) and log<sub>e</sub> minutes of MVPA for main dataset (500-m Location Buffer PAS, from Actigraph+GPS data using *Freedson-1998* MVPA conversion) and three models included for sensitivity analysis and comparison; as well as the association between green space (NDVI) and MVPA, and the interaction between quadratic daily maximum temperature and MVPA.

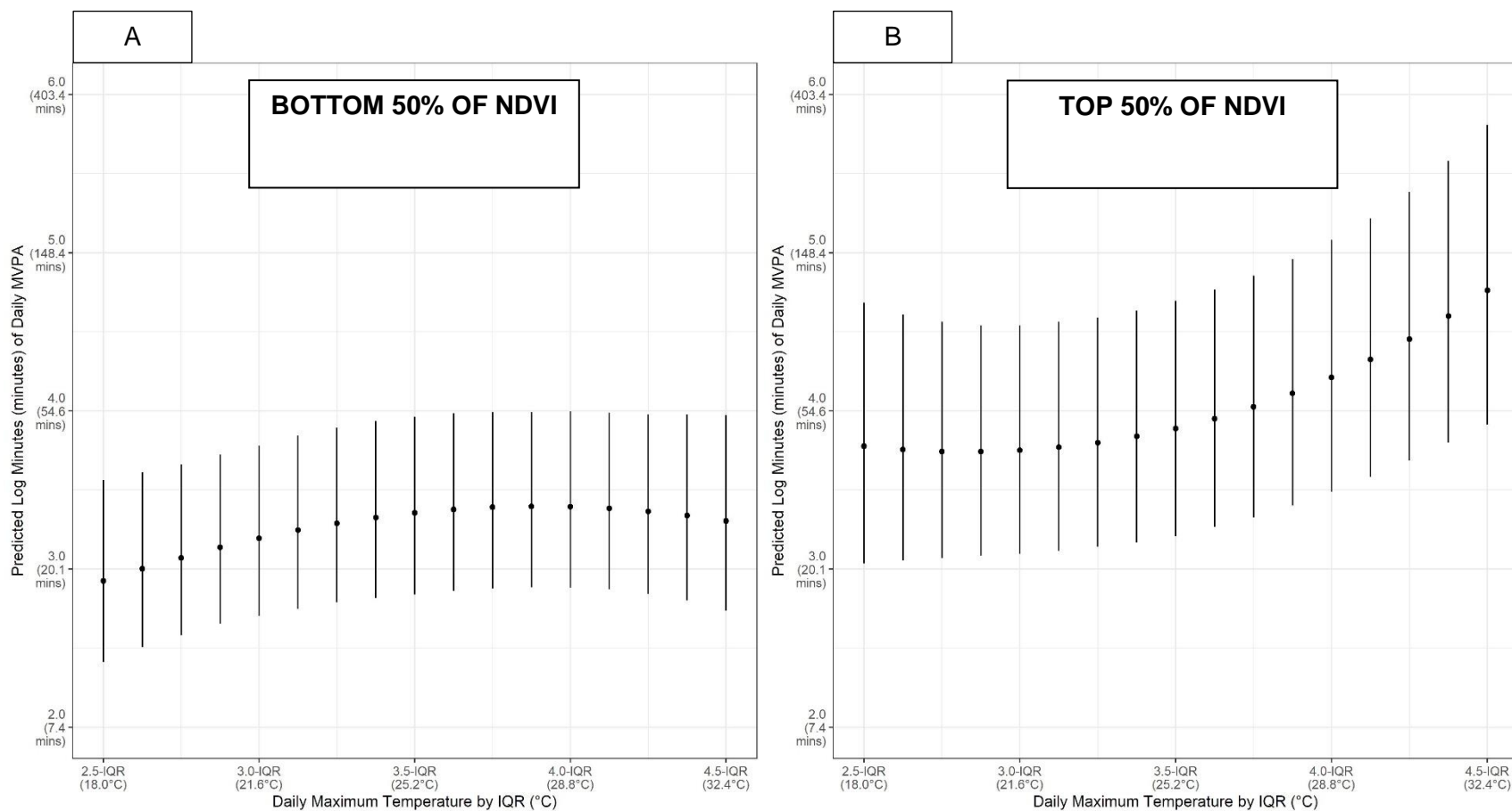
METHOD			SAMPLE		MODEL RESULTS							
PAS Method	Data Source	MVPA Formula	N	Person-Days	Temperature Associated with MVPA		Temperature <sup>2</sup> Associated with MVPA		NDVI Associated with MVPA		Temp. <sup>2</sup> X NDVI Associated with MVPA	
					Yes/No	Sign	Yes/No	Sign	Yes/No	Sign	Yes/No	Sign
500-m Location Buffer	Act+GPS	<i>Freedson</i>	122	1105	N		N		Y**	+	Y <sup>†</sup>	+
	Act+GPS	<i>Abel</i>	119	828	Y <sup>†</sup>	-	N		Y***	+	Y*	+
Minimum Convex Polygon	Act+GPS	<i>Freedson</i>	120	894	N		N		N		N	
	Act+GPS	<i>Abel</i>	115	710	N		N		N		N	

\*\*\* p < 0.001; \*\* p < 0.01; \* p < 0.05; † p < 0.1



**Figure 4.2:** Predicted MVPA associated with daily maximum temperature, stratified by median NDVI

Predicted  $\log_e$  minutes of daily MVPA associated with daily maximum temperature (scaled by IQR of 7.2°C) – for the bottom 50% (< median) of attributed NDVI by person-day (A) and the top 50% (> median) of attributed NDVI by person-day (B); figures generated using point estimates and 95% confidence intervals derived from linear mixed-effected regression model coefficients, including interaction  $\beta_9(\text{Maximum Daily Temperature})^2_{ij}X(\text{NDVI})_{ij}$ , applied to means (continuous covariates) and modes (categorical covariates).



#### 4.6 APPENDIX A. Supplemental Table 1: Description of sample from four exposure methods

Description of sample, minutes of MVPA per person-day, size of PAS polygons, daily maximum temperature, and areal mean NDVI (NAIP 2018) from activity and location data for four methods.

PAS →	500-m Location Buffer		Minimum Convex Polygon	
	Freedson et al., 1998	Abel et al., 2011	Freedson et al., 1998	Abel et al., 2011
<b>MVPA conversion →</b>				
N	122	119	120	115
N Person-days	1105	828	894	710
Daily MVPA (mins)				
M±SD	6.31±9.30	7.55±8.48	7.48±9.42	8.71±8.59
Median (Range)	3.00(0.17, 70.00)	4.83(0.17, 62.31)	4.00(0.83, 65.72)	6.01(0.83, 62.31)
PAS area (km <sup>2</sup> )				
M±SD	1.973±1.177	1.788±1.030	9.274±39.432	1.908±10.496
Median (Range)	1.771(0.785, 9.291)	1.652(0.785, 15.140)	0.026(1.0m <sup>2</sup> , 526.978)	0.014(1.0m <sup>2</sup> , 211.279)
Daily max. temp. (°C)				
M±SD	25.5±5.4	25.1±5.4	25.6±5.3	24.9±5.4
Median (Range)	25.8(14.1, 42.2)	25.2(13.8, 39.0)	26.0(14.4, 42.2)	25.2(13.9, 39.0)
IQR	7.2	7.6	7.0	7.9
2018 NDVI				
M±SD	0.045±0.060	0.051±0.064	0.033±0.077	0.032±0.088
Median (Range)	0.039 (-0.132, 0.234)	0.048 (-0.159, 0.301)	0.025 (-0.195, 0.504)	0.023 (-0.228, 0.409)
IQR	0.078	0.088	0.086	0.109

**4.7 APPENDIX B. Supplemental Table 2:** Adjusted models of association for temperature and MVPA – for four exposure methods

Adjusted models of association between daily maximum temperature and daily minutes of MVPA. Model sample size is variable due to exclusions that occur based on either difference in MVPA classification (Freedson vs. Abel) or restrictions on the number of observations needed to draw polygons (i.e., Minimum Convex Polygons require a minimum of three observations while 500-m buffers only require one.)

<b>A. Actigraph+GPS:</b> Log MVPA by <b>Freedson 1998</b> (vertical-axis count)	N=122 (1,105 pers.-days)			N=120 (894 pers.-days)		
	500-meter Location Buffer			Minimum Convex Polygon		
	IRR	CI		IRR	CI	
Daily maximum temperature <sup>a</sup>	1.014	0.602	1.716	0.968	0.572	1.638
Daily maximum temperature <sup>2</sup>	1.012	0.940	1.088	1.015	0.944	1.090
2018 NDVI <sup>b</sup>	1.117	1.032	1.210	1.034	0.973	1.100
Age (years) <sup>c</sup>	0.861	0.778	0.954	0.927	0.848	1.014
Sex <sup>d</sup>	0.693	0.564	0.851	0.759	0.631	0.912
BMI <sup>e</sup>	1.025	0.936	1.122	1.028	0.948	1.114
High school education <sup>f</sup>	0.977	0.719	1.327	0.805	0.614	1.053
Ethnicity <sup>g</sup>	1.061	0.862	1.305	1.033	0.854	1.247

<b>B. Actigraph+GPS:</b> Log MVPA by <b>Abel 2011</b> (steps)	N=119 (828 pers.-days)			N=115 (710 pers.-days)		
	500-meter Location Buffer			Minimum Convex Polygon		
	IRR	CI		IRR	CI	
Daily maximum temperature <sup>a</sup>	0.565	0.297	1.072	0.595	0.312	1.121
Daily maximum temperature <sup>2</sup>	1.070	0.973	1.178	1.072	0.972	1.186
2018 NDVI <sup>b</sup>	1.262	1.148	1.388	1.000	0.929	1.078
Age (years) <sup>c</sup>	0.874	0.778	0.981	0.888	0.799	0.987
Sex <sup>d</sup>	0.815	0.648	1.027	0.898	0.728	1.109
BMI <sup>e</sup>	0.938	0.845	1.042	0.955	0.869	1.050
High school education <sup>f</sup>	0.959	0.680	1.352	0.806	0.592	1.095
Ethnicity <sup>g</sup>	0.936	0.738	1.187	1.029	0.824	1.283

<sup>a</sup>Daily maximum temperature scaled by interquartile range (IQR)

<sup>b</sup>Areal mean 2018 NDVI by PAS, scaled by IQR

<sup>c</sup>Z-score of age (continuous years)

<sup>d</sup>Female = 1; Male = 0

<sup>e</sup>Z-score of BMI (continuous kg/m<sup>2</sup>)

<sup>f</sup>Completed high school = 1; did not complete high school = 0

<sup>g</sup>White = 1; non-White = 0

**4.8 APPENDIX C. Supplemental Table 1: Adjusted models of association for temperature and MVPA, including interaction between temperature<sup>2</sup> and NDVI – for four exposure methods**

Adjusted models of association between daily maximum temperature and daily minutes of MVPA, including adjustment for the interaction between quadratic temperature and NDVI. Model sample size is variable due to exclusions that occur based on either difference in MVPA classification (Freedson vs. Abel) or restrictions on the number of observations needed to draw polygons (i.e., Minimum Convex Polygons require a minimum of three observations while 500-m buffers only require one.)

<b>A. Actigraph+GPS:</b> Log MVPA by <b>Freedson 1998</b> (vertical-axis count)	N=122 (1,105 pers.-days)			N=120 (894 pers.-days)		
	500-meter Location Buffer			Minimum Convex Polygon		
	IRR	CI		IRR	CI	
Daily maximum temperature <sup>a</sup>	1.053	0.623	1.786	1.004	0.592	1.702
Daily maximum temperature <sup>2</sup>	1.001	0.929	1.078	1.006	0.936	1.082
2018 NDVI <sup>b</sup>	0.999	0.832	1.204	0.940	0.811	1.092
Age (years) <sup>c</sup>	0.858	0.775	0.951	0.925	0.846	1.012
Sex <sup>d</sup>	0.693	0.564	0.851	0.753	0.626	0.906
BMI <sup>e</sup>	1.024	0.936	1.121	1.027	0.947	1.113
High school education <sup>f</sup>	0.976	0.718	1.326	0.807	0.616	1.056
Ethnicity <sup>g</sup>	1.059	0.860	1.303	1.031	0.852	1.246
Max. daily temp. <sup>2</sup> X 2018 NDVI	1.008	0.996	1.021	1.007	0.997	1.017

<b>B. Actigraph+GPS:</b> Log MVPA by <b>Abel 2011</b> (steps)	N=119 (828 pers.-days)			N=115 (710 pers.-days)		
	500-meter Location Buffer			Minimum Convex Polygon		
	IRR	CI		IRR	CI	
Daily maximum temperature <sup>a</sup>	0.668	0.344	1.284	0.619	0.323	1.173
Daily maximum temperature <sup>2</sup>	1.030	0.931	1.141	1.063	0.961	1.177
2018 NDVI <sup>b</sup>	1.006	0.805	1.265	0.928	0.772	1.118
Age (years) <sup>c</sup>	0.871	0.775	0.979	0.888	0.799	0.987
Sex <sup>d</sup>	0.810	0.643	1.022	0.893	0.724	1.103
BMI <sup>e</sup>	0.938	0.845	1.042	0.955	0.869	1.051
High school education <sup>f</sup>	0.955	0.676	1.349	0.806	0.593	1.096
Ethnicity <sup>g</sup>	0.921	0.725	1.170	1.026	0.822	1.280
Max. daily temp. <sup>2</sup> X 2018 NDVI	1.020	1.002	1.038	1.007	0.991	1.024

<sup>a</sup>Daily maximum temperature scaled by interquartile range (IQR)

<sup>b</sup>Areal mean 2018 NDVI by PAS, scaled by IQR

<sup>c</sup>Z-score of age (continuous years)

<sup>d</sup>Female = 1; Male = 0

<sup>e</sup>Z-score of BMI (continuous kg/m<sup>2</sup>)

<sup>f</sup>Completed high school = 1; did not complete high school = 0

<sup>g</sup>White = 1; non-White = 0

**4.9 APPENDIX D. Supplemental Table 4: Adjusted models of association for temperature and MVPA – for four exposure methods using overlapping samples by PAS type**

Adjusted models of association between daily maximum temperature and daily minutes of MVPA. Only overlapping person-days are utilized to compare between Actigraph+GPS (Freedson) and Actigraph+GPS (Abel) for the same PAS polygon method (i.e., 500-m buffer and minimum convex polygon.)

<b>A. Actigraph+GPS:</b> Log MVPA by <b>Freedson 1998</b> (vertical-axis count)	N=118 (744 pers.-days)			N=110 (561 pers.-days)		
	500-meter Location Buffer			Minimum Convex Polygon		
	IRR	CI		IRR	CI	
Daily maximum temperature <sup>a</sup>	1.005	0.519	1.921	0.825	0.422	1.576
Daily maximum temperature <sup>2</sup>	1.010	0.922	1.109	1.039	0.950	1.140
2018 NDVI <sup>b</sup>	1.123	1.013	1.245	1.029	0.947	1.121
Age (years) <sup>c</sup>	0.857	0.762	0.966	0.938	0.840	1.048
Sex <sup>d</sup>	0.745	0.591	0.937	0.744	0.598	0.925
BMI <sup>e</sup>	1.088	0.979	1.208	1.059	0.961	1.167
High school education <sup>f</sup>	1.002	0.711	1.410	0.808	0.590	1.104
Ethnicity <sup>g</sup>	1.128	0.886	1.433	1.108	0.877	1.398
<b>B. Actigraph+GPS:</b> Log MVPA by <b>Abel 2011</b> (steps)	N=118 (744 pers.-days)			N=110 (561 pers.-days)		
	500-meter Location Buffer			Minimum Convex Polygon		
	IRR	CI		IRR	CI	
Daily maximum temperature <sup>a</sup>	0.560	0.288	1.088	0.672	0.329	1.357
Daily maximum temperature <sup>2</sup>	1.072	0.971	1.184	1.053	0.944	1.177
2018 NDVI <sup>b</sup>	1.214	1.102	1.339	0.981	0.901	1.070
Age (years) <sup>c</sup>	0.898	0.795	1.014	0.911	0.812	1.021
Sex <sup>d</sup>	0.814	0.641	1.034	0.905	0.720	1.136
BMI <sup>e</sup>	0.918	0.824	1.024	0.947	0.855	1.049
High school education <sup>f</sup>	0.896	0.629	1.276	0.766	0.551	1.065
Ethnicity <sup>g</sup>	0.915	0.714	1.172	1.024	0.803	1.305

<sup>a</sup>Daily maximum temperature scaled by interquartile range (IQR)

<sup>b</sup>Areal mean 2018 NDVI by PAS, scaled by IQR

<sup>c</sup>Z-score of age (continuous years)

<sup>d</sup>Female = 1; Male = 0

<sup>e</sup>Z-score of BMI (continuous kg/m<sup>2</sup>)

<sup>f</sup>Completed high school = 1; did not complete high school = 0

<sup>g</sup>White = 1; non-White = 0

**4.10 APPENDIX E. Supplemental Table 5: Adjusted models of association for temperature and MVPA, including interaction between temperature<sup>2</sup> and NDVI – for four exposure methods using overlapping samples by PAS type**

Adjusted models of association between Daily maximum temperature and daily minutes of MVPA, including adjustment for the interaction between quadratic temperature and NDVI. Only overlapping person-days are utilized to compare between Actigraph+GPS (Freedson) and Actigraph+GPS (Abel) for the same PAS polygon method (i.e., 500-m buffer and minimum convex polygon.)

<b>Actigraph+GPS:</b> Log MVPA by <b>Freedson 1998</b> (vertical-axis count)	N=118 (744 pers.-days)			N=110 (561 pers.-days)		
	500-meter Location Buffer			Minimum Convex Polygon		
	IRR	CI	CI	IRR	CI	CI
Daily maximum temperature <sup>a</sup>	0.619	0.323	1.173	0.937	0.475	1.804
Daily maximum temperature <sup>2</sup>	1.063	0.961	1.177	1.012	0.923	1.114
2018 NDVI <sup>b</sup>	0.928	0.772	1.118	0.853	0.701	1.044
Age (years) <sup>c</sup>	0.888	0.799	0.987	0.941	0.843	1.052
Sex <sup>d</sup>	0.893	0.724	1.103	0.733	0.588	0.912
BMI <sup>e</sup>	0.955	0.869	1.051	1.050	0.952	1.159
High school education <sup>f</sup>	0.806	0.593	1.096	0.807	0.588	1.105
Ethnicity <sup>g</sup>	1.026	0.822	1.280	1.111	0.878	1.403
Max. daily temp. <sup>2</sup> X 2018 NDVI	1.007	0.991	1.024	1.015	1.000	1.030

<b>B. Actigraph+GPS:</b> Log MVPA by <b>Abel 2011</b> (steps)	N=118 (744 pers.-days)			N=110 (561 pers.-days)		
	500-meter Location Buffer			Minimum Convex Polygon		
	IRR	CI	CI	IRR	CI	CI
Daily maximum temperature <sup>a</sup>	0.682	0.346	1.338	0.701	0.342	1.424
Daily maximum temperature <sup>2</sup>	1.022	0.921	1.135	1.041	0.931	1.166
2018 NDVI <sup>b</sup>	0.907	0.721	1.147	0.888	0.714	1.104
Age (years) <sup>c</sup>	0.894	0.791	1.011	0.913	0.813	1.022
Sex <sup>d</sup>	0.807	0.635	1.028	0.897	0.714	1.127
BMI <sup>e</sup>	0.918	0.823	1.025	0.946	0.854	1.048
High school education <sup>f</sup>	0.893	0.625	1.274	0.769	0.554	1.069
Ethnicity <sup>g</sup>	0.898	0.700	1.153	1.021	0.801	1.301
Max. daily temp. <sup>2</sup> X 2018 NDVI	1.026	1.007	1.044	1.010	0.990	1.029

<sup>a</sup>Daily maximum temperature scaled by interquartile range (IQR)

<sup>b</sup>Areal mean 2018 NDVI by PAS, scaled by IQR

<sup>c</sup>Z-score of age (continuous years)

<sup>d</sup>Female = 1; Male = 0

<sup>e</sup>Z-score of BMI (continuous kg/m<sup>2</sup>)

<sup>f</sup>Completed high school = 1; did not complete high school = 0

<sup>g</sup>White = 1; non-White = 0

**4.11 APPENDIX F. Supplemental Table 6:** Adjusted models of association for temperature and MVPA—for four exposure methods using overlapping samples by MVPA conversion equation

Adjusted models of association between daily maximum temperature and daily minutes of MVPA. Only overlapping person-days are utilized to compare between 500-meter location buffer and minimum convex polygon for the same MVPA conversion (Freedson vs. Abel).

<b>Actigraph+GPS:</b> Log MVPA by <b>Freedson 1998</b> (vertical-axis count)	N=118 (744 pers.-days)			N=110 (561 pers.-days)		
	500-meter Location Buffer		CI	Minimum Convex Polygon		CI
	IRR	CI		IRR	CI	
Daily maximum temperature <sup>a</sup>	0.968	0.566	1.657	0.968	0.572	1.638
Daily maximum temperature <sup>2</sup>	1.016	0.943	1.095	1.015	0.944	1.090
2018 NDVI <sup>b</sup>	1.108	1.018	1.208	1.034	0.973	1.100
Age (years) <sup>c</sup>	0.939	0.860	1.027	0.927	0.848	1.014
Sex <sup>d</sup>	0.766	0.638	0.918	0.759	0.631	0.912
BMI <sup>e</sup>	1.035	0.956	1.121	1.028	0.948	1.114
High school education <sup>f</sup>	0.862	0.658	1.127	0.805	0.614	1.053
Ethnicity <sup>g</sup>	1.024	0.849	1.232	1.033	0.854	1.247

<b>B. Actigraph+GPS:</b> Log MVPA by <b>Abel 2011</b> (steps)	N=118 (744 pers.-days)			N=110 (561 pers.-days)		
	500-meter Location Buffer		CI	Minimum Convex Polygon		CI
	IRR	CI		IRR	CI	
Daily maximum temperature <sup>a</sup>	0.704	0.380	1.292	0.595	0.312	1.121
Daily maximum temperature <sup>2</sup>	1.043	0.953	1.144	1.072	0.972	1.186
2018 NDVI <sup>b</sup>	1.194	1.086	1.312	1.000	0.929	1.078
Age (years) <sup>c</sup>	0.903	0.814	1.003	0.888	0.799	0.987
Sex <sup>d</sup>	0.883	0.718	1.087	0.898	0.728	1.109
BMI <sup>e</sup>	0.956	0.871	1.050	0.955	0.869	1.050
High school education <sup>f</sup>	0.881	0.649	1.196	0.806	0.592	1.095
Ethnicity <sup>g</sup>	1.038	0.835	1.291	1.029	0.824	1.283

<sup>a</sup>Daily maximum temperature scaled by interquartile range (IQR)

<sup>b</sup>Areal mean 2018 NDVI by PAS, scaled by IQR

<sup>c</sup>Z-score of age (continuous years)

<sup>d</sup>Female = 1; Male = 0

<sup>e</sup>Z-score of BMI (continuous kg/m<sup>2</sup>)

<sup>f</sup>Completed high school = 1; did not complete high school = 0

<sup>g</sup>White = 1; non-White = 0

**4.12 APPENDIX G. Supplemental Table 7: Adjusted models of association for temperature and MVPA, including interaction between temperature<sup>2</sup> and NDVI – for four exposure methods using overlapping samples by MVPA conversion equation**

Adjusted models of association between daily maximum temperature and daily minutes of MVPA, including adjustment for the interaction between quadratic temperature and NDVI. Adjusted models of association between daily maximum temperature and daily minutes of MVPA. Only overlapping person-days are utilized to compare between 500-meter location buffer and minimum convex polygon for the same MVPA conversion (Freedson vs. Abel).

<b>Actigraph+GPS:</b> Log MVPA by <b>Freedson 1998</b> (vertical-axis count)	N=120 (894 pers.-days)			N=120 (894 pers.-days)		
	500-meter Location Buffer			Minimum Convex Polygon		
	IRR	CI		IRR	CI	
Daily maximum temperature <sup>a</sup>	0.985	0.574	1.689	1.004	0.592	1.702
Daily maximum temperature <sup>2</sup>	1.011	0.936	1.091	1.006	0.936	1.082
2018 NDVI <sup>b</sup>	1.041	0.847	1.286	0.940	0.811	1.092
Age (years) <sup>c</sup>	0.938	0.859	1.026	0.925	0.846	1.012
Sex <sup>d</sup>	0.765	0.638	0.918	0.753	0.626	0.906
BMI <sup>e</sup>	1.035	0.955	1.120	1.027	0.947	1.113
High school education <sup>f</sup>	0.861	0.658	1.126	0.807	0.616	1.056
Ethnicity <sup>g</sup>	1.022	0.847	1.230	1.031	0.852	1.246
Max. daily temp. <sup>2</sup> X 2018 NDVI	1.004	0.991	1.018	1.007	0.997	1.017

<b>B. Actigraph+GPS:</b> Log MVPA by <b>Abel 2011</b> (steps)	N=115 (710 pers.-days)			N=115 (710 pers.-days)		
	500-meter Location Buffer			Minimum Convex Polygon		
	IRR	CI		IRR	CI	
Daily maximum temperature <sup>a</sup>	0.851	0.449	1.595	0.619	0.323	1.173
Daily maximum temperature <sup>2</sup>	0.998	0.905	1.104	1.063	0.961	1.177
2018 NDVI <sup>b</sup>	0.949	0.757	1.194	0.928	0.772	1.118
Age (years) <sup>c</sup>	0.899	0.810	0.999	0.888	0.799	0.987
Sex <sup>d</sup>	0.875	0.711	1.078	0.893	0.724	1.103
BMI <sup>e</sup>	0.958	0.872	1.052	0.955	0.869	1.051
High school education <sup>f</sup>	0.874	0.643	1.188	0.806	0.593	1.096
Ethnicity <sup>g</sup>	1.031	0.829	1.284	1.026	0.822	1.280
Max. daily temp. <sup>2</sup> X 2018 NDVI	1.020	1.002	1.039	1.007	0.991	1.024

<sup>a</sup>Daily maximum temperature scaled by interquartile range (IQR)

<sup>b</sup>Areal mean 2018 NDVI by PAS, scaled by IQR

<sup>c</sup>Z-score of age (continuous years)

<sup>d</sup>Female = 1; Male = 0

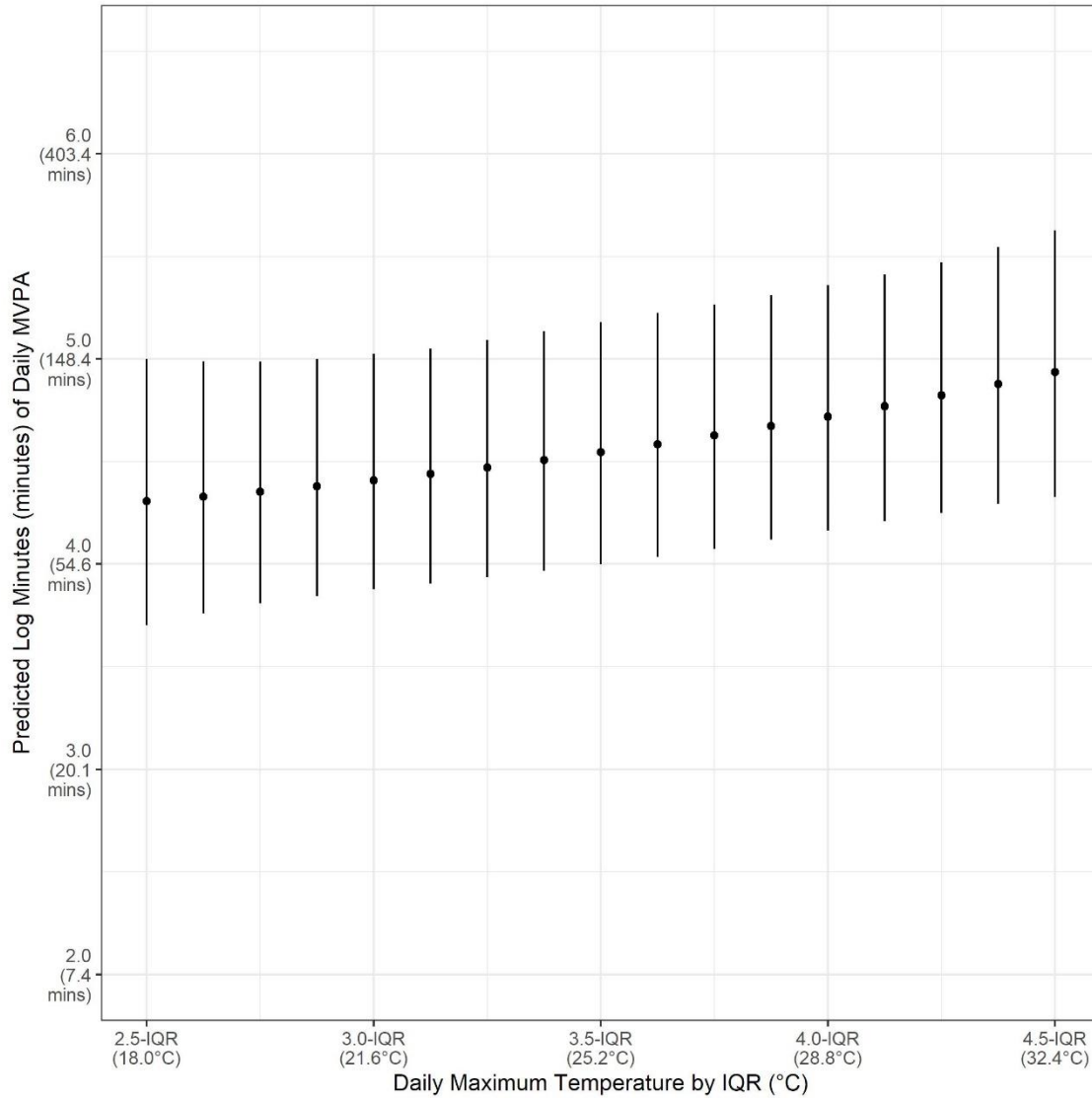
<sup>e</sup>Z-score of BMI (continuous kg/m<sup>2</sup>)

<sup>f</sup>Completed high school = 1; did not complete high school = 0

<sup>g</sup>White = 1; non-White = 0

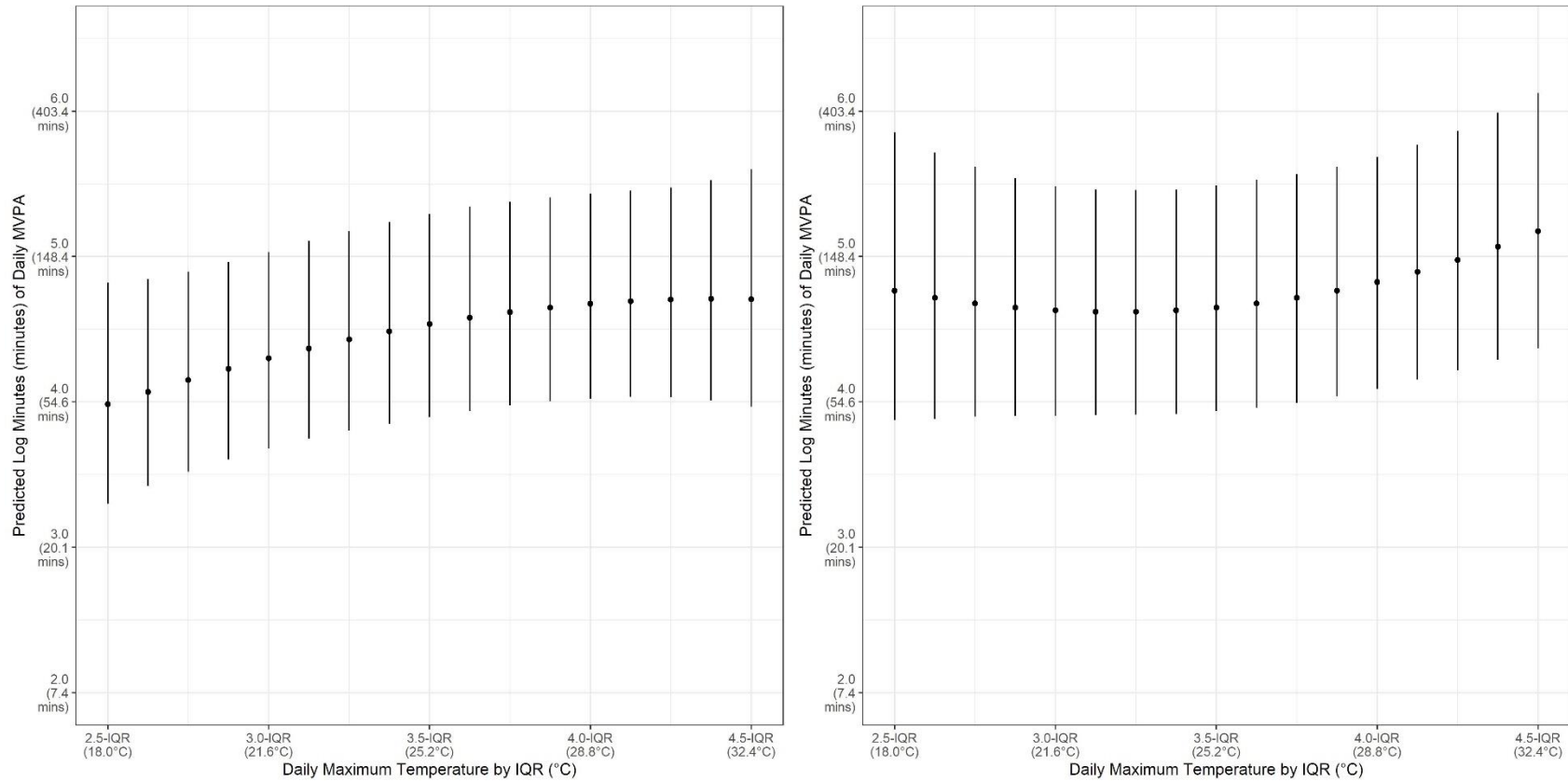
#### 4.13 APPENDIX H. Supplemental Figure 1: Predicted MVPA associated with daily maximum temperature for minimum convex polygon PASs created from *Freedson 1998* MVPA

Sensitivity analysis using dataset from minimum convex polygon PASs, derived from Actigraph+GPS data with MVPA categorized using vertical-axis counts (Freedson et al., 1998) – Predicted  $\log_e$  minutes of daily MVPA associated with daily maximum temperature (scaled by IQR of 7.2°C); figure generated using point estimates and 95% confidence intervals derived from linear mixed-effected regression model coefficients applied to means (continuous covariates) and modes (categorical covariates).



**4.14 APPENDIX I. Supplemental Figure 2:** Predicted MVPA associated with daily maximum temperature, stratified by median NDVI, for minimum convex polygon PASs created from *Freedson 1998* MVPA

Sensitivity analysis using dataset from minimum convex polygon PASs, derived from Actigraph+GPS data with MVPA categorized using vertical-axis counts (Freedson et al., 1998) – Predicted  $\log_e$  minutes of daily MVPA associated with daily maximum temperature (scaled by IQR of 7.2°C) – for the bottom 50% (< median) of attributed NDVI by person-day (LEFT) and the top 50% (> median) of attributed NDVI by person-day (RIGHT); figures generated using point estimates and 95% confidence intervals derived from linear mixed-effected regression model coefficients, including interaction  $\beta_9(\text{Maximum Daily Temperature})^2_{ij}X(\text{NDVI})_{ij}$ , applied to means (continuous covariates) and modes (categorical covariates).



#### 4.15 REFERENCES FOR CHAPTER 4

- Abel, M., Hannon, J., Mullineaux, D., Beighle, A., 2011. Determination of step rate thresholds corresponding to physical activity intensity classifications in adults. *J. Phys. Act. Heal.* 8, 45–51. <https://doi.org/10.1123/JPAH.8.1.45>
- Actigraph Corp, 2019. What's the difference among the Cut Points available in ActiLife? [WWW Document]. URL <https://actigraphcorp.my.site.com/support/s/article/What-s-the-difference-among-the-Cut-Points-available-in-ActiLife> (accessed 5.2.22).
- Alaimo, P., Loro, D., Mingione, M., Lipsitt, J., Jerrett, M., Banerjee, S., 2021. Bayesian Hierarchical Modeling and Analysis for Physical Activity Trajectories Using Actigraph Data. *arxiv Pre-Print*, 1–36. <https://doi.org/https://arxiv.org/abs/2101.01624>
- Almanza, E., Jerrett, M., Dunton, G., Seto, E., Ann Pentz, M., 2012. A study of community design, greenness, and physical activity in children using satellite, GPS and accelerometer data. *Health Place* 18, 46–54. <https://doi.org/10.1016/j.healthplace.2011.09.003>
- Amoly, E., Dadvand, P., Forn, J., López-Vicente, M., Basagaña, X., Julvez, J., Alvarez-Pedrerol, M., Nieuwenhuijsen, M.J., Sunyer, J., 2015. Green and blue spaces and behavioral development in barcelona schoolchildren: The BREATHE project. *Environ. Health Perspect.* 122. <https://doi.org/10.1289/ehp.1408215>
- Avila-Palencia, I., Int Panis, L., Dons, E., Gaupp-Berghausen, M., Raser, E., Götschi, T., Gerike, R., Brand, C., de Nazelle, A., Orjuela, J.P., Anaya-Boig, E., Stigell, E., Kahlmeier, S., Iacorossi, F., Nieuwenhuijsen, M.J., 2018. The effects of transport mode use on self-perceived health, mental health, and social contact measures: A cross-sectional and longitudinal study. *Environ. Int.* 120. <https://doi.org/10.1016/j.envint.2018.08.002>
- Aybar, C., Wu, Q., Bautista, L., Yali, R., Barja, A., 2020. rgee: An R package for interacting with Google Earth Engine. *J. Open Source Softw.*
- Bates, D., Mächler, M., Bolker, B., Walker, S., 2015. Fitting Linear Mixed-Effects Models Using {lme4}. *J. Stat. Softw.* 67, 1–48. <https://doi.org/10.18637/jss.v067.i01>
- Beekhuizen, J., Kromhout, H., Huss, A., Vermeulen, R., 2013. Performance of GPS-devices for environmental exposure assessment. *J. Expo. Sci. Environ. Epidemiol.* 23. <https://doi.org/10.1038/jes.2012.81>
- Benzinger, T.H., 1959. ON PHYSICAL HEAT REGULATION AND THE SENSE OF TEMPERATURE IN MAN. *Proc. Natl. Acad. Sci.* 45, 645. <https://doi.org/10.1073/pnas.45.4.645>

- Branion-Calles, M., Götschi, T., Nelson, T., Anaya-Boig, E., Avila-Palencia, I., Castro, A., Cole-Hunter, T., de Nazelle, A., Dons, E., Gaupp-Berghausen, M., Gerike, R., Int Panis, L., Kahlmeier, S., Nieuwenhuijsen, M., Rojas-Rueda, D., Winters, M., 2020. Cyclist crash rates and risk factors in a prospective cohort in seven European cities. *Accid. Anal. Prev.* 141. <https://doi.org/10.1016/j.aap.2020.105540>
- Brooke Anderson, G., Bell, M.L., Peng, R.D., 2013. Methods to calculate the heat index as an exposure metric in environmental health research. *Environ. Health Perspect.* <https://doi.org/10.1289/ehp.1206273>
- Chaix, B., Méline, J., Duncan, S., Merrien, C., Karusisi, N., Perchoux, C., Lewin, A., Labadi, K., Kestens, Y., 2013. GPS tracking in neighborhood and health studies: A step forward for environmental exposure assessment, a step backward for causal inference? *Health Place* 21, 46–51. <https://doi.org/10.1016/j.healthplace.2013.01.003>
- Chan, C.B., Ryan, D.A.J., Tudor-Locke, C., 2006. Relationship between objective measures of physical activity and weather: A longitudinal study. *Int. J. Behav. Nutr. Phys. Act.* 3, 1–9. <https://doi.org/10.1186/1479-5868-3-21/FIGURES/2>
- Chen, Y.-C., Dobra, A., 2017. Measuring Human Activity Spaces With Density Ranking Based on GPS Data 1–28.
- Dadvand, P., de Nazelle, A., Figueras, F., Basagaña, X., Su, J., Amoly, E., Jerrett, M., Vrijheid, M., Sunyer, J., Nieuwenhuijsen, M.J., 2012a. Green space, health inequality and pregnancy. *Environ. Int.* 40. <https://doi.org/10.1016/j.envint.2011.07.004>
- Dadvand, P., de Nazelle, A., Triguero-Mas, M., Schembari, A., Cirach, M., Amoly, E., Figueras, F., Basagaña, X., Ostro, B., Nieuwenhuijsen, M., 2012b. Surrounding greenness and exposure to air pollution during pregnancy: An analysis of personal monitoring data. *Environ. Health Perspect.* 120. <https://doi.org/10.1289/ehp.1104609>
- Dadvand, P., Villanueva, C.M., Font-Ribera, L., Martinez, D., Basagaña, X., Belmonte, J., Vrijheid, M., Gražulevičienė, R., Kogevinas, M., Nieuwenhuijsen, M.J., 2015. Risks and benefits of green spaces for children: A cross-sectional study of associations with sedentary behavior, obesity, asthma, and allergy. *Environ. Health Perspect.* 122. <https://doi.org/10.1289/ehp.1308038>
- Deeks, J.J., Dinnes, J., D'Amico, R., Sowden, A.J., Sakarovich, C., Song, F., Petticrew, M., Altman, D.G., 2003. Evaluating non-randomised intervention studies. *Health Technol. Assess. (Rockv)*. <https://doi.org/10.3310/hta7270>
- Dzhambov, A., Hartig, T., Markevych, I., Tilov, B., Dimitrova, D., 2018. Urban residential greenspace and mental health in youth: Different approaches to testing multiple pathways

- yield different conclusions. *Environ. Res.* 160. <https://doi.org/10.1016/j.envres.2017.09.015>
- Evenson, K.R., Catellier, D.J., Gill, K., Ondrak, K.S., McMurray, R.G., 2008. Calibration of two objective measures of physical activity for children. *J. Sports Sci.* 26. <https://doi.org/10.1080/02640410802334196>
- Freedson, P., Melanson, E., Sirard, J., 1998. Calibration of the Computer Science and Applications, Inc. accelerometer. *Med. Sci. Sport. Exerc.* 30.
- Gascon, M., Triguero-Mas, M., Martínez, D., Dadvand, P., Rojas-Rueda, D., Plasència, A., Nieuwenhuijsen, M.J., 2016. Residential green spaces and mortality: A systematic review. *Environ. Int.* 86, 60–67. <https://doi.org/10.1016/j.envint.2015.10.013>
- GlobalSat WorldCom Corporation, 2022a. DG-500 GPS Data Logger Quick Start Guide [WWW Document]. URL [https://www.globalsat.com.tw/ftp/download/DG-500\\_QSG\\_ENG\\_V1.3\\_20170105.pdf](https://www.globalsat.com.tw/ftp/download/DG-500_QSG_ENG_V1.3_20170105.pdf) (accessed 5.9.22).
- GlobalSat WorldCom Corporation, 2022b. BT-335 Bluetooth Data Logger User Manual [WWW Document]. URL <https://www.gpscentral.ca/products/usglobalsat/bt-335-user-manual.pdf> (accessed 5.9.22).
- Hamada, S., Ohta, T., 2010. Seasonal variations in the cooling effect of urban green areas on surrounding urban areas. *Urban For. Urban Green.* 9, 15–24. <https://doi.org/10.1016/J.UFUG.2009.10.002>
- Hayhoe, K., Cayan, D., Field, C.B., Frumhoff, P.C., Maurer, E.P., Miller, N.L., Moser, S.C., Schneider, S.H., Cahill, K.N., Cleland, E.E., Dale, L., Drapek, R., Hanemann, R.M., Kalkstein, L.S., Lenihan, J., Lunch, C.K., Neilson, R.P., Sheridan, S.C., Verville, J.H., 2004. Emissions pathways, climate change, and impacts on California. *Proc. Natl. Acad. Sci. U. S. A.* 101, 12422–12427. [https://doi.org/10.1073/PNAS.0404500101/SUPPL\\_FILE/04500FIG17.JPG](https://doi.org/10.1073/PNAS.0404500101/SUPPL_FILE/04500FIG17.JPG)
- Higgs, G., Fry, R., Langford, M., 2012. Investigating the Implications of Using Alternative GIS-Based Techniques to Measure Accessibility to Green Space. *Environ. Plan. B Plan. Des.* 39, 326–343. <https://doi.org/10.1068/b37130>
- Hirsch, J.A., Winters, M., Clarke, P., McKay, H., 2014. Generating GPS activity spaces that shed light upon the mobility habits of older adults: A descriptive analysis. *Int. J. Health Geogr.* 13, 1–14. <https://doi.org/10.1186/1476-072X-13-51>
- Ho, J.Y., Zijlema, W.L., Triguero-Mas, M., Donaire-Gonzalez, D., Valentín, A., Ballester, J., Chan, E.Y.Y., Goggins, W.B., Mo, P.K.H., Kruize, H., van den Berg, M., Gražulevičienė, R., Gidlow, C.J., Jerrett, M., Seto, E.Y.W., Barrera-Gómez, J., Nieuwenhuijsen, M.J., 2021. Does surrounding greenness moderate the relationship between apparent temperature and

- physical activity? Findings from the PHENOTYPE project. *Environ. Res.* 197, 110992. <https://doi.org/10.1016/J.ENVRES.2021.110992>
- Holliday, K.M., Howard, A.G., Emch, M., Rodríguez, D.A., Evenson, K.R., 2017. Are buffers around home representative of physical activity spaces among adults? *Heal. Place* 45, 181–188. <https://doi.org/10.1016/j.healthplace.2017.03.013>
- Humpel, N., 2002. Environmental factors associated with adults' participation in physical activity: A review. *Am. J. Prev. Med.* 22, 188–199. [https://doi.org/10.1016/S0749-3797\(01\)00426-3](https://doi.org/10.1016/S0749-3797(01)00426-3)
- Jerrett, M., Almanza, E., Davies, M., Wolch, J., Dunton, G., Spruitj-Metz, D., Ann Pentz, M., 2013. Smart growth community design and physical activity in children. *Am. J. Prev. Med.* 45, 386–392. <https://doi.org/10.1016/j.amepre.2013.05.010>
- Keadle, S.K., Shiroma, E.J., Freedson, P.S., Lee, I.M., 2014. Impact of accelerometer data processing decisions on the sample size, wear time and physical activity level of a large cohort study. *BMC Public Health* 14. <https://doi.org/10.1186/1471-2458-14-1210>
- Kerr, J., Duncan, S., Schipperjin, J., 2011. Using global positioning systems in health research: A practical approach to data collection and processing. *Am. J. Prev. Med.* 41. <https://doi.org/10.1016/j.amepre.2011.07.017>
- Kong, F., Yin, H., James, P., Hutyra, L.R., He, H.S., 2014. Effects of spatial pattern of greenspace on urban cooling in a large metropolitan area of eastern China. *Landsc. Urban Plan.* 128, 35–47. <https://doi.org/10.1016/j.landurbplan.2014.04.018>
- Kuznetsova, A., Brockhoff, P.B., Christensen, R.H.B., 2017. {lmerTest} Package: Tests in Linear Mixed Effects Models. *J. Stat. Softw.* 82, 1–26. <https://doi.org/10.18637/jss.v082.i13>
- Lachowycz, K., Jones, A.P., Page, A.S., Wheeler, B.W., Cooper, A.R., 2012. What can global positioning systems tell us about the contribution of different types of urban greenspace to children's physical activity? *Health Place* 18, 586–594. <https://doi.org/10.1016/j.healthplace.2012.01.006>
- Lafortezza, R., Carrus, G., Sanesi, G., Davies, C., 2009. Benefits and well-being perceived by people visiting green spaces in periods of heat stress. *Urban For. Urban Green.* 8, 97–108. <https://doi.org/10.1016/j.ufug.2009.02.003>
- Lee, J.H., Davis, A.W., Yoon, S.Y., Goulias, K.G., 2016. Activity space estimation with longitudinal observations of social media data. *Transportation (Amst.)* 43. <https://doi.org/10.1007/s11116-016-9719-1>
- Lee, N.C., Voss, C., Frazer, A.D., Hirsch, J.A., McKay, H.A., Winters, M., 2016. Does activity space size influence physical activity levels of adolescents?-A GPS study of an urban environment. *Prev. Med. Reports* 3. <https://doi.org/10.1016/j.pmedr.2015.12.002>

- Leslie, E., Sugiyama, T., Ierodiaconou, D., Kremer, P., 2010. Perceived and objectively measured greenness of neighbourhoods: Are they measuring the same thing? *Landsc. Urban Plan.* 95. <https://doi.org/10.1016/j.landurbplan.2009.11.002>
- Li, R., Tong, D., 2016. Constructing human activity spaces: A new approach incorporating complex urban activity-travel. *JTRG* 56, 23–35. <https://doi.org/10.1016/j.jtrangeo.2016.08.013>
- Li, X., Zhang, C., Li, W., Ricard, R., Meng, Q., Zhang, W., 2015. Assessing street-level urban greenery using Google Street View and a modified green view index. *Urban For. Urban Green.* 14. <https://doi.org/10.1016/j.ufug.2015.06.006>
- McCrorie, P.R., Fenton, C., Ellaway, A., 2014. Combining GPS, GIS, and accelerometry to explore the physical activity and environment relationship in children and young people - a review. *Int. J. Behav. Nutr. Phys. Act.* 11. <https://doi.org/10.1186/s12966-014-0093-0>
- McMorris, O., Villeneuve, P.J., Su, J., Jerrett, M., 2015. Urban greenness and physical activity in a national survey of Canadians. *Environ. Res.* 137, 94–100. <https://doi.org/10.1016/J.ENVRES.2014.11.010>
- NASA Earth Observatory, 2011. Measuring Vegetation (NDVI & EVI) [WWW Document]. URL [https://earthobservatory.nasa.gov/features/MeasuringVegetation/measuring\\_vegetation\\_2.php](https://earthobservatory.nasa.gov/features/MeasuringVegetation/measuring_vegetation_2.php) (accessed 5.9.22).
- Nazarian, N., Lee, J.K.W., 2021. Personal assessment of urban heat exposure: a systematic review. *Environ. Res. Lett.* 16, 033005. <https://doi.org/10.1088/1748-9326/ABD350>
- Oak Ridge National Laboratory, NASA, 2022. Daymet V4: Daily Surface Weather and Climatological Summaries [WWW Document]. URL <https://daymet.ornl.gov/> (accessed 5.15.22).
- Obradovich, N., Fowler, J.H., 2017. Climate change may alter human physical activity patterns. *Nat. Hum. Behav.* 2017 15 1, 1–7. <https://doi.org/10.1038/s41562-017-0097>
- Oliveira, S., Andrade, H., Vaz, T., 2011. The cooling effect of green spaces as a contribution to the mitigation of urban heat: A case study in Lisbon. *Build. Environ.* 46, 2186–2194. <https://doi.org/10.1016/j.buildenv.2011.04.034>
- Perchoux, C., Chaix, B., Cummins, S., Kestens, Y., 2013. Conceptualization and measurement of environmental exposure in epidemiology: Accounting for activity space related to daily mobility. *Heal. Place* 21, 86–93. <https://doi.org/10.1016/j.healthplace.2013.01.005>
- Puyau, M.R., Adolph, A.L., Vohra, F.A., Butte, N.F., 2002. Validation and calibration of physical activity monitors in children. *Obes. Res.* 10. <https://doi.org/10.1038/oby.2002.24>
- Raser, E., Gaupp-Berghausen, M., Dons, E., Anaya-Boig, E., Avila-Palencia, I., Brand, C., Castro,

- A., Clark, A., Eriksson, U., Götschi, T., Int Panis, L., Kahlmeier, S., Laeremans, M., Mueller, N., Nieuwenhuijsen, M., Orjuela, J.P., Rojas-Rueda, D., Standaert, A., Stigell, E., Gerike, R., 2018. European cyclists' travel behavior: Differences and similarities between seven European (PASTA) cities. *J. Transp. Heal.* 9. <https://doi.org/10.1016/j.jth.2018.02.006>
- Reid, C.E., O'Neill, M.S., Gronlund, C.J., Brines, S.J., Brown, D.G., Diez-Roux, A. V., Schwartz, J., 2009. Mapping Community Determinants of Heat Vulnerability. *Environ. Health Perspect.* 117, 1730–1736. <https://doi.org/10.1289/ehp.0900683>
- Stamatakis, E., Nnoaham, K., Foster, C., Scarborough, P., 2013. The Influence of Global Heating on Discretionary Physical Activity: An Important and Overlooked Consequence of Climate Change. *J. Phys. Act. Heal.* 10, 765–768. <https://doi.org/10.1123/jpah.10.6.765>
- Stone, B., Hess, J.J., Frumkin, H., 2010. Urban Form and Extreme Heat Events: Are Sprawling Cities More Vulnerable to Climate Change Than Compact Cities? *Environ. Health Perspect.* 118, 1425–1428. <https://doi.org/10.1289/ehp.0901879>
- Su, J.G., Dadvand, P., Nieuwenhuijsen, M.J., Bartoll, X., Jerrett, M., 2019. Associations of green space metrics with health and behavior outcomes at different buffer sizes and remote sensing sensor resolutions. *Environ. Int.* 126. <https://doi.org/10.1016/j.envint.2019.02.008>
- Sun, F., Walton, D.B., Hall, A., 2015. A Hybrid Dynamical–Statistical Downscaling Technique. Part II: End-of-Century Warming Projections Predict a New Climate State in the Los Angeles Region. *J. Clim.* 28, 4618–4636. <https://doi.org/10.1175/JCLI-D-14-00197.1>
- Trost, S.G., Loprinzi, P.D., Moore, R., Pfeiffer, K.A., 2011. Comparison of accelerometer cut points for predicting activity intensity in youth. *Med. Sci. Sports Exerc.* 43. <https://doi.org/10.1249/MSS.0b013e318206476e>
- Tucker, J.M., Welk, G.J., Beyler, N.K., 2011. Physical activity in U.S. adults: Compliance with the physical activity guidelines for Americans. *Am. J. Prev. Med.* 40. <https://doi.org/10.1016/j.amepre.2010.12.016>
- Tucker, P., Gilliland, J., 2007. The effect of season and weather on physical activity: A systematic review. *Public Health* 121, 909–922. <https://doi.org/10.1016/j.puhe.2007.04.009>
- van den Berg, A.E., Maas, J., Verheij, R.A., Groenewegen, P.P., 2010. Green space as a buffer between stressful life events and health. *Soc. Sci. Med.* 70. <https://doi.org/10.1016/j.socscimed.2010.01.002>
- Vienneau, D., de Hoogh, K., Faeh, D., Kaufmann, M., Wunderli, J.M., Rösli, M., 2017. More than clean air and tranquillity: Residential green is independently associated with decreasing mortality. *Environ. Int.* 108. <https://doi.org/10.1016/j.envint.2017.08.012>
- Villeneuve, P.J., Jerrett, M., G. Su, J., Burnett, R.T., Chen, H., Wheeler, A.J., Goldberg, M.S.,

2012. A cohort study relating urban green space with mortality in Ontario, Canada. *Environ. Res.* 115, 51–58. <https://doi.org/10.1016/j.envres.2012.03.003>
- Wang, J., Kwan, M.P., Chai, Y., 2018. An innovative context-based crystal-growth activity space method for environmental exposure assessment: A study using GIS and GPS trajectory data collected in Chicago. *Int. J. Environ. Res. Public Health* 15. <https://doi.org/10.3390/ijerph15040703>
- Ward Thompson, C., Roe, J., Aspinall, P., Mitchell, R., Clow, A., Miller, D., 2012. More green space is linked to less stress in deprived communities: Evidence from salivary cortisol patterns. *Landsc. Urban Plan.* 105, 221–229. <https://doi.org/10.1016/j.landurbplan.2011.12.015>
- Wehener, S., Raser, E., Gaupp, M., Anata, E., De Nazelle, A., Eriksoon, U., Gerike, R., Horvath, I., Iacorossi, F., Int Panis, L., Kahlmeier, S., Nieuwenhuijsen, M., Mueller, N., Sanchez, J., Rothballer, C., 2017. Active Mobility, the New Health Trend in Smart Cities, or even More? REAL CORP.
- Wolch, J.R., Byrne, J., Newell, J.P., 2014. Urban green space, public health, and environmental justice: The challenge of making cities “just green enough.” *Landsc. Urban Plan.* 125, 234–244. <https://doi.org/10.1016/j.landurbplan.2014.01.017>
- Zenk, S.N., Schulz, A.J., Matthews, S.A., Odoms-young, A., Wilbur, J., Wegrzyn, L., Gibbs, K., Braunschweig, C., Stokes, C., 2011. Health & Place Activity space environment and dietary and physical activity behaviors: A pilot study. *Health Place* 17, 1150–1161. <https://doi.org/10.1016/j.healthplace.2011.05.001>

## CHAPTER 5: SUMMARY OF DISSERTATION FINDINGS AND FUTURE RESEARCH RECOMMENDATIONS

### 5.1 INTRODUCTION

The goal of this dissertation was to investigate emerging geospatial methods for constructing ‘big data’ datasets from multiple spatiotemporally misaligned data sources. Models of association require multiple descriptors, factors, or covariates, and spatial models are often derived from multiple sources recorded at disparate times and locations. In the study of Environmental Health Sciences, models often include environmental exposures or contexts which can be quantified from data of very different temporal (e.g., 5-second instantaneous vs. 1-year average) or spatial (e.g., 60-centimeter vs. 1-kilometer) resolutions. Over-simplification when combining these data sources can lead to misclassification of key variables (e.g., exposure). Through three case studies, this dissertation offered alternative methods to quantifying spatiotemporally misaligned variables and investigated how choice in geospatial method could impact modeling results.

In the case study reported in **Chapter 2**, we report on a small-area study of COVID-19 and traffic-related air pollution. We demonstrated the use of residential-building footprints as an intermediate spatial-aggregation geography, to combine intersecting areal population data—in this case, COVID-19 outcomes (at the neighborhood level) and population demographics (at the census-tract level). In **Chapter 3**, we presented multiple methodologies for using location and activity data from accelerometers, GPS units, and smartphones to define physical activity spaces and then to quantify green space exposure within those spaces. We demonstrated these methodologies on free-living study participants and compared results on attributed exposure from 21 geospatial methods. Finally, in the case study reported in **Chapter 4**, we provided an example for how the methods in Chapter 3 could be utilized in the modeling of heat exposure and physical

activity, as modified by exposure to green space. Again, we demonstrated how choice in geospatial methods (used to attribute exposure from misaligned data) may impact study conclusions.

## 5.2 COVID-19 AND TRAFFIC-RELATED AIR POLLUTION

The research in **Chapter 2** described some of the first small-area analyses on the association of environmental exposure with COVID-19 incidence and mortality. Since this chapter was published in *Environment International* (Lipsitt et al., 2021), more research utilizing small-area and individual-level COVID-19 outcome data has been conducted (Kerr et al., 2021; Konstantinou et al., 2021) and corroborated our findings. After adjusting for selected confounders, we found NO<sub>2</sub> to be positively associated with COVID-19 incidence and mortality. This result was the same across all three of our statistical models. We also found NO<sub>2</sub> exposure to be positively associated with COVID-19 case-fatality in one of the three statistical models. These results were largely consistent with available literature (Gupta et al., 2021; Liang et al., 2020a; Srivastava, 2021; Xiao Wu et al., 2020a; Zhu et al., 2020) and demonstrate that spatial models, including small-area models accounting for population density variability, show a relationship between traffic-related air pollution and COVID-19 case and mortality rates.

To our knowledge, this study remains the only areal-level COVID-19 research to use an intermediate aggregation step, i.e., using residential building footprints to account for population density variation when aggregating between spatially misaligned datasets, in this case, neighborhoods and census tracts. Although this aggregation method has limitations, it may further the discussion on other potential intermediate spatial aggregation methods to overcome areal misalignment.

### 5.3 PHYSICAL ACTIVITY SPACE METHODS

The research presented in **Chapter 3** was, to our knowledge, the first research to use “physical activity space (PAS)” polygons to attribute environmental exposure during periods of moderate-to-vigorous physical activity (MVPA). Although activity space methodologies have become more widely used to describe the regions of daily activity (Jerrett et al., 2005a; Klompaker et al., 2018; Shin et al., 2020; Tribby et al., 2017), they have not yet been used to describe regions of MVPA. We used physical activity space polygons to describe surroundings of individuals during periods of active behavior, and attributed values from overlapping datasets that were misaligned in time and/or space. We utilized PASTA-LA study data to demonstrate 21 approaches to quantifying green space exposure using PASs using: three activity and location-tracking devices (Actigraph accelerometer, GlobalSat GPS, and the MOVES smartphone app); two equations to categorize raw accelerometry and step data into activity levels (*Freedson et al., 1998* and *Abel et al., 2011*); and seven geospatial methods to draw PAS polygons (e.g., 500-meter location buffer, minimum convex polygon, 95% ellipse, etc.). We compare these results to those derived from the commonly-used home address buffer exposure attribution. In addition, we compare green space attribution from two years of data from the United States Department of Agriculture, National Agriculture Imagery Program (NAIP) (NAIP NDVI for 2018 and 2016).

This study had three major findings. First, we found that green space exposures (areal mean NDVI per person-day within each PAS) derived from the 21 PAS methods were only weakly correlated ( $r < 0.32$ ) with that attributed from home-address buffers. This was an important finding because many studies have quantified environmental exposures using home location, and this would likely lead to exposure misclassification. This finding is generalizable to exposure attribution of activity spaces, in general, and given there is more activity than *physical* activity away from the home, there could be even greater misclassification using home buffers.

Second, all 21 PAS methods showed high correlation between green space exposure attributed from 2018 imagery and exposure attributed from 2016 imagery ( $r > 0.82$ ). This finding suggests that choice of year to define green space is not a major source of exposure misclassification.

Third, we found a large range in correlation ( $0.30 < r < 0.80$ ) depending on the location/activity device used and the way MVPA was categorized (i.e., Actigraph+GPS with MVPA by vertical-axis count vs. Actigraph+GPS with MVPA by step count vs. MOVES with MVPA by step count) across the 21 PAS methods. Thus, when correlating green space exposures from different devices and MVPA equations, the PAS method selected can determine the strength of the relationship. Therefore, when using cost-effective alternatives (such as smartphones) for location and activity tracking, researchers should carefully select PAS polygon methods to attribute exposures most comparable to current best practices (i.e., Actigraph+GPS using vertical-axis count).

#### **5.4 HEAT, GREEN SPACE, AND PHYSICAL ACTIVITY**

The study presented in **Chapter 4** builds from the methods described in **Chapter 3** to model the relationship between heat exposure and physical activity and the effect modification by green space. Based on the literature and results from **Chapter 3**, we selected as the main method for heat and green space exposure attribution the 500-meter location buffer PASs derived from Actigraph+GPS data with MVPA categorized using *Freedson et al., 1998*. A linear mixed-effects regression model utilizing the exposure data produced by this main method demonstrated that increasing heat exposure was associated with increased physical activity (MVPA). The results also showed that in hotter than normal temperatures, individuals were likely to engage in more MVPA if they were near 'more-green' green space (higher NDVI), and likely to engage in less

MVPA if they were near 'less-green' green space. This result was consistent with the literature, although we had limited data at extreme temperatures.

There was inconsistency, however, between the results of the main model and the alternative models. As an example, models using different MVPA equations differed in their results in that the positive association between heat and physical activity using the Freedson (Freedson et al., 1998) model was no longer observed in the Abel (Abel et al., 2011) models, regardless of the PAS polygon method. These differences demonstrate that even with the same data, the geospatial methods selected may yield different results.

## **5.5 CONCLUDING REMARKS ON GIS METHODS FOR MISALIGNED VARIABLE QUANTIFICATION IN ENVIRONMENTAL HEALTH SCIENCES**

This dissertation is comprised of three case studies in which we utilized methods to account for spatiotemporal misalignment: (1) a study of COVID-19 where population-level covariates were misaligned; (2) a study of the attribution of daily green space exposure for physically-active regions where activity, location, and green space data were misaligned; and (3) a study of the association between heat exposure and physical activity in which temperature, green space, and participant-level covariates were misaligned. In this dissertation, we aimed to develop methods to account for misalignment so that these multiple data sources can be utilized in combination to assess exposure and health outcomes. The methods we used not only allow for comparison of many approaches but also demonstrate exposure attribution protocols that may improve computer-processing hours, analyst hours, and costs of similar research by utilizing open-source technologies, spatial data science, and cloud computing.

Data has become easier to collect and process due to advancements in hardware and software, leading to new opportunities in the field of public health and exposure modeling. Utilizing the best and newest spatial datasets, however, leads to questions of spatiotemporal misalignment

when combining those from multiple sources. We have demonstrated the importance not only of accounting for spatiotemporal misalignment but to carefully choose between geospatial methods available, as in many cases this choice can impact study results and conclusions. We hope that the methods we utilized and the results we found may help guide future researchers on best practices for exposure attribution using activity and location information.

## 5.6 REFERENCES FOR CHAPTER 5

- Abel, M., Hannon, J., Mullineaux, D., Beighle, A., 2011. Determination of step rate thresholds corresponding to physical activity intensity classifications in adults. *J. Phys. Act. Heal.* 8, 45–51. <https://doi.org/10.1123/JPAH.8.1.45>
- Actigraph Corp, 2019. What's the difference among the Cut Points available in ActiLife? [WWW Document]. URL <https://actigraphcorp.my.site.com/support/s/article/What-s-the-difference-among-the-Cut-Points-available-in-ActiLife> (accessed 5.2.22).
- Ailshire, J., García, C., 2018. Unequal places: The impacts of socioeconomic and race/ethnic differences in neighborhoods. *Generations* 42.
- Alaimo, P., Loro, D., Mingione, M., Lipsitt, J., Jerrett, M., Banerjee, S., 2021. Bayesian Hierarchical Modeling and Analysis for Physical Activity Trajectories Using Actigraph Data. *arxiv Pre-Print*, 1–36. <https://doi.org/https://arxiv.org/abs/2101.01624>
- Almanza, E., Jerrett, M., Dunton, G., Seto, E., Ann Pentz, M., 2012. A study of community design, greenness, and physical activity in children using satellite, GPS and accelerometer data. *Health Place* 18, 46–54. <https://doi.org/10.1016/j.healthplace.2011.09.003>
- Almaraz, M., Bai, E., Wang, C., Trousdell, J., Conley, S., Faloona, I., Houlton, B.Z., 2018. Agriculture is a major source of NO<sub>x</sub> pollution in California. *Sci. Adv.* 4. <https://doi.org/10.1126/sciadv.aao3477>
- Alvarado, K., Hewitt, A., 2017. Bruin Bike Share now reaches from Santa Monica to West Hollywood | UCLA [WWW Document]. UCLA Newsroom. URL <https://newsroom.ucla.edu/stories/bruin-bike-share-now-reaches-from-santa-monica-to-west-hollywood> (accessed 5.2.22).
- Amoly, E., Dadvand, P., Fornas, J., López-Vicente, M., Basagaña, X., Julvez, J., Alvarez-Pedrerol, M., Nieuwenhuijsen, M.J., Sunyer, J., 2015. Green and blue spaces and behavioral development in barcelona schoolchildren: The BREATHE project. *Environ. Health Perspect.*

122. <https://doi.org/10.1289/ehp.1408215>

Anderson, T.K., 2009. Kernel density estimation and K-means clustering to profile road accident hotspots. *Accid. Anal. Prev.* 41. <https://doi.org/10.1016/j.aap.2008.12.014>

Apte, J.S., Messier, K.P., Gani, S., Brauer, M., Kirchstetter, T.W., Lunden, M.M., Marshall, J.D., Portier, C.J., Vermeulen, R.C.H., Hamburg, S.P., 2017. High-Resolution Air Pollution Mapping with Google Street View Cars: Exploiting Big Data. *Environ. Sci. Technol.* 51. <https://doi.org/10.1021/acs.est.7b00891>

Auchincloss, A.H., Diez Roux, A. V, Mujahid, M.S., Shen, M., Bertoni, A.G., Carnethon, M.R., 2009. Neighborhood resources for physical activity and healthy foods and incidence of type 2 diabetes mellitus: the Multi-Ethnic study of Atherosclerosis. *Arch. Intern. Med.* 169, 1698–1704. <https://doi.org/10.1001/archinternmed.2009.302>

Avila-Palencia, I., Int Panis, L., Dons, E., Gaupp-Berghausen, M., Raser, E., Götschi, T., Gerike, R., Brand, C., de Nazelle, A., Orjuela, J.P., Anaya-Boig, E., Stigell, E., Kahlmeier, S., Iacorossi, F., Nieuwenhuijsen, M.J., 2018. The effects of transport mode use on self-perceived health, mental health, and social contact measures: A cross-sectional and longitudinal study. *Environ. Int.* 120. <https://doi.org/10.1016/j.envint.2018.08.002>

Aybar, C., Wu, Q., Bautista, L., Yali, R., Barja, A., 2020. rgee: An R package for interacting with Google Earth Engine. *J. Open Source Softw.*

Bai, L., Chen, H., Hatzopoulou, M., Jerrett, M., Kwong, J.C., Burnett, R.T., Van Donkelaar, A., Copes, R., Martin, R. V., Van Ryswyk, K., Lu, H., Kopp, A., Weichenthal, S., 2018. Exposure to ambient ultrafine particles and nitrogen dioxide and incident hypertension and diabetes. *Epidemiology* 29. <https://doi.org/10.1097/EDE.0000000000000798>

Bakrania, K., Edwardson, C.L., Khunti, K., Henson, J., Stamatakis, E., Hamer, M., Davies, M.J., Yates, T., 2017. Associations of objectively measured moderate-to-vigorous-intensity physical activity and sedentary time with all-cause mortality in a population of adults at high

risk of type 2 diabetes mellitus. *Prev. Med. Reports* 5, 285–288.  
<https://doi.org/10.1016/j.pmedr.2017.01.013>

Banerjee, A., Pasea, L., Harris, S., Gonzalez-Izquierdo, A., Torralbo, A., Shallcross, L., Noursadeghi, M., Pillay, D., Sebire, N., Holmes, C., Pagel, C., Wong, W.K., Langenberg, C., Williams, B., Denaxas, S., Hemingway, H., 2020. Estimating excess 1-year mortality associated with the COVID-19 pandemic according to underlying conditions and age: a population-based cohort study. *Lancet* 395. [https://doi.org/10.1016/S0140-6736\(20\)30854-0](https://doi.org/10.1016/S0140-6736(20)30854-0)

Bates, D., Mächler, M., Bolker, B., Walker, S., 2015. Fitting Linear Mixed-Effects Models Using {lme4}. *J. Stat. Softw.* 67, 1–48. <https://doi.org/10.18637/jss.v067.i01>

Beekhuizen, J., Kromhout, H., Huss, A., Vermeulen, R., 2013. Performance of GPS-devices for environmental exposure assessment. *J. Expo. Sci. Environ. Epidemiol.* 23. <https://doi.org/10.1038/jes.2012.81>

Beelen, R., Hoek, G., van den Brandt, P.A., Goldbohm, R.A., Fischer, P., Schouten, L.J., Jerrett, M., Hughes, E., Armstrong, B., Brunekreef, B., 2008. Long-term effects of traffic-related air pollution on mortality in a Dutch cohort (NLCS-AIR study). *Environ. Health Perspect.* 116, 196–202. <https://doi.org/10.1289/ehp.10767>

Benzinger, T.H., 1959. ON PHYSICAL HEAT REGULATION AND THE SENSE OF TEMPERATURE IN MAN. *Proc. Natl. Acad. Sci.* 45, 645. <https://doi.org/10.1073/pnas.45.4.645>

Berg, K., Romer Present, P., Richardson, K., 2021. Long-term air pollution and other risk factors associated with COVID-19 at the census tract level in Colorado. *Environ. Pollut.* 287. [https://doi.org/10.1016/J.ENVPOL.2021.117584/LONG\\_TERM\\_AIR\\_POLLUTION\\_AND\\_OTHER\\_RISK\\_FACTORS\\_ASSOCIATED\\_WITH\\_COVID\\_19\\_AT\\_THE\\_CENSUS\\_TRACT\\_LEVEL\\_IN\\_COLORADO.PDF](https://doi.org/10.1016/J.ENVPOL.2021.117584/LONG_TERM_AIR_POLLUTION_AND_OTHER_RISK_FACTORS_ASSOCIATED_WITH_COVID_19_AT_THE_CENSUS_TRACT_LEVEL_IN_COLORADO.PDF)

- Bergman, A., Sella, Y., Agre, P., Casadevall, A., 2020. Oscillations in U.S. COVID-19 Incidence and Mortality Data Reflect Diagnostic and Reporting Factors. *mSystems* 5. <https://doi.org/10.1128/msystems.00544-20>
- Bialek, S., Bowen, V., Chow, N., Curns, A., Gierke, R., Hall, A., Hughes, M., Pilishvili, T., Ritchey, M., Roguski, K., Silk, B., Skoff, T., Sundararaman, P., Ussery, E., Vasser, M., Whitham, H., Wen, J., 2020. Geographic Differences in COVID-19 Cases, Deaths, and Incidence — United States, February 12–April 7, 2020. *MMWR. Morb. Mortal. Wkly. Rep.* 69, 465–471. <https://doi.org/10.15585/mmwr.mm6915e4>
- Bivand, R., Keitt, T., Rowlingson, B., 2021. rgdal: Bindings for the “Geospatial” Data Abstraction Library.
- Boakye, K.A., Amram, O., Schuna, J.M., Duncan, G.E., Hystad, P., 2021. GPS-based built environment measures associated with adult physical activity. *Heal. Place* 70. <https://doi.org/10.1016/j.healthplace.2021.102602>
- Bowler, D.E., Buyung-Ali, L., Knight, T.M., Pullin, A.S., 2010a. Urban greening to cool towns and cities: A systematic review of the empirical evidence. *Landsc. Urban Plan.* <https://doi.org/10.1016/j.landurbplan.2010.05.006>
- Bowler, D.E., Buyung-Ali, L.M., Knight, T.M., Pullin, A.S., 2010b. A systematic review of evidence for the added benefits to health of exposure to natural environments. *BMC Public Health* 10. <https://doi.org/10.1186/1471-2458-10-456>
- Brandt, E.B., Beck, A.F., Mersha, T.B., 2020. Air pollution, racial disparities, and COVID-19 mortality. *J. Allergy Clin. Immunol.* <https://doi.org/10.1016/j.jaci.2020.04.035>
- Branion-Calles, M., Götschi, T., Nelson, T., Anaya-Boig, E., Avila-Palencia, I., Castro, A., Cole-Hunter, T., de Nazelle, A., Dons, E., Gaupp-Berghausen, M., Gerike, R., Int Panis, L., Kahlmeier, S., Nieuwenhuijsen, M., Rojas-Rueda, D., Winters, M., 2020. Cyclist crash rates and risk factors in a prospective cohort in seven European cities. *Accid. Anal. Prev.* 141.

<https://doi.org/10.1016/j.aap.2020.105540>

- Brooke Anderson, G., Bell, M.L., Peng, R.D., 2013. Methods to calculate the heat index as an exposure metric in environmental health research. *Environ. Health Perspect.* <https://doi.org/10.1289/ehp.1206273>
- Bui, R., Buliung, R.N., Remmel, T.K., 2012. aspace: A collection of functions for estimating centrographic statistics and computational geometries for spatial point patterns.
- Burr, J.A., Mutchler, J.E., Gerst, K., 2010. Patterns of residential crowding among Hispanics in later life: immigration, assimilation, and housing market factors. *J. Gerontol. B. Psychol. Sci. Soc. Sci.* 65, 772–782. <https://doi.org/10.1093/geronb/gbq069>
- CADPH, 2020. CDC Confirms Possible First Instance of COVID-19 Community Transmission in California [WWW Document]. URL <https://www.cdph.ca.gov/Programs/OPA/Pages/NR20-006.aspx> (accessed 11.10.20).
- Calenge, C., 2006. The package adehabitat for the R software: tool for the analysis of space and habitat use by animals. *Ecol. Modell.* 197, 1035.
- Caltrans, 2020. Highway Performance Monitoring System (HPMS) Data [WWW Document]. URL <https://dot.ca.gov/programs/research-innovation-system-information/highway-performance-monitoring-system> (accessed 5.2.22).
- Campello, R.J.G.B., Moulavi, D., Sander, J., 2013. Density-Based Clustering Based on Hierarchical Density Estimates.
- Case, M.A., Burwick, H.A., Volpp, K.G., Patel, M.S., 2015. Accuracy of Smartphone Applications and Wearable Devices for Tracking Physical Activity Data. *JAMA* 313, 625–626. <https://doi.org/10.1001/JAMA.2014.17841>
- Centers for Disease Control and Prevention, 2020. COVIDView: A Weekly Surveillance Summary of US. COVID-19 Activity [WWW Document]. URL <https://www.cdc.gov/coronavirus/2019-ncov/covid-data/pdf/covidview-07-24-2020.pdf> (accessed 10.30.20).

- Centers for Disease Control and Prevention, 2019. 500 Cities Project: Local data for better health | Home page | CDC [WWW Document]. URL <https://www.cdc.gov/500cities/> (accessed 11.10.20).
- Chaix, B., Méline, J., Duncan, S., Merrien, C., Karusisi, N., Perchoux, C., Lewin, A., Labadi, K., Kestens, Y., 2013. GPS tracking in neighborhood and health studies: A step forward for environmental exposure assessment, a step backward for causal inference? *Health Place* 21, 46–51. <https://doi.org/10.1016/j.healthplace.2013.01.003>
- Chan, C.B., Ryan, D.A.J., Tudor-Locke, C., 2006. Relationship between objective measures of physical activity and weather: A longitudinal study. *Int. J. Behav. Nutr. Phys. Act.* 3, 1–9. <https://doi.org/10.1186/1479-5868-3-21/FIGURES/2>
- Charreire, H., Casey, R., Salze, P., Simon, C., Chaix, B., Banos, A., Badariotti, D., Weber, C., Oppert, J.M., 2010. Measuring the food environment using geographical information systems: A methodological review. *Public Health Nutr.* <https://doi.org/10.1017/S1368980010000753>
- Chen, Y.-C., Dobra, A., 2017. Measuring Human Activity Spaces With Density Ranking Based on GPS Data 1–28.
- Chew, V., 1966. Confidence, Prediction, and Tolerance Regions for the Multivariate Normal Distribution. *J. Am. Stat. Assoc.* 61. <https://doi.org/10.1080/01621459.1966.10480892>
- Ciencewicki, J., Jaspers, I., 2007. Air Pollution and Respiratory Viral Infection. *Inhal. Toxicol.* 19, 1135–1146. <https://doi.org/10.1080/08958370701665434>
- Clark, L.P., Millet, D.B., Marshall, J.D., 2014. National patterns in environmental injustice and inequality: Outdoor NO<sub>2</sub> air pollution in the United States. *PLoS One* 9. <https://doi.org/10.1371/journal.pone.0094431>
- Coker, E.S., Cavalli, L., Fabrizi, E., Guastella, G., Lippo, E., Parisi, M.L., Pontarollo, N., Rizzati, M., Varacca, A., Vergalli, S., 2020. The Effects of Air Pollution on COVID-19 Related

- Mortality in Northern Italy. *Environ. Resour. Econ.* 76. <https://doi.org/10.1007/s10640-020-00486-1>
- Collaco, J.M., Morrow, M., Rice, J.L., McGrath-Morrow, S.A., 2020. Impact of road proximity on infants and children with bronchopulmonary dysplasia. *Pediatr. Pulmonol.* 55. <https://doi.org/10.1002/ppul.24594>
- Commodore-Mensah, Y., Selvin, E., Aboagye, J., Turkson-Ocran, R.A., Li, X., Himmelfarb, C.D., Ahima, R.S., Cooper, L.A., 2018. Hypertension, overweight/obesity, and diabetes among immigrants in the United States: An analysis of the 2010-2016 National Health Interview Survey. *BMC Public Health.* <https://doi.org/10.1186/s12889-018-5683-3>
- Cui, Y., Zhang, Z.-F., Froines, J., Zhao, J., Wang, H., Yu, S.-Z., Detels, R., 2003. Air pollution and case fatality of SARS in the People's Republic of China: an ecologic study. *Environ. Heal.* 2. <https://doi.org/10.1186/1476-069x-2-15>
- Dadvand, P., de Nazelle, A., Figueras, F., Basagaña, X., Su, J., Amoly, E., Jerrett, M., Vrijheid, M., Sunyer, J., Nieuwenhuijsen, M.J., 2012a. Green space, health inequality and pregnancy. *Environ. Int.* 40. <https://doi.org/10.1016/j.envint.2011.07.004>
- Dadvand, P., de Nazelle, A., Triguero-Mas, M., Schembari, A., Cirach, M., Amoly, E., Figueras, F., Basagaña, X., Ostro, B., Nieuwenhuijsen, M., 2012b. Surrounding greenness and exposure to air pollution during pregnancy: An analysis of personal monitoring data. *Environ. Health Perspect.* 120. <https://doi.org/10.1289/ehp.1104609>
- Dadvand, P., Villanueva, C.M., Font-Ribera, L., Martinez, D., Basagaña, X., Belmonte, J., Vrijheid, M., Gražulevičienė, R., Kogevinas, M., Nieuwenhuijsen, M.J., 2015. Risks and benefits of green spaces for children: A cross-sectional study of associations with sedentary behavior, obesity, asthma, and allergy. *Environ. Health Perspect.* 122. <https://doi.org/10.1289/ehp.1308038>
- Dales, R., Wheeler, A., Mahmud, M., Frescura, A.M., Smith-Doiron, M., Nethery, E., Liu, L., 2008.

- The Influence of Living Near Roadways on Spirometry and Exhaled Nitric Oxide in Elementary Schoolchildren. *Environ. Health Perspect.* 116, 1423–1427. <https://doi.org/10.1289/ehp.10943>
- Dance, J., 2018. Moves is shutting down. Here are alternatives. [WWW Document]. Medium.com. URL <https://joshdance.medium.com/moves-is-shutting-down-here-are-alternatives-8341aae695b4> (accessed 5.2.22).
- de Nazelle, A., Smeds, E., Anaya Boig, E., Wang, C., Sanchez, J., Dons, E., Kahlmeier, S., Iacorossi, F., Wegener, S., Nieuwenhuijsen, M., Rojas-Rueda, D., Avila-Palencia, I., Götschi, T., 2017. A Comparison between Literature Findings and Stakeholder Perspectives on Active Travel Promotion. *J. Transp. Heal.* 5. <https://doi.org/10.1016/j.jth.2017.05.216>
- Deeks, J.J., Dinnes, J., D'Amico, R., Sowden, A.J., Sakarovitch, C., Song, F., Petticrew, M., Altman, D.G., 2003. Evaluating non-randomised intervention studies. *Health Technol. Assess. (Rockv)*. <https://doi.org/10.3310/hta7270>
- Dempsey, D., Kelliher, F., 2018. *Industry Trends in Cloud Computing*. Springer International Publishing, Cham.
- Diaz, F., Freato, R., 2018. *Cloud Data Design, Orchestration, and Management Using Microsoft Azure: Master and Design a Solution Leveraging the Azure Data Platform*. Apress.
- Divens, L.L., Chatmon, B.N., 2019. Cardiovascular Disease Management in Minority Women: Special Considerations. *Crit. Care Nurs. Clin. North Am.* <https://doi.org/10.1016/j.cnc.2018.11.004>
- Dixon, J., Tredoux, C., Davies, G., Huck, J., Hocking, B., Sturgeon, B., Whyatt, D., Jarman, N., Bryan, D., 2020. Parallel lives: Intergroup contact, threat, and the segregation of everyday activity spaces. *J. Pers. Soc. Psychol.* 118. <https://doi.org/10.1037/pspi0000191>
- Dohrn, I.-M., Sjöström, M., Kwak, L., Oja, P., Hagströmer, M., 2018. Accelerometer-measured sedentary time and physical activity—A 15 year follow-up of mortality in a Swedish

- population-based cohort. *J. Sci. Med. Sport* 21, 702–707.  
<https://doi.org/10.1016/j.jsams.2017.10.035>
- Donaire-Gonzalez, D., de Nazelle, A., Seto, E., Mendez, M., Nieuwenhuijsen, M.J., Jerrett, M., 2013. Comparison of Physical Activity Measures Using Mobile Phone-Based CalFit and Actigraph. *J. Med. Internet Res.* 15, e111. <https://doi.org/10.2196/jmir.2470>
- Dong, C., MacDonald, G., Okin, G.S., Gillespie, T.W., 2019. Quantifying drought sensitivity of mediterranean climate vegetation to recent warming: A case study in Southern California. *Remote Sens.* 11. <https://doi.org/10.3390/rs11242902>
- Dons, E., Götschi, T., Nieuwenhuijsen, M., De Nazelle, A., Anaya, E., Avila-Palencia, I., Brand, C., Cole-Hunter, T., Gaupp-Berghausen, M., Kahlmeier, S., Laeremans, M., Mueller, N., Orjuela, J.P., Raser, E., Rojas-Rueda, D., Standaert, A., Stigell, E., Uhlmann, T., Gerike, R., Int Panis, L., 2015. Physical Activity through Sustainable Transport Approaches (PASTA): protocol for a multi-centre, longitudinal study Energy balance-related behaviours. *BMC Public Health* 15. <https://doi.org/10.1186/s12889-015-2453-3>
- Du, Y., Lv, Y., Zha, W., Zhou, N., Hong, X., 2020. Association of Body mass index (BMI) with Critical COVID-19 and in-hospital Mortality: a dose-response meta-analysis. *Metabolism.* 154373. <https://doi.org/10.1016/j.metabol.2020.154373>
- Dunton, G.F., Almanza, E., Jerrett, M., Wolch, J., Pentz, M.A., 2014. Neighborhood park use by children: Use of accelerometry and global positioning systems. *Am. J. Prev. Med.* 46. <https://doi.org/10.1016/j.amepre.2013.10.009>
- Dzhambov, A., Hartig, T., Markevych, I., Tilov, B., Dimitrova, D., 2018. Urban residential greenspace and mental health in youth: Different approaches to testing multiple pathways yield different conclusions. *Environ. Res.* 160. <https://doi.org/10.1016/j.envres.2017.09.015>
- Eddelbuettel, D., 2018. CRAN Task View: High-Performance and Parallel Computing with R.
- Erdogan, S., Yilmaz, I., Baybura, T., Gullu, M., 2008. Geographical information systems aided

- traffic accident analysis system case study: city of Afyonkarahisar. *Accid. Anal. Prev.* 40.  
<https://doi.org/10.1016/j.aap.2007.05.004>
- ESRI, 2020. ArcGIS Desktop: Release 10. Redlands, CA: Environmental Systems Research Institute.
- Evenson, K.R., Catellier, D.J., Gill, K., Ondrak, K.S., McMurray, R.G., 2008. Calibration of two objective measures of physical activity for children. *J. Sports Sci.* 26.  
<https://doi.org/10.1080/02640410802334196>
- Evenson, K.R., Goto, M.M., Furberg, R.D., 2015. Systematic review of the validity and reliability of consumer-wearable activity trackers. *Int. J. Behav. Nutr. Phys. Act.* 12.  
<https://doi.org/10.1186/s12966-015-0314-1>
- Federal Highway Administration, 2019. FHWA Office of Highway Policy Information Fact Sheet: The 25 Most Traveled Route Locations by Annual Daily Traffic (AADT) [WWW Document]. URL <https://www.fhwa.dot.gov/policyinformation/tables/02.cfm> (accessed 5.2.22).
- Federico, F., Rauser, C., Gold, M., 2017. 2017 Sustainable LA Grand Challenge Environmental Report Card for Los Angeles County Energy and Air Quality [WWW Document]. Univ. Calif. Escholarsh. URL <https://escholarship.org/uc/item/6xj45381> (accessed 5.2.22).
- Franklin, B.A., Brook, R., Arden Pope, C. 3rd, 2015. Air pollution and cardiovascular disease. *Curr. Probl. Cardiol.* 40, 207–238. <https://doi.org/10.1016/j.cpcardiol.2015.01.003>
- Freedson, P., Melanson, E., Sirard, J., 1998. Calibration of the Computer Science and Applications, Inc. accelerometer. *Med. Sci. Sport. Exerc.* 30.
- Fuertes, E., Markevych, I., Bowatte, G., Gruzieva, O., Gehring, U., Becker, A., Berdel, D., von Berg, A., Bergström, A., Brauer, M., Brunekreef, B., Brüske, I., Carlsten, C., Chan-Yeung, M., Dharmage, S.C., Hoffmann, B., Klümper, C., Koppelman, G.H., Kozyrskyj, A., Korek, M., Kull, I., Lodge, C., Lowe, A., MacIntyre, E., Pershagen, G., Standl, M., Sugiri, D., Wijga, A., Heinrich, J., 2016. Residential greenness is differentially associated with childhood allergic

- rhinitis and aeroallergen sensitization in seven birth cohorts. *Allergy Eur. J. Allergy Clin. Immunol.* 71. <https://doi.org/10.1111/all.12915>
- Gaither, C.J., Afrin, S., Garcia-Menendez, F., Odman, M.T., Huang, R., Goodrick, S., da Silva, A.R., 2019. African american exposure to prescribed fire smoke in Georgia, USA. *Int. J. Environ. Res. Public Health* 16. <https://doi.org/10.3390/ijerph16173079>
- Garcetti, E., 2019. L.A.'s Green New Deal: Sustainable City Plan 2019. Los Angeles.
- Gascon, M., Triguero-Mas, M., Martínez, D., Dadvand, P., Rojas-Rueda, D., Plasència, A., Nieuwenhuijsen, M.J., 2016. Residential green spaces and mortality: A systematic review. *Environ. Int.* 86, 60–67. <https://doi.org/10.1016/j.envint.2015.10.013>
- Gastin, P.B., Cayzer, C., Dwyer, D., Robertson, S., 2018. Validity of the ActiGraph GT3X+ and BodyMedia SenseWear Armband to estimate energy expenditure during physical activity and sport. *J. Sci. Med. Sport* 21, 291–295. <https://doi.org/10.1016/j.jsams.2017.07.022>
- Gerike, R., De Nazelle, A., Nieuwenhuijsen, M., Panis, L.I., Anaya, E., Avila-Palencia, I., Boschetti, F., Brand, C., Cole-Hunter, T., Dons, E., Eriksson, U., Gaupp-Berghausen, M., Kahlmeier, S., Laeremans, M., Mueller, N., Orjuela, J.P., Racioppi, F., Raser, E., Rojas-Rueda, D., Schweizer, C., Standaert, A., Uhlmann, T., Wegener, S., Götschi, T., 2016. Physical Activity through Sustainable Transport Approaches (PASTA): A study protocol for a multicentre project. *BMJ Open* 6. <https://doi.org/10.1136/bmjopen-2015-009924>
- Gething, P.W., Noor, A.M., Gikandi, P.W., Ogara, E.A.A., Hay, S.I., Nixon, M.S., Snow, R.W., Atkinson, P.M., 2006. Improving imperfect data from health management information systems in Africa using space-time geostatistics. *PLoS Med.* 3. <https://doi.org/10.1371/journal.pmed.0030271>
- Glaeser, E.L., Kominers, S.D., Luca, M., Naik, N., 2018. BIG DATA AND BIG CITIES: THE PROMISES AND LIMITATIONS OF IMPROVED MEASURES OF URBAN LIFE. *Econ. Inq.* 56, 114–137. <https://doi.org/10.1111/ecin.12364>

- GlobalSat WorldCom Corporation, 2022a. BT-335 Bluetooth Data Logger User Manual [WWW Document]. URL <https://www.gpscentral.ca/products/usglobalsat/bt-335-user-manual.pdf> (accessed 5.9.22).
- GlobalSat WorldCom Corporation, 2022b. DG-500 GPS Data Logger Quick Start Guide [WWW Document]. URL [https://www.globalsat.com.tw/ftp/download/DG-500\\_QSG\\_ENG\\_V1.3\\_20170105.pdf](https://www.globalsat.com.tw/ftp/download/DG-500_QSG_ENG_V1.3_20170105.pdf) (accessed 5.9.22).
- Gong, L., Sato, H., Yamamoto, T., Miwa, T., Morikawa, T., 2015. Identification of activity stop locations in GPS trajectories by density-based clustering method combined with support vector machines. *J. Mod. Transp.* 23. <https://doi.org/10.1007/s40534-015-0079-x>
- Google Inc., 2022. Reducer Overview | Google Earth Engine [WWW Document]. URL [https://developers.google.com/earth-engine/guides/reducers\\_intro](https://developers.google.com/earth-engine/guides/reducers_intro) (accessed 5.6.22).
- Götschi, Thomas, de Nazelle, Audrey, Brand, Christian, Gerike, Regine, Alasya, B., Anaya, E., Avila-Palencia, I., Banister, D., Bartana, I., Benvenuti, F., Boschetti, F., Brand, C., Buekers, J., Carniel, L., Carrasco Turigas, G., Castro, A., Cianfano, M., Clark, A., Cole-Hunter, T., Copley, V., De Boever, P., de Nazelle, A., Dimajo, C., Dons, E., Duran, M., Eriksson, U., Franzen, H., Gaupp-Berghausen, M., Gerike, R., Girmenia, R., Götschi, T., Hartmann, F., Iacorossi, F., Int Panis, L., Kahlmeier, S., Khreis, H., Laeremans, M., Martinez, T., Meschik, M., Michelle, P., Muehlmann, P., Mueller, N., Nieuwenhuijsen, M., Nilsson, A., Nussio, F., Orjuela Mendoza, J.P., Pisanti, S., Porcel, J., Racioppi, F., Raser, E., Riegler, S., Robrecht, H., Rojas Rueda, D., Rothballer, C., Sanchez, J., Schaller, A., Schuthof, R., Schweizer, C., Sillero, A., Smidfeltrosqvist, L., Spezzano, G., Standaert, A., Stigell, E., Surace, M., Uhlmann, T., Vancluysen, K., Wegener, S., Wennberg, H., Willis, G., Witzell, J., Zeuschner, V., 2017. Towards a Comprehensive Conceptual Framework of Active Travel Behavior: a Review and Synthesis of Published Frameworks. *Curr. Environ. Heal. reports.* <https://doi.org/10.1007/s40572-017-0149-9>

- Graham, M., Shelton, T., 2013. Geography and the future of big data, big data and the future of geography. *Dialogues Hum. Geogr.* 3, 255–261. <https://doi.org/10.1177/2043820613513121>
- Gupta, A., Bherwani, H., Gautam, S., Anjum, S., Musugu, K., Kumar, N., Anshul, A., Kumar, R., 2021. Air pollution aggravating COVID-19 lethality? Exploration in Asian cities using statistical models. *Environ. Dev. Sustain.* 23. <https://doi.org/10.1007/s10668-020-00878-9>
- Hahsler, M., Piekenbrock, M., 2021. dbscan: Density Based Clustering of Applications with Noise (DBSCAN) and Related Algorithms.
- Hamada, S., Ohta, T., 2010. Seasonal variations in the cooling effect of urban green areas on surrounding urban areas. *Urban For. Urban Green.* 9, 15–24. <https://doi.org/10.1016/J.UFUG.2009.10.002>
- Harris, J.E., 2020. Understanding the Los Angeles County coronavirus epidemic: The critical role of intrahousehold transmission. *medRxiv.* <https://doi.org/10.1101/2020.10.11.20211045>
- Hayhoe, K., Cayan, D., Field, C.B., Frumhoff, P.C., Maurer, E.P., Miller, N.L., Moser, S.C., Schneider, S.H., Cahill, K.N., Cleland, E.E., Dale, L., Drapek, R., Hanemann, R.M., Kalkstein, L.S., Lenihan, J., Lunch, C.K., Neilson, R.P., Sheridan, S.C., Verville, J.H., 2004. Emissions pathways, climate change, and impacts on California. *Proc. Natl. Acad. Sci. U. S. A.* 101, 12422–12427. [https://doi.org/10.1073/PNAS.0404500101/SUPPL\\_FILE/04500FIG17.JPG](https://doi.org/10.1073/PNAS.0404500101/SUPPL_FILE/04500FIG17.JPG)
- Heinzerling, A., Stuckey, M.J., Scheuer, T., Xu, K., Perkins, K.M., Resseger, H., Magill, S., Verani, J.R., Jain, S., Acosta, M., Epton, E., 2020. Transmission of COVID-19 to Health Care Personnel During Exposures to a Hospitalized Patient — Solano County, California, February 2020. *MMWR. Morb. Mortal. Wkly. Rep.* 69. <https://doi.org/10.15585/mmwr.mm6915e5>
- Hekler, E.B., Buman, M.P., Grieco, L., Rosenberger, M., Winter, S.J., Haskell, W., King, A.C., 2015. Validation of Physical Activity Tracking via Android Smartphones Compared to

- ActiGraph Accelerometer: Laboratory-Based and Free-Living Validation Studies. *JMIR mHealth uHealth* 3, e36. <https://doi.org/10.2196/mhealth.3505>
- Higgs, G., Fry, R., Langford, M., 2012. Investigating the Implications of Using Alternative GIS-Based Techniques to Measure Accessibility to Green Space. *Environ. Plan. B Plan. Des.* 39, 326–343. <https://doi.org/10.1068/b37130>
- Hijmans, R.J., 2021. raster: Geographic Data Analysis and Modeling.
- Hirsch, Jana A, Winters, M., Clarke, P., McKay, H., 2014. Generating GPS activity spaces that shed light upon the mobility habits of older adults : a descriptive analysis 1–14.
- Hirsch, Jana A., Winters, M., Clarke, P., McKay, H., 2014. Generating GPS activity spaces that shed light upon the mobility habits of older adults: A descriptive analysis. *Int. J. Health Geogr.* 13, 1–14. <https://doi.org/10.1186/1476-072X-13-51>
- Ho, J.Y., Zijlema, W.L., Triguero-Mas, M., Donaire-Gonzalez, D., Valentín, A., Ballester, J., Chan, E.Y.Y., Goggins, W.B., Mo, P.K.H., Kruize, H., van den Berg, M., Gražulevičienė, R., Gidlow, C.J., Jerrett, M., Seto, E.Y.W., Barrera-Gómez, J., Nieuwenhuijsen, M.J., 2021. Does surrounding greenness moderate the relationship between apparent temperature and physical activity? Findings from the PHENOTYPE project. *Environ. Res.* 197, 110992. <https://doi.org/10.1016/J.ENVRES.2021.110992>
- Höchsmann, C., Knaier, R., Eymann, J., Hintermann, J., Infanger, D., Schmidt-Trucksäss, A., 2018. Validity of activity trackers, smartphones, and phone applications to measure steps in various walking conditions. *Scand. J. Med. Sci. Sport.* 28. <https://doi.org/10.1111/sms.13074>
- Holliday, K.M., Howard, A.G., Emch, M., Rodríguez, D.A., Evenson, K.R., 2017. Are buffers around home representative of physical activity spaces among adults? *Heal. Place* 45, 181–188. <https://doi.org/10.1016/j.healthplace.2017.03.013>
- Holt, J.B., Lo, C.P., Hodler, T.W., 2013. Dasymetric Estimation of Population Density and Areal Interpolation of Census Data. <http://dx.doi.org/10.1559/1523040041649407> 31, 103–121.

<https://doi.org/10.1559/1523040041649407>

Huang, G., Blangiardo, M., Brown, P.E., Pirani, M., 2021. Long-term exposure to air pollution and COVID-19 incidence: A multi-country study. *Spat. Spatiotemporal. Epidemiol.* 39, 100443.

<https://doi.org/10.1016/J.SSTE.2021.100443>

Humpel, N., 2002. Environmental factors associated with adults' participation in physical activity: A review. *Am. J. Prev. Med.* 22, 188–199. [https://doi.org/10.1016/S0749-3797\(01\)00426-3](https://doi.org/10.1016/S0749-3797(01)00426-3)

Imboden, M.T., Nelson, M.B., Kaminsky, L.A., Montoye, A.H., 2018. Comparison of four Fitbit and Jawbone activity monitors with a research-grade ActiGraph accelerometer for estimating physical activity and energy expenditure. *Br. J. Sports Med.* 52, 844–850.

<https://doi.org/10.1136/bjsports-2016-096990>

Jacobs, A., 2009. The pathologies of big data. *Queue* 7, 10–19.

<https://doi.org/10.1145/1563821.1563874>

Jerrett, M., Almanza, E., Davies, M., Wolch, J., Dunton, G., Spruitj-Metz, D., Ann Pentz, M., 2013a. Smart growth community design and physical activity in children. *Am. J. Prev. Med.* 45, 386–392. <https://doi.org/10.1016/j.amepre.2013.05.010>

Jerrett, M., Almanza, E., Davies, M., Wolch, J., Dunton, G., Spruitj-Metz, D., Pentz, M.A., 2013b. Smart growth community design and physical activity in children. *Am. J. Prev. Med.* 45, 386–392. <https://doi.org/10.1016/j.amepre.2013.05.010>

Jerrett, M., Arain, A., Kanaroglou, P., Beckerman, B., Potoglou, D., Sahuvaroglu, T., Morrison, J., Giovis, C., 2005a. A review and evaluation of intraurban air pollution exposure models. *J. Expo. Anal. Environ. Epidemiol.* <https://doi.org/10.1038/sj.jea.7500388>

Jerrett, M., Burnett, R.T., Ma, R., Pope, C.A., Krewski, D., Newbold, K.B., Thurston, G., Shi, Y., Finkelstein, N., Calle, E.E., Thun, M.J., 2005b. Spatial Analysis of Air Pollution and Mortality in Los Angeles. *Epidemiology* 16, 727–736. <https://doi.org/10.1097/01.ede.0000181630.15826.7d>

- Jerrett, M., Shankardass, K., Berhane, K., Gauderman, W.J., Künzli, N., Avol, E., Gilliland, F., Lurmann, F., Molitor, J.N., Molitor, J.T., Thomas, D.C., Peters, J., McConnell, R., 2008. Traffic-related air pollution and asthma onset in children: A prospective cohort study with individual exposure measurement. *Environ. Health Perspect.* 116, 1433–1438. <https://doi.org/10.1289/ehp.10968>
- Jewell, N.P., Lewnard, J.A., Jewell, B.L., 2020. Caution Warranted: Using the Institute for Health Metrics and Evaluation Model for Predicting the Course of the COVID-19 Pandemic. *Ann. Intern. Med.* <https://doi.org/10.7326/M20-1565>
- Jia, P., Xue, H., Yin, L., Stein, A., Wang, M., Wang, Y., 2019. Spatial Technologies in Obesity Research: Current Applications and Future Promise. *Trends Endocrinol. Metab.* <https://doi.org/10.1016/j.tem.2018.12.003>
- Kaisler, S., Armour, F., Espinosa, J.A., Money, W., 2013. Big Data: Issues and Challenges Moving Forward, in: 2013 46th Hawaii International Conference on System Sciences. IEEE, Wailea, HI, USA, pp. 995–1004. <https://doi.org/10.1109/HICSS.2013.645>
- Kambatla, K., Kollias, G., Kumar, V., Grama, A., 2014. Trends in big data analytics. *J. Parallel Distrib. Comput.* 74, 2561–2573. <https://doi.org/10.1016/j.jpdc.2014.01.003>
- Kamel Boulos, M.N., Resch, B., Crowley, D.N., Breslin, J.G., Sohn, G., Burtner, R., Pike, W.A., Jezierski, E., Chuang, K.-Y., 2011. Crowdsourcing, citizen sensing and sensor web technologies for public and environmental health surveillance and crisis management: trends, OGC standards and application examples. *Int. J. Health Geogr.* 10, 67. <https://doi.org/10.1186/1476-072X-10-67>
- Kamruzzaman, M., Hine, J., 2012. Analysis of rural activity spaces and transport disadvantage using a multi-method approach. *Transp. Policy* 19, 105–120. <https://doi.org/10.1016/J.TRANPOL.2011.09.007>
- Keadle, S.K., Shiroma, E.J., Freedson, P.S., Lee, I.M., 2014. Impact of accelerometer data

- processing decisions on the sample size, wear time and physical activity level of a large cohort study. *BMC Public Health* 14. <https://doi.org/10.1186/1471-2458-14-1210>
- Kerr, G.H., Goldberg, D.L., Anenberg, S.C., 2021. COVID-19 pandemic reveals persistent disparities in nitrogen dioxide pollution. *Proc. Natl. Acad. Sci. U. S. A.* 118. <https://doi.org/10.1073/pnas.2022409118>
- Kerr, J., Duncan, S., Schipperjin, J., 2011. Using global positioning systems in health research: A practical approach to data collection and processing. *Am. J. Prev. Med.* 41. <https://doi.org/10.1016/j.amepre.2011.07.017>
- Klompaker, J.O., Hoek, G., Bloemsma, L.D., Gehring, U., Strak, M., Wijga, A.H., van den Brink, C., Brunekreef, B., Lebret, E., Janssen, N.A.H., 2018. Green space definition affects associations of green space with overweight and physical activity. *Environ. Res.* 160, 531–540. <https://doi.org/10.1016/J.ENVRES.2017.10.027>
- Kong, F., Yin, H., James, P., Hutyra, L.R., He, H.S., 2014. Effects of spatial pattern of greenspace on urban cooling in a large metropolitan area of eastern China. *Landsc. Urban Plan.* 128, 35–47. <https://doi.org/10.1016/j.landurbplan.2014.04.018>
- Konstantinoudis, G., Padellini, T., Bennett, J., Davies, B., Ezzati, M., Blangiardo, M., 2021. Long-term exposure to air-pollution and COVID-19 mortality in England: A hierarchical spatial analysis. *Environ. Int.* 146. <https://doi.org/10.1016/J.ENVINT.2020.106316>
- Koo, T.K., Li, M.Y., 2016. A Guideline of Selecting and Reporting Intraclass Correlation Coefficients for Reliability Research. *J. Chiropr. Med.* 15. <https://doi.org/10.1016/j.jcm.2016.02.012>
- Kooiman, T.J.M., Dontje, M.L., Sprenger, S.R., Krijnen, W.P., van der Schans, C.P., de Groot, M., 2015. Reliability and validity of ten consumer activity trackers. *BMC Sports Sci. Med. Rehabil.* 7, 24. <https://doi.org/10.1186/s13102-015-0018-5>
- Korsiak, J., Tranmer, J., Leung, M., Borghese, M.M., Aronson, K.J., 2018. Actigraph measures of

- sleep among female hospital employees working day or alternating day and night shifts. *J. Sleep Res.* 27, e12579. <https://doi.org/10.1111/jsr.12579>
- Kozawa, K.H., Fruin, S.A., Winer, A.M., 2009. Near-road air pollution impacts of goods movement in communities adjacent to the Ports of Los Angeles and Long Beach. *Atmos. Environ.* 43. <https://doi.org/10.1016/j.atmosenv.2009.02.042>
- Ku, P.W., Steptoe, A., Liao, Y., Sun, W.J., Chen, L.J., 2018. Prospective relationship between objectively measured light physical activity and depressive symptoms in later life. *Int. J. Geriatr. Psychiatry* 33. <https://doi.org/10.1002/gps.4672>
- Kulhánová, I., Morelli, X., Le Tertre, A., Loomis, D., Charbotel, B., Medina, S., Ormsby, J.N., Lepeule, J., Slama, R., Soerjomataram, I., 2018. The fraction of lung cancer incidence attributable to fine particulate air pollution in France: Impact of spatial resolution of air pollution models. *Environ. Int.* <https://doi.org/10.1016/j.envint.2018.09.055>
- Künzli, N., Kaiser, R., Medina, S., Studnicka, M., Chanel, O., Filliger, P., Herry, M., Horak, F., Puybonnieux-Textier, V., Quénel, P., Schneider, J., Seethaler, R., Vergnaud, J.C., Sommer, H., 2000. Public-health impact of outdoor and traffic-related air pollution: A European assessment. *Lancet* 356. [https://doi.org/10.1016/S0140-6736\(00\)02653-2](https://doi.org/10.1016/S0140-6736(00)02653-2)
- Kuznetsova, A., Brockhoff, P.B., Christensen, R.H.B., 2017. {lmerTest} Package: Tests in Linear Mixed Effects Models. *J. Stat. Softw.* 82, 1–26. <https://doi.org/10.18637/jss.v082.i13>
- Kwan, M.P., 2012a. How GIS can help address the uncertain geographic context problem in social science research. *Ann. GIS* 18. <https://doi.org/10.1080/19475683.2012.727867>
- Kwan, M.P., 2012b. The Uncertain Geographic Context Problem. *Ann. Assoc. Am. Geogr.* 102, 958–968. <https://doi.org/10.1080/00045608.2012.687349>
- LAC, 2014. Countywide Building Outlines (2014) | County Of Los Angeles Enterprise GIS [WWW Document]. URL <https://egis-lacounty.hub.arcgis.com/datasets/countywide-building-outlines-2014> (accessed 11.1.20).

- LACDPH, 2021. Los Angeles County COVID-19 Dashboard - Data Dashboard - About [WWW Document]. URL [http://dashboard.publichealth.lacounty.gov/covid19\\_surveillance\\_dashboard/](http://dashboard.publichealth.lacounty.gov/covid19_surveillance_dashboard/) (accessed 2.25.21).
- LACDPH, 2020. COVID-19 Locations & Demographics - LA County Department of Public Health [WWW Document]. URL <http://publichealth.lacounty.gov/media/coronavirus/locations.htm> (accessed 11.10.20).
- LACDPH, 2018. Department of Public Health - Health Assessment Unit - Data Topics 2018 [WWW Document]. URL <http://publichealth.lacounty.gov/ha/LACHSDataTopics2018.htm> (accessed 11.10.20).
- Lachowycz, K., Jones, A.P., Page, A.S., Wheeler, B.W., Cooper, A.R., 2012. What can global positioning systems tell us about the contribution of different types of urban greenspace to children's physical activity? *Health Place* 18, 586–594. <https://doi.org/10.1016/j.healthplace.2012.01.006>
- Lafortezza, R., Carrus, G., Sanesi, G., Davies, C., 2009. Benefits and well-being perceived by people visiting green spaces in periods of heat stress. *Urban For. Urban Green.* 8, 97–108. <https://doi.org/10.1016/j.ufug.2009.02.003>
- Lane, N., Miluzzo, E., Lu, H., Peebles, D., Choudhury, T., Campbell, A., 2010. A survey of mobile phone sensing. *IEEE Commun. Mag.* 48, 140–150. <https://doi.org/10.1109/MCOM.2010.5560598>
- Laurent, O., Wu, J., Li, L., Milesi, C., 2013. Green spaces and pregnancy outcomes in Southern California. *Heal. Place* 24. <https://doi.org/10.1016/j.healthplace.2013.09.016>
- Lee, J.H., Davis, A.W., Yoon, S.Y., Goulias, K.G., 2016. Activity space estimation with longitudinal observations of social media data. *Transportation (Amst).* 43. <https://doi.org/10.1007/s11116-016-9719-1>

- Lee, K., Kwan, M.P., 2018. Physical activity classification in free-living conditions using smartphone accelerometer data and exploration of predicted results. *Comput. Environ. Urban Syst.* 67. <https://doi.org/10.1016/j.compenvurbsys.2017.09.012>
- Lee, N.C., Voss, C., Frazer, A.D., Hirsch, J.A., McKay, H.A., Winters, M., 2016. Does activity space size influence physical activity levels of adolescents?-A GPS study of an urban environment. *Prev. Med. Reports* 3. <https://doi.org/10.1016/j.pmedr.2015.12.002>
- Leslie, E., Sugiyama, T., Ierodiaconou, D., Kremer, P., 2010. Perceived and objectively measured greenness of neighbourhoods: Are they measuring the same thing? *Landsc. Urban Plan.* 95. <https://doi.org/10.1016/j.landurbplan.2009.11.002>
- Li, H., Xu, X.L., Dai, D.W., Huang, Z.Y., Ma, Z., Guan, Y.J., 2020. Air pollution and temperature are associated with increased COVID-19 incidence: A time series study. *Int. J. Infect. Dis.* 97. <https://doi.org/10.1016/j.ijid.2020.05.076>
- Li, R., Tong, D., 2016. Constructing human activity spaces: A new approach incorporating complex urban activity-travel. *JTRG* 56, 23–35. <https://doi.org/10.1016/j.jtrangeo.2016.08.013>
- Li, S., Dragicevic, S., Castro, F.A., Sester, M., Winter, S., Coltekin, A., Pettit, C., Jiang, B., Haworth, J., Stein, A., Cheng, T., 2016. Geospatial big data handling theory and methods: A review and research challenges. *ISPRS J. Photogramm. Remote Sens.* 115, 119–133. <https://doi.org/10.1016/j.isprsjprs.2015.10.012>
- Li, X., Zhang, C., Li, W., Ricard, R., Meng, Q., Zhang, W., 2015. Assessing street-level urban greenery using Google Street View and a modified green view index. *Urban For. Urban Green.* 14. <https://doi.org/10.1016/j.ufug.2015.06.006>
- Liang, D., Shi, L., Zhao, J., Liu, P., Sarnat, J.A., Gao, S., Schwartz, J., Liu, Y., Ebel, S.T., Scovronick, N., Chang, H.H., 2020a. Urban Air Pollution May Enhance COVID-19 Case-Fatality and Mortality Rates in the United States. *Innov.*

<https://doi.org/10.1016/j.xinn.2020.100047>

Liang, D., Shi, L., Zhao, J., Liu, P., Schwartz, J., Gao, S., Sarnat, J., Liu, Y., Ebel, S., Scovronick, N., Chang, H.H., 2020b. Urban Air Pollution May Enhance COVID-19 Case-Fatality and Mortality Rates in the United States. *medRxiv Prepr. Serv. Heal. Sci.* <https://doi.org/10.1101/2020.05.04.20090746>

Lippi, G., Sanchis-Gomar, F., Henry, B.M., 2020. Association between environmental pollution and prevalence of coronavirus disease 2019 (COVID-19) in Italy. <https://doi.org/10.1101/2020.04.22.20075986>

Lipsitt, J., Chan-Golston, A.M., Liu, J., Su, J., Zhu, Y., Jerrett, M., 2021. Spatial analysis of COVID-19 and traffic-related air pollution in Los Angeles. *Environ. Int.* <https://doi.org/10.1016/j.envint.2021.106531>

Los Angeles County, 2018. LA County: Our County - Landscapes and Ecosystems [WWW Document]. Our Cty. Landscapes Ecosyst. Brief. URL [https://ourcountyla.lacounty.gov/wp-content/uploads/2018/10/Our-County-Landscapes-and-Ecosystems-Briefing\\_For-Web.pdf](https://ourcountyla.lacounty.gov/wp-content/uploads/2018/10/Our-County-Landscapes-and-Ecosystems-Briefing_For-Web.pdf) (accessed 5.2.22).

Los Angeles County, 2012. County of Los Angeles: Bicycle Master Plan, Final Plan.

Los Angeles Times, 2020. California confirms 2 cases of coronavirus in L.A., Orange counties - Los Angeles Times [WWW Document]. URL <https://www.latimes.com/california/story/2020-01-25/los-angeles-area-prepared-for-coronavirus> (accessed 11.10.20).

Ma, X., Longley, I., Gao, J., Salmond, J., 2020. Assessing schoolchildren's exposure to air pollution during the daily commute - A systematic review. *Sci. Total Environ.* 737, 140389. <https://doi.org/10.1016/J.SCITOTENV.2020.140389>

Macias, E., Suarez, A., Lloret, J., 2013. Mobile Sensing Systems. *Sensors* 13, 17292–17321. <https://doi.org/10.3390/s131217292>

Martinez, D.A., Hinson, J.S., Klein, E.Y., Irvin, N.A., Saheed, M., Page, K.R., Levin, S.R., 2020.

- SARS-CoV-2 Positivity Rate for Latinos in the Baltimore–Washington, DC Region. *JAMA* 324, 392–395. <https://doi.org/10.1001/jama.2020.11374>
- Mayo Clinic, 2022. California COVID-19 Map: Tracking the Trends [WWW Document]. URL <https://www.mayoclinic.org/coronavirus-covid-19/map/california> (accessed 5.23.22).
- McCrorie, P.R., Fenton, C., Ellaway, A., 2014. Combining GPS, GIS, and accelerometry to explore the physical activity and environment relationship in children and young people - a review. *Int. J. Behav. Nutr. Phys. Act.* 11. <https://doi.org/10.1186/s12966-014-0093-0>
- McMorris, O., Villeneuve, P.J., Su, J., Jerrett, M., 2015. Urban greenness and physical activity in a national survey of Canadians. *Environ. Res.* 137, 94–100. <https://doi.org/10.1016/J.ENVRES.2014.11.010>
- Memken, J.A., Canabal, M.E., 1994. Housing tenure, structure, and crowding among Latino households. *J. Fam. Econ. Issues* 15, 349–365. <https://doi.org/10.1007/BF02353810>
- Microsoft, 2021. R developer's guide - R programming - Azure Architecture Center | Microsoft Docs [WWW Document]. URL <https://docs.microsoft.com/en-us/azure/architecture/data-guide/technology-choices/r-developers-guide> (accessed 5.2.22).
- Mooney, S.J., Pejaver, V., 2018. Big Data in Public Health: Terminology, Machine Learning, and Privacy. <https://doi.org/10.1146/annurev-publhealth-040617-014208> 39, 95–112. <https://doi.org/10.1146/ANNUREV-PUBLHEALTH-040617-014208>
- Mou, N., Yuan, R., Yang, T., Zhang, H., Tang, J., Makkonen, T., 2020. Exploring spatio-temporal changes of city inbound tourism flow: The case of Shanghai, China. *Tour. Manag.* 76. <https://doi.org/10.1016/j.tourman.2019.103955>
- Myers, L.C., Parodi, S.M., Escobar, G.J., Liu, V.X., 2020. Characteristics of Hospitalized Adults With COVID-19 in an Integrated Health Care System in California. *JAMA* 323, 2195–2198. <https://doi.org/10.1001/jama.2020.7202>
- NASA Earth Observatory, 2011. Measuring Vegetation (NDVI & EVI) [WWW Document]. URL

[https://earthobservatory.nasa.gov/features/MeasuringVegetation/measuring\\_vegetation\\_2.php](https://earthobservatory.nasa.gov/features/MeasuringVegetation/measuring_vegetation_2.php) (accessed 5.9.22).

Nazarian, N., Lee, J.K.W., 2021. Personal assessment of urban heat exposure: a systematic review. *Environ. Res. Lett.* 16, 033005. <https://doi.org/10.1088/1748-9326/ABD350>

Nemati, E., Batteate, C., Jerrett, M., 2017. Opportunistic Environmental Sensing with Smartphones: a Critical Review of Current Literature and Applications. *Curr. Environ. Heal. reports* 4, 306–318. <https://doi.org/10.1007/s40572-017-0158-8>

Neupane, B., Jerrett, M., Burnett, R.T., Marrie, T., Arain, A., Loeb, M., 2010. Long-term exposure to ambient air pollution and risk of hospitalization with community-acquired pneumonia in older adults. *Am. J. Respir. Crit. Care Med.* 181. <https://doi.org/10.1164/rccm.200901-0160OC>

O'Neill, M.S., Jerrett, M., Kawachi, I., Levy, J.I., Cohen, A.J., Gouveia, N., Wilkinson, P., Fletcher, T., Cifuentes, L., Schwartz, J., Bateson, T.F., Cann, C., Dockery, D., Gold, D., Laden, F., London, S., Loomis, D., Speizer, F., Van den Eeden, S., Zanobetti, A., 2003. Health, wealth, and air pollution: Advancing theory and methods. *Environ. Health Perspect.* <https://doi.org/10.1289/ehp.6334>

Oak Ridge National Laboratory, NASA, 2022. Daymet V4: Daily Surface Weather and Climatological Summaries [WWW Document]. URL <https://daymet.ornl.gov/> (accessed 5.15.22).

Obradovich, N., Fowler, J.H., 2017. Climate change may alter human physical activity patterns. *Nat. Hum. Behav.* 2017 15 1, 1–7. <https://doi.org/10.1038/s41562-017-0097>

Okabe, A., Satoh, T., Sugihara, K., 2009. A kernel density estimation method for networks, its computational method and a GIS-based tool. *Int. J. Geogr. Inf. Sci.* 23, 7–32. <https://doi.org/10.1080/13658810802475491>

Oliveira, S., Andrade, H., Vaz, T., 2011. The cooling effect of green spaces as a contribution to

- the mitigation of urban heat: A case study in Lisbon. *Build. Environ.* 46, 2186–2194.  
<https://doi.org/10.1016/j.buildenv.2011.04.034>
- Olsen, J.R., Mitchell, R., McCrorie, P., Ellaway, A., 2019. Children’s mobility and environmental exposures in urban landscapes: A cross-sectional study of 10–11 year old Scottish children. *Soc. Sci. Med.* 224, 11–22. <https://doi.org/10.1016/j.socscimed.2019.01.047>
- Pebesma, E., 2018. Simple Features for R: Standardized Support for Spatial Vector Data. *R J.* 10, 439–446. <https://doi.org/10.32614/RJ-2018-009>
- Perchoux, C., Chaix, B., Cummins, S., Kestens, Y., 2013a. Health & Place Conceptualization and measurement of environmental exposure in epidemiology : Accounting for activity space related to daily mobility. *Health Place* 21, 86–93.  
<https://doi.org/10.1016/j.healthplace.2013.01.005>
- Perchoux, C., Chaix, B., Cummins, S., Kestens, Y., 2013b. Conceptualization and measurement of environmental exposure in epidemiology: Accounting for activity space related to daily mobility. *Heal. Place* 21, 86–93. <https://doi.org/10.1016/j.healthplace.2013.01.005>
- Perrin, A., 2021. Mobile technology and home broadband 2021. *Mob. Technol. Home Broadband* 1–26.
- Pickering, T.A., Huh, J., Intille, S., Liao, Y., Pentz, M.A., Dunton, G.F., 2016. Physical activity and variation in momentary behavioral cognitions: An ecological momentary assessment study. *J. Phys. Act. Heal.* 13, 344–351. <https://doi.org/10.1123/jpah.2014-0547>
- Puyau, M.R., Adolph, A.L., Vohra, F.A., Butte, N.F., 2002. Validation and calibration of physical activity monitors in children. *Obes. Res.* 10. <https://doi.org/10.1038/oby.2002.24>
- Quast, T., Andel, R., 2020. Excess mortality and potential undercounting of COVID-19 deaths by demographic group in Ohio. *medRxiv* 2020.06.28.20141655.  
<https://doi.org/10.1101/2020.06.28.20141655>
- Quiros, D.C., Zhang, Q., Choi, W., He, M., Paulson, S.E., Winer, A.M., Wang, R., Zhu, Y., 2013.

- Air quality impacts of a scheduled 36-h closure of a major highway. *Atmos. Environ.* 67, 404–414. <https://doi.org/10.1016/j.atmosenv.2012.10.020>
- R Core Team, 2020. R: A language and environment for statistical computing. Vienna, Austria. R Foundation for Statistical Computing.
- Raser, E., Gaupp-Berghausen, M., Dons, E., Anaya-Boig, E., Avila-Palencia, I., Brand, C., Castro, A., Clark, A., Eriksson, U., Götschi, T., Int Panis, L., Kahlmeier, S., Laeremans, M., Mueller, N., Nieuwenhuijsen, M., Orjuela, J.P., Rojas-Rueda, D., Standaert, A., Stigell, E., Gerike, R., 2018. European cyclists' travel behavior: Differences and similarities between seven European (PASTA) cities. *J. Transp. Heal.* 9. <https://doi.org/10.1016/j.jth.2018.02.006>
- Reid, C.E., O'Neill, M.S., Gronlund, C.J., Brines, S.J., Brown, D.G., Diez-Roux, A. V., Schwartz, J., 2009. Mapping Community Determinants of Heat Vulnerability. *Environ. Health Perspect.* 117, 1730–1736. <https://doi.org/10.1289/ehp.0900683>
- Revelle, W., 2021. psych: Procedures for Psychological, Psychometric, and Personality Research.
- Rhys, H., 2020. Preventing overfitting with ridge regression, LASSO, and elastic net. *Mach. Learn. with R, tidyverse, mlr* 536.
- Roberts, H., Helbich, M., 2021. Multiple environmental exposures along daily mobility paths and depressive symptoms: A smartphone-based tracking study. *Environ. Int.* 156. <https://doi.org/10.1016/j.envint.2021.106635>
- Rogers, T.N., Rogers, C.R., VanSant-Webb, E., Gu, L.Y., Yan, B., Qeadan, F., 2020. Racial Disparities in COVID-19 Mortality Among Essential Workers in the United States. *World Med. Heal. Policy* 12. <https://doi.org/10.1002/wmh3.358>
- Salvaris, M., Dean, D., Tok, W.H., 2018. Microsoft AI Platform, in: Salvaris, M., Dean, D., Tok, W.H. (Eds.), *Deep Learning with Azure: Building and Deploying Artificial Intelligence Solutions on the Microsoft AI Platform*. Apress, Berkeley, CA, pp. 79–98.

- Sasaki, J.E., John, D., Freedson, P.S., 2011. Validation and comparison of ActiGraph activity monitors. *J. Sci. Med. Sport* 14, 411–416. <https://doi.org/10.1016/j.jsams.2011.04.003>
- Schmidberger, M., Morgan, M., Eddelbuettel, D., Yu, H., Tierney, L., Mansmann, U., 2009. State of the Art in Parallel Computing with R. *J. Stat. Softw.* 31. <https://doi.org/10.18637/jss.v031.i01>
- Schwalb-Willmann, J., Remelgado, R., Safi, K., Wegmann, M., 2020. moveVis: Animating movement trajectories in synchronicity with static or temporally dynamic environmental data in r. *Methods Ecol. Evol.* 11, 664–669. <https://doi.org/10.1111/2041-210X.13374>
- Shelley, J., Fairclough, S.J., Knowles, Z.R., Southern, K.W., McCormack, P., Dawson, E.A., Graves, L.E.F., Hanlon, C., 2018. A formative study exploring perceptions of physical activity and physical activity monitoring among children and young people with cystic fibrosis and health care professionals. *BMC Pediatr.* 18. <https://doi.org/10.1186/s12887-018-1301-x>
- Sherman, J.E., Spencer, J., Preisser, J.S., Gesler, W.M., Arcury, T.A., 2005. A suite of methods for representing activity space in a healthcare accessibility study. *Int. J. Health Geogr.* 4, 24. <https://doi.org/10.1186/1476-072X-4-24>
- Shih, P.C., Han, K., Poole, E.S., Rosson, M.B., Carroll, J.M., 2015. Use and Adoption Challenges of Wearable Activity Trackers. *iConference 2015 Proc.*
- Shin, J.C., Kwan, M.P., Grigsby-Toussaint, D.S., 2020. Do spatial boundaries matter for exploring the impact of community green spaces on health? *Int. J. Environ. Res. Public Health* 17, 1–17. <https://doi.org/10.3390/ijerph17207529>
- Shoaib, M., Bosch, S., Durmaz Incel, O., Scholten, H., Havinga, P.J.M., 2014. Fusion of smartphone motion sensors for physical activity recognition. *Sensors (Switzerland)* 14. <https://doi.org/10.3390/s140610146>
- Shrout, P.E., Fleiss, J.L., 1979. Intraclass correlations: Uses in assessing rater reliability. *Psychol. Bull.* 86. <https://doi.org/10.1037/0033-2909.86.2.420>

- Shyamasundar, R.K., 2018. Future of Computing Science. Proc. Indian Natl. Sci. Acad. 96. <https://doi.org/10.16943/ptinsa/2018/49341>
- Smith, M., Hosking, J., Woodward, A., Witten, K., MacMillan, A., Field, A., Baas, P., Mackie, H., 2017. Systematic literature review of built environment effects on physical activity and active transport - an update and new findings on health equity. Int. J. Behav. Nutr. Phys. Act. 14. <https://doi.org/10.1186/s12966-017-0613-9>
- Song, M.-L., Fisher, R., Wang, J.-L., Cui, L.-B., 2018. Environmental performance evaluation with big data: theories and methods. Ann. Oper. Res. 270, 459–472. <https://doi.org/10.1007/s10479-016-2158-8>
- Srivastava, A., 2021. COVID-19 and air pollution and meteorology-an intricate relationship: A review. Chemosphere. <https://doi.org/10.1016/j.chemosphere.2020.128297>
- Stamatakis, E., Nnoaham, K., Foster, C., Scarborough, P., 2013. The Influence of Global Heating on Discretionary Physical Activity: An Important and Overlooked Consequence of Climate Change. J. Phys. Act. Heal. 10, 765–768. <https://doi.org/10.1123/jpah.10.6.765>
- Steinhubl, S.R., Muse, E.D., Topol, E.J., 2015. The emerging field of mobile health. Sci. Transl. Med. 7, 283rv3-283rv3. <https://doi.org/10.1126/scitranslmed.aaa3487>
- Stone, B., Hess, J.J., Frumkin, H., 2010. Urban Form and Extreme Heat Events: Are Sprawling Cities More Vulnerable to Climate Change Than Compact Cities? Environ. Health Perspect. 118, 1425–1428. <https://doi.org/10.1289/ehp.0901879>
- Su, J.G., Dadvand, P., Nieuwenhuijsen, M.J., Bartoll, X., Jerrett, M., 2019. Associations of green space metrics with health and behavior outcomes at different buffer sizes and remote sensing sensor resolutions. Environ. Int. 126. <https://doi.org/10.1016/j.envint.2019.02.008>
- Su, J.G., Jerrett, M., Beckerman, B., Wilhelm, M., Ghosh, J.K., Ritz, B.R., 2009. Predicting traffic-related air pollution in Los Angeles using a distance decay regression selection strategy. Environ. Res. 109, 657–670. <https://doi.org/10.1016/j.envres.2009.06.001>

- Su, J.G., Meng, Y.-Y., Chen, X., Molitor, J., Yue, D., Jerrett, M., 2020. Predicting differential improvements in annual pollutant concentrations and exposures for regulatory policy assessment. *Environ. Int.* 143, 105942. <https://doi.org/https://doi.org/10.1016/j.envint.2020.105942>
- Su, J.G., Meng, Y.Y., Pickett, M., Seto, E., Ritz, B., Jerrett, M., 2016. Identification of Effects of Regulatory Actions on Air Quality in Goods Movement Corridors in California. *Environ. Sci. Technol.* 50. <https://doi.org/10.1021/acs.est.6b00926>
- Sun, F., Walton, D.B., Hall, A., 2015. A Hybrid Dynamical–Statistical Downscaling Technique. Part II: End-of-Century Warming Projections Predict a New Climate State in the Los Angeles Region. *J. Clim.* 28, 4618–4636. <https://doi.org/10.1175/JCLI-D-14-00197.1>
- Swan, M., 2012. Sensor Mania! The Internet of Things, Wearable Computing, Objective Metrics, and the Quantified Self 2.0. *J. Sens. Actuator Networks* 1, 217–253. <https://doi.org/10.3390/jsan1030217>
- Sydbom, A., Blomberg, A., Parnia, S., Stenfors, N., Sandström, T., Dahlén, S.-E., 2001. Health effects of diesel exhaust emissions. *Eur. Respir. J.* 17, 733 LP – 746.
- Tang, J., Liu, F., Wang, Y., Wang, H., 2015. Uncovering urban human mobility from large scale taxi GPS data. *Phys. A Stat. Mech. its Appl.* 438. <https://doi.org/10.1016/j.physa.2015.06.032>
- Tate, E.B., Shah, A., Jones, M., Pentz, M.A., Liao, Y., Dunton, G., 2015. Toward a Better Understanding of the Link between Parent and Child Physical Activity Levels: The Moderating Role of Parental Encouragement. *J. Phys. Act. Heal.* 12, 1238–1244. <https://doi.org/10.1123/jpah.2014-0126>
- Thornton, M.M., Shrestha, R., Wei, Y., Thornton, P.E., Kao, S., Wilson, B.E., 2020. Daymet: Daily Surface Weather Data on a 1-km Grid for North America, Version 4. <https://doi.org/10.3334/ORNLDAAAC/1840>

- Travaglio, M., Yu, Y., Popovic, R., Selley, L., Leal, N.S., Martins, L.M., 2021. Links between air pollution and COVID-19 in England. *Environ. Pollut.* 268, 115859. <https://doi.org/10.1016/j.envpol.2020.115859>
- Tribby, C.P., Miller, H.J., Brown, B.B., Smith, K.R., Werner, C.M., 2017. Health & Place Geographic regions for assessing built environmental correlates with walking trips: A comparison using different metrics and model designs. *Health Place* 45, 1–9. <https://doi.org/10.1016/j.healthplace.2017.02.004>
- Trifan, A., Oliveira, M., Oliveira, J.L., 2019. Passive sensing of health outcomes through smartphones: Systematic review of current solutions and possible limitations. *JMIR mHealth uHealth* 7. <https://doi.org/10.2196/12649>
- Troped, P.J., Wilson, J.S., Matthews, C.E., Cromley, E.K., Melly, S.J., 2010. The Built Environment and Location-Based Physical Activity. *Am. J. Prev. Med.* 38, 429–438. <https://doi.org/10.1016/j.amepre.2009.12.032>
- Trost, S.G., Loprinzi, P.D., Moore, R., Pfeiffer, K.A., 2011. Comparison of accelerometer cut points for predicting activity intensity in youth. *Med. Sci. Sports Exerc.* 43. <https://doi.org/10.1249/MSS.0b013e318206476e>
- Tucker, J.M., Welk, G.J., Beyler, N.K., 2011. Physical activity in U.S. adults: Compliance with the physical activity guidelines for Americans. *Am. J. Prev. Med.* 40. <https://doi.org/10.1016/j.amepre.2010.12.016>
- Tucker, P., Gilliland, J., 2007. The effect of season and weather on physical activity: A systematic review. *Public Health* 121, 909–922. <https://doi.org/10.1016/j.puhe.2007.04.009>
- Twohig-Bennett, C., Jones, A., 2018. The health benefits of the great outdoors: A systematic review and meta-analysis of greenspace exposure and health outcomes. *Environ. Res.* 166. <https://doi.org/10.1016/j.envres.2018.06.030>
- U.S. Department of Labor, 2021. AMERICAN TIME USE SURVEY — MAY TO DECEMBER 2019

- AND 2020 RESULTS [WWW Document]. News Release, Bur. Labor Stat. URL [www.bls.gov/tus](http://www.bls.gov/tus) (accessed 6.1.22).
- US Census Bureau, 2020. U.S. Census Bureau QuickFacts: Los Angeles County, California [WWW Document]. URL <https://www.census.gov/quickfacts/losangelescountycalifornia> (accessed 11.10.20).
- US Census Bureau, 2018. American Community Survey 5-Year Data (2009-2018) [WWW Document]. URL <https://www.census.gov/data/developers/data-sets/acs-5year.html> (accessed 11.10.20).
- USDA NAIP GeoHub, 2022. National Agriculture Imagery Program - NAIP Hub Site [WWW Document]. URL <https://naip-usdaonline.hub.arcgis.com/> (accessed 6.1.22).
- Ushey, K., Allaire, J.J., Tang, Y., 2021. reticulate: Interface to “Python.”
- Uyttendaele, N., 2015. How to speed up R code: an introduction. arXiv1503.00855 [cs, stat].
- van den Berg, A.E., Maas, J., Verheij, R.A., Groenewegen, P.P., 2010. Green space as a buffer between stressful life events and health. *Soc. Sci. Med.* 70. <https://doi.org/10.1016/j.socscimed.2010.01.002>
- Varghese, B., Buyya, R., 2018. Next generation cloud computing: New trends and research directions. *Futur. Gener. Comput. Syst.* 79, 849–861. <https://doi.org/10.1016/j.future.2017.09.020>
- Vienneau, D., de Hoogh, K., Faeh, D., Kaufmann, M., Wunderli, J.M., Rösli, M., 2017. More than clean air and tranquillity: Residential green is independently associated with decreasing mortality. *Environ. Int.* 108. <https://doi.org/10.1016/j.envint.2017.08.012>
- Villeneuve, P.J., Jerrett, M., G. Su, J., Burnett, R.T., Chen, H., Wheeler, A.J., Goldberg, M.S., 2012. A cohort study relating urban green space with mortality in Ontario, Canada. *Environ. Res.* 115, 51–58. <https://doi.org/10.1016/j.envres.2012.03.003>
- Wang, B., Chen, H., Chan, Y.L., Oliver, B.G., 2020. Is there an association between the level of

- ambient air pollution and COVID-19? *Am. J. Physiol. Lung Cell. Mol. Physiol.*  
<https://doi.org/10.1152/ajplung.00244.2020>
- Wang, B., Shi, W., Miao, Z., 2015. Confidence Analysis of Standard Deviation Ellipse and Its Extension into Higher Dimensional Euclidean Space. *PLoS One* 10, e0118537.  
<https://doi.org/10.1371/journal.pone.0118537>
- Wang, J., Kwan, M.P., Chai, Y., 2018. An innovative context-based crystal-growth activity space method for environmental exposure assessment: A study using GIS and GPS trajectory data collected in Chicago. *Int. J. Environ. Res. Public Health* 15.  
<https://doi.org/10.3390/ijerph15040703>
- Wang, Y., Kung, L., Byrd, T.A., 2018. Big data analytics: Understanding its capabilities and potential benefits for healthcare organizations. *Technol. Forecast. Soc. Change* 126, 3–13.  
<https://doi.org/10.1016/j.techfore.2015.12.019>
- Wang, Y., Wen, Y., Wang, Yue, Zhang, S., Zhang, K.M., Zheng, H., Xing, J., Wu, Y., Hao, J., 2020. Four-Month Changes in Air Quality during and after the COVID-19 Lockdown in Six Megacities in China. *Environ. Sci. Technol. Lett.* <https://doi.org/10.1021/acs.estlett.0c00605>
- Ward Thompson, C., Roe, J., Aspinall, P., Mitchell, R., Clow, A., Miller, D., 2012. More green space is linked to less stress in deprived communities: Evidence from salivary cortisol patterns. *Landsc. Urban Plan.* 105, 221–229.  
<https://doi.org/10.1016/j.landurbplan.2011.12.015>
- Wehener, S., Raser, E., Gaupp, M., Anata, E., De Nazelle, A., Eriksoon, U., Gerike, R., Horvath, I., Iacorossi, F., Int Panis, L., Kahlmeier, S., Nieuwenhuijsen, M., Mueller, N., Sanchez, J., Rothballer, C., 2017. Active Mobility, the New Health Trend in Smart Cities, or even More? REAL CORP.
- Wing, S.E., Larson, T. V., Hudda, N., Boonyarattaphan, S., Fruin, S., Ritz, B., 2020. Preterm birth among infants exposed to in utero ultrafine particles from aircraft emissions. *Environ. Health*

- Perspect. 128, 1–9. <https://doi.org/10.1289/EHP5732>
- Wolch, J.R., Byrne, J., Newell, J.P., 2014a. Urban green space, public health, and environmental justice: The challenge of making cities “just green enough.” *Landsc. Urban Plan.* 125, 234–244. <https://doi.org/10.1016/j.landurbplan.2014.01.017>
- Wolch, J.R., Byrne, J., Newell, J.P., 2014b. Urban green space, public health, and environmental justice: The challenge of making cities “just green enough.” *Landsc. Urban Plan.* 125, 234–244. <https://doi.org/10.1016/j.landurbplan.2014.01.017>
- World Health Organization, 2022. Physical activity: Fact Sheet [WWW Document]. URL <https://www.who.int/news-room/fact-sheets/detail/physical-activity> (accessed 5.9.22).
- World Health Organization, 2021. WHO Coronavirus Disease (COVID-19) Dashboard | WHO Coronavirus Disease (COVID-19) Dashboard [WWW Document]. URL <https://covid19.who.int/> (accessed 11.2.20).
- Wu, C.Y.H., Zaitchik, B.F., Swarup, S., Gohlke, J.M., 2019. Influence of the Spatial Resolution of the Exposure Estimate in Determining the Association between Heat Waves and Adverse Health Outcomes. *Ann. Am. Assoc. Geogr.* 109. <https://doi.org/10.1080/24694452.2018.1511411>
- Wu, Xiao, Nethery, R.C., Sabath, B.M., Braun, D., Dominici, F., 2020a. Exposure to air pollution and COVID-19 mortality in the United States. medRxiv.
- Wu, Xiao, Nethery, R.C., Sabath, B.M., Braun, D., Dominici, F., 2020b. Exposure to air pollution and COVID-19 mortality in the United States: A nationwide cross-sectional study. medRxiv Prepr. Serv. Heal. Sci. <https://doi.org/10.1101/2020.04.05.20054502>
- Wu, X., Nethery, R.C., Sabath, M.B., Braun, D., Dominici, F., 2020. Air pollution and COVID-19 mortality in the United States: Strengths and limitations of an ecological regression analysis. *Sci. Adv.* 6, eabd4049. <https://doi.org/10.1126/sciadv.abd4049>
- Yang, D.H., Goerge, R., Mullner, R., 2006. Comparing GIS-based methods of measuring spatial

accessibility to health services. *J. Med. Syst.* 30. <https://doi.org/10.1007/s10916-006-7400-5>

Yao, Y., Pan, J., Liu, Z., Meng, X., Wang, Weidong, Kan, H., Wang, Weibing, 2021. Ambient nitrogen dioxide pollution and spreadability of COVID-19 in Chinese cities. *Ecotoxicol. Environ. Saf.* 208, 111421. <https://doi.org/10.1016/J.ECOENV.2020.111421>

Yi, L., Wilson, J.P., Mason, T.B., Habre, R., Wang, S., Dunton, G.F., 2019. Methodologies for assessing contextual exposure to the built environment in physical activity studies: A systematic review. *Heal. Place.* <https://doi.org/10.1016/j.healthplace.2019.102226>

Yu, Z., Bellander, T., Bergström, A., Dillner, J., Eneroth, K., Engardt, M., Georgelis, A., Kull, I., Ljungman, P., Pershagen, G., Stafoggia, M., Melén, E., Gruzieva, O., Group, B.C.-19 S., Almqvist, C., Andersson, N., Ballardini, N., Bergström, A., Björkander, S., Brodin, P., Castel, A., Ekström, S., Georgelis, A., Hammarström, L., Pan-Hammarström, Q., Hallberg, J., Jansson, C., Kere, M., Kull, I., Lauber, A., Lövquist, A., Melén, E., Mjösberg, J., Mogensen, I., Palmberg, L., Pershagen, G., Roxhed, N., Schwenk, J., 2022. Association of Short-term Air Pollution Exposure With SARS-CoV-2 Infection Among Young Adults in Sweden. *JAMA Netw. Open* 5, e228109–e228109. <https://doi.org/10.1001/JAMANETWORKOPEN.2022.8109>

Zeldovich, Y.B., 2015. 26. Oxidation of Nitrogen in Combustion and Explosions, in: *Selected Works of Yakov Borisovich Zeldovich, Volume I.* <https://doi.org/10.1515/9781400862979.404>

Zenk, Shannon N, Schulz, A.J., Matthews, S.A., Odoms-young, A., Wilbur, J., Wegrzyn, L., Gibbs, K., Braunschweig, C., Stokes, C., 2011. Health & Place Activity space environment and dietary and physical activity behaviors: A pilot study. *Health Place* 17, 1150–1161. <https://doi.org/10.1016/j.healthplace.2011.05.001>

Zenk, Shannon N., Schulz, A.J., Matthews, S.A., Odoms-Young, A., Wilbur, J.E., Wegrzyn, L.,

- Gibbs, K., Braunschweig, C., Stokes, C., 2011. Activity space environment and dietary and physical activity behaviors: A pilot study. *Heal. Place* 17, 1150–1161. <https://doi.org/10.1016/j.healthplace.2011.05.001>
- Zhang, Z., Xue, T., Jin, X., 2020. Effects of meteorological conditions and air pollution on COVID-19 transmission: Evidence from 219 Chinese cities. *Sci. Total Environ.* 741. <https://doi.org/10.1016/j.scitotenv.2020.140244>
- Zhao, P., Kwan, M.P., Zhou, S., 2018. The uncertain geographic context problem in the analysis of the relationships between obesity and the built environment in Guangzhou. *Int. J. Environ. Res. Public Health* 15. <https://doi.org/10.3390/ijerph15020308>
- Zhou, X., Josey, K., Kamareddine, L., Caine, M.C., Liu, T., Mickley, L.J., Cooper, M., Dominici, F., 2021. Excess of COVID-19 cases and deaths due to fine particulate matter exposure during the 2020 wildfires in the United States. *Sci. Adv.* 7, 8789–8802. [https://doi.org/10.1126/SCIADV.ABI8789/SUPPL\\_FILE/SCIADV.ABI8789\\_SM.PDF](https://doi.org/10.1126/SCIADV.ABI8789/SUPPL_FILE/SCIADV.ABI8789_SM.PDF)
- Zhu, Y., Xie, J., Huang, F., Cao, L., 2020. Association between short-term exposure to air pollution and COVID-19 infection: Evidence from China. *Sci. Total Environ.* 727. <https://doi.org/10.1016/j.scitotenv.2020.138704>